LITHUANIAN UNIVERSITY OF HEALTH SCIENCES

Jolita Stabrauskienė

THE INFLUENCE OF MICROCAPSULATED AND LIPOSOMAL MODIFIED RELEASE FORMS ON THE SOLUBILITY OF NARINGIN AND NARINGENIN

Doctoral Dissertation
Medical and Health Sciences,
Pharmacy (M 003)

Kaunas, 2026

Dissertation has been prepared at the Pharmaceutical Science Laboratory of the Institute of Pharmaceutical Technologies, Faculty of Pharmacy, Medical Academy, Lithuanian University of Health Sciences during the period of 2021–2025.

Scientific Supervisor

Prof. Dr. Jurga Bernatonienė (Lithuanian University of Health Sciences, Medical and Health Sciences, Pharmacy – M 003).

Consultant

Prof. Dr. Robertas Lažauskas (Lithuanian University of Health Sciences, Medical and Health Sciences, Medicine – M 001).

Dissertation is defended at the Pharmacy Research Council of the Lithuanian University of Health Sciences:

Chairperson

Prof. Dr. Lina Raudonė (Lithuanian University of Health Sciences, Medical and Health Sciences, Pharmacy – M 003).

Members:

Dr. Kristina Zymonė (Lithuanian University of Health Sciences, Medical and Health Sciences, Pharmacy – M 003);

Prof. Dr. Ramunė Rutkaitė (Kaunas University of Technology, Technological Sciences, Chemical Engineering – T 005);

Assoc. Prof. Dr. Konstantīns Logviss (Riga Stradiņš University, Latvia, Medical and Health Sciences, Pharmacy – M 003);

Prof. Dr. Lolita Kuršvietienė (Lithuanian University of Health Sciences, Natural Sciences, Biochemistry – N 004).

Dissertation will be defended at the open session of the Pharmacy Research Council of the Lithuanian University of Health Sciences at 11 a.m. on June 2, 2026, at the Museum of the History of Lithuanian Medicine and Pharmacy. Address: Rotušės 28, LT-01100 Kaunas, Lithuania.

LIETUVOS SVEIKATOS MOKSLŲ UNIVERSITETAS

Jolita Stabrauskienė

MIKROKAPSULIUOTŲ IR LIPOSOMINIŲ MODIFIKUOTO ATPALAIDAVIMO FORMŲ ĮTAKA NARINGINO IR NARINGENINO TIRPIMUI

Daktaro disertacija
Medicinos ir sveikatos mokslai,
farmacija (M 003)

Kaunas, 2026

Disertacija rengta 2021–2025 metais Lietuvos sveikatos mokslų universiteto Medicinos akademijos Farmacijos fakulteto Farmacinių technologijų instituto Farmacijos mokslinėje laboratorijoje.

Mokslinė vadovė

prof. dr. Jurga Bernatonienė, (Lietuvos sveikatos mokslo universitetas, medicinos ir sveikatos mokslai, farmacija – M 003).

Konsultantas

prof. dr. Robertas Lažauskas, (Lietuvos sveikatos mokslo universitetas, medicinos ir sveikatos mokslai, medicina – M 001).

Disertacija ginama Lietuvos sveikatos mokslų universiteto Farmacijos mokslo krypties taryboje:

Pirmininkė

prof. dr. Lina Raudonė (Lietuvos sveikatos mokslų universitetas, medicinos ir sveikatos mokslai, farmacija – M 003).

Nariai:

dr. Kristina Zymonė (Lietuvos sveikatos mokslų universitetas, medicinos ir sveikatos mokslai, farmacija – M 003);

prof. dr. Ramunė Rutkaitė (Kauno technologijos universitetas, technologijos mokslai, chemijos inžinerija – T 005);

doc. dr. Konstantīns Logviss (Rygos Stradinio universitetas (Latvija), medicinos ir sveikatos mokslai, farmacija – M 003);

prof. dr. Lolita Kuršvietienė (Lietuvos sveikatos mokslų universitetas, gamtos mokslai, biochemija – N 004).

Disertacija bus ginama viešajame Farmacijos mokslo krypties tarybos posėdyje 2026 m. birželio 2 d. 11 val. Lietuvos medicinos ir farmacijos istorijos muziejuje.
Disertacijos gynimo vietos adresas: Rotušės a. 28, LT-01100 Kaunas, Lietuva.

CONTENTS

ACKNOWLEDGEMENTS

I would like to sincerely thank my scientific advisor, Prof. Dr. Jurga Bernatonienė, for her ongoing guidance, valuable advice, and encouragement throughout my doctoral studies. Her support and constructive feedback not only helped me complete this dissertation but also inspired me to develop as a researcher.

I am truly grateful to my colleagues at the Department of Drug Technology and Social Pharmacy, the Neuroscience Institute, and the Institute of Pharmaceutical Technologies at the Lithuanian University of Health Sciences. Collaborating with such committed and supportive people made this journey both professional and enjoyable.

Special thanks go to Dr. Lauryna Pudžiuvelytė for her kind support, thoughtful discussions, and uplifting presence during both scientific work and everyday moments — it meant more than words can say.

My heartfelt thanks go to my family, my husband, children, and close friends for their endless patience, encouragement, and love. You have been my greatest source of strength and motivation every step of the way.

Finally, I gratefully acknowledge the financial support from the Science Foundation of the Lithuanian University of Health Sciences and the Research Council of Lithuania (project No. 09.3.3-ESFA-V-711-01-0001), which made this research and the dissemination of its results possible.

LIST OF ABBREVIATIONS

ALG – sodium alginate
CAT – catalase
CD – cyclodextrins
CMC – carboxymethylcellulose
DE – dissolution efficiency
EE – encapsulation efficiency
GR – glutathione reductase
GSH – reduced glutathione
HPMC – hydroxypropyl methylcellulose
LBC – lipid-based carrier
L(FD) – lyophilised (freeze-dried) formulation
MDA – malondialdehyde
MD – maltodextrin
$AlCl_3$ – aluminum chloride
GE – Grapefruit extract
NR – naringin
NAR – naringenin
N7R – naringenin-7-O-rutinoside
PDI – polydispersity index
PVA – polyvinyl alcohol
SD – spray drying
SGF – simulated gastric fluid
SIF – simulated intestinal fluid
SKM – skim milk
SOD – superoxide dismutase
DPPH – 2,2-diphenyl-1-picrylhydrazyl
ABTS – 2,2'-azino-bis(3-ethylbenzothiazoline-6-sulfonic acid)
FRAP – ferric reducing antioxidant power
HPLC – high-performance liquid chromatography
CYP3A4 – cytochrome P450 3A4 enzyme
BCS – Biopharmaceutics classification system
Nrf2 – Nuclear factor erythroid 2–related factor 2
SEM – scanning electron microscopy
ZP – Zeta potential
TE – Trolox equivalents
ANOVA – analysis of variance

INTRODUCTION

Plant-derived bioactive compounds have been used in medicine for centuries due to their structural diversity and broad spectrum of biological activities. Unlike many synthetic molecules, phytochemicals often demonstrate better biological compatibility, lower toxicity, and the ability to interact with multiple biological targets simultaneously, which makes them attractive for pharmaceutical and nutraceutical applications [1]. In recent years, increasing attention has also been directed toward sustainability and circular bioeconomy approaches. Considerable efforts are being made to utilise food industry by-products as valuable sources of bioactive compounds. Globally, fruits and vegetables account for the largest share of food waste, at approximately 1.3 billion tons annually [2]. It is estimated that about 20% of fruits are lost during processing, leading to the disposal of materials that still contain valuable bioactive compounds with potential therapeutic value [3,4].

One such example is grapefruit (*Citrus* × *aurantium* f. aurantium, Rutaceae). Studies have shown that extracts obtained from citrus peels and juices, as well as isolated bioactive compounds, exhibit a wide range of biological activities, including antioxidant, antimicrobial, cardioprotective, anticancer, and antidiabetic effects [5]. These biological properties are largely attributed to the diversity of phytochemicals present in citrus fruits, including phenolic compounds, coumarins, limonoids, carotenoids, and essential oils.

The main flavanones found in grapefruit peel are naringin (NR) and narirutin (N7R). Naringin is a glycoside consisting of the flavanone aglycone naringenin (NAR) linked to the disaccharide rutinose (α-L-rhamnosyl-D-glucose), and is therefore commonly referred to as naringenin-7-O-rutinoside [6]. Narirutin is also a flavanone-7-O-glycoside [7–13]. During digestion, the glycosidic bond is hydrolysed, releasing the aglycone naringenin, which is considered the biologically active form. As an aglycone, NAR is more lipophilic and can more readily penetrate biological membranes, which contributes to improved absorption and biological activity compared with its glycosylated forms [14–16].

However, their practical use is often limited. Both NR and NAR suffer from poor water solubility and low bioavailability, and NR in particular is known to interfere with the cytochrome P450 3A4 enzyme (CYP3A4), leading to the so-called “grapefruit–drug interaction”. NR is classified as a biopharmaceutics classification system (BCS) class IV compound, meaning it has both low solubility and low permeability, with an oral bioavailability of less than 5% [17,18]. Both flavanones are primarily absorbed in the small intestine, where they require protection from acidic and enzymatic degradation in the stomach

[19]. Moreover, differences between animal and human digestion must be considered when interpreting experimental results [20].

Although these compounds have attracted significant scientific attention, there remains limited knowledge of how different extraction methods, hydrolysis conditions, and excipients influence flavanone yield, solubility, and stability. Addressing this research gap represents one of the main objectives of the present study.

To improve the efficiency of extraction and application, various technological solutions have been studied. Combined methods, such as ultrasound-assisted hydrolysis and extraction, increased NR by about 44% and NAR by almost threefold compared to conventional extraction [21,22].

The scientific literature also increasingly highlights the importance of excipients, such as cyclodextrins (α-, β-, and γ-CD) and magnesium aluminometasilicate, in improving the extraction and stability of flavanones. These substances can form complexes with bioactive molecules, thereby increasing their solubility and protecting them from oxidative degradation, light exposure, and unfavourable pH conditions [23]. Magnesium alumino-metasilicate has been reported to stabilise isoflavones and promote their release from plant matrices. Cyclodextrins possess a characteristic cone-shaped molecular structure with a hydrophobic internal cavity and a hydrophilic outer surface, enabling them to form inclusion complexes with the hydrophobic regions of flavanone molecules through weak noncovalent interactions, thereby improving their solubility in aqueous systems. Previous studies have shown that the use of cyclodextrins during extraction increased the recovery of bioactive compounds from plant materials such as red clover (*Trifolium pratense* L.) and peppermint (*Mentha* × *piperita* L.) [24–26].

When evaluating the practical applicability of flavanones, improving extraction efficiency and stability alone is not sufficient; it is also necessary to assess their biological activity, particularly their effects on antioxidant defence systems. *In vitro* studies provide valuable insights into the antioxidant potential of flavanones; however, they cannot fully replicate the complex biological interactions occurring in living organisms. For this reason, *in vivo* studies are required to better understand the interactions between flavanones and endogenous antioxidant systems.

Previous studies have demonstrated that NR can reduce lipid peroxidation and increase the activity of key antioxidant enzymes, including catalase (CAT), superoxide dismutase (SOD), and glutathione reductase (GR) [20,27–29]. Considering that grapefruit extracts also contain other bioactive compounds, including flavonoids, phenolic acids, and pectins, it is likely that synergistic interactions between these components may further enhance the overall antioxidant activity [12,29]. However, only a limited number of studies have

investigated this aspect, and direct *in vivo* comparisons between pure naringin and whole grapefruit peel extracts remain scarce.

Encapsulation technology is an important strategy for improving the applicability of NR and NAR. Encapsulation protects sensitive compounds from environmental and gastrointestinal degradation, enhances aqueous solubility, and enables controlled or targeted release. These advantages are particularly relevant for flavanones, which exhibit limited solubility and stability.

Given the biological activity of flavanones and their limited solubility and bioavailability, increasing attention has been directed toward advanced technological approaches that could improve their pharmacokinetic properties. One of the most promising strategies is microencapsulation, which protects bioactive compounds from environmental degradation, improves their solubility, and enables controlled release and enhanced stability.

Microencapsulation using spray-drying and freeze-drying techniques is widely used to formulate flavonoid-rich extracts. Spray-dried powders typically exhibit high encapsulation efficiency, low moisture content, and good storage stability, which are important for extending product shelf life and improving practical applicability [30–32]. In contrast, freeze-drying preserves structural integrity and produces porous matrices that facilitate rapid hydration and release of active compounds.

Previous studies have demonstrated that the use of different wall materials during freeze-drying, such as skim milk powder, sodium caseinate, or β-cyclodextrin, can significantly improve the solubility of plant extracts [32,33]. Kazlauskaitė and colleagues reported that freeze-dried microcapsules achieved yields of approximately 85% and exhibited higher total phenolic content and antioxidant activity than spray-dried powders, which reached only about 45% [34,35].

Liposomal carriers provide an effective means of protecting flavanones, such as NR, from acidic gastric conditions and enzymatic degradation [36]. Composed of phospholipid bilayers, liposomes can encapsulate hydrophobic compounds, improving their stability and enhancing intestinal absorption [37]. The study using green tea extract demonstrated that nanoliposomes enhanced stability and facilitated the controlled release of the active ingredient *in vitro* [38]. Another study with NR demonstrated that a liposome-polymer system enabled sustained release and promoted bone formation in both cell cultures and animal models [39]. These results suggest that liposome technology may be a practical approach to enhancing the stability of active ingredients and improving their bioavailability.

However, liposomal dispersions in aqueous media are prone to instability, often leading to particle aggregation and leakage of compounds during storage.

To improve their shelf life, liposomes are commonly dried via lyophilisation or spray drying. Studies have shown that cryoprotectants, such as sucrose or mannitol, help preserve liposomal structure and encapsulation efficiency [40]. Ko et al. reported that spray-dried liposomes increased vitamin C bioavailability by approximately 30%, while Wu et al. demonstrated greater stability and slower release with lyophilised NAR nanoparticles [41–43].

Double encapsulation, which involves combining two protective layers or technological processes, has recently emerged as one of the most promising strategies for improving stability and controlling the release of active compounds. Although only a limited number of studies have investigated this approach, and it has not yet been applied to naringin, research involving other bioactive compounds indicates significant potential for this strategy [44].

Buccal films represent an alternative drug delivery system that can bypass first-pass metabolism and reduce enzymatic degradation in the gastrointestinal tract, thereby improving bioavailability [45]. The physicochemical properties of these films, including dissolution rate, mechanical strength, and release kinetics, strongly depend on the excipients selected for the formulation. Polymers play a key role in determining both the technological quality and functional performance of the dosage form. Studies by Jawadi et al. and Sabra et al. have shown that mucoadhesive films composed of polyvinyl alcohol (PVA) and hydroxypropyl methylcellulose (HPMC) dissolve rapidly in simulated saliva and exhibit strong adhesion to the buccal mucosa, ensuring rapid absorption of active compounds [46,47].

This dissertation focused on optimising extraction methods to obtain flavanone-rich grapefruit peel extracts and evaluating their *in vivo* activity compared to pure naringin. Several formulation strategies (microcapsules, liposomes, and buccal films) were developed to assess solubility, stability, and *in vitro* release. The findings highlight the importance of technological factors in determining product effectiveness and functionality.

The dissertation aims to evaluate the impact of liposomal and micro-encapsulated modified-release formulations on the solubility of NR and NAR, and to determine the effect of technological parameters on the quality of microcapsules obtained by different methods and on the *in vitro* dissolution of the active substances.

Objectives

1. To investigate the effect of various extraction methods for obtaining NR and NAR from grapefruit peel**,** and to evaluate the *in vitro* antioxidant properties of the obtained extracts.
2. To investigate the effect of excipients on the yield, stability, and antioxidant activity of grapefruit peel flavanones.
3. To evaluate the *in vivo* antioxidant activity of pure NR and grapefruit peel extract in mice by analysing oxidative stress biomarkers and comparing biological responses.
4. To develop and characterise microencapsulated formulations of grapefruit flavanones using spray–drying and freeze-drying methods, focusing on encapsulation efficiency, physicochemical properties, and stability.
5. To compare *in vitro* dissolution and release profiles of spray-dried microcapsules, dual liposomal–microencapsulation systems, and buccal films under simulated gastrointestinal and saliva conditions, and to determine their potential for improving solubility, stability, and site-specific delivery of naringin.

Hypotheses

1. Using a combination of extraction methods increases the yield of NR and NAR compared to using individual methods alone.
2. Adding excipients such as magnesium aluminometasilicate and cyclodextrins improves the extraction efficiency, stability, and antioxidant activity of flavanones.
3. Grapefruit peel extract reduces oxidative stress more effectively than pure NR due to the synergistic action of multiple phytochemicals.
4. Applying microencapsulation techniques, including spray-drying and freeze-drying, enhances the stability and retention of bioactive compounds.
5. The solubility and release profile of NR and NAR depend on the type of delivery system.

SCIENTIFIC NOVELTY

This dissertation offers novel insights into the utilisation of grapefruit peel as a sustainable source of flavanones, addressing the limited research on the combined influence of extraction parameters, excipients, and delivery strategies on the performance of NR and NAR.

This study was the first to use functional excipients in the extraction of flavanones from grapefruit peel, thereby increasing flavanone yield, solubility, and antioxidant stability.

A novel aspect of this work lies in the comparative evaluation of pure NR and whole grapefruit peel extract. *In vivo* studies in mice reveal distinct antioxidant mechanisms: NR primarily enhances endogenous defence systems, whereas the entire extract more effectively reduces lipid peroxidation, highlighting the role of synergistic phytochemicals.

Furthermore, the study presented the first integrated analysis of four delivery systems for poorly water-soluble flavonoids: spray-dried and freeze-dried microcapsules, liposomal carriers, and buccal films. Each system offered specific functional advantages, ranging from enhanced dissolution and extended release to improved mucosal absorption, demonstrating the potential for targeted delivery applications.

This research provides several novel insights, including the first comparative in *vivo* evaluation of pure NR and grapefruit extract, the first integration of excipient-enhanced extraction with multiple delivery platforms, and the first systematic assessment of how formulation methods affect solubility, stability, and biological activity of flavanones from grapefruit peel.

PRACTICAL VALUE

The application of combined extraction methods (ultrasound-assisted and thermal hydrolysis) together with functional excipients enables significantly higher recovery of NR and NAR from grapefruit byproducts while reducing solvent consumption. This method not only increases extraction efficiency but also complies with the principles of green chemistry and sustainable bioeconomy.

The inclusion of excipients such as magnesium aluminiummetasilicate and cyclodextrins enhances the solubility, stability, and antioxidant activity of flavanones, protecting sensitive compounds from degradation during processing and storage. *In vitro* antioxidant studies confirmed that these excipients significantly improved the radical-scavenging capacity of the flavanone-rich extracts. Among cyclodextrins, β-cyclodextrin demonstrated the highest suitability for forming stable complexes with flavanones.

The comparative *in vivo* evaluation of pure NR and grapefruit peel extract revealed different antioxidant mechanisms. NR mainly enhanced endogenous antioxidant defences. In contrast, the whole extract was more effective at reducing lipid peroxidation, likely due to synergistic phytochemicals. These results suggest that whole-plant extracts may be more effective than isolated compounds, especially for long-term use.

Spray–drying and freeze-drying microencapsulation using carbohydrate-based wall materials improved the solubility and stability of NR and NAR in the extract. Spray-drying resulted in higher encapsulation efficiency. In contrast, freeze–drying provided faster dissolution. Liposomal encapsulation offered additional protection for bioactive compounds in the stomach. It also enabled prolonged release in the intestine.

Comparative *in vitro* evaluation of spray-dried powders, dual liposomal–microencapsulated systems, and buccal films revealed specific benefits of each delivery form. Single microencapsulation improved solubility. Dual encapsulation ensured prolonged intestinal release. Buccal films enabled rapid dissolution, strong mucosal adhesion, and bypass of first-pass metabolism.

These results offer practical approaches for creating advanced dietary supplements, functional foods, and pharmaceutical products from grapefruit by-products. The study contributes to waste reduction, sustainable processing, and increased therapeutic potential of natural antioxidants.

THE LAYOUT OF THE DISSERTATION

The dissertation is based on five original research articles. It is structured into five main thematic parts that reflect the progression from natural extract preparation to advanced formulation and release studies.

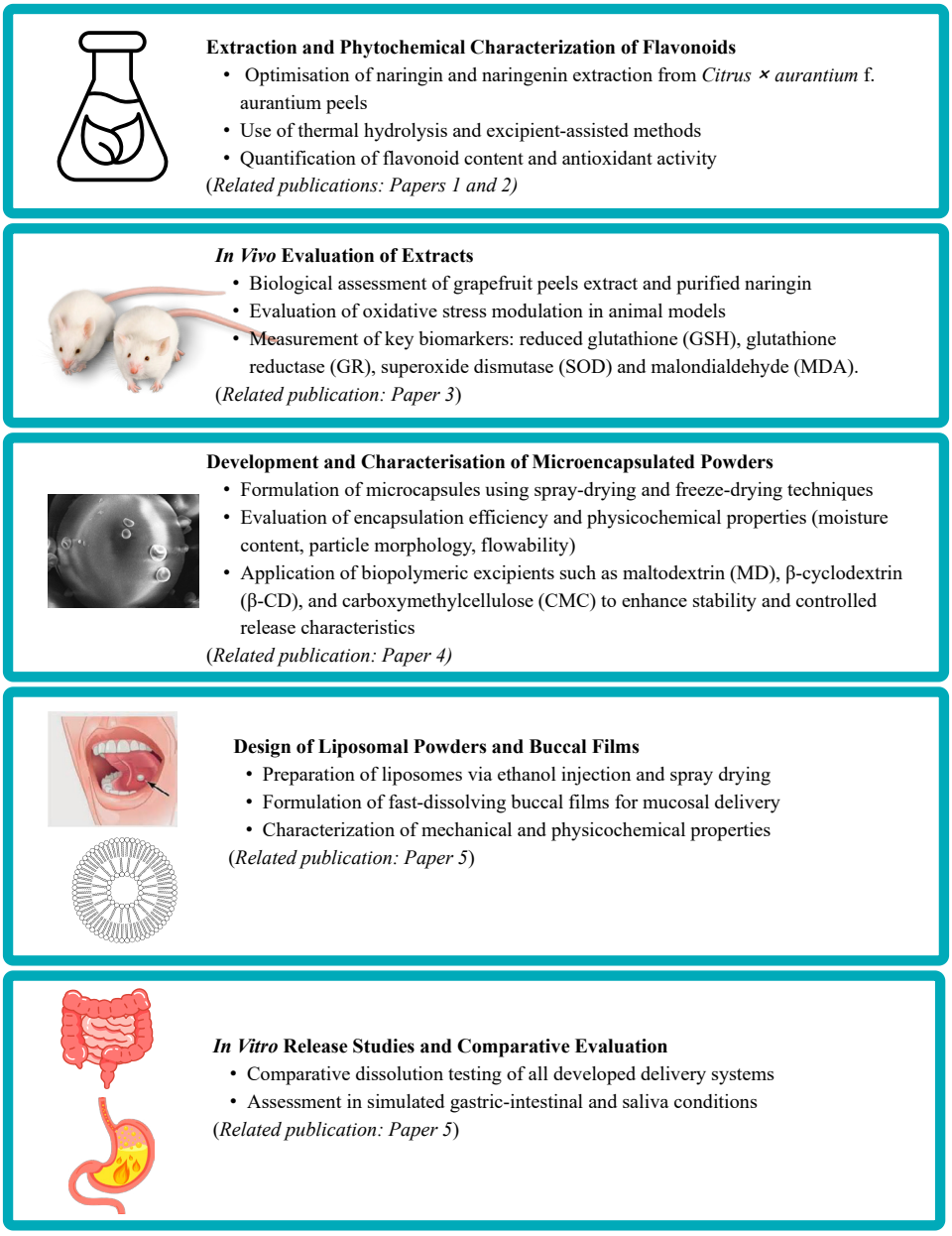

Fig. 1. *Scheme of the thesis with published scientific papers*

The thesis material is organised into five principal sections:

1. Examination of extraction strategies and excipients on the yield of NR and NAR from grapefruits by–products, with emphasis on sustainable processing, functional excipients, and their effect on *in vitro* antioxidant activity.
2. Evaluation of *in vivo* antioxidant activity, comparing pure NR and grapefruit peel extract, and identifying their distinct mechanisms of action in modulating oxidative stress biomarkers.
3. Investigation of technological factors in microencapsulation, analysing the effect of spray–drying and freeze–drying techniques, wall material composition, and structural parameters on solubility, stability, and encapsulation efficiency.
4. Design and characterisation of liposomal powders and buccal films, focusing on technological preparation methods, physicochemical and mechanical properties.
5. Comparative assessment of delivery systems, focusing on the dissolution and release behaviour of spray–dried microcapsules, dual liposomal–microencapsulation systems, and buccal films under simulated gastrointestinal and mucosal conditions.

PHD CANDIDATE'S CONTRIBUTION

Author Jolita Stabrauskiene was actively involved in all five research articles (1–5) and prepared the original drafts. Her contributions included conceptual and methodological input, experimental execution, data analysis, and dissemination of results. Specific roles per article are as follows:

Article 1: Research design, extraction techniques optimisation (naringin, naringenin), use of excipients, data handling, manuscript preparation, and visual data representation.

Article 2: Development of sustainable extraction protocols with cyclodextrins, *in vitro* antioxidant analysis and phytochemical evaluation, data processing, visualisation, and editorial contributions.

Article 3: Preparation of extracts, *in vivo* antioxidant testing in an animal model, comparative analysis (pure compound *vs.* extract), statistical evaluation, result visualisation, and text refinement.

Article 4: Design and evaluation of microencapsulation processes (spray- and freeze-drying), selection of carriers, material characterisation (solubility, moisture, structure), and contribution to data interpretation and writing.

Article 5: Creation of dual delivery systems, formulation of buccal films, release profile studies under simulated conditions, extract *vs*. pure compound comparison, data synthesis, and manuscript editing.

CO-AUTHORS' CONTRIBUTION

All co–authors actively participated in the experimental work, methodology development, data analysis, and manuscript preparation for the papers included in this dissertation.

Prof. dr. Jurga Bernatoniene served as the scientific supervisor for all five publications, provided conceptual guidance, coordinated experimental planning, and critically reviewed all manuscripts.

Prof. dr. Ilona Sadauskiene and **Dr. Arūnas Liekis** contributed to the *in vivo* experiments presented in Article 3. They were responsible for conducting animal studies, collecting tissue samples, and evaluating biochemical markers of oxidative stress (GSH, GR, SOD, MDA).

Dr. Zoja Mikniene participated in the handling of biological samples and contributed to the technical implementation of *in vivo* protocols in Article 3.

Dr. Lauryna Pudžiuvelyte contributed to the development and optimisation of encapsulation methods (spray–drying, freeze–drying) in Article 4.

Dr. Mindaugas Marksa contributed to the methodology and qualitative analysis of naringin and naringenin in Articles 1,2, and 5.

Prof. dr. Liudas Ivanauskas facilitated the resource organisation for experiments related to Articles 1, 2, and 5.

Prof. dr. Pranas Viskelis and **Dr. Jonas Viskelis** supported the preparation of grapefruit extracts and the evaluation of antioxidant potential in Article 2. They also contributed to the selection of raw plant material and the development of sample preparation techniques.

All co-authors reviewed and approved the final versions of the manuscripts and contributed to the scientific integrity and accuracy of the published research.

LIST OF SCIENTIFIC ARTICLES

1 article: Stabrauskiene, Jolita; Marksa, Mindaugas; Ivanauskas, Liudas; Bernatoniene, Jurga. Optimisation of naringin and naringenin extraction from *Citrus* × *paradisi* L. using hydrolysis and excipients as adsorbent // Pharmaceutics. Basel: MDPI, 2022, vol. 14, no. 5, p. 1-15, ISSN 1999-4923. doi:10.3390/pharmaceutics14050890. [Impact factor: 5.4, aggregate impact factor.: 4.5, quartile: Q1 (2022. InCites JCR SCIE)].

2 article: Stabrauskiene, Jolita; Marksa, Mindaugas; Ivanauskas, Liudas; Viškelis, Pranas; Viškelis, Jonas; Bernatoniene, Jurga. *Citrus* × *paradisi* L. Fruit Waste: The Impact of Eco-Friendly Extraction Techniques on the Phytochemical and Antioxidant Potential // Nutrients. Basel: MDPI, 2023, vol. 15, no. 5, p. 1-21, ISSN 2072-6643, 2072-6643. doi:10.3390/nu15051276. [Impact factor: 4.8, aggregate impact factor: 4.623, quartile Q1 (2023. InCites JCR SCIE)].

3 article: Stabrauskiene, Jolita; Sadauskiene, Ilona; Liekis, Arūnas; Mikniene, Zoja; Bernatoniene, Jurga. Naringin vs. *Citrus* × *paradisi* L. Peel Extract: An In Vivo Journey into Oxidative Stress Modulation // Antioxidants, 2025, vol. 14, no. 2, pp. 1-24, ISSN 2076-3921. doi:10.3390/antiox14020157. Science Citation Index Expanded (Web of Science); Scopus; PubMed; PubMed Central. [Impact factor: 6, aggregate impact factor: 4.725, quartile: Q1 (2023. InCites JCR SCIE)].

4 article: **Stabrauskiene, Jolita**; Pudžiuvelytė, Lauryna; Bernatoniene, Jurga. Optimising Encapsulation: Comparative Analysis of Spray-Drying and Freeze-Drying for Sustainable Recovery of Bioactive Compounds from Citrus x paradisi L. Peels // Pharmaceuticals, 2024, t. 17, nr. 5, p. 1- 15, ISSN 1424-8247. doi:10.3390/ph17050596. [Impact factor: 4.3, aggregate impact factor: 4.081, quartile: Q1 (2023. InCites JCR SCIE)].

5 article: Stabrauskiene, Jolita; Marksa, Mindaugas; Bernatoniene, Jurga. (2025). Comparative *In Vitro* Evaluation of Buccal Films, Microcapsules, and Liposomal Systems for Naringin and *Citrus* × *paradisi* L. Peel Extract: Effects of Encapsulation Strategy and Compound Origin on Release Profiles. Pharmaceutics, 2025, t. 17, nr. 10, p. 1- 24, ISSN1999-4923. doi:10.3390/pharmaceutics17101311. [Impact factor:5.5, aggregate impact factor: 4.264, quartile: Q1(2024. InCites JCR SCIE)].

CONFERENCE PRESENTATIONS

The findings of the dissertation were presented at the following scientific conferences:

1. **Stabrauskiene, Jolita**; Bernatoniene, Jurga; Marksa, Mindaugas.
   Encapsulation of Hydrophobic Naringin and *Citrus* × *paradisi* L. Peel Extract into Liposomes via Ethanol Injection and Spray Drying.
   Contemporary Pharmacy: Issues, Challenges and Expectations 2025, April 10, 2025, Abstract Book, No. 2, p. 94.
2. **Stabrauskiene, Jolita**.
   Naringin vs. *Citrus* × *paradisi* L. Extract: An In Vivo Journey into Oxidative Stress Modulation.
   Health for All 2025 "Healthy beginnings, hopeful futures", Abstract Book, April 4, 2025, p. 52–53.
3. **Stabrauskiene, Jolita**.
   Advancements in Microencapsulation Techniques for Bioactive Compounds in *Citrus* × *paradisi* L. Peels: A Comparative Analysis of Freeze-Drying and Spray-Drying Methods.
   International Health Sciences Conference for All (IHSC for All) "Precision Medicine", March 25–26, 2024, Kaunas, p. 462–464.
4. **Stabrauskiene, Jolita**; Bernatoniene, Jurga; Pudžiuvelyte, Lauryna.
   Optimisation of Spray-Drying Parameters for Enhanced Microencapsulation of Phenolic Compounds in *Citrus* × *paradisi* L. Peels: A Study on Yield, Moisture, and Solubility.
   Contemporary Pharmacy: Issues, Challenges and Expectations 2024, March 22, Kaunas, Abstract Book, No. 1, p. 109.
5. **Stabrauskiene, Jolita**; Bernatoniene, Jurga; Pudžiuvelyte, Lauryna.
   Optimisation of Spray-Drying Conditions for Microencapsulation of *Citrus* × *paradisi* L. Phenolics Using Maltodextrin and Skim Milk as Wall Materials.
   WayScience: 5th International Scientific and Practical Internet Conference "Integration of Education, Science and Business in Modern Environment: Summer Debates", August 3–4, 2023, Dnipro, Ukraine, p. 48–49.
6. **Stabrauskiene, Jolita**.
   Eco-Friendly Extraction Method Using α-, β-, and γ-Cyclodextrins for Naringin, Naringenin, and Narirutin Solubilization from *Citrus* × *paradisi* L. Fruit Parts.
   Dubai International Pharmaceutical & Technology Conference & Exhibition (DUPHAT), January 10–12, 2023, Dubai, UAE, p. 36.

7. **Stabrauskiene, Jolita**; Bernatoniene, Jurga; Marksa, Mindaugas.
   Extraction Method Using Excipients to Enhance the Yield of Naringin and Naringenin from Grapefruit (*Citrus* × *paradisi* L.).
   PLANTA+. The Third Scientific and Practical Conference with International Participation, February 18, 2022, Kyiv, Ukraine, Volume 1, p. 107–109.
8. **Stabrauskiene, Jolita**; Bernatoniene, Jurga; Marksa, Mindaugas.
   Identification of Flavanones in *Citrus* × *paradisi* L. Fresh Fruit Parts Using Different Extraction Methods.
   Medicina: Abstracts of the International Scientific Conference on Medicine, 80th International Scientific Conference of the University of Latvia, March 25–26, 2022, Riga, p. 205.
9. **Stabrauskiene, Jolita**a; Bernatoniene, Jurga; Marksa, Mindaugas.
   Novel Extraction Method Using α-Cyclodextrins to Increase Flavanone Yield from *Citrus* × *paradisi* L.
   The Joint International Scientific Practical Conference "Contemporary Pharmacy: Issues, Challenges and Expectations 2022", May 6, 2022, Kaunas, p. 31.
10. **Stabrauskiene, Jolita**; Bernatoniene, Jurga; Marksa, Mindaugas.
    Quantification of Flavanones from the Fresh Fruit Parts of *Citrus* × *paradisi* L. Using Different Extraction and Hydrolysis Methods.
    65th International Conference for Students of Physics and Natural Sciences "Open Readings 2022", March 15–18, 2022, Vilnius, p. 440.
11. **Stabrauskiene, Jolita**; Bernatoniene, Jurga; Marksa, Mindaugas.
    The Quantification of Naringin, Naringenin, and Narirutin in Different Parts of *Citrus* × *paradisi* L. Fruits.
    12th International Pharmacy Conference "Contemporary Pharmacy: Issues, Challenges and Expectations 2022 Autumn", October 21, 2022, Kaunas, p. 50.
12. **Stabrauskiene, Jolita**.
    The Impact of Excipients and Extraction Methods on the Yield of Naringin and Naringenin.
    Planta Medica: 70th International Congress and Annual Meeting of the Society for Medicinal Plant and Natural Product Research (GA), August 28–31, 2022, Thessaloniki, Greece, Vol. 88(15), p. 1549–1550.
13. **Stabrauskiene, Jolita**; Bernatoniene, Jurga.
    Investigation of Total Phenolic Content and Antioxidant Activities of the *Citrus* × *paradisi* L. Fruits Using Different Extraction Methods.
    The Joint International Pharmacy Symposium "Contemporary Pharmacy: Issues, Challenges and Expectations 2021" and "11th Conference: Pharmacy Science and Practice", October 22, 2021, Kaunas, p. 47.

1. SUMMARY OF MATERIALS AND METHODS

1.1. Plant material

Fresh fruits of *Citrus* × *aurantium* f. aurantium (Rutaceae) were collected in 2021–2022 from the local market in Mastaiciai, Kaunas district, Lithuania (origin: Italy, region unspecified). The fruits were separated into flavedo, albedo, and segmental membranes, then chopped in a food processor (Bosch, Germany) and stored frozen at –18 ± 0.9 °C until extraction.

A detailed description of the plant raw materials and processing conditions is provided in Articles 1 and 2.

Between 2023 and 2025, plant material was obtained as post-juicing residues. Grapefruit peels and segments were collected from local cafés in Kaunas, Lithuania, as industrial by-products. The material was dried in a hot-air oven (Memmert, Germany) at 60 ± 5 °C until constant weight, ground in a household coffee grinder (Philips, Netherlands), and stored in sealed containers under dry, dark conditions. The residual moisture content of the powdered samples was measured using a moisture analyser (KERN MLB, KERN & Sohn GmbH, Germany) and was 4.58 ± 0.15%.

A detailed description of the plant raw materials and processing conditions is provided in Articles 1 and 2.

1.2. Extraction

1.2.1. Conventional extraction methods

Several extraction techniques were employed to obtain flavanone-rich extracts from fresh grapefruits. Heat reflux extraction (HRE) was carried out in ethanol–water mixtures (50% and 70% *v/v*) at a 1:10 ratio and 100 ± 2 °C for 1 hour. Ultrasound-assisted extraction (UAE) was performed using either an ultrasonic bath (38 kHz) or an ultrasonic homogeniser (19–25 kHz, 250 W) under controlled temperature and extraction time. These approaches enabled evaluation of the effects of solvent concentration, temperature, and ultrasonic intensity on the recovery of NR and NAR from different grapefruit parts (flavedo, albedo, and segmental membranes).

Following extraction, hydrolysis was conducted under acidic, alkaline, and thermal conditions to cleave glycosidic bonds and obtain the aglycone form of NAR. Acidic hydrolysis (2 M HCl, pH 2.5) promoted the conversion of NR into its aglycone, followed by neutralisation with 2 M NaOH to stabilise the extract. Thermal hydrolysis (1 h at 100 ± 2 °C with reflux) further enhanced the release of bound flavanones due to heat-induced degradation. In contrast,

alkaline hydrolysis (2 M NaOH, pH 10) was used to cleave ester and glycoside bonds, although careful neutralisation with 25% acetic acid was required to avoid degradation of the compounds.

Articles 1 and 2 provide detailed information on the extraction conditions, including plant amounts, extraction times, temperatures, and solvent types and concentrations.

1.2.2. Extraction methods with excipients

Flavanones from grapefruit peels were extracted using various excipients. The samples were modified and prepared using magnesium aluminiummetasilicate and *α-, β-*, or *γ*-CDs. The conditions of use for these excipients, solvents, and extraction parameters were selected based on the flavanone yield obtained with conventional extraction methods. The following extraction methods were used with excipients: ultrasonication (20 or 30 minutes), ultrasonication combined with thermal hydrolysis (20 or 30 minutes), and thermal hydrolysis alone.

A detailed description of the extraction conditions, including the amount of raw material, extraction time, temperature, and the solvents and their concentrations, is provided in Articles 1 and 2.

1.2.3. Extraction from dried by-products

The dried biomass was ground into a powder and extracted with ethanol–water solutions (50%, 70%, and 90% *v/v*) at a 1:10 ratio. Extraction was performed in two steps: Ultrasound-assisted extraction in an ultrasonic bath (20–30 min at 50 ± 2 °C) followed by thermal hydrolysis extraction (60 min at 100 ± 2 °C).

A detailed description of the extraction conditions, including solvent concentrations, extraction times, and hydrolysis procedures, is presented in Articles 3-5.

1.3. Phytochemical characterisation methods

1.3.1. HPLC-PDA

The qualitative and quantitative analysis of flavonones in grapefruit peel extracts was performed using a validated HPLC-PDA method. Phenolic analysis was performed using an ACE 5 C18 250 × 4.6 mm column with a linear gradient elution profile, *following the parameters and conditions described in Articles 1–3,5.*

1.3.2. Spectrophotometric assays

The total phenolic content (TPC) of extracts was determined by the Folin–Ciocalteu method (λ = 765 nm), and results were expressed as mg gallic acid equivalents per gram of dry weight (mg GAE/g dw). The total flavonoid content (TFC) was measured using the aluminium chloride colourimetric assay (λ = 475 nm), with results expressed as milligrams of rutin equivalents per gram of dry weight (mg RE/g dw). Calibration curves showed high linearity ($R^2 > 0.99$).

Detailed protocols are described in Articles 2 and 4.

1.4. Antioxidant activity and biological evaluation *in vitro* and *in vivo*

1.4.1. Antioxidant activity *in vitro*

The antioxidant properties of grapefruit peel extracts were evaluated by *in vitro* spectrophotometric assays. The free radical scavenging activity was assessed using the ABTS (λ = 734 nm), DPPH (λ = 517 nm) and FRAP (λ = 593 nm) assays. The results were expressed as Trolox equivalents (TE) and reported as μg or μmol TE/g fresh weight (fw), depending on the assay conditions. The results were *described in Article 2.*

1.4.2. Antioxidant activity *in vivo*

The *in vivo* study assessed the antioxidant activity of grapefruit peel extracts and pure NR in mice by examining oxidative stress–related biomarkers in blood, liver, and brain. The parameters measured included reduced glutathione (GSH), malondialdehyde (MDA) as a marker of lipid peroxidation, and the activities of the enzymatic antioxidants catalase (CAT) and glutathione reductase (GR). GSH levels were quantified using Ellman's reagent (DTNB), with absorbance measured at λ = 412 nm, and results expressed as μmol/L in blood or μmol/g in tissue. Lipid peroxidation was determined by MDA formation using the thiobarbituric acid reactive substances (TBARS) assay, with absorbance recorded at (λ = 535 and 520 nm). Enzymatic antioxidant defence was assessed by CAT activity, measured spectrophotometrically at λ = 410 nm via hydrogen peroxide decomposition, and GR activity, measured spectrophotometrically at λ = 340 nm via NADPH oxidation during GSSG reduction. Results were normalised to protein content or tissue weight and expressed as enzymatic units or μmol equivalents. The Lithuanian State Food and Veterinary Service approved the animal study protocol, License no. G2-275

Detailed methodological parameters are provided in Article 3.

1.5. Formulation and delivery systems

1.5.1. Emulsion preparation for spray- and freeze-drying

Emulsions were prepared as an intermediate step for the microencapsulation of grapefruit extracts. Different wall-forming agents, including maltodextrin (MD), skim milk (SKM), β-cyclodextrin (β-CD), chitosan, and carboxymethylcellulose (CMC), were dissolved in purified water at a concentration of 20% (*w/v*). The solutions were homogenised using a magnetic stirrer at 25 °C for 30 min to ensure complete dissolution. Subsequently, ethanolic extracts of grapefruit peels were incorporated into the wall material solutions and stirred for an additional 30 min, yielding uniform emulsions. These emulsions served as feed solutions for both spray-drying and freeze-drying processes.

For more detailed information on the emulsion preparation process, see Articles 4 and 5.

1.5.2. Microencapsulation (spray- and freeze-drying)

The same emulsion formulation was applied for both spray- and freeze-drying processes. Before lyophilisation, the samples were frozen at –80 °C. Freeze-drying was carried out for 24 h, while spray-drying was performed at different inlet temperature settings (90–160 °C) with corresponding outlet temperatures (25–80 °C). The feed rate and air pressure were maintained at constant levels throughout the process.

Detailed methodological parameters are described in Articles 4 and 5.

1.5.3. Characterisations of the microcapsules

Spray-dried and lyophilised powders were evaluated for their physical, chemical and functional properties. The parameters analysed included moisture content, solubility, wettability, bulk and crushed volumes, process yield and encapsulation efficiency. In addition, morphological properties were evaluated using scanning electron microscopy, and total and surface phenolic content was quantified spectrophotometrically.

A more detailed description of the microcapsule characterisation and the applied methodologies is provided in Article 4.

1.6. Formulation of liposomes and characterisation

Liposomes were prepared using the ethanol injection method followed by probe sonication. Lipoid S100 and cholesterol were first dissolved in ethanol together with either grapefruit peel extract or pure NR, and the resulting

solution was injected into the aqueous phase under continuous stirring. Subsequent probe sonication enabled the formation of nanoscale vesicles. To optimise encapsulation efficiency and stability, two lipid-to-core ratios (1:1 and 2:1) were investigated. Liposomes were characterised by dynamic light scattering (DLS) to determine particle size, polydispersity index (PDI), and zeta potential, thereby ensuring vesicle stability and homogeneity.

A detailed description of the methodology is provided in Article 5.

1.7. Double encapsulation formulation and characterisation

Double encapsulation was achieved by incorporating grapefruit peel extract and pure NR into liposomal vesicles using the ethanol injection method, followed by size reduction via probe sonication. The resulting nanoscale liposomes were then spray-dried using MD, β-CD, and CMC as wall-forming agents. Spray-dried powders of microencapsulated and double-encapsulated systems prepared with grapefruit peel extract and pure NR were analysed to determine their technological and functional parameters. Moisture content was assessed using a moisture analyser, and equilibrium solubility tests, followed by HPLC quantification, were used to evaluate solubility. The process yield was calculated as the ratio of collected dry powder to total solids in the feed solution. The encapsulation efficiency (EE) of naringin and grapefruit peel extract was determined by centrifugation followed by HPLC anal ysis of the supernatant.

The morphological properties of the powders were examined by scanning electron microscopy (SEM) to assess particle shape, surface topography, and potential structural differences between the microencapsulated and double-encapsulated systems.

A full description of the preparation procedure and the formulation composition is available in Article 5.

1.8. Preparation for buccal films and characterisation

Buccal films were prepared by solvent casting. Extract or NR-based formulations were obtained by dissolving hydroxypropyl methylcellulose (12% *w/v*) in ethanolic solutions, followed by the addition of sodium alginate or polyvinyl alcohol (2% *w/v*) with glycerol (4% *w/v*). The mixtures were homogenised, cast onto glass plates at a thickness of 2 mm, and dried at 40 °C for 2 hours. The films were cut into 3 × 2.5 cm strips, sealed in foil sachets, and stored at 22 ± 2 °C.

Conditions and equipment used for buccal film preparation are described in Article 5.

1.9. *In vitro* release studies

The release of NR from different delivery systems (microcapsules, liposomal powders, and buccal film) was evaluated under simulated physiological conditions. Microcapsules and liposomal powders were tested using a Sotax AT7 Smart Dissolution System (SOTAX AG, Switzerland). Samples were incubated in simulated gastric fluid (SGF, pH 1.2) for 0–90 min. and in simulated intestinal fluid (SIF, pH 6.8) for 90–180 min. Aliquots were collected every 30 min, filtered (0.45 μm), and analysed by HPLC.

Buccal film samples (3 × 2.5 cm) were immersed in 25 mL of artificial saliva (pH 6.8, 37 ± 1 °C) under stirring. Aliquots (1 mL) were collected at 5, 10, 15, and 30 min, filtered, and analysed by HPLC. Artificial saliva was prepared according to the reported composition of inorganic salts and urea and adjusted to pH 6.8.

For a more detailed description of the methods and reagents used, see Article 5.

1.10. Data analysis and statistics

Experimental data from *Articles 1–5* were processed and visualised using IBM SPSS Statistics version 20.0 (IBM Corp., Armonk, NY, USA), Microsoft Excel 2021, and GraphPad Prism 8. All experiments were performed at least in triplicate, and results are presented as mean ± standard deviation (SD), where applicable.

Depending on data distribution, parametric (ANOVA) or non-parametric tests were applied. The Friedman test, followed by the Wilcoxon signed-rank test, was used for repeated-measures data across three groups, while the Mann–Whitney U test was used for comparisons between two independent groups. Correlation and regression analyses were performed using Spearman's rank correlation coefficient.

For the *in vivo* experiments, differences among the seven experimental groups were analysed using one-way analysis of variance (ANOVA) followed by Tukey's post hoc test. Oxidative stress biomarkers (GSH, MDA, CAT, and GR) were measured in blood, liver, and brain.

Statistical significance was set at $p < 0.05$.

2. SUMMARY OF RESULTS

2.1. Optimisation of conventional extraction techniques to enhance the recovery of flavanones

NR was detected in all fractions of fresh grapefruit peel, with the albedo showing the highest yield under UAE conditions (17.45 ± 0.87 mg/g, 50% ethanol, 30 min, 50 °C). In comparison, the segmental membrane produced the lowest values (4.31 ± 0.96 mg/g). NAR was only found in the albedo, reaching a maximum of 4.63 ± 0.23 μg/g with 70% ethanol. Increasing ethanol concentration from 50% to 70% improved extraction in several cases, particularly in flavedo and albedo fractions. Prolonged sonication further increased yields, as indicated by higher NR and NAR concentrations after 30 minutes than after shorter treatment times. Heat reflux extraction produced significantly higher NAR levels, especially in albedo and segmental membranes (up to 35.80 ± 1.77 μg/g) ($p < 0.05$). The homogeniser–assisted UAE method also increased aglycone release, yielding the highest NAR concentration of 7.40 ± 0.37 μg/g in the segmental part using 70% ethanol. Statistically significant differences were especially evident in the albedo fraction, which contained the highest concentrations of the analysed compounds, related to solvent concentration, ultrasonication time, and temperature ($p < 0.05$).

The application of acidic, alkaline, and thermal hydrolysis, in combination with UAE, significantly enhanced flavanone yields compared with non–hydrolysed extracts ($p < 0.05$). Thermal hydrolysis was the most effective, particularly for albedo samples, where NR content increased from 17.39 ± 0.87 mg/g to 25.05 ± 1.25 mg/g. Similarly, the segmental fraction nearly doubled its NR yield under these conditions (from 5.26 ± 0.26 mg/g to 11.07 ± 0.55 mg/g). For aglycones, NAR release was strongly promoted by thermal hydrolysis, reaching 4.21 ± 0.21 μg/g in segmental membranes, whereas no NAR was detected in the absence of hydrolysis. Acidic hydrolysis resulted in a moderate increase in aglycone release, whereas alkaline treatment showed comparatively weaker effects. Overall, thermal hydrolysis proved to be the most efficient strategy for enhancing both glycoside and aglycone recovery under UAE conditions ($p < 0.05$).

To assess differences between fresh and dried raw materials, dried grapefruit peel extracts were also analysed to determine the effect of processing on flavonoid recovery. The contents of NR and NAR were quantified in dried peel extracts obtained using various extraction methods and ethanol concentrations. The extraction methods employed were ultrasonic

extraction and a combination of ultrasonic and reflux extraction, using ethanol concentrations of 50%, 70%, and 90%.

The analysis demonstrated that the highest NR content was found in the UH70 sample, yielding 51.94 ± 2.6 mg/g ($p < 0.05$), followed by UH50 with 49.13 ± 2.46 mg/g ($p < 0.05$). Lower yields were observed in the ultrasound-only samples: U50 (42.04 ± 2.1 mg/g) and U70 (40.36 ± 2.02 mg/g). However, in a following series of extractions carried out under the same methodological parameters, the yields were considerably lower: NR was quantified at only 14.58–15.62 mg/g, and NAR at 1.41–1.82 μg/g. Since the extraction procedure, solvent concentration, and processing conditions were identical, the difference most likely reflects natural variability of the raw material. Factors such as fruit ripeness, harvest season, storage conditions or environmental influences may explain the significant decrease in flavonoid content. Despite these differences, NR was the dominant flavanone in all cases, confirming its majority in grapefruit peel extracts.

The conditions and impact of all extraction methods are described in Articles 1, 2, 3 and 5.

2.2. Impact of excipients on flavanone extraction

Incorporating 1% magnesium aluminometasilicate during extraction selectively increased flavanone recovery. Across flavedo, albedo and segmental fractions, the excipient consistently increased NAR (aglycone) levels (e.g., up to 6.8 μg/g) in segmental membranes under UAE conditions. However, for NR (glycoside), yields decreased by an average of 15% relative to matched controls across all samples.

Cyclodextrins (CDs) have been shown to significantly enhance flavanone recovery by forming inclusion complexes that increase their solubility and stability ($p < 0.05$). To evaluate this effect, α-, β-, and γ-cyclodextrins were added at 1% concentration during the extraction of grapefruit peels. Their functioning was compared with control samples obtained under identical conditions but without excipients.

In the case of NR, the highest yield was obtained with the segmental membrane when β-CD was used with 70% ethanol, yielding 58.06 ± 2.9 mg/g (SB2), compared with 7.8 ± 0.39 mg/g in the control (ST2). In the albedo fraction, the NR content increased from 11.58 ± 0.58 mg/g (control, AT1) to 18.87 ± 0.94 mg/g with α-CD (AA1).

For NAR, the highest yield was observed in the segmental membrane using β-CD with 50% ethanol, reaching 91.19 ± 4.55 μg/g (SA1), compared with 65.84 ± 3.29 μg/g in the control (ST1). In the albedo fraction, β-CD

also enhanced NAR concentration from 23.58 ± 1.17 μg/g (AT1) to 43.44 ± 2.17 μg/g (AA1).

In the *in vitro* evaluation, the total phenolic content (TPC) and total flavonoid content (TFC) were determined in various parts of grapefruit peel using ultrasound-assisted extraction with and without the addition of CDs. Results showed that most samples extracted with CDs contained significantly higher levels of total phenolic compounds than control samples ($p < 0.05$). In the albedo part, TPC increased from 3.58 ± 0.17 mg GAE/g DW to 18.42 ± 0.92 mg GAE/g DW when β-CD was applied, and in the segmental membrane, it increased from 2.56 ± 0.12 mg GAE/g DW to 17.8 ± 0.89 mg GAE/g DW. In the flavedo part, the flavonoid concentration increased from 2.52 ± 0.13 mg RE/g DW in control samples to 4.66 ± 1.26 mg RE/g DW in extracts prepared with β-CD. In juice samples, the TFC increased from 1.78 ± 0.09 mg RE/g DW to 2.52 ± 0.13 mg RE/g DW under the same conditions.

The impact of excipients on extraction processes and phenolic and flavonoid content is discussed in detail in Articles 1 and 2.

2.3. Antioxidant activity of grapefruit peel extract (*in vitro*)

The antioxidant activity of grapefruit peel extracts and fresh juice was evaluated using three in vitro assays: the DPPH radical scavenging assay, the ABTS radical cation decolourisation assay, and the FRAP (ferric reducing antioxidant power) assay.

The DPPH assay showed that fresh juice exhibited the highest radical scavenging activity (1429.25 ± 71.01 μmol TE/g), followed by flavedo (517.14 ± 25.86 μmol TE/g), segmental membranes (500.27 ± 22.54 μmol TE/g), and albedo (368.50 ± 15.42 μmol TE/g). The addition of β-CD slightly increased the antioxidant activity of flavedo extracts (from 517.14 ± 25.86 to 630.76 ± 31.54 μmol TE/g), whereas in segmental membranes and fresh juice, the activity decreased.

The ABTS assay showed that antioxidant capacity ranged from 4.36 ± 0.218 μg TE/g in segmental membranes to 18.61 ± 0.93 μg TE/g in fresh juice. In flavedo extracts, antioxidant activity increased from 8.97 ± 0.448 to 18.61 ± 0.93 μg TE/g after the addition of β-CD, while fresh juice samples increased from 18.61 ± 0.93 to 20.56 ± 1.028 μg TE/g. In all cases, the application of β-CD significantly enhanced antioxidant capacity compared with control samples ($p < 0.05$).

The FRAP assay showed the highest reducing activity in fresh juice (12336 ± 616.8 μmol TE/g), followed by flavedo (8969.91 ± 448.50 μmol TE/g), while the lowest activity was observed in segmental membranes

(4359.57 ± 24.89 μmol TE/g). The addition of β-CD resulted in a statistically significant increase ($p < 0.05$) in reducing power in all tested samples, with some values nearly doubling, as observed in the flavedo extract (from 10.44 ± 0.522 to 20.44 ± 1.02 μg TE/g). *The detailed findings and descriptions of all applied methods are presented in Article 2.*

2.4. Antioxidant activity of grapefruit peel extract (*in vivo*)

This part of the study aimed to compare the effects of grapefruit peel extract and pure NR on oxidative stress in a mouse model. Oxidative stress was induced using $AlCl_3$, and animals were divided into seven groups: control (K), ethanol (EtOH), aluminium (Al), extract (GE), extract + Al (GE + Al), naringin (NR), and naringin + Al (NR + Al). Antioxidant activity was assessed by measuring key biomarkers in blood, liver, and brain, including reduced glutathione (GSH), malondialdehyde (MDA), and the enzymatic antioxidants catalase (CAT) and glutathione reductase (GR).

The concentration of GSH in mouse blood ranged from 602.83 ± 28.27 to 1735.46 ± 111.02 μmol/g protein. The lowest value was observed in the NR group (602.83 ± 28.27 μmol/g protein), while the highest was detected in the NR + $AlCl_3$ group (1735.46 ± 111.02 μmol/g protein), followed by the extract (GE) + $AlCl_3$ group with 1377.26 ± 175.06 μmol/g protein. Compared to the control (673.28 ± 14.21 μmol/g protein), both E and NR alone significantly modulated GSH levels ($p \leq 0.05$). Importantly, co-administration with $AlCl_3$ resulted in a statistically significant increase in GSH levels compared with the $AlCl_3$ group (1089.33 ± 95.68 μmol/g protein), confirming the protective effect of both treatments.

The MDA levels in mouse blood varied between 110.78 ± 24.19 and 351.59 ± 92.21 μmol/g protein. The highest concentration was recorded in the ethanol group (351.59 ± 92.21 μmol/g protein), while the lowest was found in the GE + $AlCl_3$ group (110.78 ± 24.19 μmol/g protein). Compared to the control (193.05 ± 17.92 μmol/g protein), ethanol significantly increased MDA levels ($p \leq 0.05$), indicating enhanced lipid peroxidation. In contrast, treatment with the extract or synthetic NR reduced MDA levels: NR + $AlCl_3$ (163.59 ± 20.93 μmol/g protein) and GE + $AlCl_3$ (110.78 ± 24.19 μmol/g protein) showed significant reductions compared to $AlCl_3$ alone (241.32 ± 11.10 μmol/g protein) ($p < 0.05$). These data indicate that E was more effective at preventing lipid peroxidation, whereas NR had a greater effect on GSH synthesis.

The GSH content in mouse brain tissues ranged from 0.0023 ± 0.0006 to 0.0193 ± 0.0049 μmol/g protein. The lowest concentration was found in the $AlCl_3$ group (0.0023 ± 0.0006 μmol/g protein), confirming the

intense oxidative stress induced by $AlCl_3$, and the highest in the NR + $AlCl_3$ group (0.0193 ± 0.0049 µmol/g protein). Compared to the control (0.005 ± 0.0015 µmol/g protein), ethanol slightly reduced GSH levels (0.004 ± 0.0009 µmol/g protein), whereas treatment with NR significantly enhanced GSH (0.0095 ± 0.0021 µmol/g protein; $p \leq 0.05$). Co-treatment with NR + $AlCl_3$ restored GSH levels to near-control values, demonstrating NR's capacity to stimulate GSH synthesis and neutralise oxidative stress.

MDA levels in brain tissues varied from 56.21 ± 9.94 to 104.07 ± 9.24 µmol/g protein. The ethanol group displayed the highest level of lipid peroxidation (104.07 ± 9.24 µmol/g protein), while the lowest was recorded in the E + $AlCl_3$ group (56.21 ± 9.94 µmol/g protein). Compared to the control (77.01 ± 10.87 µmol/g protein), $AlCl_3$ alone increased MDA levels (87.66 ± 4.57 µmol/g protein). In contrast, both E and NR treatments significantly reduced lipid peroxidation, with NR + $AlCl_3$ (60.61 ± 1.65 µmol/g protein) showing the better protection ($p \leq 0.05$).

CAT activity in the brain ranged from 22.69 ± 4.05 to 73.11 ± 12.75 U/mg protein. The lowest activity was detected in the $AlCl_3$ group (22.69 ± 3.95 U/mg protein), while the highest was in the control group (73.11 ± 12.75 U/mg protein). Ethanol (24.24 ± 3.95 U/mg protein) strongly suppressed CAT, whereas NR treatment (72.15 ± 5.18 U/mg protein) maintained activity at levels close to those of the control. In the NR + $AlCl_3$ group, CAT activity (63.44 ± 8.44 U/mg protein) was significantly higher than in the $AlCl_3$ group ($p \leq 0.05$), highlighting NR's ability to restore enzymatic antioxidant defences. By contrast, E + $AlCl_3$ (29.01 ± 2.32 U/mg protein) provided limited protection.

In the liver, GSH levels ranged from 0.1 ± 0.03 to 0.31 ± 0.10 µmol/g protein. The control group exhibited baseline activity (0.1 ± 0.03 µmol/g protein), while the highest concentration was observed in the NR + $AlCl_3$ group (0.31 ± 0.10 µmol/g protein), followed by the $AlCl_3$ group (0.30 ± 0.07 µmol/g protein). Ethanol increased GSH slightly (0.18 ± 0.02 µmol/g protein), while treatment with E (0.23 ± 0.04 µmol/g protein) and NR (0.14 ± 0.04 µmol/g protein) demonstrated enhanced antioxidant capacity. Importantly, co-treatment with NR + $AlCl_3$ significantly restored GSH levels compared with $AlCl_3$ alone, confirming NR's strong protective role ($p \leq 0.05$).

MDA levels in the liver varied between 47.52 ± 8.97 and 99.69 ± 10.97 µmol/g protein. The highest lipid peroxidation was observed in the $AlCl_3$ group (99.69 ± 10.97 µmol/g protein), while the lowest was in the E + $AlCl_3$ group (47.52 ± 8.97 µmol/g protein). Compared with the control (93.03 ± 7.89 µmol/g protein), ethanol had no significant effect (93.25 ± 10.03 µmol/g protein), whereas both the GE and NR treatments reduced MDA. Notably, NR

+ $AlCl_3$ (51.13 ± 9.71 µmol/g protein) and GE + $AlCl_3$ (47.52 ± 8.97 µmol/g protein) demonstrated statistically significant decreases compared with the $AlCl_3$ group, confirming strong protective effects against lipid peroxidation ($p \leq 0.05$).

CAT activity in the liver ranged widely from 98.04 ± 36.97 to 585.57 ± 38.18 U/mg protein. The highest activity was observed in the E group (585.57 ± 38.18 U/mg protein), suggesting intense stimulation of enzymatic defences, while the lowest was detected in the E + $AlCl_3$ group (98.04 ± 36.97 U/mg protein). Compared to the control (379.21 ± 34.33 U/mg protein), ethanol (488.83 ± 53.14 U/mg protein) and $AlCl_3$ (489.75 ± 53.24 U/mg protein) increased CAT activity, possibly as an adaptive response to increased production of reactive oxygen species (ROS). Interestingly, NR + $AlCl_3$ (132.33 ± 11.67 U/mg protein) partially restored CAT activity relative to the E + $AlCl_3$ group, although levels remained below those of the control.

Detailed findings, methodology, and comparative analyses with other natural antioxidants are presented in Article 3.

2.5. Formulation strategies for naringin and grapefruit peel extract emulsions

2.5.1. Formulation of emulsions

Emulsions for microencapsulation were formulated using ethanolic grapefruit peel extracts as the active ingredient. The wall materials included maltodextrin (MD), skim milk (SK), β-cyclodextrin (β-CD), chitosan, and carboxymethylcellulose (CMC), each at 20% (*w/v*). Each excipient had a different function: MD improved drying efficiency and reduced residual moisture; SK enhanced capsule stability through protein interactions; β-CD facilitated solubility and wettability; CMC contributed to water retention due to its hydrophilic nature; and chitosan exhibited additional film-forming properties.

Spray-dried samples exhibited yields ranging from 48.0 ± 2.4% (M7, 170/116 °C) to 52.95 ± 2.64% (M3, 160/80 °C). The highest yield was achieved at an inlet temperature of 160 °C and an outlet temperature of 80 °C. However, a higher inlet temperature (170 °C) reduced the yield, most likely due to phenolic degradation or the formation of a surface crust. Adjustments to drying parameters further enhanced efficiency: in MBC2 and MBC3, reducing the inlet temperature from 160 °C to 145 °C and simultaneously increasing the flow rate from 30 to 60 mL/min substantially increased yields, from 14.15% to 27.2% in MBC2 and from 8.55% to 38.5% in MBC3.

Freeze-drying yielded the highest yields, ranging from 69.7% (L1) to 79.2% (L3), compared with spray-drying. The highest yield was achieved with the L3 formulation containing MD 17%, β-CD 2.5%, and CMC 0.5%, suggesting that this wall-material composition provided optimal drying performance.

Detailed findings and methods are discussed in Article 4.

2.5.2. Physicochemical properties of microcapsules

The drying method and the type of wall material had an apparent effect on the physicochemical characteristics of the microcapsules. For the spray-dried variants, the moisture content ranged from 5.31 ± 0.26% to 7.60 ± 0.38%. Notably, lower moisture was typically found at higher drying temperatures and when β-CD was included in the formulation. The samples MBC2 and MBC3 (MD 15–17%, β-CD 2.5–4.1%, CMC 0.5–0.9%) exhibited lower residual moisture (5.52 ± 0.27% and 5.10 ± 0.26%) compared to formulations without β-CD. Wettability was strongly affected by wall materials, ranging from 1170 s (MBC3) to 1461 s (MBC1). The addition of β-CD shortened the wetting time due to its amphiphilic properties, whereas a higher CMC content prolonged it.

Freeze-dried samples contained comparable or lower residual moisture levels: L1, 5.8 ± 0.29%; L2, 4.74 ± 0.19%; and L3, 5.07 ± 0.25%. Wettability tests confirmed that lyophilisation led to more rapid hydration, with L2 exhibiting the fastest wetting, despite its composition being similar to that of L1. This highlights that optimising the MD:β-CD: CMC ratio is more critical than the absolute concentrations of the wall materials.

Powder flowability, assessed by Carr's compressibility index and Hausner ratio, also differed between techniques. Spray-dried powders exhibited compressibility indices ranging from 30.43% to 38.89% and Hausner ratios of 1.438 to 1.636. MBC1 exhibited the lowest flowability (Hausner ratio: 1.636). It was most likely due to its higher content of β-CD and CMC. By contrast, MBC3, which contained more MD, showed better flow. The freeze-dried powders performed slightly better, with compressibility indices ranging from 30.11 to 34.65% and Hausner ratios ranging from 1.438 to 1.520, indicating satisfactory or acceptable flow characteristics.

The solubility values further highlighted the influence of formulation and drying methods. The solubility of spray-dried samples ranged from 30.11 ± 1.50% (MBC1) to 65.68 ± 3.35% (MBC4), and of lyophilised powders from 31.47 ± 1.57% (L1) to 61.58 ± 3.07% (L2). Higher MD content increased solubility, whereas higher β-CD and CMC contents decreased it.

SEM analysis revealed apparent morphological differences. The spray–dried samples (M3, MBC1–MBC4) mainly formed spherical or hemispherical

capsules. M3 had a wrinkled surface, while MBC4, which is rich in SK, had a smoother morphology. A higher MD concentration yielded more uniform, smoother capsules, whereas a higher β-CD content led to a rougher surface. In contrast, the lyophilised powders (L1–L3) had a porous, irregular and brittle, lamellar morphology. These structural differences directly affected wettability, solubility and encapsulation efficiency.

Physical parameters of microcapsules are presented in Article 4.

2.5.3. Phenolic content and encapsulation efficiency

Encapsulation efficiency (EE%) varied across formulations, ranging from 76.72% (MBC1) to 91.41% (MBC3). Increasing MD concentrations improved encapsulation, as demonstrated by the progression 76.72% < 87.27% < 91.41% in spray–dried (M) samples. However, higher β-CD or CMC concentrations slightly reduced EE, likely due to weaker binding capacity. Freeze-dried samples achieved EE values of 76.77%–88.57%, which are slightly lower than those of the spray–dried samples; however, they showed superior preservation of phenolic compounds ($p < 0.05$).

Phenolic content and encapsulation efficiency are present in Article 4.

2.6. Formulation of liposomes

2.6.1. Liposome composition and physicochemical characterisation

Liposomal formulations were prepared using grapefruit peel extract (GE) and pure naringin (NR) at two lipid–to–core ratios (1:1 and 2:1).

The average liposome particle size ranged from 93.93 ± 4.70 nm for EL2 to 101.5 ± 5.08 nm for EL1, all in the nanoscale range. It confirmed that all formulations were suitable for biomedical and nutraceutical applications. EL2 vehicles were significantly smaller than those of EL1 ($p < 0.05$), indicating that higher lipid content favoured the formation of more compact bilayers. The sizes of NL1 (98.57 ± 4.93 nm) and NL2 (96.96 ± 4.85 nm) were intermediate, and the difference between them was not statistically significant. These observations suggest that lipid concentration had a greater impact on vesicle size than the type of encapsulated compound.

The polydispersity index (PDI) ranged between 0.144 ± 0.007 for EL2 and 0.362 ± 0.018 for EL1. The low PDI value of EL2 indicated a narrow size distribution and a more homogeneous vesicle population. By contrast, EL1 (0.362 ± 0.018) and NL1 (0.225 ± 0.011) exhibited higher PDI values, indicating greater heterogeneity among the vesicles.

Zeta potential (ζ) values ranged from –10.4 ± 0.52 mV (NL1) to –25.8 ± 1.29 mV (NL2). The most negative charge was recorded for NL2, indicating

strong electrostatic stability and reduced risk of aggregation. EL formulations displayed intermediate values (–17.5 ± 0.88 to –20.3 ± 1.02 mV).

Based on these characteristics, EL2 and NL2 were selected as optimal liposomal systems for subsequent spray-drying and double-encapsulation experiments.

The liposome composition and physicochemical characterisation are presented in Article 5.

2.7. Double encapsulation

2.7.1. Liposomes implanted into spray-dried microcapsules

Spray-dried powders from both single- and double-encapsulation exhibited yields ranging from 36.7 ± 1.83% (NR) to 43.0 ± 2.15% (GE). Extract-based formulations (ES, ELS) yielded higher results (41 – 43%) compared to pure NR powders (NS, NLS; 36 –38%). Liposomal encapsulation slightly reduced yield compared to non-liposomal systems, possibly due to lipids interfering with droplet atomization and powder collection.

The moisture content was below 6%, the acceptable stability limit for spray-dried powders, and ranged from 3.81 ± 0.19% (ELS) to 5.58 ± 0.28% (NLS). NLS exhibited the highest residual moisture (5.58 ± 0.28%), significantly higher than the other samples, likely due to interactions between lipids and naringin crystals that hindered complete water removal ($p < 0.05$).

Encapsulation efficiency (EE) differed markedly across the formulations. The best result was obtained for ELS (99.36 ± 4.96%), whereas NS had the lowest value (81.08 ± 4.05%). The higher EE observed in the liposomal powders can be attributed to the phospholipid bilayer structure, which accommodates compounds in both its hydrophilic and hydrophobic regions, thereby improving retention.

Solubility was observed among the formulations and ranged from 17.36 ±1.01 μg/mL (ELS – liposomal form) to 306.42 ± 10.34 μg/mL (NS – non–liposomal form). NS displayed the highest solubility (306.42 ± 10.34 μg/mL), followed by ES (138.80 ± 4.25 μg/mL). Liposomal powders exhibited lower solubility values, with NLS reaching 93.32 ± 6.01 μg/mL and ELS only 17.36 ± 1.01 μg/mL. This reduced solubility can be partly attributed to the lower absolute amounts of active compound used in these formulations, especially in ELS, where the initial extract loading was considerably lower than in the other samples.

Despite the lower absolute solubility, liposomal formulations showed improved dissolution efficiency (DE) relative to their NR content. NLS achieved a 42.7 ± 2.13% DE, while ELS reached 55.3 ± 2.76%. In comparison,

NS exhibited only 5.6 ± 0.28% DE, despite containing the highest theoretical naringin content. ES demonstrated the best overall performance, releasing nearly all of its NR content (91.8 ± 4.59% DE).

SEM analysis revealed that all powders formed predominantly spherical particles with diameters of 5–10 μm. Spray-dried ES and NS powders displayed typical surface indentations and wrinkles. Compared with the other samples, the liposome formulations (ELS and NLS) yielded particles with smoother, more uniform surfaces and fewer defects. *Double–encapsulation results are presented in Article 5.*

2.8. Buccal film development and characterisation

2.8.1. Film formulation

Buccal films were prepared using a solvent-casting method with four formulations (EP1, EP2, NP1, and NP2) that differed in their polymer and active-ingredient compositions. EP1 and EP2 included 70% grapefruit peel extract, while NP1 and NP2 included pure NR (50 mg/ml in 70% ethanol). Hydroxypropyl methylcellulose (HPMC) served as the primary polymer across all samples. As secondary polymers, sodium alginate (ALG) was applied in EP1 and NP1, whereas polyvinyl alcohol (PVA) was used in EP2 and NP2. Glycerol acted as the plasticiser in each formulation.

All the prepared films appeared uniform, smooth, and free from cracks or air bubbles, confirming good compatibility between the polymers and the incorporated actives. Visual differences were evident between extract-loaded and NR–loaded films. Extract-based samples (EP1 and EP2) showed yellow to light brown tones, consistent with flavonoid and polyphenol content. At the same time, NR-based films were more transparent: NP1 was nearly colourless, and NP2 had only a faint yellow hue.

Polymer type also influenced the appearance and texture. PVA-based films (EP2, NP2) were more transparent, flexible, and smooth, whereas ALG–based films (EP1, NP1) appeared slightly more rigid. These differences may influence not only consumer acceptability but also functional performance, such as mucoadhesion.

The moisture content varied with both the active compound and the polymer. Extract-based films had higher values (EP1: 13.48 ± 0.45%; EP2: 15.25 ± 0.52%), likely due to the hygroscopic nature of sugars and phenolics. In contrast, NP1 and NP2 contained less moisture (11.46 ± 0.40% and 11.49 ± 0.42%).

Dissolution testing in artificial saliva (pH 6.8) highlighted apparent differences. The NR–loaded films released the highest amounts of active

compounds, with NP2 reaching 69.97 ± 3.01 μg/mL (40.9% efficiency) and NP1 reaching 63.99 ± 2.64 μg/mL (37.5%). Extract-based films released less NR overall (EP1: 27.08 ± 1.42 μg/mL; EP2: 18.45 ± 1.05 μg/mL). However, EP1 (40.2%) exhibited higher efficiency than EP2 (26.6%), likely due to the slower erosion and controlled alginate release compared with the rapid hydration and degradation promoted by PVA.

Texture analysis further confirmed polymer-dependent effects. NP2 (PVA-based) exhibited the highest peak adhesion force (0.09 ± 0.01 N) and work of adhesion (0.47 ± 0.11 N·s). NP1 showed comparable work of adhesion (0.46 ± 0.10 N·s), likely reflecting ionic interactions between alginate and mucin. In contrast, Extract-based films (EP1, EP2) demonstrated lower mucoadhesive properties, with EP2 showing the lowest work of adhesion (–0.25 ± 0.008 N·s). This reduction may be attributed to polyphenols interfering with hydrogen bonding between the polymers and mucin. Nevertheless, visual observations indicated that all films hydrated rapidly and adhered well to the glass surface, suggesting that surface swelling facilitated attachment even in samples with weaker mucoadhesive properties.

Film disintegration time also reflected the influence of polymer composition. EP2 dissolved the fastest (5 min), consistent with PVA's rapid hydration. NP1 and NP2 disintegrated within 15–20 min, whereas EP1 exhibited the longest disintegration time (35 min), suggesting slower alginate erosion and a more prolonged release profile. *Physical characterisation of buccal films is presented in Article 5.*

2.9. *In vitro* release from different formulations

NR release was assessed from spray-dried microcapsules, dual liposomal powders, and buccal films in SGF (pH 1.2), SIF (pH 6.8), and artificial saliva (pH 6.8). This allowed comparison of each system's efficiency and release profile under simulated gastric, intestinal, and oral conditions. Spray-dried microcapsules of pure NR exhibited the highest release in SGF, reaching 274.26 ± 2.15 μg/mL after 30 min; however, this represented only 6% of the theoretical drug loading (163.8 mg). The rapid saturation was followed by recrystallisation, reflecting poor solubility of crystalline NR in acidic media. In contrast, the dual liposomal powders of NR remained stable at 55.36 ± 0.44 μg/mL after 30 min, then increased to 55.87 ± 0.33 μg/mL at 90 min. This study indicates a diffusion-limited process controlled by the lipid bilayer and carbohydrate matrix, representing 59–60% of its aqueous solubility (93.3 μg/mL). The Extract-based systems showed different results: 130.67 ± 3.21 μg/ml after 30 min and 135.71 ± 2.16 μg/ml after 90 min, corresponding to almost complete release of the theoretical amount of

4.53 mg (94–98%). The dual liposomal powders of GE showed the lowest absolute NR levels (9.87–10.85 μg/ml), accounting for 32–36% of the limiting dose (0.94 mg), indicating effective retention of active ingredients during gastric emptying. In the intestinal phase, the release patterns changed. NR–based microcapsule concentrations declined from the gastric peak to 208.53 ± 1.95 μg/mL at 120 min, with a modest recovery to 220.82 ± 1.65 μg/mL at 180 min, indicating precipitation–redissolution dynamics at neutral pH.

Extract–based microcapsules maintained high values of 148.35 ± 2.37 μg/mL at 120 min and 146.88 ± 2.01 μg/mL at 180 min, indicating stable diffusion without strong pH dependence. Dual liposomal powders of NR showed a slight increase, reaching 56.89 ± 0.68 μg/mL at 120 min and stabilising at 52.07 ± 0.55 μg/mL at 180 min, consistent with pH-dependent liposome destabilisation and controlled diffusion. Dual liposomal powders of GE released 11.24 ± 0.41 μg/mL at 120 min and 9.94 ± 0.36 μg/mL at 180 min, showing delayed but sustained intestinal release compared with SGF.

Buccal films offered an alternative route for release. NP2 (PVA–HPMC, NR) achieved the highest release (72.13 ± 2.85 μg/mL at 10 min; 69.97 ± 3.01 μg/mL at 30 min), corresponding to 41% dissolution efficiency. NP1 (ALG–HPMC, NR) showed slightly lower values (63.99 ± 2.64 μg/mL at 10–30 min), reflecting slower hydration of alginate gels and diffusion-limited transport (38% efficiency). EP1 (ALG–HPMC, GE) released 27.08 ± 1.42 μg/mL after 30 min (40% efficiency), with the longest dissolution time (35 min). EP2 (PVA–HPMC, GE) exhibited faster disintegration (5 min), but due to lower initial loading, release was limited to 18.45 ± 1.05 μg/mL at 30 min (27% efficiency).

In comparison, single encapsulation yielded higher initial release but exhibited low solubility efficiency. Dual encapsulation, by contrast, slowed release in SGF while improving stability in SIF. Additionally, buccal films enabled rapid salivary release, with the polymer type substantially affecting both the release rate and adhesion. Each system displayed complementary benefits: powders appeared more suitable for intestinal delivery, whereas buccal films offered fast oromucosal administration.

In vitro release from different formulations is presented in Article 5.

3. DISCUSSION

In this study, grapefruit peel was selected as a rich source of bioactive compounds because it is among the most widely consumed citrus fruits globally, yet nearly half of its mass is discarded during juice production [48,49]. These by–products, mainly peel and segment membranes, remain underutilised and contribute to environmental pollution [50]. At the same time, they are abundant in biologically active components, including phenolics, pectins, essential oils, and flavonoids, particularly naringin (NR) and its aglycone naringenin (NAR) [15,51]. Both NR and NAR exhibit well-documented antioxidant, anti-inflammatory, and potential anticancer properties, making them valuable in pharmaceutical and nutraceutical applications [13,20,29,52–58]. Therefore, increasing the utilisation of grapefruit processing waste aligns with current trends in sustainable biorecycling and presents an opportunity to transform waste into value-added products.

One of the main challenges in utilising citrus by–products is the development of efficient, environmentally sustainable extraction methods. Conventional solvent-based extraction is often limited by high solvent consumption, extended processing times, and the risk of degrading thermolabile compounds [49,59–61]. To address these limitations, this study compared several extraction techniques, including ultrasound-assisted extraction (UAE), heat–reflux extraction, and their combinations. Optimisation parameters included solvent composition, extraction time, temperature, and hydrolysis conditions. Based on previous findings with other plant matrices, ultrasonic cavitation and controlled thermal input were expected to promote cellular disruption and enhance mass transfer, thereby improving the recovery of flavonoid compounds [22,62,63].

These results are consistent with those of Jeyaraj et al., who reported that NR is most abundant in albedo and segment membranes. However, low amounts or no NAR are found in flavedo membranes [8,64]. The choice of raw material is an essential factor for maximising flavonoid yield [21].

In the current study, ultrasound-assisted extraction (UAE) alone was not more effective than heat–reflux or combined extraction. However, prolonged ultrasound treatment (30 min *vs* 10 min*)* improved the extraction of both NR and NAR, suggesting that prolonged cavitation promotes solvent diffusion into plant tissues. This trend has also been reported by Tundis et al. and Kadam et al., who observed that longer sonication times increased the extraction of phenolic compounds and flavonoids due to enhanced cell wall disruption [65,66]. However, excessively long processing times or high energy levels may pose a risk of compound degradation [67,68]. Extraction at 50 °C

was more efficient than at lower temperatures, supporting the hypothesis that gentle heating enhances solubility and accelerates diffusion without significant degradation. These results further support previous observations by Brglez Mojzer et al., who demonstrated that moderate heating enhances the extraction of thermolabile antioxidants while preserving their activity [67].

The ethanol concentration also had a moderate impact on flavanone recovery. Ultrasound-assisted extraction with 70% ethanol yielded higher levels of NR and NAR than extraction with 50% ethanol. This observation aligns with data from Muti et al. and Zulkifli et al., who demonstrated that 70% ethanol provides the optimal polarity balance for extracting flavanone glycosides and phenolic compounds from citrus matrices [69–71]. However, when ultrasound was combined with heat reflux, yields were comparable at both concentrations. This indicates that heating compensates for the lower ethanol strength. From a sustainability perspective, using 50% ethanol reduces environmental impact and cost without sacrificing efficiency.

Combining extraction with acidic, alkaline, or thermal hydrolysis significantly affected the flavanone profile of grapefruit peel extracts.

Acid hydrolysis was particularly effective in promoting NAR formation, especially in segment membranes, where NAR was otherwise undetectable. In the present study, acid hydrolysis promoted the conversion of glycosides into aglycones, increasing aglycone yields. Comparable observations were reported by Kazlauskaitė et al. in studies on legume isoflavones, in which acid hydrolysis facilitated cleavage of glycosidic bonds [72]. In contrast, alkaline hydrolysis enhanced NR recovery in the albedo but was less effective in promoting aglycone formation, likely due to stabilisation of glycosidic structures under alkaline conditions, consistent with observations reported by Sant et al [22].

Thermal hydrolysis was the most effective in increasing NR content (20–25%) in all grapefruit tissues and stimulated NAR release in segment membranes. This is consistent with the results of Ghasemi et al. [69], who reported improved flavonoid recovery and transformation following moderate heat treatment during extraction from plant matrices. These results indicate that hydrolysis conditions significantly impact flavanone composition, which directly affects bioavailability, and should be considered when developing dietary supplement formulations. The appropriate choice of hydrolysis method can also contribute to more environmentally friendly processing, reducing the need for harsh solvents and improving the availability of the target compound.

The use of excipients improved flavanone solubility and stability during extraction. Magnesium aluminometasilicate showed a selective effect. At 1% concentration, it consistently increased NAR levels in segment membranes.

However, it reduced NR recovery by approximately 15% compared to control samples.

This suggests that the excipient stabilises aglycones more effectively than glycosides. Previous studies by Kazlauskaitė et al. and Matulytė et al. also demonstrated that magnesium aluminometasilicate can act as a carrier with preferential affinity for specific phytochemicals. Such selectivity is likely influenced by the physicochemical properties of the compounds, particularly polarity and molecular size [23,73].

Cyclodextrins (CDs) had a more substantial effect on flavanone recovery than other excipients. All three types tested: α-, β-, and γ-CD, improved the extraction results. However, their efficiency varied with cavity size and molecular compatibility.

α-CD slightly increased naringin levels but had a minimal effect on NAR. γ-CD, with the largest cavities, showed broader stabilisation but was less effective overall. β-CD consistently gave the best results. It increased both NAR and NAR yields by more than three times compared to extracts without excipients.

This effect is likely due to the optimal cavity size of β-CD, which fits well with the aromatic ring of flavanones. As a result, stable inclusion complexes can form. These complexes improve flavonoid solubility and protect them from oxidative and hydrolytic degradation. The positive effect of CDs was also evident in total phenolic content (TPC) and total flavonoid content (TFC). Extracts prepared with β-CD contained several times more phenolics and flavonoids compared to controls, particularly in albedo and segmental membranes.

In the present study, cyclodextrins enhanced the recovery of phenolic compounds during extraction. Previous studies have also demonstrated that cyclodextrins can increase isoflavone yields from *Trifolium pratense* L. extracts and improve the solubility and antioxidant stability of phenolics from *Aspalathus linearis*. These effects are attributed to cyclodextrins' ability to form inclusion complexes with phenolic molecules, which remain associated in the extract and thereby improve their solubility and stability in aqueous systems [25,74–76].

The findings of this work indicate that the addition of β- and γ-cyclodextrins significantly enhanced the recovery of flavanones compared with control extracts ($p < 0.05$). Moreover, the use of CDs enabled higher yields even at reduced solvent concentrations. They can be adapted to achieve different goals. Magnesium aluminometasilicate can be used when a higher aglycone content is required. The CDs are more suitable for stabilising glycosides or ensuring solubility in aqueous formulations.

The antioxidant activity of grapefruit extracts strongly depended on both the extraction method and the use of excipients. Chemical antioxidant assays (ABTS, DPPH, and FRAP) showed that extracts obtained with β-cyclodextrin exhibited the highest antioxidant capacity, in some cases exceeding that of control extracts by more than 50%. This increase is likely related to improved solubility and stability of flavanones due to inclusion complex formation with β-cyclodextrin rather than to any intrinsic antioxidant activity of the cyclodextrin itself [77,78].

In vivo experiments also confirmed the antioxidant potential of grapefruit extracts. This part of the study compared the antioxidant effects of grapefruit peel extract (GE) with pure NR in an aluminium chloride ($AlCl_3$)–induced oxidative stress mouse model. Oxidative stress was assessed by measuring reduced glutathione (GSH), malondialdehyde (MDA), and the enzymatic antioxidants catalase (CAT) and glutathione reductase (GR) in blood, liver, and brain tissues.

In the blood, NR significantly increased GSH levels, especially when co-administered with $AlCl_3$. GSH concentrations were more than twice as high as in the control. Grapefruit extract also elevated GSH, but to a lesser extent. However, MDA levels were lowest in the GE + $AlCl_3$ group, with 50% reduction relative to the $AlCl_3$ group. This suggests that the extract offers stronger protection against lipid peroxidation. The results indicate complementary effects: NR mainly enhanced endogenous GSH synthesis, while the extract directly protected lipid membranes.

In the brain, NR again significantly restored GSH levels, which were more than 3-fold higher than in the $AlCl_3$ group. This confirms its role in stimulating antioxidant defences. Meanwhile, E reduced MDA levels more effectively, with a 40% decrease compared to the control group. This contributes to better membrane protection in neuronal tissue. Regarding CAT activity, NR maintained levels close to control levels, whereas GE was less effective. These results suggest that NR more strongly supports brain enzymatic antioxidant systems.

In the liver, the pattern was reversed. Grapefruit extract significantly increased CAT activity, exceeding control values by more than 50%. This indicates activation of adaptive enzymatic defence. In contrast, NR combined with $AlCl_3$ was more effective in elevating GSH levels, supporting its hepatoprotective potential [79].

The *in vivo* data demonstrate a complementary antioxidant profile: grapefruit peel extract is more effective at reducing oxidative lipid damage. At the same time, pure NR has more potent effects on glutathione metabolism and enzymatic antioxidant defences. This highlights the importance of whole

extracts rather than isolated compounds, as the synergistic presence of polyphenols, vitamin C, and organic acids.

Microencapsulation was performed to improve the technological and functional properties of grapefruit peel extracts. Given the limited solubility and stability of NR and NAR, both spray-drying and freeze-drying were applied using different wall materials (MD, SKM, β-CDs, CH, and CMC), to evaluate their impact on powder characteristics, encapsulation efficiency, and dissolution.

The drying method significantly affected the process yield. Spray drying yielded 48%–53%, with the highest at 160 °C (M3, 52.95%). Increasing the inlet temperature to 170 °C reduced the yield to 48%, most likely due to phenolic compound degradation and the formation of a surface crust that hindered solvent evaporation. Higher inlet temperatures may accelerate moisture removal but can also promote the degradation of heat-sensitive bioactive compounds. Comparable observations were reported by Nguyen et al., who noted yield losses at higher spray-drying temperatures during citrus extract processing [80]. In contrast, freeze drying produced significantly higher yields (69.7–79.2%), indicating greater retention of extract mass under mild processing conditions. This effect may be attributed to the low-temperature environment, which minimises degradation of heat-sensitive compounds and prevents the loss of volatile substances. Consistent observations were reported by Da Silva Junior et al., who found greater flavonoid retention in *Spondias purpurea* peel extract after freeze-drying than after spray-drying [30].

Moisture content showed a comparable trend. Spray-dried powders exhibited moisture contents ranging from 5.3% to 7.6%, with lower values observed at higher inlet temperatures and in formulations containing β-CD in the wall matrix. Samples MBC2 and MBC3 exhibited residual moisture levels below 5.5%, whereas in β-CD–free systems, the values exceeded 7%. Freeze-dried samples showed comparable moisture contents (4.7–5.8%), although with slightly greater variability.

The reduced moisture content in β-CD formulations may be attributed to cyclodextrins' ability to promote closer molecular packing and the formation of less porous structures. Comparable observations were reported by Ćujić Nikolić et al., who found that cyclodextrin-based encapsulation systems, either alone or in combination with other carriers, exhibited significantly lower moisture content than systems using conventional carriers such as whey protein or maltodextrin [81].

The composition of the wall material significantly influenced wettability. Spray-dried powders containing the highest levels of CMC and β-cyclodextrin (β-CD) exhibited the longest wetting times (>1400 s). This effect may be attributed to the formation of more structured and less permeable particle

surfaces promoted by β-CD. Freeze-dried powders generally hydrated more rapidly, with L2 exhibiting the shortest wetting time, despite its composition being similar to L1, suggesting that the ratio of wall components was more important than their total concentration. Comparable observations were reported by Shi Li et al. in lyophilised polyphenol systems, where porous structures facilitated faster water penetration [82].

The flowability, measured by the Carr index and Hausner ratio, is statistically significantly dependent on the wall material. The Hausner ratio of the spray–dried powders ranged from 1.438 to 1.636, with MBC1 exhibiting the weakest flow due to the high content of β-CD and CMC. The inclusion of maltodextrin improved its flowability by reducing stickiness and particle cohesion, consistent with reports by Sidlagatta et al. on its use as a flow-improving carrier [83]. Freeze–dried powders exhibited slightly higher compressibility indices (30–34%) and Hausner ratios below 1.52, indicating acceptable flowability.

Solubility values reflected both wall material composition and drying method. Spray-dried capsules showed solubility from 30% (MBC1) to 66% (MBC4), while lyophilised powders ranged from 31% (L1) to 62% (L2). Higher MD levels enhanced solubility, whereas β-CD and CMC decreased it, possibly by forming less water-dispersible matrices. This is consistent with the previous findings of Xiao et al., who showed that maltodextrin enhances solubility by reducing particle aggregation and by forming a porous matrix that facilitates water dispersion [30,84].

Encapsulation efficiency (EE%) ranged from 76.7% to 91.4%, with the highest values observed in spray-dried β-CD–containing formulations (MBC3). While β-CD provided strong protective effects through inclusion complex formation, excessive amounts of β-CD or CMC slightly reduced EE, likely due to weaker binding with polyphenols. Freeze-dried samples showed slightly lower EE (76.8–88.6%) but retained higher overall phenolic content, indicating less degradation during drying. Comparable results were reported by Zhao et al. for the encapsulation of citrus flavonoids, with spray–drying yielding higher EE but freeze–drying better preserving phenolic integrity [85].

SEM analysis highlighted distinct surface structures. Spray-dried capsules were mainly spherical or semi-spherical, with smooth or wrinkled surfaces depending on wall composition. SK–rich formulations (e.g., MBC4) had smoother morphologies, whereas β-CD–rich capsules displayed more wrinkled surfaces. Lyophilised samples exhibited porous, lamellar structures with irregularly shaped particles. These structural differences explain functional variations: porous freeze–dried particles favoured hydration and solubility, while smoother spray–dried capsules improved encapsulation efficiency and

stability. Such correlations between morphology and function have also been noted in studies of phenolic microencapsulation [86].

To further enhance the solubility and bioavailability of flavanones, lipid–based carriers (liposomes) were developed that incorporated either the grapefruit extract (GE) or pure naringin (NR). Physicochemical characterisation confirmed that both liposome types were within the nanoscale range (94 –102 nm) and exhibited polydispersity indices below 0.4, indicating suitability for oral delivery. Increasing the lipid-to-core ratio from 1:1 to 2:1 (EL2 *vs*. EL1) resulted in smaller vesicles, more compact bilayers, and narrower particle-size distributions. These findings align with previous research on citrus- and quercetin-based liposomes, in which higher phospholipid concentrations have been shown to promote vesicle stability and homogeneity [87,88].

Zeta potential values ranged from –10.4 mV to –25.8 mV, with more negative values observed in lipid-rich formulations (NL2). In general, ζ-potential values exceeding ±20 mV is considered indicative of improved colloidal stability due to stronger electrostatic repulsion between particles. Accordingly, the higher surface charge observed in NL2 may enhance electrostatic repulsion, thereby preventing particle aggregation and improving dispersion stability [89]. Previous studies have reported comparable findings for rutin- and hesperidin-loaded liposomes, where increasing the phospholipid content enhanced colloidal stability and improved encapsulation efficiency [90,91]. Based on these properties, EL2 and NL2 were selected for spray drying and subsequent double encapsulation.

To ensure liposome stability, extend shelf life, and increase their applicability in formulations, liposomal emulsions were converted into powders via spray drying using wall materials such as β-CD, MD, and CMC. Spray drying is less expensive and less time– and energy–intensive than freeze drying, making it a suitable strategy for drying liposomal dispersions [92].

A comparative study was conducted between spray–dried powders without liposomes and those encapsulated in liposomes, as well as between formulations prepared with pure NR and those obtained from grapefruit peel extract (GE).

Spray–drying powder yields of 36–43%, with GE–based powders 43.00 ± 2.15 % and 41.05 ± 1.60% (ES, ELS, respectively) performing better than pure NR powders 36.70 ± 1.83% and 38.15 ± 1.91% (NS, NLS, respectively). Lower yields of liposomal powders may result from differences in formulation and drying behaviour, consistent with the findings of Panizzon et al. [93].

The residual moisture content remained below 6%, ensuring long–term stability. However, lipid–based NR had the highest moisture (5.58%),

suggesting that crystalline NR interfered with water removal when combined with lipids.

Encapsulation efficiency (EE) clearly differentiated the systems. The highest EE (99.4%) was achieved for the double-encapsulated GE formulation, compared with 81% for the spray-dried NR system. These results indicate that liposomal bilayers significantly improve flavonoid retention by incorporating the compounds within both the aqueous core and the lipid bilayer. Comparable protective effects of liposomal microencapsulation have been reported in previous studies, in which nanoliposomes prepared using a pH-driven method successfully encapsulated poorly soluble polyphenols such as NR and NAR, thereby improving their aqueous solubility and protecting them from degradation during processing and storage [37]. In addition, Hussein et al. demonstrated that liposomal encapsulation of ketoprofen combined with higher carbohydrate carrier concentrations improved encapsulation efficiency and stability after spray drying [94].

Absolute solubility was highest for NR (306 μg/mL), where NR was present in crystalline form within a carbohydrate-based microcapsule. In contrast, liposomal powders (GE, NR) exhibited significantly lower apparent solubility (17–93 μg/mL) because the lipid bilayer impeded immediate dissolution. However, the dissolution efficiency (DE%) relative to the actual NR content was significantly higher in liposomal formulations. Lipid–based NR reached 42.7%, and lipid–based GE achieved 55.3%. In comparison, NR single microcapsules showed only 5.6% DE. This was observed even though the liposomal powders contained 5 times less NR (10 mg/mL) than the non-liposomal powders (50 mg/mL).

SEM images confirmed that spray-dried particles were mostly spherical (5–10 μm). Non-liposomal GE and NR powders showed irregular wrinkling and indentations typical of rapid moisture loss. By contrast, liposomal GE and NR displayed smoother, more uniform surfaces, suggesting that lipids stabilised the droplet films during atomisation and drying.

Buccal films were developed as an alternative drug delivery route to overcome gastrointestinal degradation and the limited solubility of flavanones. Films prepared from HPMC–alginate (E1, NR1) and HPMC–PVA (E2, NR2) matrices exhibited distinct physicochemical and functional properties, confirming the significant influence of both polymer composition and the type of incorporated flavanone. Pure NR films (NP1, NP2) exhibited the highest dissolution efficiency in artificial saliva, reaching 37.5% and 40.9%, respectively. By comparison, extract–loaded films (E1 and E2) released significantly less NR, with lower DE (40.2% and 26.6%, respectively). The dissolution time further differed depending on the polymer used: GE-based films with ALG–HPMC dissolved the slowest (35 min), indicating the

formation of a dense alginate gel that limits diffusion, while GE-based films with PVA–HPMC disintegrated quickly (5 min), due to the higher hydration capacity of PVA and rapid erosion. Pure NR films showed intermediate values (15–20 min). Comparable effects of polymer type on dissolution kinetics have been described by Maslii et al., who compared alginate-, CMC-, HEC-, HPC-, and PVA-based films and demonstrated that alginate–containing matrices dissolved more slowly due to gel formation, whereas PVA–based systems hydrated and eroded faster, in line with the present findings [95].

GE-based films (EP1, EP2) exhibited higher moisture content (13.5–15.2%) compared with pure NR films (11.5%). This effect was attributed to the presence of hygroscopic sugars and polyphenols in the grapefruit peel extract. Comparable observations have been reported for other polymer films containing extract. For example, chitosan films incorporating *Aloe vera* extract showed higher moisture content than pure chitosan films due to the hydrophilic polysaccharides present in the extract. Likewise, pectin–propolis films and starch–gelatin films containing green tea extract exhibited higher moisture contents than their extract-free counterparts. In all these cases, the presence of complex plant-derived components, such as sugars and polyphenols, increased the hygroscopicity of the film matrix [96–98].

NR films exhibited the strongest mucoadhesive properties. The highest peak adhesion force and work of adhesion were observed for NR films (NP2: 0.09 ± 0.01 N and 0.47 ± 0.11 N·s; NP1: 0.08 ± 0.01 N and 0.46 ± 0.10 N·s), highlighting the strong contribution of PVA and alginate to mucoadhesion through hydrogen bonding and ionic interactions with mucin. In contrast, GE-loaded films exhibited lower work of adhesion (EP1: –0.53 ± 0.12 N·s; EP2: –0.25 ± 0.01 N·s), suggesting that extract components may interfere with optimal polymer–mucin interactions.

However, visual observations revealed that all films hydrated quickly and adhered well to glass, indicating that surface swelling facilitated attachment, even in samples with weaker mucoadhesive properties.

Grapefruit extract-based films were darker (yellow-brown) due to flavonoids and phenolic pigments, while NR films were more transparent, with NP1 being nearly colourless.

In vitro release studies demonstrated that the delivery strategy strongly influenced NR solubility and release efficiency. Spray-dried microcapsules showed high initial release but low dissolution efficiency due to recrystallisation. Dual encapsulation with liposomes significantly improved stability in gastric conditions. It provided sustained intestinal release, while buccal films enabled rapid release in saliva, with the polymer composition (alginate *vs*. PVA) influencing both the release rate and mucoadhesion [47].

4. SUMMARY OF THE CONCLUSIONS

1. Combined ultrasound-assisted extraction and hydrolysis proved to be the most effective strategy for flavanone recovery from grapefruit peel. The combined approach enabled similar extraction yields to be obtained using a lower ethanol concentration, indicating that the process can be optimised by reducing solvent strength.
2. Excipients significantly influenced flavanone recovery, stability, and antioxidant activity. β-Cyclodextrin increased the yield of both naringin and naringenin more than threefold and enhanced antioxidant capacity, whereas magnesium aluminometasilicate showed selective stabilisation of the aglycone form.
3. *In vivo* experiments demonstrated different antioxidant mechanisms of pure naringin and grapefruit peel extract. Naringin significantly increased glutathione levels and maintained enzymatic antioxidant defence, whereas the grapefruit extract more effectively reduced lipid peroxidation, suggesting a synergistic effect of multiple phytochemicals.
4. Microencapsulation method and wall material composition significantly affected flavanone stability and powder properties. Freeze-dried powders exhibited higher yield and better preservation of bioactive compounds, while spray-dried systems showed higher encapsulation efficiency and more uniform particle morphology.
5. Liposomal systems improved the solubility, stability, and controlled release of flavanones. Increasing the lipid-to-core ratio reduced particle size and enhanced colloidal stability, while double encapsulation prolonged naringin release and increased dissolution efficiency compared with non-encapsulated compounds.
6. Mucoadhesive buccal films based on PVA–HPMC and alginate–HPMC matrices proved suitable for rapid naringin delivery through the oral mucosa. Polymer composition significantly influenced dissolution behaviour, release kinetics, and mucoadhesive properties, thereby enabling modulation of the delivery system to achieve the desired therapeutic effect.

SUMMARY IN LITHUANIAN

Įvadas

Augalinės kilmės bioaktyvūs junginiai jau šimtmečius naudojami medicinoje dėl struktūrinės įvairovės ir plataus biologinio poveikio spektro. Kitaip nei sintetinės molekulės, daugelis fitocheminių junginių geriau dera biologiškai, mažiau toksiški, geba veikti keletą biologinių taikinių vienu metu [1–4]. Pastaraisiais metais daug dėmesio skiriama tvarumui. Ieškoma būdų, kaip panaudoti maisto pramonės atliekas vertingoms medžiagoms išgauti. Pasaulio mastu vaisiai ir daržovės sudaro didžiausią maisto atliekų dalį – apie 1,3 mlrd. tonų per metus [5–7]. Apie 20 proc. vaisių prarandama juos perdirbant, kartu pašalinami ir naudingi bioaktyvūs junginiai [8–10].

Vienas tokių pavyzdžių yra greipfrutų vaisiai (lot. *Citrus* × *aurantium* f. aurantium) priklausantys rūtininių Rutaceae šeimai. Tyrimai rodo, kad citrusinių vaisių žievelių ir sulčių ekstraktai bei iš jų izoliuoti biologiškai aktyvūs komponentai pasižymi plačiu biologinio aktyvumo spektru, apimančiu antioksidacinį, antimikrobinį, kardiovaskulinę sistemą apsaugantį, priešvėžinį ir antidiabetinį veikimą [11–13]. Šis biologinis aktyvumas siejamas su didele citrusiniuose vaisiuose aptinkamų fitocheminių junginių įvairove, įskaitant fenolinius junginius, kumarinus, limonoidus, karotinoidus ir eterinius aliejus.

Pagrindiniai flavanonai, randami greipfrutų žievėje, yra naringinas (NR) ir narirutinas (N7R). Naringinas yra flavanono naringenino (NAR) glikozidas, kuriame aglikonas susijungęs su disacharidu rutinoze (α-L-ramnozil-D-gliukoze), todėl jis dar vadinamas naringenin-7-O-rutinozidu. Narirutinas taip pat priklauso flavanonų 7-O-glikozidams. Virškinimo metu glikozidinė dalis hidrolizuojama, išlaisvinant aglikoną naringeniną, kuris yra lipofiliškesnis ir lengviau prasiskverbia per biologines membranas [14–17].

Nepaisant vertingų farmakologinių savybių, NR ir NAR praktinis taikymas yra ribotas. Pagrindinės priežastys – prastas tirpumas vandeninėje terpėje ir menkas biologinis pasisavinimas. NR taip pat žinomas kaip fermento CYP3A4 inhibitorius, o tai lemia galimą sąveiką su vaistiniais preparatais. Pagal Bioprieinamumo klasifikavimo sistemą (BCS), NR priskiriamas IV klasei. Šiai klasei būdingas žemas tirpumas ir silpna žarnyno absorbcija. Nustatyta, kad geriamoji NR absorbcija siekia mažiau nei 5 proc. [17,18]. Flavanonai dažniausiai pasisavinami plonajame žarnyne. Todėl skiriamas didelis dėmesys technologijoms, kurios leidžia apsaugoti junginius nuo skrandžio rūgščių ir virškinimo fermentų poveikio [19,20].

Nors šie junginiai sulaukia didelio mokslinio susidomėjimo, šiuo metu vis dar trūksta duomenų apie tai, kaip įvairūs ekstrahavimo metodai, hidrolizės

sąlygos bei pagalbinės medžiagos veikia flavanonų išeigą, tirpumą ir stabilumą. Šiame darbe siekiama prisidėti užpildant šią tyrimų spragą.

Siekiant padidinti ekstrakcijos veiksmingumą ir pagerinti biologiškai aktyvių junginių išgavimo galimybes, pastaraisiais metais vis dažniau taikomi įvairūs technologiniai sprendimai, įskaitant kombinuotus ekstrakcijos metodus. Nustatyta, kad hidrolizės derinimas su ultragarso poveikiu gali reikšmingai padidinti aktyvių junginių išeigą, kai kuriais atvejais net iki 44 proc., palyginti su tradicinėmis ekstrakcijos sąlygomis [21,22].

Mokslinėje literatūroje vis dažniau akcentuojama pagalbinių medžiagų, tokių kaip (α-, β-, γ-) ciklodekstrinai (CD) arba magnio aliuminio metasilikatas, svarba, didinant flavanonų išsiskyrimą iš augalinės žaliavos, bei gerinant jų fizines ir chemines savybes. Tyrimų duomenimis, šios medžiagos statistiškai reikšmingai padidina flavanonų išeigą, tirpumą ir stabilumą, sudarydamos kompleksus su jų molekulėmis ir taip apsaugodamos nuo oksidacinio skilimo, šviesos poveikio bei nepalankių pH pokyčių [23].

Nustatyta, kad magnio aliuminio metasilikatas gali stabilizuoti izoflavonus ir skatinti jų išsiskyrimą iš augalinės žaliavos [24,25]. α-, β- ir γ-CD pasižymi kūgine molekuline struktūra su hidrofobine vidine ertme ir hidrofiliniu išoriniu paviršiumi, todėl gali sudaryti inkluzinius kompleksus su hidrofobinėmis flavanonų dalimis per silpnas nekovalentines sąveikas ir taip pagerinti jų tirpumą vandeninėje terpėje. Kai kurių tyrimų duomenimis, ciklodekstrinų taikymas ekstrakcijos metu, naudojant raudonųjų dobilų (*Trifolium pratense* L.) ir pipirinių mėtų (*Mentha* × *piperita* L.) žaliavą, lėmė didesnį biologiškai aktyvių junginių kiekį galutiniuose ekstraktuose [24–26].

Vertinant flavanonų praktinį pritaikomumą, vien tik jų išgavimo ir stabilumo didinimo nepakanka – būtina įvertinti ir jų biologinį aktyvumą, ypač poveikį antioksidacinėms organizmo sistemoms. *In vitro* tyrimai suteikia reikšmingų įžvalgų apie flavanonų antioksidacinį potencialą, tačiau neatskleidžia sudėtingų biologinių sąveikų, vykstančių gyvuose organizmuose. Dėl šios priežasties būtini *in vivo* tyrimai, leidžiantys įvertinti flavanonų poveikį endogeninėms antioksidacinėms sistemoms.

Literatūros duomenys rodo, kad NR mažina lipidų peroksidaciją ir didina pagrindinių antioksidacinių fermentų – katalazės (CAT), superoksido dismutazės (SOD) ir glutationo reduktazės (GR) – aktyvumą [20,27,28]. Atsižvelgiant į tai, kad greipfrutų ekstraktuose aptinkama ir kitų biologiškai aktyvių junginių, įskaitant flavonoidus, fenolines rūgštis ir pektinus, tikėtina, jog jų sinerginis poveikis gali papildomai prisidėti prie bendro antioksidacinio aktyvumo [12,29]. Tačiau iki šiol tik pavieniai autoriai yra nagrinėję šį aspektą, o tiesioginių *in vivo* palyginamųjų tyrimų, kuriuose būtų lyginamas gryno NR ir viso greipfrutų žievelių ekstrakto biologinis poveikis, nėra atlikta, todėl jų santykinis biologinis veiksmingumas išlieka nepakankamai ištirtas.

Atsižvelgiant į flavanonų biologinį aktyvumą bei jų ribotą tirpumą ir žemą biologinį prieinamumą, vis didesnis dėmesys skiriamas pažangioms technologijoms, galinčioms pagerinti šių junginių farmakokinetines savybes. Viena perspektyviausių priemonių – mikrokapsuliavimo technologijos, leidžiančios apsaugoti bioaktyvias medžiagas nuo nepalankių aplinkos veiksnių, pagerinti jų tirpumą, kontroliuoti veikliųjų junginių išsiskyrimą, padidinti jų stabilumą. Mikrokapsuliacijos technologija pasitelkiant purškiamojo ir sublimacinio džiovinimo metodus plačiai taikoma flavonoidų ekstraktams formuluoti. Purškiamojo džiovinimo metodu gauti milteliai dažniausiai pasižymi aukštu inkapsuliacijos veiksmingumu, mažesniu drėgmės kiekiu ir geru stabilumu, o tai svarbu užtikrinant ilgesnį produkto tinkamumo laiką bei jo praktinį pritaikymą [30–32].

Literatūros duomenys rodo, kad sublimacinio džiovinimo metu naudojant skirtingas pagalbines medžiagas, pavyzdžiui, lieso pieno miltelius, natrio kazeinatą ar β-ciklodekstriną, galima žymiai pagerinti ekstraktų tirpumą [32,33]. Kito tyrimo metu Kazlauskaitė ir kolegos nustatė, kad sublimacinio džiovinimo būdu gautų mikrokapsulių išeiga siekė apie 85 proc., ir pasižymėjo aukštesniu bendru fenolinių junginių kiekiu bei didesniu antioksidaciniu aktyvumu. O purškiamojo džiovinimo metu gautų miltelių išeiga tesiekė 45 proc. [34,35].

Kita strategiškai reikšminga technologija – lipidinių nano–nešiklių pritaikymas. Fosfolipidinių dvisluoksnių sudaryti lipidiniai nano–nešikliai geba apsaugoti hidrofobinius flavanonus nuo rūgštinės ir fermentinės degradacijos skrandyje bei pagerinti jų absorbciją plonajame žarnyne [36,37].

Nagrinėti tyrimai rodo, kad veikliųjų medžiagų įterpimas į liposomas laikomas vienu būdų pagerinti veikliosios medžiagos tirpumą ir kontroliuojamą išsiskyrimą. Pavyzdžiui, eksperimentuose su žaliosios arbatos ekstraktu nanoliposomos padidino medžiagos stabilumą ir užtikrino lėtesnį išsiskyrimą *in vitro* sąlygomis [38]. Kitame tyrime buvo sukurta naringino liposomų sistema su polimeriniais nešikliais (sacharozės acetato izobutiratu), kuri ląstelių kultūrose ir gyvūnų modeliuose skatino kaulinio audinio formavimąsi, išlaikydama ilgalaikį veikliosios medžiagos išsiskyrimą [39].

Nors liposominiai nano–nešikliai veiksmingi gerinant biologiškai aktyvių junginių savybes, jiems dažnai būdingi ir reikšmingi trūkumai, daugiausia susiję su ribotu stabilumu biologinėse matricose bei ilgalaikio laikymo metu. Pagrindinės su stabilumu susijusios problemos apima cheminį ir fizikinį nestabilumą bei mikrobiologinės taršos riziką.

Cheminio ir fizikinio stabilumo problemas galima spręsti liposomas konvertuojant į sausas formas, taikant purškiamojo arba sublimacinio (liofilizacijos) džiovinimo metodus [40]. Moksliniai tyrimai parodė, kad purškiamuoju būdu džiovintos liposomos padidino vitamino C biologinį prieinamumą 30

proc., o liofilizuotos naringenino nanodalelės pasižymėjo didesniu stabilumu ir ilgesniu kontroliuojamo išsiskyrimo laikotarpiu [41,42].

Dviguba inkapsuliacija, kurios metu derinami du apsauginiai sluoksniai arba technologiniai etapai, laikoma vienu pažangiausių būdų stabilumui ir veikliųjų medžiagų kontroliuojamam išsiskyrimui užtikrinti. Literatūroje aprašyta vos keletas atvejų, nors ši strategija nebuvo taikyta NR, tyrimai su kitomis bioaktyviosiomis medžiagomis rodo reikšmingą potencialą [43].

Žandinės plėvelės (angl. buccal films) yra alternatyvi veikliųjų medžiagų tiekimo forma, padedanti apeiti pirmojo kepenų metabolizmo etapą ir sumažinti fermentinės degradacijos virškinamajame trakte riziką, taip padidinant biologinį pasisavinimą [44]. Plėvelių fizikinės ir cheminės savybės, tokios kaip tirpimo greitis, mechaninis stiprumas ir veikliosios medžiagos atpalaidavimo kinetika, reikšmingai priklauso nuo pagalbinių medžiagų parinkimo formulėse. Polimerų pasirinkimas turi esminės reikšmės tiek technologinei preparato kokybei, tiek jo funkciniam veiksmingumui. Jawadi ir kt. bei Sabra ir kt. tyrimuose nustatyta, kad žandinės plėvelės, sudarytos iš polivinilo alkoholio (PVA) ir hidroksipropilmetilceliuliozės (HPMC), pasižymi greitu tirpimu imituojamoje seilių terpėje ir stipriu sukibimu su burnos gleivine, taip užtikrinant greitą veikliosios medžiagos pasisavinimą [45,46]. Tokios savybės ypač svarbios junginiams, kuriems būdingas mažas biologinis pasisavinimas vartojant per *os*.

Šio tyrimo metu sistemiškai įvertinti flavanonų ekstrakcijos metodai ir parametrai, nagrinėtas pagalbinių medžiagų poveikis flavanonų išeigai, tirpumui, stabilumui ir *in vitro* antioksidaciniam aktyvumui. *In vivo* sąlygomis palygintas greipfrutų žievelių ekstrakto ir gryno naringino (NR) antioksidacinis aktyvumas.

Suformuluotos skirtingos dozavimo formos – mikrokapsulės, liposomos ir žandinės plėvelės. *In vitro* eksperimentais įvertintas šių formų stabilumas, tirpumas ir veikliųjų medžiagų išsiskyrimo charakteristikos. Remiantis gautais rezultatais, atrinktos veiksmingiausios taikytos technologijos ir formulės.

Disertacijos tikslas – įvertinti liposominių ir mikrokapsuliuotų modifikuoto atpalaidavimo formų įtaką naringino ir naringenino tirpumui bei nustatyti technologinių parametrų įtaką skirtingais metodais gautų mikrokapsulių kokybei ir veikliųjų medžiagų tirpimui *in vitro*.

Uždaviniai

1. Išanalizuoti ir palyginti skirtingus ekstrakcijos metodus, įvertinti jų įtaką NR ir NAR išeigai iš greipfrutų apyvaisio skirtingų dalių bei įvertinti gautų ekstraktų antioksidacinį aktyvumą.
2. Nustatyti pagalbinių medžiagų įtaką flavanonų išeigai, stabilumui ir antioksidaciniam aktyvumui *in vitro* sąlygomis.

3. Įvertinti gryno NR ir greipfrutų žievelių ekstrakto antioksidacinį aktyvumą *in vivo* tyrimuose pelių modelyje, stebint oksidacinio streso žymenis bei palyginti biologinį poveikį audiniuose ir kraujyje
4. Įvertinti technologinių veiksnių įtaką formuojant mikrokapsuliuotas formas, įvertinti jų įkapsuliavimo veiksmingumą, fizikines–chemines savybes ir stabilumą.
5. Palyginti purškiamuoju būdu džiovintų mikrokapsulių, liposominių miltelių ir mukoadhezinių plėvelių tirpumo bei veikliosios medžiagos išsiskyrimo profilius imituotomis virškinamojo trakto ir seilių sąlygomis, siekiant įvertinti šių dozavimo formų tinkamumą flavanonų tirpumui, stabilumui ir tikslingam atpalaidavimui gerinti.

Hipotezės

1. Kombinuotų ekstrakcijos metodų taikymas padidins NR ir NAR išeigą, palyginti su tradiciniais ekstrakcijos metodais.
2. Pagalbinių medžiagų (magnio aliuminio metasilikato ir ciklodekstrinų) įtraukimas į ekstrakcijos procesą pagerins flavanonų išeigą, stabilumą ir antioksidacinį aktyvumą.
3. Greipfrutų žievelių ekstraktai veiksmingiau mažins oksidacinį stresą nei grynas NR dėl kelių fitocheminių junginių sinerginio poveikio.
4. Mikrokapsuliavimo technologijų pritaikymas pagerins biologiškai aktyvių junginių stabilumą.
5. Pasirinktos formulavimo sistemos padidins NR ir NAR tirpumą bei leis veiksmingai atpalaiduoti tiriamus junginius.

Mokslinis naujumas ir praktinė reikšmė

Atsižvelgiant į didėjantį agropramoninių atliekų kiekį ir tvarumo siekius, taip pat augantį susidomėjimą natūralios kilmės biologiškai aktyviais junginiais, ši disertacija orientuota kompleksiškai išgauti, stabilizuoti ir technologiškai pritaikyti flavanonus (NR ir NAR) iš greipfruto žievelių, kurios dažnai laikomos maisto pramonės šalutiniu produktu.

Greipfrutų žievelių ekstraktų sudėtis buvo išsamiai ištirta taikant efektyviosios skysčių chromatografijos metodiką, kuri leido identifikuoti ir kiekybiškai nustatyti tiriamuosius flavanonus – NR ir NAR. Papildomai spektrofotometriniais metodais įvertintas bendras fenolinių junginių, flavonoidų kiekis ir antioksidacinis aktyvumas. Tyrimo metu taikyti įvairūs flavanonų išgavimo metodai, paremti hidrolizės procesais ir pagalbinių medžiagų taikymu. Rezultatai atskleidė, kad tokių junginių kaip magnio aliuminio metasilikato bei (α-, β-, γ-) ciklodekstrinų įtraukimas žymiai pagerino fenolinių junginių ir flavanonų išeigas ir sustiprino antioksidacinį ekstraktų aktyvumą. Tokios metodi-

kos padeda spręsti žemo flavanonų tirpumo problemą, kartu išlaikant aplinkai draugišką ir ekonomišką procesą, atitinkantį žaliosios chemijos principus.

Šiame darbe pirmą kartą atliktas tiesioginis gryno NR ir viso greipfrutų žievelių ekstrakto (GE) palyginimas *in vivo* modelyje su pelėmis. Rezultatai parodė, kad NR daugiausia skatino endogeninių antioksidacinių fermentų (CAT, SOD ir GR) aktyvumą, o visas greipfrutų žievelių ekstraktas veiksmingiau mažino lipidų peroksidacijos lygį. Tokiu būdu buvo užpildyta esminė tyrimų spraga, nes iki šiol tokio sisteminio palyginimo literatūroje nebuvo atlikta.

Mikrokapsulių gamybai buvo taikyti du metodai – purškiamojo džiovinimo ir sublimacijos (liofilizacijos) metodai. Apvalkalo struktūrai formuoti naudoti maltodekstrinas, β-ciklodekstrinai ir karboksimetilceliuliozė, kurie užtikrino mikrokapsulių formavimąsi bei kontroliuojamą veikliųjų junginių atpalaidavimą. Visos gautos mikrokapsulės atitiko kokybės reikalavimus, tačiau purškiamojo džiovinimo būdu paruoštos formulės pasižymėjo geresniais technologiniais parametrais, todėl laikytinos tolimesniems tyrimams.

Liposominiams nano nešikliams formuoti naudojamas etanolio injekcijos ir ultragarsinio apdorojimo metodas. Siekiant padidinti šių nešiklių fizikinį ir cheminį stabilumą ilgalaikio laikymo sąlygomis, liposomos buvo konvertuotos į sausą miltelių formą taikant purškiamojo džiovinimo metodą. Papildomai liposomos buvo įterptos į matricą, sudarytą iš MD, β-CD ir CMC. Tokia dvigubos inkapsuliacijos sistema padėjo reikšmingai pagerinti liposomų stabilumą ir kontroliuoti NR bei NAR atpalaidavimo profilį.

Atlikta palyginamoji *in vitro* atpalaidavimo analizė tarp skirtingų farmacinių formų: mikrokapsulių, gautų purškiamojo džiovinimo metodu; dvigubai inkapsuliuotų sistemų, kuriose liposominiai nešikliai buvo įterpti į polisacharidinę matricą; ir mukoadhezinių burnos gleivinei skirtų plėvelių. Kiekviena šių formų buvo suformuota tiek su grynu naringinu (NR), tiek su greipfrutų žievelių ekstraktu, turinčiu natūralų kompleksą. Tai suteikė galimybę ne tik įvertinti formuluočių poveikį tirpumui ir atpalaidavimo kinetikai, bet ir tiesiogiai palyginti dviejų skirtingos kilmės veikliųjų medžiagų (gryno junginio ir augalinio ekstrakto) išsiskyrimo charakteristikas. Gauti rezultatai leido įvertinti technologinių sprendimų ir žaliavos kilmės įtaką flavanonų tirpumui ir išsiskyrimo charakteristikoms *in vitro*.

Tyrimo objektas ir metodai

Švieži greipfrutų vaisiai buvo surinkti 2021–2022 m. iš vietinės prekybos vietos Mastaičiuose (Kauno r.), vaisių kilmės šalis – Italija (regionas nenurodytas). Vaisiai buvo atskirti į išorinį žievelės sluoksnį – egzokarpį, vidinį sluoksnį – mezokarpį ir endokarpinę segmentinę pertvarą. Žaliava buvo

susmulkinta elektriniu smulkintuvu („Bosch“, Vokietija) ir užšaldyta –18 ± 0,9 °C temperatūroje iki ekstrakcijos.

2023–2025 m. greipfrutų žievelės ir segmentinės pertvaros, kaip pramoninės kilmės šalutiniai produktai, buvo surinktos iš vietinių kavinių Kaune. Žaliava buvo džiovinama 60 ± 5 °C temperatūroje iki pastovios masės, sumalama ir laikoma sandariuose induose sausoje ir tamsioje aplinkoje. Drėgmės kiekis nustatytas drėgmės analizatoriumi (KERN MLB, Vokietija) ir siekė 4,58 ± 0,15 proc.

Tyrime taikyti skirtingi ekstrahavimo metodai: ultragarsinė ekstrakcija su homogenizatoriumi, ultragarsinė ekstrakcija vandens vonelėje bei terminė ekstrakcija su kondensatoriumi. Vertinta ekstrahavimo parametrų (temperatūros, trukmės, galios, tirpiklio koncentracijos) įtaka flavanonų išeigai. Analizuota šarminės, rūgštinės bei terminės hidrolizės įtaka NR ir NAR išsiskyrimui. Taip pat įvertinta pagalbinių medžiagų (magnio aliuminio metasilikato, α-, β-, γ-ciklodekstrinų) įtaka ekstraktų stabilumui, išeigai ir antioksidaciniam aktyvumui.

Tiriamųjų junginių kiekiui nustatyti taikytas efektyviosios skysčių chromatografijos (ESC) metodas. Bendras fenolinių junginių bei flavonoidų kiekis įvertintas spektrofotometriniais metodais.

Antioksidacinės savybės vertintos *in vitro* taikant standartizuotus testus: ABTS (λ = 734 nm), DPPH (λ = 517 nm) ir FRAP (λ = 593 nm).

In vivo tyrime naudotas pelių modelis, kuriuo vertintas gryno NR ir viso greipfrutų ekstrakto antioksidacinis poveikis. Buvo analizuojami oksidacinio streso žymenys: sumažinto glutationo (GSH) kiekis (λ = 412 nm), malondialdehido (MDA) koncentracija (λ = 535/520 nm), fermentų – katalazės (CAT) ir glutationo reduktazės (GR) – aktyvumas (λ = 410 ir 340 nm) pelių kraujyje, kepenyse bei smegenyse. Gyvūnų tyrimas buvo patvirtintas Valstybinės maisto ir veterinarijos tarnybos (leidimo Nr. G2-275).

Mikrokapsulių gamybai taikyti purškiamojo džiovinimo ir liofilizacijos (sublimacinio džiovinimo) metodai, naudojant įvairias apvalkalą formuojančios medžiagas ir jų koncentracijas: maltodekstriną, liesą pieną, β-ciklodekstriną, chitozaną bei karboksimetilceliuliozę (CMC). Kokybiniai parametrai įvertinti pagal Europos farmakopėjos metodikas: miltelių birumo tankis (Hausner‘io) koeficientas, kūgio kampas, drėgmės kiekis, drėkinamumas, morfologija, proceso išeiga (Y, proc.), tirpumas bei bendras ir paviršinis fenolinių junginių kiekis.

Lipidinių nešiklių gamyba atlikta etanolio injekcijos metodu, taikant zondo tipo ultragarsinį poveikį (5 ciklai po 1 min. įjungta / 1 min. išjungta, 16 ± 5 proc. galia). Nešiklių sudėčiai naudotas Lipoid S100 (fosfatidilcholinas) ir cholesterolis, kurie buvo ištirpinti etanolyje kartu su greipfrutų ekstraktu arba

grynu NR tirpalu ir įšvirkšti į vandeninę terpę maišant. Tyrime naudoti lipidų ir šerdies masės santykiai (1:1 ir 2:1).

Lipidinių nešiklių fizikinės – cheminės savybės nustatytos naudojant dinaminės šviesos sklaidos (DLS) metodą („Nano ZS 3600“, JK). Nustatytas vidutinio dalelių dydžio ir polidispersiškumo indeksas (PDI). Lipidinių nešiklių paviršiaus ζ (dzeta) potencialas nustatytas taikant ζ (dzeta) režimą. Liposomų struktūriniam vientisumui išsaugoti jos buvo konvertuotos į miltelių formą taikant purškiamojo džiovinimo metodą ir derinant su pagalbinėmis medžiagomis (MD, β-CD ir CMC).

Žandinės plėvelės buvo pagamintos tirpinimo-liejimo būdu, naudojant HPMC (12 proc.), PVA ar natrio alginatą (2 proc.) ir gliceroli (4 proc.). Plėvelės džiovintos 40 °C temperatūroje. Mechaninės savybės įvertintos tekstūros analizatoriumi (TA.XT Plus), fizikinės–cheminės savybės nustatytos matuojant drėgmę, tirpimą ir ištirpimo laiką.

In vitro atpalaidavimo tyrimai atlikti naudojant „Sotax AT7“ išmaniąją sistemą, imituojančią burnos (dirbtinės seilės), skrandžio (SGF, pH 1,2) ir žarnyno (SIF, pH 6,8) sąlygas. Tyrimo metu buvo lyginamas NR atpalaidavimas iš įvairių farmacinių formų: mikrokapsulių, liposomų bei žandinių plėvelių, naudojant tiek gryną NR, tiek greipfrutų žievelių ekstraktą kaip šaltinį. Kiekybinis NR įvertinimas atliktas efektyviosios skysčių chromatografijos (ESC) metodu.

Eksperimentiniai duomenys iš 1–5 straipsnių buvo analizuojami ir vizualizuojami naudojant „IBM SPSS Statistics 20.0“, „Microsoft Excel 2021“ ir „GraphPad Prism 8“ programas. Visi eksperimentai atlikti ne mažiau kaip trimis pakartojimais, o rezultatai pateikiami kaip vidurkis ± standartinis nuokrypis (SD).

Skirtumai tarp grupių vertinti taikant neparametrinius statistinius testus: Friedmano testą su Wilcoxono rangų ženklų testu pakartotiniams matavimams bei Mann–Whitney U testą dviejų nepriklausomų grupių palyginimui. Koreliacija ir regresija nustatyta naudojant Spearmano ranginės koreliacijos koeficientą.

In vivo eksperimentuose skirtumai tarp septynių grupių analizuoti taikant vienfaktorinę dispersinę analizę (ANOVA) su Tukey post hoc testu. Statistiškai reikšmingais laikyti skirtumai, kai $p < 0,05$. *Naudotos medžiagos ir taikyti metodai išsamiai aprašyti su šiuo darbu susijusiuose moksliniuose straipsniuose (1–5).*

Diskusija ir rezultatų apžvalga

Greipfrutų vaisiai yra vieni populiariausių citrusinių vaisių pasaulyje, tačiau beveik pusė jų biomasės tampa atliekomis po sulčių gamybos [46,47].

Šios atliekos (žievelės ir segmentinės pertvaros) ne tik kelia aplinkosaugos problemų, bet ir yra turtingas fenolinių junginių, flavonoidų, pektinų bei eterinių aliejų šaltinis [15,48,49]. Didžiausios reikšmės turi flavanonai – naringinas (NR) ir jo aglikonas naringeninas (NAR), pasižymintys antioksidacinėmis, priešuždegiminėmis ir priešvėžinėmis savybėmis [13,20,29,50–56]. Todėl veiksmingai išgauti šiuos junginius iš greipfrutų perdirbimo atliekų aktualu tiek farmacijos, tiek maisto pramonės srityse.

Vienas šio tyrimo tikslų buvo optimizuoti ekstrakcijos parametrus, taikant eksperimentinę technologinę optimizavimo strategiją, pagrįstą kombinuotu ekstrakcijos metodu su rūgštine, šarmine ir termine hidrolize. Optimizavimo metu buvo vertinama žaliavos apdorojimo trukmės, tirpiklio tipo, hidrolizės sąlygų bei skirtingų ekstrakcijos metodų (ultragarsinės ekstrakcijos, virinimo tirpiklio virimo temperatūroje su grįžtamuoju kondensatoriumi) ir jų derinių – įtaka tikslinių junginių išeigai. Ekstrakcija buvo taikyta tiek iš šviežios žaliavos atskirų dalių (egzokarpio, mezokarpio ir segmentinių pertvarų), tiek iš džiovintų greipfrutų žievelių, susidarančių kaip sulčių gamybos šalutinis produktas.

Ultragarsinės ekstrakcijos metu buvo nustatyti statistiškai reikšmingi skirtumai ($p < 0,05$) tarp atskirų greipfrutų vaisiaus dalių: mezokario dalyje NR koncentracija siekė $17,45 \pm 0,87$ mg/g, egzokarpio dalyje – $8,12 \pm 0,41$ mg/g, o segmentinėse pertvarose – tik $4,31 \pm 0,96$ mg/g. Taip pat fiksuotas statistiškai reikšmingas skirtumas ($p < 0,05$) tarp NAR išeigos mezokarpio dalyje ($4,63 \pm 0,23$ μg/g), lyginant su kitomis dalimis, kuriose NAR kiekiai buvo žemiau aptikimo ribos. Panaši flavanonų pasiskirstymo tendencija skirtingose greipfrutų audinių dalyse aprašyta ir kituose tyrimuose. Pavyzdžiui, Jeyaraj ir kt. nustatė, kad didesnės NR koncentracijos dažniausiai aptinkamos mezokarpio audiniuose ir segmentinėse pertvarose [8,62–66].

Tiriant etanolio koncentracijos (50 proc. ir 70 proc. (*v/v*)) poveikį nustatyta, kad kai kuriuose mėginiuose 70 proc. (*v/v*) etanolis statistiškai reikšmingai padidino tiriamų junginių koncentraciją. Pavyzdžiui, egzokarpio mėginiuose NR kiekis padidėjo nuo $14,79 \pm 0,73$ mg/g (7-A) iki $17,39 \pm 1.10$ mg/g (9-A). Mezokarpio dalyje NAR koncentracija padidėjo nuo $3,36 \pm 0,16$ μg/g (7-A) iki $4,57 \pm 0,22$ μg/g (9-A) ($p < 0,05$). Tikėtina, kad didesnė etanolio koncentracija pagerino mažiau polinių flavanonų tirpumą, todėl padidėjo jų ekstrakcijos efektyvumas. Ši variacija nebuvo vienoda visoms tirtoms vaisiaus dalims, kas rodo, kad ekstrakcijos efektyvumą gali lemti ir audinių struktūra bei junginių pasiskirstymas skirtinguose greipfrutų audiniuose. Gauti rezultatai iš esmės sutampa su kitų autorių pateiktais duomenimis, rodančiais, kad didesnė etanolio koncentracija gali padidinti fenolinių junginių ir flavonoidų ekstrakcijos efektyvumą [64,65]. Tačiau šiame tyrime gauti duomenys papil-

do informaciją apie šio poveikio pasireiškimą skirtingose greipfrutų vaisiaus dalyse.

Virinimas tirpiklio virimo temperatūroje su grįžtamuoju kondensatoriumi statistiškai reikšmingai ($p < 0,05$) padidino NAR išeigą, ypač segmentinėse pertvarose, kur ji siekė 35,80 ± 1,77 µg/g. Segmentinėse pertvarose NAR kiekis padidėjo beveik dešimt kartų, palyginti su mėginiais, kurie nebuvo veikiami šilumos. Tikėtina, kad aukšta temperatūra skatino glikozidinių jungčių hidrolizę, dėl kurios glikozidinė NR forma buvo paverčiama į aglikoną NAR, taip pat pagerino tirpiklio skvarbą į augalinius audinius ir padidino fenolinių junginių tirpumą bei difuziją. Literatūros duomenys taip pat rodo, kad padidinta temperatūra gali skatinti flavonoidų glikozidų hidrolizę ir aglikonų susidarymą ekstrakcijos metu [66,67].

Rūgštinė, šarminė ir terminė hidrolizė statistiškai reikšmingai ($p < 0,05$) padidino flavanonų išeigą, palyginti su kontroliniais ekstraktais. Didžiausias poveikis nustatytas taikant terminę hidrolizę: NR kiekis mezokarpio dalyje padidėjo nuo 17,39 ± 0,87 mg/g iki 25,05 ± 1,25 mg/g, o segmentinėse pertvarose – nuo 5,26 ± 0,26 mg/g iki 11,07 ± 0,55 mg/g. Segmentinėje dalyje NAR nebuvo aptiktas be terminės hidrolizės, tačiau po terminio apdorojimo jo kiekis statistiškai reikšmingai ($p < 0,05$) padidėjo iki 4,21 ± 0,21 µg/g. Tokie rezultatai gali būti siejami su flavanonų glikozidų hidrolize ir aglikonų susidarymu esant padidintai temperatūrai, kas aprašyta ir ankstesniuose tyrimuose [68]. Taikant kombinuotą ekstrakcijos metodą (ultragarsinę ekstrakciją su terminiu apdorojimu), abiejų flavanonų koncentracijos buvo panašios naudojant 70 proc. ir 50 proc. (*v/v*) etanolį. Tai rodo, kad kombinuoti ekstrakcijos metodai gali užtikrinti panašų flavanonų išgavimo efektyvumą ir naudojant mažesnės koncentracijos tirpiklį, taip sumažinant tirpiklio poreikį neprarandant ekstrakcijos veiksmingumo, kaip nurodoma ir kituose tyrimuose [69].

Rūgštinė hidrolizė sudarė sąlygas vidutiniam NAR kiekiui susidaryti, o šarminė hidrolizė labiau skatino glikozidų skilimą, tačiau aglikonų išeiga išliko ribota. Tai gali būti susiję su flavonoidų glikozidų stabilumo skirtumais skirtingose pH terpėse. Literatūroje taip pat nurodoma, kad flavonoidų glikozidų hidrolizė priklauso nuo aplinkos pH ir temperatūros, kurios gali skatinti aglikonų susidarymą [70].

Iš džiovintos greipfrutų žaliavos didžiausios flavanonų išeigos buvo gautos taikant kombinuotą ultragarsu asistuotą ekstrakciją kartu su terminiu apdorojimu. NR koncentracija siekė 49,13 ± 2,46 mg/g ir 51,94 ± 2,60 mg/g (50 proc. ir 70 proc. etanolį *v/v,*) ir statistiškai reikšmingai ($p < 0,05$) viršijo vien tik ultragarsu atliktos ekstrakcijos rezultatus (42,00 ± 2,10 mg/g ir 40,36 ± 2,00 mg/g). NAR koncentracija siekė 64,22 ± 3,21 µg/g.

Tačiau džiovintos žaliavos mėginių rezultatų variacija leidžia daryti prielaidą, kad tam tikrą įtaką galėjo turėti žaliavos biologinė įvairovė, vaisių brandos laipsnis ar sezoniškumas, nors žaliavos džiovinimo ir laikymo sąlygos buvo standartizuotos. Visais atvejais žaliava buvo džiovinama vienodomis sąlygomis (60 ± 5 °C temperatūroje iki pastovios masės), sumalama vienodu būdu ir laikoma sandariuose induose sausoje bei tamsioje aplinkoje. Tai gali būti susiję su tuo, kad naudota žaliava buvo gauta kaip sulčių gamybos šalutinis produktas, todėl jos cheminė sudėtis galėjo kisti priklausomai nuo vaisių kilmės, brandos laipsnio, laikymo ar perdirbimo sąlygų. Literatūroje taip pat nurodoma, kad citrusinių vaisių bioaktyvių junginių kiekio svyravimus gali lemti biologiniai ir aplinkos veiksniai [48].

Pagalbinių medžiagų naudojimas ekstrakcijos metu pagerino flavanonų tirpumą ir stabilumą. Magnio aliuminio metasilikatas pasižymėjo selektyviu poveikiu: padidino NAR kiekį segmentinėse pertvarose, tačiau sumažino NR išeigą maždaug 15 proc., lyginant su kontroliniais mėginiais ($p < 0,05$). Šis poveikis leidžia teigti, kad ši medžiaga veiksmingiau stabilizuoja aglikonus nei glikozidus. Kitų autorių tyrimuose taip pat nustatyta, kad magnio aliuminio metasilikatas gali veikti kaip nešiklis ir padidinti tam tikrų fitocheminių junginių išsiskyrimą iš augalinės žaliavos. Manoma, kad jo sąveika su junginiais gali priklausyti nuo jų poliarumo ir molekulinio dydžio [23,72].

Ciklodekstrinai (CD) turėjo skirtingą poveikį flavanonų išeigai. α-CD ir γ-CD flavanonų išeigos statistiškai reikšmingai nepakeitė ($p > 0,05$), tuo tarpu β-CD reikšmingai padidino tiek NR, tiek NAR koncentraciją ($p < 0,05$). Segmentinių pertvarų mėginiuose NR koncentracija padidėjo nuo 7,8 ± 0,39 iki 58,06 ± 2,9 mg/g, o NAR – nuo 65,84 ± 3,39 iki 91,19 ± 4,55 μg/g. Toks β-CD poveikis gali būti siejamas su jo gebėjimu sudaryti stabiliausius inkluzinius kompleksus su flavanonų molekulėmis, nes β-CD ertmės dydis laikomas optimaliai pritaikytu daugeliui flavonoidų struktūrų. Tokie kompleksai gali pagerinti flavonoidų tirpumą ir stabilumą. Literatūroje taip pat nurodoma, kad ciklodekstrinai gali didinti fitocheminių junginių tirpumą ir stabilumą augaliniuose ekstraktuose, pavyzdžiui, padidinti izoflavonų išeigą iš *Trifolium pratense* L. ekstraktų bei pagerinti fenolinių junginių tirpumą ir antioksidacinį stabilumą *Aspalathus linearis* (Burm.f.) ekstraktuose [25,73–75].

Teigiamas CD poveikis buvo akivaizdus ir vertinant bendrą fenolinių junginių kiekį (TPC) bei bendrą flavonoidų kiekį (TFC): TPC ir TFC padidėjo daugiau kaip du kartus, ypač mėginiuose iš mezokarpio ir segmentinės pertvaros ($p < 0,05$).

Naudojant β-CD, mėginiuose iš egzokarpinės dalies antioksidacinis aktyvumas (DPPH metodu) padidėjo nuo 517,14 ± 25,86 iki 630,76 ± 31,54 μmol/g TE ($p < 0,05$). ABTS metodu aktyvumo padidėjimas – nuo 8,97 ± 0,45 iki

18,61 ± 0,93 μg TE/g ($p < 0,05$). Greipfrutų sultyse β-CD įtaka buvo mažiau ryškesnė (18,61 ± 0,93 iki 20,56 ± 1,03 μg TE/g), tačiau pokytis taip pat buvo statistiškai reikšmingas ($p < 0,05$). Didžiausias redukcinis aktyvumas (FRAP metodu) buvo nustatytas greipfrutų sultyse (12336 ± 616,8 μmol/g TE) ir egzokarpio dalyje (8969 ± 448,5 μmol/g TE). Literatūroje nurodoma, kad ciklodekstrinai gali sudaryti inkluzinius kompleksus su flavonoidais ir taip pagerinti jų tirpumą bei stabilumą. Vis dėlto šio tyrimo rezultatai rodo, kad β-CD poveikis antioksidaciniam aktyvumui gali skirtis priklausomai nuo žaliavos tipo ir flavanonų sudėties ekstraktuose [76,77]. Mažesnis β-CD poveikis greipfrutų sultyse gali būti susijęs su skirtinga bioaktyvių junginių sudėtimi, nes žievelės ekstraktuose paprastai aptinkama didesnė flavanonų koncentracija.

In vivo tyrimų dalyje buvo lyginamas greipfrutų žievelės ekstrakto ir gryno NR poveikis pelėms, kurioms oksidacinis stresas buvo sukeltas aliuminio chloridu ($AlCl_3$). Oksidacinis stresas buvo vertinamas matuojant redukuoto glutationo (GSH), malondialdehido (MDA) ir fermentinių antioksidantų – katalazės (CAT) bei glutationo reduktazės (GR) – aktyvumą kraujyje, kepenyse ir smegenyse.

Kraujyje NR statistiškai reikšmingai ($p < 0,05$) padidino GSH kiekį, ypač vartojant kartu su $AlCl_3$. GSH koncentracija buvo daugiau nei dvigubai didesnė, palyginti su kontroline grupe. Greipfrutų ekstraktas (GE) taip pat padidino GSH kiekį, tačiau šis padidėjimas buvo mažesnis nei NR grupėje. MDA koncentracija buvo mažiausia E + $AlCl_3$ grupėje ir statistiškai reikšmingai ($p < 0,05$) sumažėjo beveik 50 proc., palyginti su $AlCl_3$ grupe, o tai rodo stipresnį GE apsauginį poveikį nuo lipidų peroksidacijos. Gauti rezultatai rodo skirtingą veikimo mechanizmą: NR labiau skatino endogeninio GSH kiekio padidėjimą, o GE veiksmingiau slopino lipidų peroksidacijos procesus.

Smegenų audinyje NR statistiškai reikšmingai ($p < 0,05$) padidino GSH koncentraciją, pasiekdamas daugiau nei tris kartus didesnį lygį nei $AlCl_3$ grupėje, kas rodo jo gebėjimą aktyvinti endogenines antioksidacines sistemas. Tuo tarpu greipfrutų ekstraktas veiksmingiau sumažino MDA kiekį – nustatytas apie 40 proc. statistiškai reikšmingas ($p < 0,05$) sumažėjimas, palyginti su $AlCl_3$ grupe. Vertinant katalazės (CAT) aktyvumą, grynas NR išlaikė reikšmes, artimas kontrolinės grupės lygiui, o GE poveikis buvo mažiau ryškus. Šie rezultatai leidžia daryti prielaidą, kad grynas NR labiau palaiko fermentinių antioksidacinių sistemų aktyvumą smegenų audinyje.

Kepenyse stebėtas priešingas modelis. Greipfrutų ekstraktas statistiškai reikšmingai ($p < 0,05$) padidino CAT aktyvumą, daugiau nei 50 proc. viršydamas kontrolinės grupės reikšmes, kas rodo adaptacinės fermentinės antioksidacinės gynybos aktyvaciją. Tuo tarpu grynas NR, vartojamas kartu su $AlCl_3$, reikšmingiau padidino GSH koncentraciją ($p < 0,05$), kas gali rodyti

stipresnį jo poveikį hepatocitų redokso pusiausvyros palaikymui. Literatūroje taip pat nurodoma, kad flavonoidai gali moduliuoti kepenų antioksidacines sistemas tiek aktyvindami fermentinius mechanizmus, tokius kaip katalazė, tiek didindami nefermentinių antioksidantų, įskaitant glutationą, kiekį [78].

In vivo duomenys parodė skirtingą antioksidacinį profilį: greipfrutų žievelių ekstraktas veiksmingiau sumažino oksidacinį lipidų pažeidimą. Pastebėta, kad grynas naringinas stipriai padidino GSH koncentraciją, kas rodo ryškią glutationo metabolizmo aktyvaciją. Manoma, kad šis poveikis gali būti susijęs su NR gebėjimu moduliuoti Nrf2 faktoriaus signalinį kelią, kuris reguliuoja pagrindinių antioksidacinių fermentų ir glutationo sintezėje dalyvaujančių fermentų ekspresiją. Staigus šios sistemos aktyvinimas gali būti siejamas su kompensaciniu atsaku į oksidacinį stresą arba su tiesioginiu flavonoidų poveikiu redokso reguliacijos mechanizmams. Tačiau pernelyg intensyvi antioksidacinių sistemų aktyvacija gali sutrikdyti fiziologinę redokso pusiausvyrą, nes pernelyg didelis antioksidantų aktyvumas gali slopinti ląstelių signalinius procesus, kuriuose reaktyviosios deguonies formos veikia kaip svarbūs signaliniai mediatoriai. Tokie duomenys rodo, kad izoliuotų flavonoidų poveikis gali būti stipresnis ir labiau nukreiptas į specifinius antioksidacinius kelius nei kompleksinių augalinių ekstraktų, kuriuose skirtingi bioaktyvūs komponentai gali veikti sinergiškai ir palaikyti subalansuotą antioksidacinį atsaką [13,56].

Siekiant pagerinti greipfrutų žievelių ekstraktų technologines ir funkcines savybes, buvo atliktas jų įkapsuliavimas taikant purškiamojo ir sublimacinio (liofilizacinio) džiovinimo metodus. Mikrokapsulių apvalkalui suformuoti naudoti įvairūs pagalbiniai komponentai (MD, SK, β-CD ir CMC). Įvertintas šių medžiagų poveikis gautų miltelių išeigai, likutiniam drėgmės kiekiui, sudrėkimo laikui, byrėjimui, tirpumui, įkapsuliavimo veiksmingumui bei morfologinėms savybėms.

Džiovinimo metodas reikšmingai paveikė galutinę produkto išeigą ir biologiškai aktyvių junginių išsaugojimą. Purškiamojo džiovinimo metu išeiga siekė 48–53 proc., o didžiausia vertė nustatyta esant 160 °C įėjimo temperatūrai (M3 formulė – 52,95 proc.). Temperatūrai padidėjus iki 170 °C, išeiga sumažėjo iki 48 proc., greičiausiai dėl fenolinių junginių terminės degradacijos ir paviršiaus plutelės susidarymo, ribojančio tirpiklio išgaravimą. Literatūroje taip pat nurodoma, kad didesnės purškiamojo džiovinimo temperatūros gali skatinti bioaktyviųjų junginių degradaciją citrusinių vaisių ekstraktuose, ypač viršijus 180 °C ribą [78].

Liofilizuoti mėginiai pasižymėjo statistiškai reikšmingai ($p < 0,05$) didesne išeiga 69,7–79,2 proc., o tai rodo, kad ekstrakto masė išsaugojama veiksmingiau ir švelnesnėmis proceso sąlygomis. Literatūroje taip pat nurodoma, kad liofilizavimas dažnai leidžia išsaugoti didesnį sausųjų medžiagų kiekį au-

galiniuose ekstraktuose. Pavyzdžiui, Da Silva Júnior ir kt. nustatė, kad liofilizuojant *Spondias purpurea* (ciriguelos) žievelės ekstraktą gaunama didesnė bendroji sausųjų medžiagų išeiga nei taikant purškiamojo džiovinimo metodą [30].

Drėgmės kiekis purškiamojo džiovinimo metu gautuose milteliuose kito nuo 5,3 iki 7,6 proc., mažiausios reikšmės nustatytos β-CD turinčiuose mėginiuose (pvz., MBC2 ir MBC3 < 5,5 proc., palyginti su sistemomis be β-CD, > 7 proc.; $p < 0,05$). Liofilizuotuose mėginiuose drėgmės kiekis siekė 4,7–5,8 proc. Mažesnis drėgmės kiekis β-CD turinčiuose mėginiuose gali būti siejamas su ciklodekstrinų gebėjimu sudaryti inkluzinius kompleksus su bioaktyviais junginiais ir taip modifikuoti susidarančių dalelių struktūrą bei vandens absorbcines savybes. Literatūroje taip pat nurodoma, kad ciklodekstrinai gali prisidėti prie stabilesnių mikroenkapsuliuotų sistemų susidarymo ir pagerinti bioaktyviųjų junginių stabilumą džiovintuose ekstraktuose [79].

Purškiamojo džiovinimo metu gautos kapsulės, turinčios didesnę β-CD koncentraciją, pasižymėjo ilgesniu sudrėkimo laiku (>1400 s), kas gali būti siejama su mažiau laidžios dalelių struktūros formavimusi. Liofilizuoti mėginiai sudrėko greičiau; trumpiausias sudrėkimo laikas nustatytas L2 mėginyje, nors jo sudėtis buvo panaši į L1, kas rodo, kad svarbus ne tik bendras komponentų kiekis, bet ir jų tarpusavio santykis. Literatūroje taip pat nurodoma, kad liofilizacijos metu susidariusi porėta struktūra gali palengvinti vandens įsiskverbimą į daleles [80,81].

Miltelių birumo savybės, vertintos pagal Carr indeksą ir Hausner santykį, priklausė nuo apvalkalą formuojančių medžiagų sudėties. Purškiamuoju džiovinimu gautų miltelių Hausner santykis svyravo nuo 1,438 iki 1,636, o prasčiausias birumas nustatytas MBC1 mėginyje, kuriame naudota didžiausia β-CD ir CMC koncentracija. MD įtraukimas statistiškai reikšmingai ($p < 0,05$) pagerino miltelių tekamumą, tikėtina dėl sumažėjusio dalelių lipnumo ir agregacijos. Liofilizuoti mėginiai pasižymėjo geresnėmis birumo savybėmis (Carr indeksas 30–34 proc.; Hausner santykis < 1,52).

Mikrokapsulių tirpumas priklausė nuo apvalkalą formuojančių medžiagų sudėties ir taikyto džiovinimo metodo. Purškiamuoju džiovinimu gautų kapsulių tirpumas siekė 30–66 proc., o liofilizuotų – 31–62 proc. Didesnė MD koncentracija padidino tirpumą, tikėtina dėl geresnės dalelių dispergacijos ir mažesnės agregacijos. Tuo tarpu β-CD ir CMC turinčiose sistemose tirpumas buvo mažesnis, kas gali būti siejama su tankesnės struktūros formavimusi ir ribota vandens difuzija. Literatūroje taip pat nurodoma, kad MD gali pagerinti mikrokapsulių tirpumą ir dalelių pasiskirstymą, nes mažina dalelių sulipimą ir palengvina vandens difuziją į matricą, kaip parodė Xiao ir kt. tyrimas [30,83].

Įkapsuliavimo efektyvumas (EE) svyravo nuo 76,7 iki 91,4 proc., o didžiausia vertė nustatyta purškiamuoju džiovinimu gautame β-CD turinčiame mėginyje (MBC3). Didesnis EE gali būti siejamas su β-CD gebėjimu stabilizuoti flavanonus ir sumažinti jų degradaciją džiovinimo metu. Vis dėlto mėginiuose, kuriuose β-CD ar CMC koncentracija buvo didesnė, EE sumažėjo, nors šie pokyčiai ne visais atvejais buvo statistiškai reikšmingi ($p > 0,05$), kas gali rodyti ribotą komponentų suderinamumą sistemoje. Zhao ir kt. tyrimuose taip pat nurodoma, kad ciklodekstrinai gali prisidėti prie flavonoidų stabilumo didinimo mikroenkapsuliuotose sistemose, tačiau šio poveikio mastas priklauso nuo pagalbinių medžiagų sudėties ir jų tarpusavio suderinamumo [83–84].

Liofilizuotų mėginių EE buvo mažesnis (76,8–88,6 proc.), tačiau jie išsaugojo daugiau bendrojo fenolinių junginių kiekio. Tai rodo, kad švelnesnės liofilizacijos sąlygos veiksmingiau apsaugo bioaktyviąsias medžiagas nuo skaidymosi, ypač jautrias oksidacijai ar termodegradacijai. Tokia tendencija atitinka literatūroje aprašytus rezultatus, pabrėžiančius liofilizacijos pranašumus išsaugant antioksidacinius komponentus įvairių augalinės kilmės ekstraktų įkapsuliavimo metu [32–35].

Skenuojančios elektroninės mikroskopijos (SEM) analizė atskleidė ryškius morfologinius skirtumus tarp skirtingais būdais gautų mikrokapsulių. Purškiamojo džiovinimo metu suformuotos dalelės buvo sferinės arba pusiau sferinės formos, o jų paviršiaus struktūra priklausė nuo naudojamų apvalkalą formuojančių medžiagų. Mėginiai, turintys daug lieso pieno miltelių (pvz., MBC4), pasižymėjo lygesniu ir tolygesniu paviršiumi, o β-CD turintys mėginiai dažniau sudarė labiau raukšlėtus paviršius. Tai siejama su β-CD gebėjimu formuoti tankesnes struktūras, kurios džiovinimo metu gali sukelti paviršiaus susitraukimų ir deformacijų.

Priešingai, liofilizacijos metu gautos mikrokapsulės pasižymėjo netaisyklinga, porėta ir sluoksniuota struktūra. Toks morfologinis vaizdas atspindi būdingus liofilizacijos proceso bruožus – švelnų vandens šalinimą per sublimaciją, kuris nesukelia greito išorinio paviršiaus kietėjimo, bet sudaro erdvę trapios tekstūros matricai. Nors liofilizuotų mikrokapsulių porėta struktūra gali palengvinti tirpimą, purškiamuoju džiovinimu gautos kapsulės pasižymėjo vienodesne morfologija ir geresnėmis technologinėmis savybėmis, todėl šis metodas buvo pasirinktas tolesniems tyrimams.

Siekiant pagerinti flavanonų tirpumą ir biologinį pasisavinimą, papildomai buvo suformuoti lipidiniai nešikliai – liposomos, į kurių sudėtį buvo įtrauktas greipfrutų ekstraktas arba grynas NR. Liposomų fizikinė ir cheminė charakteristika parodė, kad visos sistemos buvo nanoskalės ribose (94–102 nm), o polidispersijos indeksai nesiekė $PDI < 0,4$. Tai rodo gerą jų tinkamumą geriamajam vartojimui. Padidinus lipidų ir veikliosios medžiagos santykį nuo 1:1

iki 2:1 (EL2 *vs*. EL1), sumažėjo pūslelių dydis, susiformavo kompaktiškesni dvisluoksniai, siauriau pasiskirstė dalelių dydžiai. Kitų tyrimų, nagrinėjančių kvercetino ir kitų citrusiniuose vaisiuose randamų bioaktyviųjų junginių liposomas, duomenimis, didesnė fosfolipidų koncentracija yra susijusi su padidėjusiu liposomų stabilumu ir homogeniškumu [86,87].

Paviršiaus ζ (dzeta) potencialo reikšmės kito nuo –10,4 iki –25,8 mV, o didesnė neigiama paviršiaus įkrova siejama su geresniu koloidiniu stabilumu, nes tai padeda apsaugoti daleles nuo agregacijos elektrostatinio atstūmimo jėgų pagalba [87–90]. Remiantis šiais parametrais, stabiliausiomis buvo pasirinktos EL2 ir NL2 formulės.

Siekiant išsaugoti struktūrinį liposomų vientisumą ir padidinti veikliųjų medžiagų stabilumą, buvo pasitelktas dvigubo įkapsuliavimo principas – flavanonai pirmiausia buvo įkapsuliuoti į liposomų dvisluoksnę membraną, o vėliau liposominis tirpalas buvo paverstas milteliais naudojant purškiamojo džiovinimo metodą su β-CD, MD ir CMC apvalkalą formuojančiomis medžiagomis. Šio tyrimo metu, buvo įvertinta miltelių išeiga, drėgmės kiekis ir įkapsuliavimo efektyvumas, siekiant įvertinti šių sistemų tinkamumą praktiniam taikymui.

Purškiamuoju džiovinimu gautų miltelių išeiga svyravo nuo 36 iki 43 proc. Didesnė išeiga nustatyta greipfrutų ekstrakto pagrindu paruoštuose mėginiuose (43,0 ± 2,15 proc. ir 41,05 ± 1,60 proc.), o mažesnė – gryno NR sistemose (36,70 ± 1,83 proc. ir 38,15 ± 1,91 proc.) ($p < 0,05$). Įtraukus lipidinius nešiklius, išeiga šiek tiek sumažėjo, kas gali būti siejama su sudėtingesne lašelių atomizacija ir lipidinių dalelių adhezija prie purškiamojo džiovinimo kameros sienelių [91].

Likutinis drėgmės kiekis visuose mėginiuose neviršijo 6 proc., kas laikoma tinkama riba džiovintų miltelių stabilumui užtikrinti, nors didžiausia vertė nustatyta lipidinėse NR sistemose (5,58 proc.). Įkapsuliavimo veiksmingumas buvo didžiausias liposominėse sistemose su greipfrutų ekstraktu (99,4 proc.), palyginti su neliposominėmis sistemomis (81–91 proc.), kas gali būti siejama su fosfolipidinio dvi sluoksnio gebėjimu apsaugoti bioaktyvius junginius nuo degradacijos [37,92].

Liposomų stabilizuojantis poveikis bioaktyviems junginiams aprašytas ir kituose tyrimuose, kuriuose nanoliposomos sėkmingai įkapsuliavo hidrofobinius polifenolius, tokius kaip naringinas ir naringeninas [37]. Taip pat nustatyta, kad angliavandenių nešikliai gali didinti įkapsuliavimo veiksmingumą ir stabilumą purškiamuoju džiovinimu gautose sistemose [93].

Absoliutus tirpumas buvo didžiausias gryno NR ne liposominėse mikrokapsulėse (306 μg/mL), tačiau jų tirpumo veiksmingumas tesiekė 5,6 proc. Liposominiai milteliai (NLS, ELS) pasižymėjo daug mažesniu absoliučiu tirpumu (17–93 μg/mL), bet kelis kartus didesniu tirpumo veiksmingumu

(42,7–55,3 proc.). SEM analizė parodė, kad purškiant gautos liposominės kapsulės buvo lygesnio paviršiaus ir vienodesnės, palyginti su ne liposominiais mėginiais, kurių paviršius buvo labiau raukšlėtas ir netolygus.

Žandinės burnos plėvelės buvo sukurtos kaip alternatyvus peroralinis veikliųjų medžiagų tiekimo būdas, siekiant išvengti flavanonų skilimo virškinamajame trakte. Iš HPMC – alginato (EP1, NP1) ir HPMC – PVA (EP2, NP2) matricų sukurtos plėvelės parodė akivaizdžius fizikinių–cheminių ir funkcinių savybių skirtumus, patvirtinančius reikšmingą polimero tipo ir veikliosios medžiagos šaltinio įtaką. Gryno NR plėvelės (NP1, NP2) pasižymėjo didžiausiu atpalaidavimu dirbtinėse seilėse: jų tirpumo efektyvumas (DE) atitinkamai siekė 37,5 proc. ir 40,9 proc. Priešingai, ekstrakto pagrindu sukurtose plėvelėse (E1 ir E2) naringino atpalaidavimas buvo žymiai mažesnis, o tirpumo efektyvumas atitinkamai sudarė 40,2 proc. ir 26,6 proc. Tirpimo trukmė taip pat skyrėsi priklausomai nuo naudoto polimero: EP1 (alginatas – HPMC) plėvelės tirpo lėčiausiai (35 min) dėl tankaus alginato gelio formavimosi, kuris riboja difuziją, o EP2 (PVA–HPMC) plėvelės greičiau suiro (5 min) dėl didesnio polimero gebėjimo prisijungti vandenį ir spartesnio irimo. Gryno NR plėvelės pasižymėjo vidutine tirpimo trukme (15–20 min). Panašų polimero tipo poveikį tirpimo kinetikai aprašė ir Maslii su bendraautoriais, kurie, lygindami alginato, CMC, HEC, HPC ir PVA pagrindu sukurtas plėveles, nustatė, jog alginato turinčios matricos tirpo lėčiau dėl gelio formavimosi, o PVA pagrindu sukurtos sistemos greičiau suiro, tai sutampa su šio tyrimo rezultatais [93].

Tyrimai parodė, kad ekstrakto pagrindu sukurtos plėvelės (EP1, EP2) turėjo didesnį drėgmės kiekį (13,5–15,2 proc.), palyginti su gryno NR plėvelėmis (11,5 proc.). Šis skirtumas siejamas su higroskopinių cukrų ir polifenolių, esančių greipfrutų žievelių ekstrakte, buvimu. Literatūroje taip pat nurodoma, kad chitozano plėvelės, papildytos Aloe vera ekstraktu, pasižymi didesniu drėgmės kiekiu nei grynos chitozano plėvelės dėl ekstrakte esančių polisacharidų hidrofiliškumo. Padidėjęs drėgmės kiekis taip pat nustatytas pektino–propolio ir krakmolo–želatinos plėvelėse, papildytose žaliosios arbatos ekstraktu, palyginti su atitinkamomis kontrolinėmis (be ekstrakto) plėvelėmis [94–96]. Tokiais atvejais augalinės kilmės komponentai, tokie kaip cukrūs ir polifenoliai, gali padidinti plėvelės matricos higroskopiškumą.

Didžiausias gleivinės sukibimo stiprumas (mukoadhezinis stiprumas) buvo nustatytas NP2 (0,09 N, 0,47 N·s) ir NP1 (0,08 N, 0,46 N·s) mėginiuose, tai patvirtina stiprų PVA ir alginato indėlį į mukoadheziją per vandenilinius ryšius ir jonines sąveikas su mucinu. Ekstraktu prisotintos plėvelės pasižymėjo mažesne adhezijos energija (EP1: 0,53 N·s; EP2: 0,25 N·s), tai rodo, jog ekstrakto komponentai galėjo trikdyti optimaliai polimero ir mucino sąveikai. Vis dėlto vizualiniai stebėjimai parodė, kad visos plėvelės pasižymėjo greitu

drėkimu ir geru sukibimu su stikliniu paviršiumi, o tai rodo, kad paviršiaus brinkimas skatino prisitvirtinimą net ir mažesnio sukibimo atvejais. Nustatyta, kad ekstrakto pagrindu sukurtos plėvelės buvo tamsesnės (geltonai rudos) dėl flavonoidų ir fenolinių pigmentų, o NR plėvelės buvo skaidresnės.

In vitro atpalaidavimo tyrimai parodė, kad pasirinkta veikliųjų medžiagų tiekimo sistema turėjo reikšmingos įtakos NR tirpumui ir atpalaidavimo veiksmingumui. Purškiamojo džiovinimo metodu gautos mikrokapsulės pasižymėjo dideliu pradiniu NR atpalaidavimu rūgščioje terpėje (SGF. pH 1,2) – 274,26 ± 2,15 μg/mL po 30 min, tačiau šis kiekis sudarė tik apie 6 proc. teorinio veikliosios medžiagos kiekio (163,8 mg). Tolesnį atpalaidavimą ribojo rekristalizacijos procesai, rodantys prastą NR tirpumą rūgštinėje aplinkoje.

Dvigubai įkapsuliuotas NR pasižymėjo žymiai mažesniu atpalaidavimu po 30 min (55,36 ± 0,44 μg/ml), tačiau koncentracija išliko stabili net ir po 90 min (55,87 ± 0,33 μg/ml). Tokia dinamika rodo, kad veikliosios medžiagos išsiskyrimą ribojo difuzija, kuri buvo reguliuojama lipidinės dvisluoksnės membranos ir angliavandenių matricos.

Ekstrakto pagrindu sukurtos mikrokapsulės pasižymėjo kitokiu atpalaidavimo pobūdžiu: po 30 min NR koncentracija siekė 130,67 ± 3,21 μg/ml, po 90 min – 135,71 ± 2,16 μg/ml, o tai atitiko beveik visą teorinį veikliosios medžiagos kiekį (4,53 mg, t. y. 94–98 proc.). Dvigubai įkapsuliuotas greipfrutų ekstraktas pasižymėjo žemiausiu absoliučiu atpalaidavimo lygiu (9,87–10,85 μg/ml), tačiau šis kiekis atitiko 32–36 proc. teorinio kiekio (0,94 mg).

Perėjus į žarnyno sąlygas (SIF, pH ~6,8), buvo pastebėtas atpalaidavimo profilio pokytis. Gryno NR formulėse, NR koncentracija po pradinio piko sumažėjo iki 208,53 ± 1,95 μg/ml (po 120 min), bet vėliau vėl padidėjo iki 220,82 ± 1,65 μg/ml (po 180 min), tai rodo, kad neutralioje terpėje įvyksta tirpumo pusiausvyra tarp nusodinimo ir pakartotinio ištirpimo procesų.

GE mikrokapsulėse, NR koncentracijos žarnyno terpėje išliko stabilios (148,35 ± 2,37 μg/mL po 120 min ir 146,88 ± 2,01 μg/mL po 180 min). Šie duomenys rodo, kad NR atpalaidavimas vyko pastoviu difuzijos būdu, beveik nepriklausomu nuo pH pokyčių.

Dvigubai įkapsuliuotos sistemos (NR ir GE) pasižymėjo lėtesniu ir stabilesniu NR atpalaidavimu žarnyno terpėje. NR formulėse – NR koncentracija po 120 min. siekė 56,89 ± 0,68 μg/ml ir stabilizavosi ties 52,07 ± 0,55 μg/ml po 180 min., o GE sistemose išliko dar mažesnė (11,24 ± 0,41 ir 9,94 ± 0,36 μg/ml). Tai rodo, kad dviguba įkapsuliacija moduliuoja NR išsiskyrimo kinetiką ir užtikrina labiau kontroliuojamą atpalaidavimą.

Žandinės burnos plėvelės buvo tiriamos kaip alternatyvus NR tiekimo būdas, siekiant apeiti virškinamojo trakto fermentinį skaidymą. Gryno NR plėvelė (PVA – HPMC) pasižymėjo didžiausiu atpalaidavimu: 72,13 ± 2,85 μg/ml (po 10 min) ir 69,97 ± 3,01 μg/ml (po 30 min). Ištirpusio NR kiekis

sudarė 41 proc. nuo įkapsuliuoto kiekio; (alginatas – HPMC) atpalaidavo 63,99 ± 2,64 μg/ml (38 proc.), kas siejama su lėtesniu alginato išbrinkimu ir ribota difuzija. Ekstrakto pagrindu sukurtos plėvelės (alginatas – HPMC) atpalaidavo 27,08 ± 1,42 μg/ml (40 proc.), tačiau pasižymėjo ilgiausia ištirpimo trukme (35 min); (PVA – HPMC) suiro per trumpiausią laiką (5 min), tačiau dėl mažesnės pradinės NR įkrovos atpalaidavo tik 18,45 ± 1,05 μg/ml (27 proc.) [98].

Apibendrinant galima teigti, kad purškiamuoju džiovinimu gautos mikrokapsulės užtikrina greitą pradinį NR išsiskyrimą, tačiau pasižymi ribotu tirpumo veiksmingumu. Dvigubas įkapsuliavimas lėtina atpalaidavimą rūgščioje terpėje ir padidina stabilumą žarnyno sąlygomis. Žandinės burnos plėvelės leidžia pasiekti greitą vietinį veikliosios medžiagos tiekimą, o polimero tipas reikšmingai veikia tiek tirpimo kinetiką, tiek adhezines savybes.

Išvados

1. Ultragarsinė ekstrakcija derinama su terminę hidrolizė buvo veiksmingiausia flavanonų išgavimo strategija iš greipfrutų žievelių. Nustatyta, kad taikant kombinuotą metodą galima pasiekti panašią flavanonų išeigą naudojant mažesnės koncentracijos etanolį, todėl ekstrakcijos procesas gali būti optimizuotas sumažinant tirpiklio koncentraciją.
2. Pagalbinių medžiagų (β-, α-, γ- CD ir magnio aluminio metasilikato) taikymas ekstrakcijos metu turėjo statistiškai reikšmingą poveikį flavanonų išeigai, stabilumui bei antioksidaciniam aktyvumui. β-CD padidino tiek NR, tiek NAR išeigą daugiau nei tris kartus ($p < 0,05$) ir sustiprino bendrą antioksidacinį aktyvumą. Magnio aluminio metasilikatas selektyviai stabilizavo aglikoninę formą (NAR), tačiau sumažino NR išeigą (15 proc.).
3. *In vivo* tyrimai parodė skirtingus antioksidacinio veikimo mechanizmus. Grynas naringinas reikšmingai padidino glutationo kiekį ir palaikė fermentinių antioksidacinių sistemų aktyvumą, o greipfrutų žievelių ekstraktas veiksmingiau mažino lipidų peroksidaciją, kas rodo kompleksinių fitocheminių junginių sinerginį poveikį.
4. Mikroenkapsuliavimo metodai ir apvalkalą formuojančių medžiagų parinkimas turėjo statistiškai reikšmingos įtakos flavanonų stabilumui ir miltelių technologinėms savybėms. Liofilizacijos būdu gauti milteliai pasižymėjo didesne išeiga (69,7–79,2 proc.), o purškiamojo džiovinimo metu pasiektas didžiausias įkapsuliavimo veiksmingumas (iki 91,4 proc.). SEM analizė patvirtino, kad purškiamojo džiovinimo metodu gauti milteliai turėjo tolygesnę, sferinę morfologiją.

5. Liposominės sistemos pagerino flavanonų (NR ir NAR) tirpumą, stabilumą ir atpalaidavimo kontrolę. Padidinus lipidų ir veikliosios medžiagos santykį nuo 1:1 iki 2:1 sumažėjo dalelių dydis (iki 94 nm) ir padidėjo sistemos stabilumas. Dviguba įkapsuliacija pailgino NR išsiskyrimą žarnyno terpėje ir reikšmingai padidino tirpumo veiksmingumą, palyginti su neinkapsuliuotu NR.
6. Žandinės burnos plėvelės (PVA–HPMC ir alginato–HPMC matricose) pasirodė tinkamos greitam naringino tiekimui per burnos gleivinę, apeinant virškinimo traktą. Gryno NR plėvelės pasižymėjo didžiausiu atpalaidavimo kiekiu, o ekstrakto pagrindu sukurtos plėvelės – ilgesne tirpimo trukme ir didesniu drėgmės kiekiu. Nustatyta, kad polimerų sudėtis reikšmingai lemia plėvelių tirpimo kinetiką ir mukoadhezinį stiprumą.

REFERENCES

1. Mulat, M.; Banicod, R.J.S.; Tabassum, N.; Javaid, A.; Karthikeyan, A.; Jeong, G.-J.; Kim, Y.-M.; Jung, W.-K.; Khan, F. Multiple Strategies for the Application of Medicinal Plant-Derived Bioactive Compounds in Controlling Microbial Biofilm and Virulence Properties. *Antibiotics* **2025**, *14*, 555, doi:10.3390/antibiotics14060555.
2. Cederberg, C.; Sonesson, U. *Global Food Losses and Food Waste: Extent, Causes and Prevention; Study Conducted for the International Congress Save Food! At Interpack 2011, [16 - 17 May], Düsseldorf, Germany*; Gustavsson, J., Ed.; Food and Agriculture Organization of the United Nations: Rome, 2011; ISBN 978-92-5-107205-9.
3. Nirmal, N.; Khanashyam, A.; Mundanat, A.; Shah, K.; Babu, K.; Thorakkattu, P.; Al-Asmari, F.; Pandiselvam, R. Valorization of Fruit Waste for Bioactive Compounds and Their Applications in the Food Industry. *Foods* **2023**, *12*, 556, doi:10.3390/foods12030556.
4. Faulisi, M.V.; Palmeri, R.; Restuccia, C. Multifunctional Application of Food Grade Extracts from Fruit Processing Industry Wastes: A Sustainable Approach to Food and Health Preservation. *Food Bioscience* **2024**, *62*, 105204, doi:10.1016/j.fbio.2024.105204.
5. Andrade, M.A.; Barbosa, C.H.; Shah, M.A.; Ahmad, N.; Vilarinho, F.; Khwaldia, K.; Silva, A.S.; Ramos, F. Citrus By-Products: Valuable Source of Bioactive Compounds for Food Applications. *Antioxidants* **2022**, *12*, 38, doi:10.3390/antiox12010038.
6. Li, P.; Yao, X.; Zhou, Q.; Meng, X.; Zhou, T.; Gu, Q. Citrus Peel Flavonoid Extracts: Health-Beneficial Bioactivities and Regulation of Intestinal Microecology in Vitro. *Front. Nutr.* **2022**, *9*, 888745, doi:10.3389/fnut.2022.888745.
7. Bacanlı, M.; Başaran, A.A.; Başaran, N. The Major Flavonoid of Grapefruit: Naringin. In *Polyphenols: Prevention and Treatment of Human Disease*; Elsevier, 2018; pp. 37–44 ISBN 978-0-12-813008-7.
8. Shilpa, V.; Shams, R.; Dash, K.K.; Pandey, V.K.; Dar, A.H.; Ayaz Mukarram, S.; Harsányi, E.; Kovács, B. Phytochemical Properties, Extraction, and Pharmacological Benefits of Naringin: A Review. *Molecules* **2023**, *28*, 5623, doi:10.3390/molecules28155623.
9. Cai, J.; Wen, H.; Zhou, H.; Zhang, D.; Lan, D.; Liu, S.; Li, C.; Dai, X.; Song, T.; Wang, X.; et al. Naringenin: A Flavanone with Anti-Inflammatory and Anti-Infective Properties. *Biomedicine & Pharmacotherapy* **2023**, *164*, 114990, doi:10.1016/j.biopha.2023.114990.
10. Ahmed, O.M.; Ahmed, A.A.; Fahim, H.I.; Zaky, M.Y. Quercetin and Naringenin Abate Diethylnitrosamine/Acetylaminofluorene-Induced Hepatocarcinogenesis in Wistar Rats: The Roles of Oxidative Stress, Inflammation and Cell Apoptosis. *Drug and Chemical Toxicology* **2022**, *45*, 262–273, doi:10.1080/01480545.2019.1683187.
11. Xin, Z.; Gao, Y.; He, L.; Xiu, Z.; Sun, L. Bioactive Antioxidants from Avocado By-Products: Mechanistic Study and Laboratory-Scale Extraction Optimization. *Antioxidants* **2025**, *14*, 1225, doi:10.3390/antiox14101225.
12. Alam, M.A.; Subhan, N.; Rahman, M.M.; Uddin, S.J.; Reza, H.M.; Sarker, S.D. Effect of Citrus Flavonoids, Naringin and Naringenin, on Metabolic Syndrome and Their Mechanisms of Action. *Advances in Nutrition* **2014**, *5*, 404–417, doi:10.3945/an.113.005603.
13. Stabrauskiene, J.; Kopustinskiene, D.M.; Lazauskas, R.; Bernatoniene, J. Naringin and Naringenin: Their Mechanisms of Action and the Potential Anticancer Activities. *Biomedicines* **2022**, *10*, 1686, doi:10.3390/biomedicines10071686.
14. Peng, Y.; Qu, R.; Xu, S.; Bi, H.; Guo, D. Regulatory Mechanism and Therapeutic Potentials of Naringin against Inflammatory Disorders. *Heliyon* **2024**, *10*, e24619, doi:10.1016/j.heliyon.2024.e24619.

15. Wedamulla, N.E.; Fan, M.; Choi, Y.-J.; Kim, E.-K. Citrus Peel as a Renewable Bioresource: Transforming Waste to Food Additives. *Journal of Functional Foods* **2022**, *95*, 105163, doi:10.1016/j.jff.2022.105163.
16. Chen; Wang; Tan; Hu; Sundararajan; Zhou Profiling of Flavonoid and Antioxidant Activity of Fruit Tissues from 27 Chinese Local Citrus Cultivars. *Plants* **2020**, *9*, 196, doi:10.3390/plants9020196.
17. Ravetti, S.; Garro, A.G.; Gaitán, A.; Murature, M.; Galiano, M.; Brignone, S.G.; Palma, S.D. Naringin: Nanotechnological Strategies for Potential Pharmaceutical Applications. *Pharmaceutics* **2023**, *15*, 863, doi:10.3390/pharmaceutics15030863.
18. Zeng, X.; Su, W.; Zheng, Y.; He, Y.; He, Y.; Rao, H.; Peng, W.; Yao, H. Pharmacokinetics, Tissue Distribution, Metabolism, and Excretion of Naringin in Aged Rats. *Front. Pharmacol.* **2019**, *10*, 34, doi:10.3389/fphar.2019.00034.
19. Yang, Y.; Trevethan, M.; Wang, S.; Zhao, L. Beneficial Effects of Citrus Flavanones Naringin and Naringenin and Their Food Sources on Lipid Metabolism: An Update on Bioavailability, Pharmacokinetics, and Mechanisms. *The Journal of Nutritional Biochemistry* **2022**, *104*, 108967, doi:10.1016/j.jnutbio.2022.108967.
20. Zeng, X.; Zheng, Y.; He, Y.; Zhang, J.; Peng, W.; Su, W. Microbial Metabolism of Naringin and the Impact on Antioxidant Capacity. *Nutrients* **2022**, *14*, 3765, doi:10.3390/nu14183765.
21. Stabrauskiene, J.; Marksa, M.; Ivanauskas, L.; Bernatoniene, J. Optimization of Naringin and Naringenin Extraction from Citrus × Paradisi L. Using Hydrolysis and Excipients as Adsorbent. *Pharmaceutics* **2022**, *14*, 890, doi:10.3390/pharmaceutics14050890.
22. Sant, A.; Ahmad, I.; Bhatia, S. Extraction and Hydrolysis of Naringin from Citrus Fruit Peels. *IOP Conf. Ser.: Mater. Sci. Eng.* **2022**, *1263*, 012031, doi:10.1088/1757-899X/1263/1/012031.
23. Kazlauskaite, J.A.; Ivanauskas, L.; Bernatoniene, J. Novel Extraction Method Using Excipients to Enhance Yield of Genistein and Daidzein in Trifolium Pratensis L. *Pharmaceutics* **2021**, *13*, 777, doi:10.3390/pharmaceutics13060777.
24. Van Der Merwe, J.; Steenekamp, J.; Steyn, D.; Hamman, J. The Role of Functional Excipients in Solid Oral Dosage Forms to Overcome Poor Drug Dissolution and Bioavailability. *Pharmaceutics* **2020**, *12*, 393, doi:10.3390/pharmaceutics12050393.
25. Kazlauskaite, J.A.; Ivanauskas, L.; Bernatoniene, J. Cyclodextrin-Assisted Extraction Method as a Green Alternative to Increase the Isoflavone Yield from Trifolium Pratensis L. Extract. *Pharmaceutics* **2021**, *13*, 620, doi:10.3390/pharmaceutics13050620.
26. Vassilis Athanasiadis , Dimitrios Palaiogiannis, Eleni Bozinou; , Stavros I. Lalas andDimitrisP. Makris * β-Cyclodextrin-Aided Aqueous Extraction of Antioxidant Polyphenols from Peppermint (Mentha × Piperita L.). **2022**, doi:DOI:%2010.3390/oxygen2040029.
27. Raja Kumar, S.; Mohd Ramli, E.S.; Abdul Nasir, N.A.; Ismail, N.H.M.; Mohd Fahami, N.A. Preventive Effect of Naringin on Metabolic Syndrome and Its Mechanism of Action: A Systematic Review. *Evidence-Based Complementary and Alternative Medicine* **2019**, *2019*, 1–11, doi:10.1155/2019/9752826.
28. Elsawy, H.; Algefare, A.I.; Alfwuaires, M.; Khalil, M.; Elmenshawy, O.M.; Sedky, A.; Abdel-Moneim, A.M. Naringin Alleviates Methotrexate-Induced Liver Injury in Male Albino Rats and Enhances Its Antitumor Efficacy in HepG2 Cells. *Bioscience Reports* **2020**, *40*, BSR20193686, doi:10.1042/BSR20193686.
29. Han, H.-W.; Kwak, J.-H.; Jang, T.-S.; Knowles, J.C.; Kim, H.-W.; Lee, H.-H.; Lee, J.-H. Grapefruit Seed Extract as a Natural Derived Antibacterial Substance against Multidrug-Resistant Bacteria. *Antibiotics* **2021**, *10*, 85, doi:10.3390/antibiotics10010085.
30. Da Silva Júnior, M.E.; Araújo, M.V.R.L.; Martins, A.C.S.; Dos Santos Lima, M.; Da Silva, F.L.H.; Converti, A.; Maciel, M.I.S. Microencapsulation by Spray-Drying and

Freeze-Drying of Extract of Phenolic Compounds Obtained from Ciriguela Peel. *Sci Rep* **2023**, *13*, 15222, doi:10.1038/s41598-023-40390-4.
31. Baeza, R.; Chirife, J. Anthocyanin Content and Storage Stability of Spray/Freeze Drying Microencapsulated Anthocyanins from Berries: A Review. *International Journal of Food Engineering* **2021**, *17*, 927–944, doi:10.1515/ijfe-2021-0184.
32. Pudziuvelyte, L.; Marksa, M.; Jakstas, V.; Ivanauskas, L.; Kopustinskiene, D.M.; Bernatoniene, J. Microencapsulation of Elsholtzia Ciliata Herb Ethanolic Extract by Spray-Drying: Impact of Resistant-Maltodextrin Complemented with Sodium Caseinate, Skim Milk, and Beta-Cyclodextrin on the Quality of Spray-Dried Powders. *Molecules* **2019**, *24*, 1461, doi:10.3390/molecules24081461.
33. Pudziuvelyte, L.; Marksa, M.; Sosnowska, K.; Winnicka, K.; Morkuniene, R.; Bernatoniene, J. Freeze-Drying Technique for Microencapsulation of Elsholtzia Ciliata Ethanolic Extract Using Different Coating Materials. *Molecules* **2020**, *25*, 2237, doi:10.3390/molecules25092237.
34. Kazlauskaite, J.A.; Matulyte, I.; Marksa, M.; Bernatoniene, J. Nutmeg Essential Oil, Red Clover, and Liquorice Extracts Microencapsulation Method Selection for the Release of Active Compounds from Gel Tablets of Different Bases. *Pharmaceutics* **2023**, *15*, 949, doi:10.3390/pharmaceutics15030949.
35. Matulyte, I.; Marksa, M.; Bernatoniene, J. Development of Innovative Chewable Gel Tablets Containing Nutmeg Essential Oil Microcapsules and Their Physical Properties Evaluation. *Pharmaceutics* **2021**, *13*, 873, doi:10.3390/pharmaceutics13060873.
36. Ang, S.-S.; Thoo, Y.Y.; Siow, L.F. Encapsulation of Hydrophobic Apigenin into Small Unilamellar Liposomes Coated with Chitosan Through Ethanol Injection and Spray Drying. *Food Bioprocess Technol* **2024**, *17*, 424–439, doi:10.1007/s11947-023-03140-y.
37. Chen, M.; Li, R.; Gao, Y.; Zheng, Y.; Liao, L.; Cao, Y.; Li, J.; Zhou, W. Encapsulation of Hydrophobic and Low-Soluble Polyphenols into Nanoliposomes by pH-Driven Method: Naringenin and Naringin as Model Compounds. *Foods* **2021**, *10*, 963, doi:10.3390/foods10050963.
38. Ahmadi, N.; Ahranjani, P.J.; Rashidi, L. Encapsulation of Green Tea Extract (GTE) in Nanoliposome and Assessment of Its Characterization and In€Vitro Release Study of GTE. *Food Science* **2025**.
39. Meng, D.; Song, J.; Yi, Y.; Li, J.; Zhang, T.; Shu, Y.; Wu, X. Controlled Released Naringin-Loaded Liposome/Sucrose Acetate Isobutyrate Hybrid Depot for Osteogenesis in Vitro and in Vivo. *Front. Bioeng. Biotechnol.* **2023**, *10*, 1097178, doi:10.3389/fbioe.2022.1097178.
40. Guimarães, D.; Noro, J.; Silva, C.; Cavaco-Paulo, A.; Nogueira, E. Protective Effect of Saccharides on Freeze-Dried Liposomes Encapsulating Drugs. *Front. Bioeng. Biotechnol.* **2019**, *7*, 424, doi:10.3389/fbioe.2019.00424.
41. Ko, J.; Yoo, C.; Xing, D.; Gonzalez, D.E.; Jenkins, V.; Dickerson, B.; Leonard, M.; Nottingham, K.; Kendra, J.; Sowinski, R.; et al. Pharmacokinetic Analyses of Liposomal and Non-Liposomal Multivitamin/Mineral Formulations. *Nutrients* **2023**, *15*, 3073, doi:10.3390/nu15133073.
42. Wu, C.; Ji, P.; Yu, T.; Liu, Y.; Jiang, J.; Xu, J.; Zhao, Y.; Hao, Y.; Qiu, Y.; Zhao, W. Naringenin-Loaded Solid Lipid Nanoparticles: Preparation, Controlled Delivery, Cellular Uptake, and Pulmonary Pharmacokinetics. *DDDT* **2016**, 911, doi:10.2147/DDDT.S97738.
43. Abbassi, M.; Nejad Ebrahimi, S.; Rahimi, M. Optimized Spray-Drying of Zinc Sulfate-Loaded Liposomes: Physicochemical Characterization and in Vitro Release Assessment. *Sci Rep* **2025**, *15*, 20955, doi:10.1038/s41598-025-05948-4.

44. Radeva, L.; Yordanov, Y.; Spassova, I.; Kovacheva, D.; Tzankova, V.; Yoncheva, K. Double Encapsulation of Resveratrol and Doxorubicin in Composite Nanogel—An Opportunity to Reduce Cardio- and Neurotoxicity of Doxorubicin. *Gels* **2024**, *10*, 699, doi:10.3390/gels10110699.
45. Bahraminejad, S.; Almoazen, H. Sublingual and Buccal Delivery: A Historical and Scientific Prescriptive. *Pharmaceutics* **2025**, *17*, 1073, doi:10.3390/pharmaceutics17081073.
46. Jawadi, Z.; Yang, C.; Haidar, Z.S.; Santa Maria, P.L.; Massa, S. Bio-Inspired Muco-Adhesive Polymers for Drug Delivery Applications. *Polymers* **2022**, *14*, 5459, doi:10.3390/polym14245459.
47. Sabra, R.; Kirby, D.; Chouk, V.; Malgorzata, K.; Mohammed, A.R. Buccal Absorption of Biopharmaceutics Classification System III Drugs: Formulation Approaches and Mechanistic Insights. *Pharmaceutics* **2024**, *16*, 1563, doi:10.3390/pharmaceutics16121563.
48. Agudelo, C.; Barros, L.; Santos-Buelga, C.; Martínez-Navarrete, N.; Ferreira, I.C.F.R. Phytochemical Content and Antioxidant Activity of Grapefruit (Star Ruby): A Comparison between Fresh Freeze-Dried Fruits and Different Powder Formulations. *LWT* **2017**, *80*, 106–112, doi:10.1016/j.lwt.2017.02.006.
49. Ilayda Sanli; ,; Gulay Ozkan; ,; Neşe Şahin-Yeşilçubuk Green Extractions of Bioactive Compounds from Citrus Peels and Their Applications in the Food Industry. *Food Research International Volume 212, July 2025, 116352* **2025**, doi:https://doi.org/10.1016/j.foodres.2025.116352.
50. Negrea, M.; Cocan, I.; Jianu, C.; Alexa, E.; Berbecea, A.; Poiana, M.-A.; Silivasan, M. Valorization of Citrus Peel Byproducts: A Sustainable Approach to Nutrient-Rich Jam Production. *Foods* **2025**, *14*, 1339, doi:10.3390/foods14081339.
51. Ciupei, D.; Colişar, A.; Leopold, L.; Stănilă, A.; Diaconeasa, Z.M. Polyphenols: From Classification to Therapeutic Potential and Bioavailability. *Foods* **2024**, *13*, 4131, doi:10.3390/foods13244131.
52. Allameh, A.; Niayesh-Mehr, R.; Aliarab, A.; Sebastiani, G.; Pantopoulos, K. Oxidative Stress in Liver Pathophysiology and Disease. *Antioxidants* **2023**, *12*, 1653, doi:10.3390/antiox12091653.
53. Cai, J.; Wen, H.; Zhou, H.; Zhang, D.; Lan, D.; Liu, S.; Li, C.; Dai, X.; Song, T.; Wang, X.; et al. Naringenin: A Flavanone with Anti-Inflammatory and Anti-Infective Properties. *Biomedicine & Pharmacotherapy* **2023**, *164*, 114990, doi:10.1016/j.biopha.2023.114990.
54. Ghanbari-Movahed, M.; Jackson, G.; Farzaei, M.H.; Bishayee, A. A Systematic Review of the Preventive and Therapeutic Effects of Naringin Against Human Malignancies. *Front. Pharmacol.* **2021**, *12*, 639840, doi:10.3389/fphar.2021.639840.
55. Koolaji, N.; Shammugasamy, B.; Schindeler, A.; Dong, Q.; Dehghani, F.; Valtchev, P. Citrus Peel Flavonoids as Potential Cancer Prevention Agents. *Current Developments in Nutrition* **2020**, *4*, nzaa025, doi:10.1093/cdn/nzaa025.
56. Memariani, Z.; Abbas, S.Q.; ul Hassan, S.S.; Ahmadi, A.; Chabra, A. Naringin and Naringenin as Anticancer Agents and Adjuvants in Cancer Combination Therapy: Efficacy and Molecular Mechanisms of Action, a Comprehensive Narrative Review. *Pharmacological Research* **2021**, *171*, 105264, doi:10.1016/j.phrs.2020.105264.
57. Miles, E.A.; Calder, P.C. Effects of Citrus Fruit Juices and Their Bioactive Components on Inflammation and Immunity: A Narrative Review. *Front. Immunol.* **2021**, *12*, 712608, doi:10.3389/fimmu.2021.712608.
58. Manchope, M.F.; Casagrande, R.; Verri, W.A. Naringenin: An Analgesic and Anti-Inflammatory Citrus Flavanone. *Oncotarget* **2017**, *8*, 3766–3767, doi:10.18632/oncotarget.14084.

59. Priyanka Prajapati, Meenakshi Garg, Rajni Chopra & Neha Singh Novel Strategies to Obtain Valuable and Sustainable Molecules from Citrus By-Products. *Springer Nature Link* **2024**, doi:Prajapati,%20P.,%20Garg,%20M.,%20Chopra,%20R.,%20Singh,%20N.%20(2024).%20Novel%20Strategies%20to%20Obtain%20Valuable%20and%20Sustainable%20Molecules%20from%20Citrus%20By-products.%20In:%20Gupta,%20A.K.,%20Kour,%20J.,%20Mishra,%20P.%20(eds)%20Citrus%20Fruits%20and%20Juice.%20Springer,%20Singapore.%20https://doi.org/10.1007/978-981-99-8699-6_17.
60. Liqin ZhangLi SongPeipei ZhangShow all 8 authorsJiye ZhangJiye Zhang Solubilities of Naringin and Naringenin in Different Solvents and Dissociation Constants of Naringenin.
61. Suetsugu, T.; Iwai, H.; Tanaka, M.; Hoshino, M.; Quitain, A.; Sasaki, M.; Goto, M. Extraction of Citrus Flavonoids from Peel of Citrus Junos Using Supercritical Carbon Dioxide with Polar Solvent. *CES* **2013**, *1*, 87–90, doi:10.12691/ces-1-4-7.
62. Kazlauskaitė, J.A.; Bernatonienė, J. Identification of Isoflavones Aglycones in Trifolium Pratense L. Blossoms Using Different Extraction Methods. *International e-conference "Contemporary Pharmacy: Issues, Challenges and Expectations 2020 Autumn" : abstract book : 23rd October 2020, Kaunas, Lithuania = Mokslinė praktinė konferencija „Farmacija šiandien. Ruduo 2020." : nuotolinė konferencija : 2020 m. spalio 23 d. / is organized by Lithuanian University of Health Sciences. Faculty of Pharmacy. Department of Drug Technology and Social Pharmacy. Kaunas : Lietuvos sveikatos mokslų universiteto Leidybos namai, 2020* 2020.
63. Kaur, A.; Singh, S.; Singh, R.S.; Schwarz, W.H.; Puri, M. Hydrolysis of Citrus Peel Naringin by Recombinant α-L-Rhamnosidase from Clostridium Stercorarium. *J. Chem. Technol. Biotechnol.* **2010**, *85*, 1419–1422, doi:10.1002/jctb.2433.
64. Peterson, J.J.; Beecher, G.R.; Bhagwat, S.A.; Dwyer, J.T.; Gebhardt, S.E.; Haytowitz, D.B.; Holden, J.M. Flavanones in Grapefruit, Lemons, and Limes: A Compilation and Review of the Data from the Analytical Literature. *Journal of Food Composition and Analysis* **2006**, *19*, S74–S80, doi:10.1016/j.jfca.2005.12.009.
65. Xue, H.; Li, J.; Wang, G.; Zuo, W.; Zeng, Y.; Liu, L. Ultrasound-Assisted Extraction of Flavonoids from Potentilla Fruticosa L. Using Natural Deep Eutectic Solvents. *Molecules* **2022**, *27*, 5794, doi:10.3390/molecules27185794.
66. Garcia-Castello, E.M.; Rodriguez-Lopez, A.D.; Mayor, L.; Ballesteros, R.; Conidi, C.; Cassano, A. Optimization of Conventional and Ultrasound Assisted Extraction of Flavonoids from Grapefruit (Citrus Paradisi L.) Solid Wastes. *LWT - Food Science and Technology* **2015**, *64*, 1114–1122, doi:10.1016/j.lwt.2015.07.024.
67. Hiranpradith, V.; Therdthai, N.; Soontrunnarudrungsri, A.; Rungsuriyawiboon, O. Optimisation of Ultrasound-Assisted Extraction of Total Phenolics and Flavonoids Content from Centella Asiatica. *Foods* **2025**, *14*, 291, doi:10.3390/foods14020291.
68. Bhadange, Y.A.; Carpenter, J.; Saharan, V.K. A Comprehensive Review on Advanced Extraction Techniques for Retrieving Bioactive Components from Natural Sources. *ACS Omega* **2024**, *9*, 31274–31297, doi:10.1021/acsomega.4c02718.
69. Muti, L.; Nascimento, L.B.D.S.; Goracci, G.; Detti, C.; Brunetti, C.; Bilia, A.R.; Ferrini, F.; Gori, A. From Waste to Value: Optimization of Ultrasound-Assisted Extraction of Anthocyanins and Flavonols from Pistacia Lentiscus L. Oilcakes. *Molecules* **2025**, *30*, 237, doi:10.3390/molecules30020237.
70. Zulkifli, M.Z.A.; Benjamin, M.A.Z.; Mohd Rosdan, M.D.E.; Saini, A.; Rusdi, N.A.; Awang, M.A. Optimisation of Yield, Flavonoids, and Antioxidant Activity via Ultrasound-Assisted Extraction of Bamboo Leaves from Dinochloa Sublaevigata S. Dransf. (Wadan) in Sabah, Malaysia. *Advances in Bamboo Science* **2025**, *10*, 100128, doi:10.1016/j.bamboo.2025.100128.

71. Mohammed, E.A.; Abdalla, I.G.; Alfawaz, M.A.; Mohammed, M.A.; Al Maiman, S.A.; Osman, M.A.; Yagoub, A.E.A.; Hassan, A.B. Effects of Extraction Solvents on the Total Phenolic Content, Total Flavonoid Content, and Antioxidant Activity in the Aerial Part of Root Vegetables. *Agriculture* **2022**, *12*, 1820, doi:10.3390/agriculture12111820.
72. Kazlauskaitė, J.A.; Marksa, M.; Bernatonienė, J. Quantification of Isoflavones Aglycones in the Late Harvest Aerial Parts of Trifolium Pratense L. Using Different Hydrolysis Methods. 5.
73. Matulyte, I.; Marksa, M.; Ivanauskas, L.; Kalvėnienė, Z.; Lazauskas, R.; Bernatoniene, J. GC-MS Analysis of the Composition of the Extracts and Essential Oil from Myristica Fragrans Seeds Using Magnesium Aluminometasilicate as Excipient. *Molecules* **2019**, *24*, 1062, doi:10.3390/molecules24061062.
74. Bernatoniene, J.; Nemickaite, E.; Majiene, D.; Marksa, M.; Kopustinskiene, D.M. In Vitro and In Silico Anti-Glioblastoma Activity of Hydroalcoholic Extracts of Artemisia Annua L. and Artemisia Vulgaris L. *Molecules* **2024**, *29*, 2460, doi:10.3390/molecules29112460.
75. Lucas-Abellán, C.; Pérez-Abril, M.; Castillo, J.; Serrano, A.; Mercader, M.T.; Fortea, M.I.; Gabaldón, J.A.; Núñez-Delicado, E. Effect of Temperature, pH, β- and HP-β-Cds on the Solubility and Stability of Flavanones: Naringenin and Hesperetin. *LWT* **2019**, *108*, 233–239, doi:10.1016/j.lwt.2019.03.059.
76. Vhangani, L.N.; Favre, L.C.; Rolandelli, G.; Van Wyk, J.; Del Pilar Buera, M. Optimising the Polyphenolic Content and Antioxidant Activity of Green Rooibos (Aspalathus Linearis) Using Beta-Cyclodextrin Assisted Extraction. *Molecules* **2022**, *27*, 3556, doi:10.3390/molecules27113556.
77. Fenyvesi, F.; Klusóczki, Á.; Rusznyák, Á.; Zsebik, B.; Bácskay, I.; Váradi, J. Cyclodextrin-Based Delivery Systems for Flavonoids: Mechanisms, Advances, Formulation, and Application Opportunities. *Antioxidants* **2025**, *14*, 998, doi:10.3390/antiox14080998.
78. Nicolaescu, O.E.; Ionescu, C.; Samide, A.; Tigae, C.; Spînu, C.I.; Oprea, B. Advancements in Cyclodextrin Complexes with Bioactive Secondary Metabolites and Their Pharmaceutical Applications. *Pharmaceutics* **2025**, *17*, 506, doi:10.3390/pharmaceutics17040506.
79. Stabrauskiene, J.; Sadauskiene, I.; Liekis, A.; Mikniene, Z.; Bernatoniene, J. Naringin vs. Citrus x Paradisi L. Peel Extract: An In Vivo Journey into Oxidative Stress Modulation. *Antioxidants* **2025**, *14*, 157, doi:10.3390/antiox14020157.
80. Nguyen, T.N.P.; Van, C.K.; Nguyen, T.T.T.; Van Tran, T.; Hoang, Q.B.; Bach, L.G. Influence of Spray Drying Parameters on the Physicochemical Characteristics of Microencapsulated Pomelo (Citrus Grandis (L.) Osbeck) Essential Oil. *Food Sci Biotechnol* **2022**, *31*, 1679–1689, doi:10.1007/s10068-022-01161-5.
81. Ćujić Nikolić, N.; Jovanović, M.; Radan, M.; Lazarević, Z.; Bigović, D.; Marković, S.; Jovanović Lješković, N.; Šavikin, K. Development of Cyclodextrin-Based Mono and Dual Encapsulated Powders by Spray Drying for Successful Preservation of Everlasting Flower Extract. *Pharmaceutics* **2024**, *16*, 861, doi:10.3390/pharmaceutics16070861.
82. Li, S.; Fu, X.; Wen, J.; Jiang, L.; Shao, L.; Du, Y.; Shan, C. Characterization of Physicochemical Properties, Bioactivities, and Sensory Attributes of Sea Buckthorn–Fava Bean Composite Instant Powder: Spray-Drying Versus Freeze-Drying Coupled with Carriers. *Foods* **2024**, *13*, 3944, doi:10.3390/foods13233944.
83. Sidlagatta, V.; Chilukuri, S.V.V.; Devana, B.R.; Dasi, S.D.; Rangaswamy, L. Effect of Maltodextrin Concentration and Inlet Air Temperature on Properties of Spray Dried Powder from Reverse Osmosis Concentrated Sweet Orange Juice. *Braz. arch. biol. technol.* **2020**, *63*, e20190538, doi:10.1590/1678-4324-2020190538.

84. Xiao, Z.; Xia, J.; Zhao, Q.; Niu, Y.; Zhao, D. Maltodextrin as Wall Material for Microcapsules: A Review. *Carbohydrate Polymers* **2022**, *298*, 120113, doi:https://doi.org/10.1016/j.carbpol.2022.120113.
85. Zhao, J.; Qin, X.; Liu, Y.; He, Q.; Qin, J.; Shen, F.; Wu, Z. Comparative Evaluation of Spray-Drying Versus Freeze-Drying Techniques on the Encapsulation Efficiency and Biofunctional Performance of Chenpi Extract Microcapsules. *Foods* **2025**, *14*, 1825, doi:10.3390/foods14101825.
86. Da Silva Júnior, M.E.; Araújo, M.V.R.L.; Martins, A.C.S.; Dos Santos Lima, M.; Da Silva, F.L.H.; Converti, A.; Maciel, M.I.S. Microencapsulation by Spray-Drying and Freeze-Drying of Extract of Phenolic Compounds Obtained from Ciriguela Peel. *Sci Rep* **2023**, *13*, 15222, doi:10.1038/s41598-023-40390-4.
87. Rahim, M.A.; Zahran, H.A.; Jaffar, H.M.; Ambreen, S.; Ramadan, M.F.; Al-Asmari, F.; Castro-Muñoz, R.; Zongo, E. Liposomal Encapsulation in Food Systems: A Review of Formulation, Processing, and Applications. *Food Science & Nutrition* **2025**, *13*, e70587, doi:10.1002/fsn3.70587.
88. Osojnik Črnivec, I.G.; Skrt, M.; Polak, T.; Šeremet, D.; Mrak, P.; Komes, D.; Vrhovšek, U.; Poklar Ulrih, N. Aspects of Quercetin Stability and Its Liposomal Enhancement in Yellow Onion Skin Extracts. *Food Chemistry* **2024**, *459*, 140347, doi:10.1016/j.foodchem.2024.140347.
89. Wang, D.-Y.; Van Der Mei, H.C.; Ren, Y.; Busscher, H.J.; Shi, L. Lipid-Based Antimicrobial Delivery-Systems for the Treatment of Bacterial Infections. *Front. Chem.* **2020**, *7*, 872, doi:10.3389/fchem.2019.00872.
90. Arneth, B.; Abdelmonem, R.; El-Nabarawi, M.A.; Teaima, M.H.; Rashwan, K.O.; Soliman, M.A.; Al-Samadi, I.E.I. Optimized Hesperidin-Loaded Lipid Nanoparticles with Tea Tree Oil for Enhanced Wound Healing: Formulation, Characterization, and Evaluation. *Pharmaceuticals* **2025**, *18*, 290, doi:10.3390/ph18030290.
91. Dejeu, I.L.; Vicaș, L.G.; Marian, E.; Ganea, M.; Frenț, O.D.; Maghiar, P.B.; Bodea, F.I.; Dejeu, G.E. Innovative Approaches to Enhancing the Biomedical Properties of Liposomes. *Pharmaceutics* **2024**, *16*, 1525, doi:10.3390/pharmaceutics16121525.
92. Sepúlveda, C.T.; Alemán, A.; Zapata, J.E.; Montero, M.P.; Gómez-Guillén, M.C. Characterization and Storage Stability of Spray Dried Soy-Rapeseed Lecithin/Trehalose Liposomes Loaded with a Tilapia Viscera Hydrolysate. *Innovative Food Science & Emerging Technologies* **2021**, *71*, 102708, doi:10.1016/j.ifset.2021.102708.
93. Panizzon, G.; Bueno, F.; Ueda-Nakamura, T.; Nakamura, C.; Dias Filho, B. Preparation of Spray-Dried Soy Isoflavone-Loaded Gelatin Microspheres for Enhancement of Dissolution: Formulation, Characterization and in Vitro Evaluation. *Pharmaceutics* **2014**, *6*, 599–615, doi:10.3390/pharmaceutics6040599.
94. Hussein, N. Spray-Dried Liposomes: A Study of the Effect of Carbohydrate Carrier and Concentrations on Liposome Size and Drug Entrapment. *Zanco J. Med. Sci.* **2019**, *23*, 345–353, doi:10.15218/zjms.2019.043.
95. Maslii, Y.; Herbina, N.; Dene, L.; Ivanauskas, L.; Matulis, G.; Bernatoniene, J. Mucoadhesive Polymeric Film with Plant-Based Compounds for Dental Applications: Formulation, Characterization and Evaluation. *Pharmaceutical Development and Technology* **2025**, *30*, 505–520, doi:10.1080/10837450.2025.2498368.
96. Veras, J.M.L.; Plácido, G.R.; Romani, V.P.; Alves, J.D.S.; Sousa, T.L.D.; Célia, J.A.; Oliveira, D.E.C.D.; Monteiro, L.B. Hygroscopicity of Pectin-Propolis Films: Sorption Isotherms and Thermodynamic Properties. *Cienc. Rural* **2025**, *55*, e20230667, doi:10.1590/0103-8478cr20230667.
97. Yoshida, C.M.P.; Pacheco, M.S.; De Moraes, M.A.; Lopes, P.S.; Severino, P.; Souto, E.B.; Da Silva, C.F. Effect of Chitosan and Aloe Vera Extract Concentrations on

the Physicochemical Properties of Chitosan Biofilms. *Polymers* **2021**, *13*, 1187, doi:10.3390/polym13081187.
98. Mikus, M.; Galus, S. The Effect of Phenolic Acids on the Sorption and Wetting Properties of Apple Pectin-Based Packaging Films. *Molecules* **2025**, *30*, 1960, doi:10.3390/molecules30091960.

CURRICULUM VITAE

Name, Surname:	**Jolita Stabrauskienė**
E-mail:	Jolita.stabrauskiene@lsmu.lt

Work experience

01/09/2021 – CURRENT	LSMU, Department of Drug Technology and Social Pharmacy, Assistant
01/09/2025 – CURRENT	LSMU, Department of Drug Technology and Social Pharmacy, Serial Production Coordinator
01/07/2021 – 01/09/2025	UAB Gintarinė vaistinė Advanced Practice Pharmacist/Pharmacist
01/09/2020 – 01/07/2021	UAB Apotheka pharma, Pharmacist
01/09/2019 – 01/09/2020	UAB Aconitum, Product development specialist
01/12/2014 – 01/09/2019	UAB Benu vaistinė, Pharmacist
01/07/2011 – 01/12/2014	UAB Eurovaistine Pharmaceutical Operations Manager / Pharmacist

Education

01/09/1999 – 01/07/2011	Lithuanian University of Health Sciences, Faculty of Pharmacy, Master of Pharmacy
01/09/1987 – 01/07/1999	Kaunas Veršvų Gymnasium
01/09/1987 – 01/07/1994	Gruodžio music school

Awards

12/12/2024	3nd place award in the contest “Best PhD Student 2024” organised by the Science Foundation of the Lithuanian University of Health Sciences.
10/06/2025	Giedrius Andžiukevičius Scholarship.

International experience

09/07/2022 – 22/07/2022	“3D printing in pharmacy”, summer school in Masaryk University, Chechia, Brno.
01/12/2024 – 01/11/2024	Internship at the University of Ljubljana, Slovėnija

COPIES OF PUBLICATIONS

Paper 1

Title: Optimisation of Naringin and Naringenin Extraction from *Citrus* × *paradisi* L. Using Hydrolysis and Excipients as Adsorbent
Authors: Jolita Stabrauskiene, Mindaugas Marksa, Liudas Ivanauskas and Jurga Bernatoniene
Pharmaceutics 14, 890 (2022)

pharmaceutics

MDPI

Article

Optimization of Naringin and Naringenin Extraction from *Citrus* × *paradisi* L. Using Hydrolysis and Excipients as Adsorbent

Jolita Stabrauskiene [1,2], Mindaugas Marksa [3], Liudas Ivanauskas [3] and Jurga Bernatoniene [1,2,*]

[1] Department of Drug Technology and Social Pharmacy, Lithuanian University of Health Sciences, LT-50161 Kaunas, Lithuania; jolita.stabrauskiene@lsmu.lt
[2] Institute of Pharmaceutical Technologies, Lithuanian University of Health Sciences, LT-50161 Kaunas, Lithuania
[3] Department of Analytical and Toxicological Chemistry, Lithuanian University of Health Sciences, LT-50161 Kaunas, Lithuania; mindaugas.marksa@lsmuni.lt (M.M.); liudas.ivanauskas@lsmuni.lt (L.I.)
* Correspondence: jurga.bernatoniene@lsmuni.lt; Tel.: +370-6006-3349

Abstract: While flavanones exist in a variety of chemical forms, their favorable health effects are most prominent in their free form—aglycones. Their concentrations in grapefruit (*Citrus* × *paradisi* L.) extracts vary according to the extraction and hydrolysis methods used. The primary aim of this work was to maximize the yields of naringin and naringenin from various parts of fresh grapefruit fruits (*flavedo*, *albedo*, *and segmental*) using different extraction and hydrolysis methods. In addition, we aimed to evaluate the excipient—magnesium aluminometasilicate—and determine its influence on the qualitative composition of grapefruit extracts. Extracts were obtained by heat reflux extraction (HRE), ultrasound-assisted extraction with an ultrasonic homogenizer (UAE*), and ultrasound-assisted extraction with a bath (UAE). Ultrasound-assisted extraction using a bath (UAE) was modulated using acidic, thermal, and alkaline hydrolysis. The highest yield of naringin 8A (17.45 ± 0.872 mg/g) was obtained from an *albedo* sample under optimal conditions using ultrasound-assisted extraction; a high yield of naringenin 23-SHR (35.80 ± 1.79 µg/g) was produced using the heat reflux method from the *segmental* part. Meanwhile, ultrasonic combined with thermal hydrolysis significantly increased flavanone extraction from the *albedo* and *segmental* parts: naringin from sample 9-A (from 17.45 ± 0.872 mg/g to 25.05 ± 1.25 mg/g) and naringenin from sample 15-S (from 0 to 4.21 ± 0.55 µg/g). Additionally, magnesium aluminometasilicate demonstrated significant increases of naringenin from all treated grapefruit parts. To our knowledge, this is the first report of magnesium aluminometasilicate used as an adsorbent in flavanone extractions.

Keywords: *Citrus* × *paradisi* L.; grapefruit; flavanones; glycosides; aglycones; extractions; excipient; magnesium aluminometasilicate; adsorbent

Citation: Stabrauskiene, J.; Marksa, M.; Ivanauskas, L.; Bernatoniene, J. Optimization of Naringin and Naringenin Extraction from *Citrus* × *paradisi* L. Using Hydrolysis and Excipients as Adsorbent. *Pharmaceutics* **2022**, *14*, 890. https://doi.org/10.3390/pharmaceutics14050890

Academic Editors: Donatella Paolino and Cinzia Anna Ventura

Received: 7 March 2022
Accepted: 15 April 2022
Published: 19 April 2022

1. Introduction

Citrus × *paradisi* L. is an essential member of the Citrus genus in the *Rutaceae* family. Grapefruit is a delicious fruit used in the juice and food industry. However, around half of all fruit waste is discarded as a waste product, even though it includes a huge number of biologically active components with distinct health benefits. Therefore, numerous studies have been conducted to extract and identify biologically active components present in various citrus fruits to understand the relationship between their presence in diet and health benefits and reduced risk of disease [1,2]. Citrus peels contain significant amounts of vitamin C, fiber, pectin, essential oils, and polyphenols. Therefore, they have high potential for use as value-adding products, particularly in the biotechnology and pharmaceutical industries [3,4].

Previous research has found that flavonoid types in citrus fruits varied between species and cultivars (Durand-Hulak et al., 2015), as did their contents and distribution in different fruit tissues (Antonio Cano et al., 2007) (p. 64, [5]) and [6].

Citrus peels are rich in phenolic components and essential flavonoids, which are widely studied and positively affect human health [7–9]. The main bioflavonoids in citrus fruits, flavanones narirutin, naringin, and aglycon naringenin, display high biological activity and antioxidant, anti-inflammatory, metabolic, antivirus, neuroprotective, and antitumor effects [10–12]. There is considerable evidence of how naringenin works synergistically with anticancer drugs, especially in resistant cancer forms. Therefore, the development of new pharmaceutical forms will significantly impact cancer treatment [11]. Other essential and beneficial flavonoids are hesperidin, rutin, diosmin, didymin, and quercetin.

Flavanones in citrus fruits are in glycoside or aglycone forms [13]. Of the aglycone forms, the essential flavanones are naringenin and hesperetin. Glycosides are divided into two types: neohesperidosides (e.g., naringin), which have a bitter taste, and rutinosides (e.g., hesperidin, narirutin, and didymin) (Figure 1) [14,15]. The characteristic flavor of citrus fruits is caused by flavanones, usually diglycosides. The molecular structures of flavonoids are provided in Figure 1.

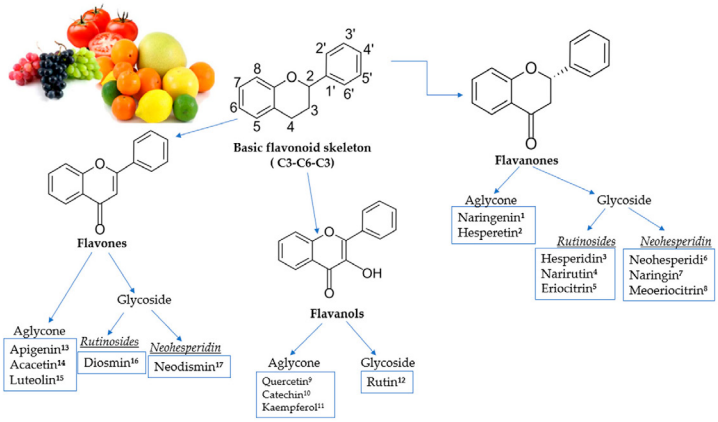

Naringenin[1] R4=R3=R2=R1=H	Quercetin[9] R4=R1=OH, R3=R2=H
Hesperetin[2] R4=H, R3=OH, R2=H, R1=Me	Catechin[10] R4=R2=R1=OH, R3=H
Hesperidin[3] R4=H, R3=rutinose, R2=OH, R1=Me	Kaempferol[11] R4=R2=OH, R3=R1=H
Narirutin[4] R4=H, R3=rutinose, R2=R1=H	Rutin[12] R4=neohesperidose, R3=H, R2=R1=OH
Eriocitrin[5] R4=H, R3=rutinose, R2=OH, R1=H	Apigenin[13] R4=R2=OH, R3=R1=H
Neohesperidi[6] R4=H, R3=neohesperidose, R2=OH, R1=Me	Acacetin[14] R4=OH, R2=OMe, R3=R1=H
Naringin[7] R4=H, R3=neohesperidose, R2=R1=H	Luteolin[15] R4=R2=R1=OH, R3=H
Neoeriocitrin[8] R4=H, R3=neohesperidose, R2=OH, R1=Me	Diosmin[16] R4=O-rutinose, R3=H, R2=OMe, R1=OH
	Neodismin[17] R4=O-neohesperidose, R3=H, R2=OMe, R1=OH

Figure 1. Molecular structures of flavonoids and their subclasses.

Natural flavanone glycosides, such as naringin, are not easily absorbed in intestinal absorptive cells because of their large hydrophilic structures—this reduces the expected effects of flavanones. As a result, the conjugated flavanones are inactive compounds but become active in aglycone form (naringenin). This bioflavonoid can be obtained from

naringin hydrolysis with naringinase when the glucose molecule is removed from the structure [16].

Naringin is hydrolyzed into rhamnose and prunin by the naringinase exhibiting α-l-rhamnosidase activity, and then β-D-glucosidase catalyzes the hydrolysis of prunin to glucose and naringenin [17]. Hydrolysis of naringin to naringenin is shown in Figure 2.

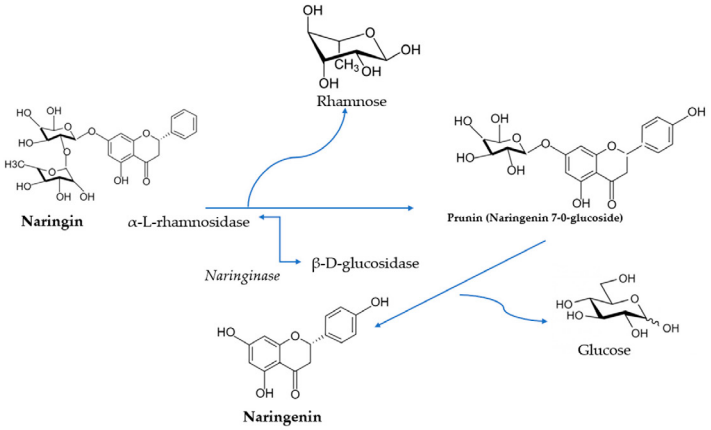

Figure 2. Hydrolysis of naringin by naringinase to produce naringenin.

Conventional extraction methods are based on the use of chemical solvents and the heating of the sample to maximize the solubility of active substances and accelerate their transfer. The extraction yield depends on various factors, including the type, concentration, and amount of the solvent used; its treatment time; and temperature. According to Sarah Luisa Rodriguez De Luna, 2020, the extraction time is a parameter that needs to be optimized in each experiment [18]. An increase in temperature may increase the release of flavonoids, but it also depends on the properties of the solvent used. The most appropriate extraction technique depends on the type of plant, so the defined selection criteria must be followed [19]. Different extraction methods, such as maceration, percolation, heat refluxing, Soxhlet extraction, supercritical extraction, microwave-assisted extraction, ultrasound-assisted extraction, and others, are the most commonly used methods for bioactive compound recovery from natural materials [20–22]. All these methods have their own advantages and disadvantages. However, maceration, percolation, continuous stirring, and Soxhlet extraction come with big disadvantages, such as long extraction times, complicated extraction operations, inflated costs, hazardous flammable liquid organic solvents, and large amounts of extraction solvents.

Meanwhile, green and sustainable extraction techniques, such as supercritical CO_2 extraction method or ultrasound-assisted extraction, are environmentally friendly, safe, and non-toxic and are promising alternatives to conventional extraction methods [21,23,24].

Ultrasound-assisted extraction is widely used to extract biologically active compounds such as flavonoids, anthocyanins, and phenolic acids. According to Londono Londono et al. (2010), ultrasound-assisted extraction demonstrated a higher efficiency of flavonoid extraction from citrus peels in 60 min using methanol as a solvent than Soxhlet extraction with a more extensive solvent selection [22]. The biological activity of phenolic compounds is strongly dependent on the conditions of ultrasound-assisted extraction, such as temperature, type of solvent, and extraction time [21]. Cavitation is the primary

action mechanism of ultrasound-assisted methods, causing cellular disruption, high solvent penetration, and particle size reduction.

Transformation of flavanone glycosides to aglycone can be achieved using an extraction method combined with hydrolysis. Chemical (using bases and acids) or thermal (high temperatures) hydrolysis can increase aglycon content [25,26].

The previous research demonstrated that magnesium aluminometasilicate can work as an adsorbent to increase the solubility of bioflavonoids in extracts [27,28].

Indeed, this study aimed to maximize the yields of naringin and naringenin from various parts of fresh grapefruit fruits using different extraction and hydrolysis methods, as well as to evaluate how magnesium aluminometasilicate affects the qualitative content of grapefruit extracts.

2. Materials and Methods

2.1. Materials

The grapefruit fruits (*Citrus* × *paradisi* L., variety Star Ruby, Italy, region—unknown) were collected from the local market in Mastaičiai, Kaunas district, Lithuania. The fruit were separated into the *flavedo*, *albedo*, and *segmental* parts, then chopped up with a food processor and frozen in a freezer (−18 ± 0.9 °C) until extraction. The parts of the fruit used in this study are shown in Figure 3.

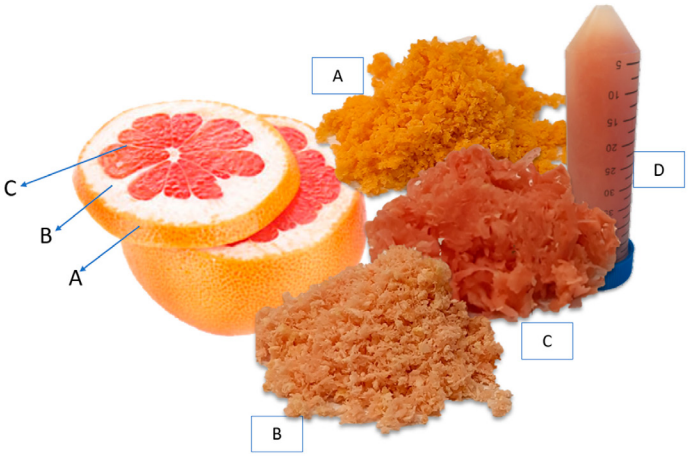

Figure 3. Fresh *Flavedo* (**A**), fresh *Albedo* (**B**), fresh *Segmental* (**C**), and frozen Juice (**D**) of *Citrus* × *paradisi* L.

Magnesium aluminometasilicate (Neusilin® US2, Fuji Chemical Industries Co., Ltd., Toyoma, Japan) was used as excipient. Ethanol 96% (Vilniaus degtine, Vilnius, Lithuania) was used as a solvent for extraction.

2.2. Methods

Three different extraction techniques were used. In the first experiment, extracts were obtained by heat reflux extraction (Section 2.2.1), ultrasound-assisted extraction with an ultrasonic homogenizer (Section 2.2.3), and ultrasound-assisted extraction with a bath (Section 2.2.2). In the second experiment, the same methods and conditions were used with magnesium aluminometasilicate (Neusilin®), and in the third experiment, ultrasound-assisted extraction with a bath was modulated with acidic, thermal, and alkaline hydrolysis. The operational conditions for each extraction method are shown in Table 1.

Table 1. Operational conditions of the different extraction methods.

Extract ID	Extraction Temp. °C	Extraction Time, min	Material:Solvent Ratio (g/mL)	Solvent	Excipient	Hydrolysis Methods
HRE—Heat-Reflux Extraction						
21-FHR 22-AHR 23-SHR	100 ± 2	60	1:10	Ethanol 70% (*v*/*v*)	*Magnesium aluminometasilicate*	- - -
UAE—Ultrasound-Assisted Extraction Bath						
1-F	50 ± 2	20	1:10	Ethanol 50% (*v*/*v*)		-
2-F	50 ± 2	30	1:10	Ethanol 50% (*v*/*v*)		-
3-F	50 ± 2	20	1:10	Ethanol 70% (*v*/*v*)		AC*/AL*/T*
4-F	50 ± 2	30	1:10	Ethanol 70% (*v*/*v*)		-
5-F	70 ± 2	30	1:10	Ethanol 50% (*v*/*v*)		-
6-F	70 ± 2	30	1:10	Ethanol 70% (*v*/*v*)		-
7-A	50 ± 2	20	1:10	Ethanol 50% (*v*/*v*)		-
8-A	50 ± 2	30	1:10	Ethanol 50% (*v*/*v*)		-
9-A	50 ± 2	20	1:10	Ethanol 70% (*v*/*v*)	*Magnesium aluminometasilicate*	AC*/AL*/T*
10-A	50 ± 2	30	1:10	Ethanol 70% (*v*/*v*)		-
11-A	70 ± 2	30	1:10	Ethanol 50% (*v*/*v*)		-
12-A	70 ± 2	30	1:10	Ethanol 70% (*v*/*v*)		-
13-S	50 ± 2	20	1:10	Ethanol 50% (*v*/*v*)		-
14-S	50 ± 2	30	1:10	Ethanol 50% (*v*/*v*)		-
15-S	50 ± 2	20	1:10	Ethanol 70% (*v*/*v*)		AC*/AL*/T*
16-S	50 ± 2	30	1:10	Ethanol 70% (*v*/*v*)		-
17-S	70 ± 2	30	1:10	Ethanol 50% (*v*/*v*)		-
18-S	70 ± 2	20	1:10	Ethanol 70% (*v*/*v*)		-
UAE*—Ultrasound-Assisted Extraction Using an Ultrasonic Homogenizer						
27-SUX1	from 33.2 to 40 ± 2	1	1:5	Ethanol 70% (*v*/*v*)	-	-
28-SUX2	from 33.2 to 40 ± 2	3	1:5	Ethanol 70% (*v*/*v*)	-	-
29-SUX3	from 33.2 to 40 ± 2	5	1:5	Ethanol 70% (*v*/*v*)	-	-
30-FUX1	from 33.2 to 40 ± 2	1	1:5	Ethanol 70% (*v*/*v*)	-	-
31-FUX2	from 33.2 to 40 ± 2	3	1:5	Ethanol 70% (*v*/*v*)	-	-
32-FUX3	from 33.2 to 40 ± 2	5	1:5	Ethanol 70% (*v*/*v*)	-	-
33-AUX1	from 33.2 to 40 ± 2	1	1:5	Ethanol 70% (*v*/*v*)	-	-
34-AUX2	from 33.2 to 40 ± 2	3	1:5	Ethanol 70% (*v*/*v*)	-	-
35-AUX3	from 33.2 to 40 ± 2	5	1:5	Ethanol 70% (*v*/*v*)	-	-

UAE—ultrasound-assisted extraction bath, UAE*—ultrasound-assisted extraction using an ultrasonic homogenizer; HRE—heat reflux extraction. AC*—acidic hydrolysis, AL*—alkaline hydrolysis, T*—thermal hydrolysis.

HPLC-grade and analytical-grade reagents were used: hydrochloric acid, sodium hydroxide, methanol, acetonitrile (Sigma Aldrich, Hamburg, Germany); standards of naringin and naringenin (Sigma Aldrich, Steinheim, Germany); and ethanol (96%) (Vilniaus Degtine, Vilnius, Lithuania).

2.2.1. Heat Reflux Extraction (HRE)

The frozen, raw material was defrosted at room temperature and allowed to warm up to 25 ± 2 °C. A sample of 1 ± 0.05 g of defrosted grapefruit (*flavedo*, *albedo*, or *segmental* parts) was mixed with the solvent (70% ethanol (*v*/*v*)) at 1:10 ratio in a 250 mL round-bottom flask and refluxed in a sand bath at 100 ± 2 °C for one hour. The mixture was left to cool down at room temperature, and then centrifuged with Sigma 3-18K centrifuge (Sigma, Osterode am Harz, Germany) for 10 min at RCP 1789× *g*, followed by the decantation of the supernatant. The extracts were filtered through PVDF syringe filters (pore size 0.22 µm, Frisenette, Knebel, Denmark) prior to HPLC (high-performance liquid chromatography) analysis. All the extraction conditions are displayed in Table 1.

2.2.2. Ultrasound-Assisted Extraction Bath (UAE)

Ultrasonic extraction was performed using an ultrasonic bath (Cambridge, UK, Grant Instruments ™ XUB12 Digital) (frequency of 38 kHz). A sample of 1 ± 0.05 g of defrosted *flavedo*, *albedo*, or *segmental* parts was macerated with the 50% or 70% ethanol solvent (*v*/*v*) at a ratio of 1:10, and extraction time (10 or 30 min), with the processing temperature of

50 ± 2 °C or 70 ± 2 °C (the temperature was regulated automatically by the ultrasonic bath). The mixture was allowed to cool down at room temperature (20 ± 5 °C) and then centrifuged with Sigma 3-18K centrifuge (Sigma, Osterode am Harz, Germany) for 10 min at RCP 1789× *g*, followed by the decantation of the supernatant. Next, the extracts were filtered through PVDF syringe filters (pore size 0.22 µm, Frisenette, Knebel, Denmark) before analyzing with HPLC (high-performance liquid chromatography). All the extraction conditions are displayed in Table 1.

2.2.3. Ultrasound-Assisted Extraction Using an Ultrasonic Homogenizer (UAE*)

Ultrasound-assisted extraction was performed using an UP-250 ultrasonic homogenizer (frequency range 19–25 kHz, 250 W, probes amplitude 35 µm). Firstly, 5 ± 0.25 g of samples (*albedo*, *flavedo*, or *segmental* parts) were defrosted at room temperature before being mixed with the 70% ethanol solvent (*v*/*v*) at a 1:5 ratio in a 100 mL chemical beaker and extracted for 1, 3, and 5 min at a temperature of from 33.2 to 40 ± 2 °C. Next, the mixture was centrifuged with Sigma 3-18K centrifuge at room temperature (25 ± 5 °C) (Sigma, Osterode am Harz, Germany) for 10 min at RCF 3382× *g*, followed by the decantation of the supernatant. Then, the extracts were filtered through PVDF syringe filters (pore size 0.22 µm, Frisenette, Knebel, Denmark) before analyzing with HPLC (high-performance liquid chromatography). All the extraction conditions are displayed in Table 1.

2.2.4. The Use of Magnesium Aluminometasilicate in the Preparation of Extracts

Samples were modified with magnesium aluminometasilicate. The extracts were made under the same conditions as previously listed (Sections 2.2.1 and 2.2.2). Again, 50% or 70% ethanol (*v*/*v*) or purification water was used as the solvent at a ratio of 1:10, and the excipient was added to the extraction mixture. The excipient concentration was 1% (*w*/*v*). Magnesium aluminometasilicate (g) was based on ethanol quantity. The samples were centrifuged for 10 min at RCF 1789× *g*, followed by decantation of the supernatant, and then the extracts were filtered through PVDF syringe filters (pore size 0.22 µm) before HPLC analysis. Sample preparation conditions are listed in Table 1.

2.3. *Hydrolysis and Neutralization*

2.3.1. Acidic Hydrolysis and Neutralization Using *Albedo*, *Flavedo*, and *Segmental* Parts

The applied modified acidic hydrolysis method was based on Keun Young Min et al.'s 2014 studies [29]. Firstly, the extracts were made under the previously listed conditions (Section 2.2.2). Then, 70% ethanol (*v*/*v*) was used as a solvent (ratio of 1:10), and the pH was adjusted with 2 M HCl to pH 2.5. After that, the extracts were sonicated using the UAE method at 50 ± 2 °C for 20 min. Next, the hydrolyzed extracts were allowed to cool down to 25 ± 2 °C and adjusted to pH 8 by adding an aqueous solution of 2 M NaOH while stirring. Finally, the neutralized extracts were centrifuged for 10 min at RCF 1789× *g* and filtered through PVDF syringe filters (pore size 0.22 µm) before HPLC analysis.

2.3.2. Thermal Hydrolysis Using *Albedo*, *Flavedo*, and *Segmental* Parts

Firstly, we used an ultrasonic bath (frequency of 38 kHz) (Cambridge, UK, Grant Instruments ™ XUB12 Digital) to macerate 1 ± 0.05 g of *flavedo*, *albedo*, or *segmental* parts in 10 mL of 70% *v*/*v* ethanol solvent for a duration of 20 min at a temperature of 50 ± 2 °C (the temperature was regulated automatically by the ultrasonic bath). Thermal hydrolysis was completed by transferring the extract to a 250 mL round-bottom flask and refluxing in a sand bath at 100 ± 2 °C for 1 h. After cooling, the mixture was centrifuged for 10 min at 1789× *g* using a Sigma 3-18K centrifuge (Sigma, Osterode am Harz, Germany), followed by decantation of the supernatant. Before HPLC analysis, the extracts were filtered through PVDF syringe filters (pore size 0.22 m, Frisenette, Knebel, Denmark). The parameters of sample preparation are listed in Table 1.

2.3.3. Alkaline Hydrolysis and Neutralization Using *Albedo*, *Flavedo*, and *Segmental* Parts

The applied modified alkaline hydrolysis method was based on Liuting Zhu's 2020 studies. Firstly, 1 ± 0.05 g of raw material was macerated with 70% ethanol (*v*/*v*) (ratio of 1:10). Next, the pH was adjusted with 2 M NaOH to pH 10 (measured with Thermo Scientific Orion Versa Star™, an advanced electrochemistry meter). Next, the extracts were sonicated using the UAE method at 50 ± 2 °C for 20 min (Section 2.2.2). Finally, the neutralized extracts were centrifuged for 10 min at RCF 1789× *g*, followed by decantation of the supernatant. Before HPLC analysis, the extracts were filtered through PVDF syringe filters (pore size 0.22 m, Frisenette, Knebel, Denmark). The parameters of sample preparation are listed in Table 1.

2.4. Hydro Distillation (HD)

Essential oil was extracted from the grapefruit peels (*flavedo* and *albedo* parts) using a hydro distillation technique. The procedure was as follows. Firstly, 44.5 ± 0.5 g of peels was placed in a round-bottom flask with 500 mL of distilled water and connected to a Clevenger's distillation unit. Then, the essential oil was extracted by hydro distillation for 120 min. Next, the obtained essential oil, which was collected in a Clevenger's receiver, was separated. Finally, the essential oil was stored in a glass bottle refrigerated at −4 °C until we determined the yield. Each extraction was performed three times under the same conditions. The yield of oil from the grapefruit peels' *flavedo* and *albedo* parts (Y) obtained in each extraction was calculated by the formula:

$$Y\ (\%) = \text{Volume of essential oil (mL)} / \text{Amount of row material (g)} \times 100\% \quad (1)$$

2.5. HPLC–PDA Conditions

A Waters 2695 liquid chromatography with a photodiode array detector (Waters 996, 200–400 nm wavelength range) was used in the study. In addition, a chromatographic column ACE C18 (250 mm × 4.6 mm) with a sorbent particle size of 5 µm was used to separate the biologically active compounds.

The following are the procedure details of HPLC method. The tested compounds were separated using gradient elution. Then, 10 µL of each extract was injected and analyzed at 280 nm. Eluent A: acetonitrile; eluent B: water at a rate of 1 mL/min. Gradient elution: 0.0 min, 10% A; 5 min, 20% A; 25 min, 40% A; 30 min, 100% A; 35 min, 100% A; 36 min, 10% A. The temperature of the column was 25 °C. The peaks were identified by comparing their UV-vis spectra and retention times to those of authentic reference standards. The samples were analyzed twice. The chromatograms of naringenin and naringin standards are shown in Figure 4.

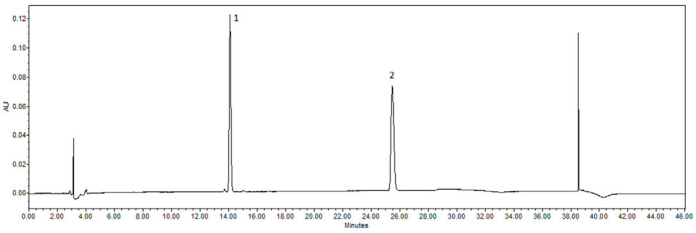

Figure 4. Chromatograms of standards detected by HPLC. Peaks identified: 1—naringin; 2—naringenin.

The quantification and validation followed the methodical revision of natural products presented by Wolfender (2009) [30]. Standard stock solutions of primary concentrations of 100 µg/mL for naringin and naringenin were freshly prepared in 70% methanol, and calibration curves constructed using 6 different standard solution concentrations. Three

injections per concentration were performed to determine linearity. Naringin and naringenin were plotted against the known concentrations of their associated standard solutions to establish calibration equations. A linear regression equation was calculated by the least-squares method. The regression coefficients of all calibration curves were $R^2 > 0.999$, confirming the linearity of the concentration ranges.

The method sensitivity was evaluated by determining the limit of detection (LOD) and quantitation (LOQ). LOD and LOQ were calculated as the concentrations that gave signal-to-noise ratios of 3 to 10, respectively.

A standard mixture of naringin and naringenin was used for intra-day and inter-day precision testing. The method precision was demonstrated by performing five replicate non-consecutive injections of the usual mix on the same day on four different days. The results are reported in terms of RSD. In this study, standards (naringin and naringenin) were analyzed, and their retention time and spectra were compared with the prepared extracts. The linearity was determined by estimating the correlation coefficient R^2 of the calibration curve (Figure 5) (naringin $R^2 = 0.99992$, naringenin $R^2 = 0.99992$), and the peak areas were used for quantification, Table 2. The linearity range of naringin was 1.166 to 33.343 µg/mL, and naringenin was 0.472 to 15.125 µg/mL. The results were expressed as µg/g and mg/g dry weight (DW) of naringenin and naringin, respectively.

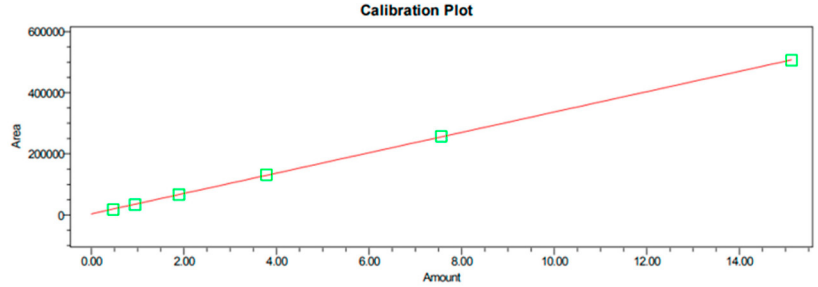

Naringenin calibration curve, range of linearity 0.472 – 15.125 µg/mL ; R^2 =0.999924

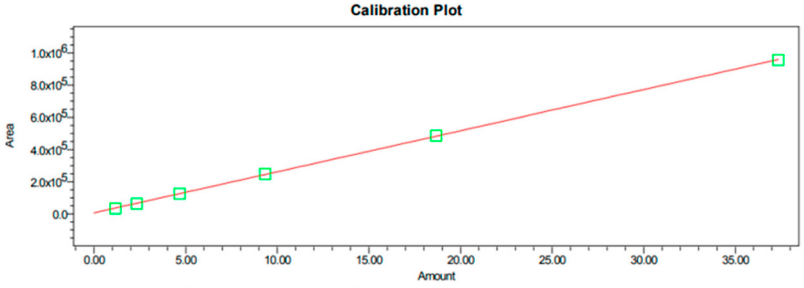

Naringin calibration curve, range of linearity 1.66 – 33.343 µg/mL; R^2 =0.999923

Figure 5. Naringin and naringenin calibration curves.

Table 2. The linearities of calibration curves of flavanones.

Component	Calibration Equation	Coefficient of Determination R^2	Coefficient of Correlation R	LOD* µg/mL	LOQ** µg/mL
Naringin	Y = 25.500x + 6720	0.999923	0.99996	0.146	0.583
Naringenin	±Y = 33.300x + 3570	0.999924	0.99996	0.118	0.430

LOD*—limit of detection; LOQ**—limit of quantification.

2.6. Statistical Analysis

The data are presented as the mean and standard deviation (SD). Statistical analysis was performed with SPSS 20.0 (IBM Corporation, Armonk, NY, USA). One-way ANOVA was used to analyze the differences between extractions. In addition, post hoc comparisons of the means were conducted according to Tukey's HSD test. The means of the compared samples were considered significantly different when $p < 0.05$.

3. Results and Discussion

The extracts from fresh fruit materials were obtained using the UAE, HER, and UAE* methods (Table 1). Two different ethanol concentrations (50% and 70% v/v) were used for the extraction. Some of the samples were modified with magnesium aluminometasilicate.

The yield of naringin and naringenin was determined using HPLC-PDA.

3.1. Flavanone Determination in Citrus × paradisi L. Extracts

Naringin was obtained from all extracts of different parts (*flavedo*, *albedo*, and *segmental*) of fresh *Citrus* × *paradisi* L. fruit. The yields of naringin and naringenin obtained using different extraction methods are shown in Table 3.

Using the UAE extraction method, the highest yield of naringin was obtained from the *albedo* fraction using 50% ethanol (v/v) as a solvent with ultrasonic time of 30 min at 50 ± 2 °C, resulting in 8-A (17.45 ± 0.87 mg/g). In contrast, the lowest amount of naringin was obtained from the *segmental* part using 50% ethanol (v/v) with ultrasonic time of 30 min at 50 ± 2°C—17-S (4.31 ± 0.96 mg/g) ($p < 0.05$). Meanwhile, naringenin was found only in *albedo*, and its highest concentration was detected using 70% ethanol (v/v) for 30 min at 50 ± 2 °C, 12-A (4.63 ± 0.23 µg/g).

When the effect of ethanol concentration (50% or 70% (v/v)) was analyzed, it was discovered that 70% (v/v) ethanol produced better results in some cases. For example, samples taken from *flavedo* parts had increased naringin from 7-A (14.79 ± 0.73 mg/g) to 9-A (17.39 ± 1.10 mg/g), and the *albedo* part had increased naringenin from 7-A (3.36 ± 0.16 µg/g) to 9-A (4.57 ± 0.22 µg/g) (50% and 70% (v/v) ethanol, respectively) ($p < 0.05$).

The differences between samples 7-A and 8-A (shown in Table 3 with 50% (v/v) ethanol showed that an increase in the sonication time statistically significantly increased flavanone yield from the *flavedo* part, 14.79 ± 0.73 mg/g to 17.45 ± 0.87 mg/g and 3.36 ± 0.168 µg/g to 3.55 ± 0.17 µg/g (naringin and naringenin, respectively).

When compared to the UAE method, the HRE extraction method produced a significant yield, with naringenin qualitatively doubled in extracts from the *albedo* 22-AHR (12.60 ± 0.63 µg/g) and *segmental* parts 23-SHR (35.80 ± 1.77 µg/g).

In the case of the UAE* method, the maximum yield was obtained when naringenin was released from the segmental part using 70% (v/v) ethanol in a temperature range of 33.5 to 40 ± 2 °C; the highest amount of naringenin detected was from the sample 28-SUX2 (7.40 ± 0.37 µg/g).

Unfortunately, the supercritical CO_2 extraction method from fresh fruit flavedo did not produce statistically meaningful results (total amount of extract 0.79 ± 0.039 g/100 g) ($p > 0.05$). However, given that the findings were not statistically significant, they are not included in Table 3.

Table 3. Yields of flavanones recovered using different extraction methods.

Extraction Methods	Extract ID *	Naringin mg/g	Naringenin µg/g
Ultrasound-assisted extraction bath	1-F	5.41 ± 0.27 [d]	-
	2-F	5.38 ± 0.267	-
	3-F	5.59 ± 0.279 [d]	-
	4-F	6.08 ± 0.304	-
	5-F	7.18 ± 0.359	-
	6-F	4.82 ± 0.241 [b]	-
	7-A	14.79 ± 0.739 [d]	3.36 ± 0.168 [d,b]
	8-A	17.45 ± 0.872	3.55 ± 0.1775 [b]
	9-A	17.39 ± 0.869 [d]	4.57 ± 0.228 [d,b]
	10-A	16.46 ± 0.823	4.63 ± 0.231 [b]
	11-A	16.08 ± 0.820	3.53 ± 0.176 [b]
	12-A	15.86 ± 0.793	4.34 ± 0.207 [b]
	13-S	5.91 ± 0.295 [b,d,e]	- [b,e]
	14-S	5.06 ± 0.253 [b,e]	- [b,e]
	15-S	5.26 ± 0.263 [d,b,e]	- [b,e]
	16-S	5.40 ± 0.27 [b,e]	- [b,e]
	17-S	4.31 ± 0.215 [b,e]	- [b,e]
	18-S	5.65 ± 0.282 [b,e]	- [b,e]
Heat reflux extraction	21-FHR	5.16 ± 0.258 [a]	-
	22-AHR	14.17 ± 0.708 [a]	12.60 ± 0.63
	23-SHR	6.68 ± 0.334	35.80 ± 1.79
Ultrasound-assisted extraction using an ultrasonic homogenizer	27-SUX1	5.15 ± 0.257 [a,b]	4.39 ± 0.219
	28-SUX2	6.38 ± 0.319 [b]	7.40 ± 0.37
	29-SUX3	5.56 ± 0.279 [a,b]	5.88 ± 0.294
	30-FUX1	0.96 ± 0.048 [a,b]	-
	31-FUX2	1.05 ± 0.0525 [a,b]	-
	32-FUX3	0.98 ± 0.049 [a,b]	-
	33-AUX1	5.75 ± 0.287 [a,b]	- [a,b]
	34-AUX2	6.67 ± 0.333 [a,b]	- [a,b]
	35-AUX3	6.13 ± 0.306 [a,b]	- [a,b]

* The meanings of the abbreviations are presented in Table 1. [d] $p < 0.05$ when UAE with 50% ethanol (v/v) were compared with UAE with 70% ethanol (v/v). [a] $p < 0.05$ vs. ultrasound-assisted extraction bath; [b] $p < 0.05$ vs. heat reflux extraction; [e] $p < 0.05$ vs. ultrasound-assisted extraction using an ultrasonic homogenizer.

3.1.1. Flavanones Extraction Using the UAE Method with Acidic, Alkaline, and Thermal Hydrolysis

The extracted sample was prepared using the UAE method with acidic, alkaline, and thermal hydrolysis and 70% (v/v) ethanol as a solvent (Sections 2.3.1–2.3.3). Using UAE with thermal hydrolysis, naringin yields were increased from all parts, for example, from the *flavedo* part (from 5.59 ± 0.279 mg/g to 6.25 ± 0.312 mg/g), doubled yield from the *albedo* part (from 17.39 ± 0.869 mg/g to 25.05 ±1.25 mg/g), and from the *segmental* part (from 5.26 ± 0.263 mg/g to 11.07 ± 0.55 mg/g) (Table 4). The highest amount of aglycon naringenin was obtained from the *segmental* part using thermal and acidic hydrolysis: 0–1.12 ± 0.056 µg/g–4.21 ± 0.21 µg/g (UAE without hydrolysis, acidic, and thermal hydrolysis, respectively) ($p < 0.05$ when compared to extraction without hydrolysis). Statistically significant results are shown in Figure 6.

Wenbin Chen et al. (2017) demonstrated that the complete hydrolysis of the flavonoid glycosides was achieved only by refluxing at 80 ± 2 °C [31]. This tendency was also observed in this study using thermal hydrolysis.

Table 4. Yields of flavanones recovered using UAE extraction methods with and without hydrolysis.

	Naringin mg/g				*Naringenin* µg/g			
Extract ID **	**No Hydrolysis**	**AC ***	**AK ***	**T ***	**No Hydrolysis**	**AC ***	**AK ***	**T ***
3-F	5.59 ± 0.279 [a]	2.14 ± 0.10	3.36 ± 0.168	6.25 ± 0.312 [a]	-	-	-	-
9-A	17.39 ± 0.869 [a]	11.39 ± 0.56	12.59 ± 0.629	25.05 ± 1.25 [a]	4.57 ± 0.249	1.78 ± 0.089	-	1.87 ± 0.09
15-S	5.26 ± 0.263 [a]	6.39 ± 0.319	5.13 ± 0.256	11.07 ± 0.55 [a]	0 [a]	1.12 ± 0.065	-	4.21 ± 0.21 [a]

* The meanings of the abbreviations are in Table 1. ** The meanings of the abbreviations are in Table 1. [a] $p < 0.05$ when compared to extraction without hydrolysis.

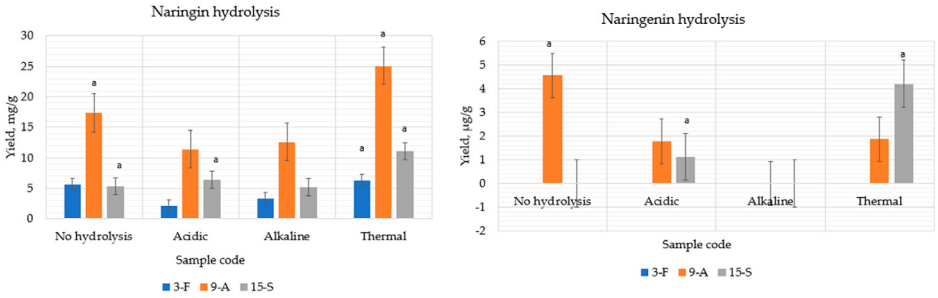

Figure 6. Comparison of the extraction yields of naringin and naringenin obtained with and without hydrolysis. [a] $p < 0.05$ when compared to extraction without hydrolysis. Extract ID and preparation conditions are displayed in Table 1.

3.1.2. Flavanone Extraction Using an Excipient as Adsorbent 1% Magnesium Aluminometasilicate

Using excipients as adsorbent may improve the solubility of certain active substances in drugs that have poor water solubility [27,32]. Therefore, in this study, we decided to use excipients during extractions to determine whether they could increase the yields of flavanones. The used heat reflux extraction and ultrasound-assisted extraction bath methods obtained most flavanones (Section 2.2.4). These extraction conditions using additional compounds were applied to improve the solubility of flavanones.

The use of magnesium aluminometasilicate during extraction significantly affected the release of naringenin in all samples. There was a statistically significant improvement in naringenin self-efficacy in the HRE from the *flavedo* (samples 21-FHR—2.92 ± 0.503 µg/g). There was also a statistically significant increase of naringenin yield in samples from *segmental* parts using the UAE method: 13-S (4.07 ± 0.203 µg/g); 14-S (5.11 ± 0.257 µg/g); 15-S (2.66 ± 0.133 µg/g); 16-S (2.83 ± 0.141 µg/g); 17-S (6.78 ± 0.34 µg/g); 18-S (3.75 ± 0.19 µg/g). The operational conditions for each extraction method are shown in Table 1. The quantitative yield of flavanone glycosides and aglycone using magnesium aluminometasilicate are shown in Figures 7 and 8.

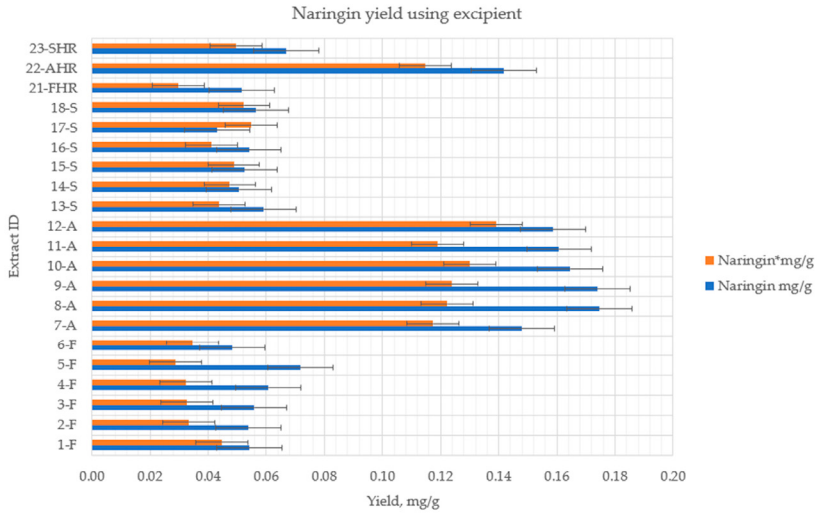

Figure 7. The quantitative yield of flavanone glycosides using excipient (1%). $p < 0.05$ when control samples without excipients were compared to samples with magnesium aluminometasilicate *. Extract ID and preparation conditions are displayed in Table 1.

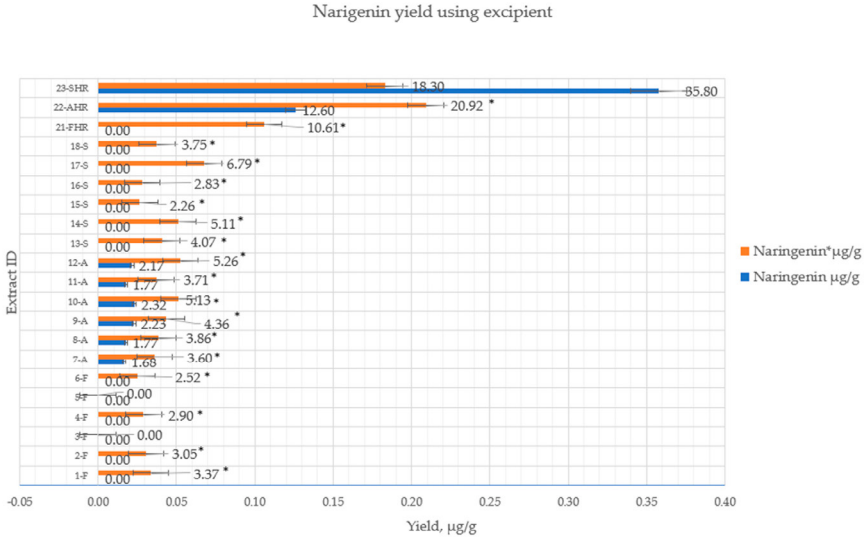

Figure 8. The quantitative yield of flavanone aglycones using excipients (1%). $p < 0.05$ when control samples without excipients were compared to samples with magnesium aluminometasilicate *. Extract ID and preparation conditions are displayed in Table 1.

Using the UAE technique (50 ± 2 °C, 30 min sonication time, and the solvent of purified water with 1% magnesium aluminometasilicate), naringenin was detected in samples from the *flavedo* part, with a yield of 2.38 ± 0.119 μg/g. However, given that the findings were not statistically significant, they are not included in Table 3.

4. Conclusions

The results indicated that the highest yields of naringin can be obtained using an ultrasound-assisted extraction bath with optimal conditions (50% of ethanol *v*/*v* as a solvent, sonication time 30 min at 50 ± 2 C°) from the *albedo* part 8-A (17.45 ± 0.872 mg/g); meanwhile, the highest yield of naringenin was obtained by heat reflux extraction method from the *segmental* part with 70% of ethanol (*v*/*v*) 23-SHR (35.80 ± 1.79 μg/g). Significant results of naringenin yield in terms of ultrasound-assisted extraction using an ultrasonic homogenizer were obtained using extracts from the *segmental* part—in a short time (3 min), the quantity of naringenin increased up to 28-SUX2 (7.40 ± 0.37 μg/g) compared with UAE method (Table 3).

The solvent, extraction time, and temperature influenced the recovery of flavanones from fruit materials. The high temperatures could increase active compound quantities, so using the UAE method combined with thermal hydrolysis, the amount of naringin in the *segmental* and *albedo* portions was at least doubled: 15-S (11.07 ± 0.55 mg/g); 9-A (25.05 ± 1.25 mg/g). The acidic and thermal hydrolysis influenced the amount of aglycon naringenin from the *segmental* part and demonstrated better quantification when compared with extraction without hydrolysis, (0 μg/g–1.12 ± 0.056 μg/g–4.21 ± 0.21 μg/g) (Table 4).

The magnesium aluminometasilicate, which was used as an adsorbent to increase flavanone yields from different fruits parts, increased the amount of naringenin in all samples from the *flavedo*, *albedo,* and *segmental* parts, using 50% or 70% of ethanol (*v*/*v*). Meanwhile, when purified water was used as the solvent, naringenin was detected in a small amount from the *flavedo* part (2.38 ± 0.119 μg/g). Thus, we could achieve the same quantity of aglycone with a lower concentration of solvent (ethanol) when using additional adsorbent magnesium aluminometasilicate. However, the quantity of naringin was reduced by 15% in extracts from different parts of the fruits (Figure 7).

After reviewing the studies, we found that flavanone solubility may be increased in the aqueous solvent or a lower concentration of ethanol by adding additional agents, such as cyclodextrin, to improve the release and stability of the active compounds.

The majority of the active compounds were extracted from the *Citrus* × *paradisi* L. *albedo* and *segmental* parts using the UAE and HRE methods, so these parts are a promising material for further research and can be used to develop novel pharmaceutical products.

Author Contributions: Conceptualization J.B. and J.S.; methodology, J.B., L.I., M.M. and J.S.; investigation, J.S.; resources, J.B. and L.I.; writing—original draft preparation, J.S.; writing—review and editing, J.B. and J.S.; visualization, J.S.; supervision, J.B. All authors have read and agreed to the published version of the manuscript.

Funding: This research received no external funding.

Institutional Review Board Statement: Not applicable.

Informed Consent Statement: Not applicable.

Data Availability Statement: Not applicable.

Acknowledgments: The authors would like to thank the Open Access Centre for the Advanced Pharmaceutical and Health Technologies (Lithuanian University of Health Sciences) for the possibility to use their research infrastructure and fulfill this research.

Conflicts of Interest: The authors declare no conflict of interest.

References

1. Lü, Z.; Zhang, Z.; Wu, H.; Zhou, Z.; Yu, J. Phenolic Composition and Antioxidant Capacities of Chinese Local Pummelo Cultivars' Peel. *Hortic. Plant J.* **2016**, *2*, 133–140. [CrossRef]
2. Mahmoud, A.M.; Bautista, R.J.H.; Sandhu, M.A.; Hussein, O.E. Beneficial Effects of Citrus Flavonoids on Cardiovascular and Metabolic Health. *Oxidative Med. Cell. Longev.* **2019**, *2019*, 1–19. [CrossRef] [PubMed]
3. Deng, W.; Liu, K.; Cao, S.; Sun, J.; Zhong, B.; Chun, J. Chemical Composition, Antimicrobial, Antioxidant, and Antiproliferative Properties of Grapefruit Essential Oil Prepared by Molecular Distillation. *Molecules* **2020**, *25*, 217. [CrossRef] [PubMed]
4. Koolaji, N.; Shammugasamy, B.; Schindeler, A.; Dong, Q.; Dehghani, F.; Valtchev, P. Citrus Peel Flavonoids as Potential Cancer Prevention Agents. *Curr. Dev. Nutr.* **2020**, *4*, nzaa025. [CrossRef]
5. Durand-Hulak, M.; Dugrand, A.; Duval, T.; Bidel, L.P.R.; Jay-Allemand, C.; Froelicher, Y.; Bourgaud, F.; Fanciullino, A.-L. Mapping the genetic and tissular diversity of 64 phenolic compounds in Citrus species using a UPLC–MS approach. *Ann. Bot.* **2015**, *115*, 861–877. [CrossRef]
6. Cano, A.; Medina, A.; Bermejo, A. Bioactive compounds in different citrus varieties. Discrimination among cultivars. *J. Food Compos. Anal.* **2008**, *21*, 377–381. [CrossRef]
7. Alam, M.A.; Subhan, N.; Rahman, M.M.; Uddin, S.J.; Reza, H.M.; Sarker, S.D. Effect of Citrus Flavonoids, Naringin and Naringenin, on Metabolic Syndrome and Their Mechanisms of Action. *Adv. Nutr.* **2014**, *5*, 404–417. [CrossRef]
8. Suleria, H.A.R.; Barrow, C.J.; Dunshea, F.R. Screening and Characterization of Phenolic Compounds and Their Antioxidant Capacity in Different Fruit Peels. *Foods* **2020**, *9*, 1206. [CrossRef]
9. Ribeiro, I.A.; Rocha, J.; Sepodes, B.; Mota-Filipe, H.; Ribeiro, M.H. Effect of naringin enzymatic hydrolysis towards naringenin on the anti-inflammatory activity of both compounds. *J. Mol. Catal. B Enzym.* **2008**, *52–53*, 13–18. [CrossRef]
10. Cirmi, S.; Ferlazzo, N.; Lombardo, G.E.; Ventura-Spagnolo, E.; Gangemi, S.; Calapai, G.; Navarra, M. Neurodegenerative Diseases: Might Citrus Flavonoids Play a Protective Role? *Molecules* **2016**, *21*, 1312. [CrossRef]
11. Memariani, Z.; Abbas, S.Q.; ul Hassan, S.S.; Ahmadi, A.; Chabra, A. Naringin and naringenin as anticancer agents and adjuvants in cancer combination therapy: Efficacy and molecular mechanisms of action, a comprehensive narrative review. *Pharmacol. Res.* **2021**, *171*, 105264. [CrossRef]
12. Qurtam, A.A.; Mechchate, H.; Es-Safi, I.; Al-Zharani, M.; Nasr, F.A.; Noman, O.M.; Aleissa, M.; Imtara, H.; Aleissa, A.M.; Bouhrim, M.; et al. Citrus Flavanone Narirutin, In Vitro and In Silico Mechanistic Antidiabetic Potential. *Pharmaceutics* **2021**, *13*, 1818. [CrossRef]
13. Di Majo, D.; Giammanco, M.; La Guardia, M.; Tripoli, E.; Giammanco, S.; Finotti, E. Flavanones in Citrus fruit: Structure–antioxidant activity relationships. *Food Res. Int.* **2005**, *38*, 1161–1166. [CrossRef]
14. Tripoli, E.; La Guardia, M.; Giammanco, S.; Di Majo, D.; Giammanco, M. Citrus flavonoids: Molecular structure, biological activity and nutritional properties: A review. *Food Chem.* **2007**, *104*, 466–479. [CrossRef]
15. Mahato, N.; Sinha, M.; Sharma, K.; Koteswararao, R.; Cho, M.H. Modern Extraction and Purification Techniques for Obtaining High Purity Food-Grade Bioactive Compounds and Value-Added Co-Products from Citrus Wastes. *Foods* **2019**, *8*, 523. [CrossRef] [PubMed]
16. Felgines, C.; Texier, O.; Morand, C.; Manach, C.; Scalbert, A.; Régerat, F.; Rémésy, C. Bioavailability of the flavanone naringenin and its glycosides in rats. *Am. J. Physiol. Liver Physiol.* **2000**, *279*, G1148–G1154. [CrossRef]
17. Vila-Real, H.; Alfaia, A.J.; Bronze, M.R.; Calado, A.R.T.; Ribeiro, M.H.L. Enzymatic Synthesis of the Flavone Glucosides, Prunin and Isoquercetin, and the Aglycones, Naringenin and Quercetin, with Selective α-L-Rhamnosidase and β-D-Glucosidase Activities of Naringinase. *Enzym. Res.* **2011**, *2011*, 1–11. [CrossRef]
18. Rodríguez De Luna, S.L.; Ramírez-Garza, R.E.; Serna Saldívar, S.O. Environmentally Friendly Methods for Flavonoid Extraction from Plant Material: Impact of Their Operating Conditions on Yield and Antioxidant Properties. *Sci. World J.* **2020**, *2020*, 1–38. [CrossRef]
19. Chaves, J.O.; De Souza, M.C.; Da Silva, L.C.; Lachos-Perez, D.; Torres-Mayanga, P.C.; Machado, A.P.D.F.; Forster-Carneiro, T.; Vázquez-Espinosa, M.; González-de-Peredo, A.V.; Fernández Barbero, G. Extraction of Flavonoids from Natural Sources Using Modern Techniques. *Front. Chem.* **2020**, *8*, 507887. [CrossRef]
20. Giannuzzo, A.N.; Boggetti, H.J.; Nazareno, M.A.; Mishima, H.T. Supercritical fluid extraction of naringin from the peel of Citrus paradisi. *Phytochem. Anal.* **2003**, *14*, 221–223. [CrossRef]
21. Khan, M.K.; Abert-Vian, M.; Fabiano-Tixier, A.-S.; Dangles, O.; Chemat, F. Ultrasound-assisted extraction of polyphenols (flavanone glycosides) from orange (*Citrus sinensis* L.) peel. *Food Chem.* **2010**, *119*, 851–858. [CrossRef]
22. M'hiri, N.; Ioannou, I.; Paris, C.; Ghoul, M.; Mihoubi Boudhrioua, N. Ecophysiology and Agri Processes, Higher Institute of Biotechnology of Sidi Thabet, University of Manouba, BP-66, 2020 Ariana-Tunis, Tunisie, Boudhrioua N. Comparison of the Efficiency of Different Extraction Methods on Antioxidants of Maltease Orange Peel. *IJFNS* **2016**, *3*, 1–13.
23. Rozzi, N.L.; Singh, R.K. Supercritical Fluids and the Food Industry. *Compr. Rev. Food Sci. Food Saf.* **2006**, *1*, 33–44. [CrossRef] [PubMed]
24. Ioannou, I.; M'Hiri, N.; Chaaban, H.; Boudhrioua, N.M.; Ghoul, M. Effect of the process, temperature, light and oxygen on naringin extraction and the evolution of its antioxidant activity. *Int. J. Food Sci. Technol.* **2018**, *53*, 2754–2760. [CrossRef]
25. Nuutila, A.; Kammiovirta, K.; Oksman-Caldentey, K.-M. Comparison of methods for the hydrolysis of flavonoids and phenolic acids from onion and spinach for HPLC analysis. *Food Chem.* **2002**, *76*, 519–525. [CrossRef]

26. Walle, T.; Browning, A.M.; Steed, L.L.; Reed, S.G.; Walle, U.K. Flavonoid Glucosides Are Hydrolyzed and Thus Activated in the Oral Cavity in Humans. *J. Nutr.* **2005**, *135*, 48–52. [CrossRef]
27. Kazlauskaite, J.; Ivanauskas, L.; Bernatoniene, J. Novel Extraction Method Using Excipients to Enhance Yield of Genistein and Daidzein in *Trifolium pratensis* L. *Pharmaceutics* **2021**, *13*, 777. [CrossRef]
28. Matulyte, I.; Jekabsone, A.; Jankauskaite, L.; Zavistanaviciute, P.; Sakiene, V.; Bartkiene, E.; Ruzauskas, M.; Kopustinskiene, D.M.; Santini, A.; Bernatoniene, J. The Essential Oil and Hydrolats from Myristica fragrans Seeds with Magnesium Aluminometasilicate as Excipient: Antioxidant, Antibacterial, and Anti-inflammatory Activity. *Foods* **2020**, *9*, 37. [CrossRef]
29. Min, K.Y.; Kim, H.J.; Lee, K.A.; Kim, K.-T.; Paik, H.-D. Antimicrobial activity of acid-hydrolyzed Citrus unshiu peel extract in milk. *J. Dairy Sci.* **2014**, *97*, 1955–1960. [CrossRef]
30. Wolfender, J.-L. HPLC in Natural Product Analysis: The Detection Issue. *Planta Med.* **2009**, *75*, 719–734. [CrossRef]
31. Tu, X.; Ma, S.; Gao, Z.; Wang, J.; Huang, S.; Chen, W. One-Step Extraction and Hydrolysis of Flavonoid Glycosides in Rape Bee Pollen Based on Soxhlet-Assisted Matrix Solid Phase Dispersion: A Modified MSPD Method for the Determination of Flavonoid Aglycones. *Phytochem. Anal.* **2017**, *28*, 505–511. [CrossRef] [PubMed]
32. Matulyte, I.; Marksa, M.; Ivanauskas, L.; Kalvėnienė, Z.; Lazauskas, R.; Bernatoniene, J. GC-MS Analysis of the Composition of the Extracts and Essential Oil from Myristica fragrans Seeds Using Magnesium Aluminometasilicate as Excipient. *Molecules* **2019**, *24*, 1062. [CrossRef] [PubMed]

Paper 2

Title: *Citrus* × *paradisi* L. Fruit Waste: The Impact of Eco-Friendly Extraction Techniques on the Phytochemical and Antioxidant Potential
Authors: Jolita Stabrauskiene, Mindaugas Marksa, Liudas Ivanauskas, Pranas Viskelis, Jonas Viskelis and Jurga Bernatoniene.
Nutrients 2023,15, 1276.

nutrients

MDPI

Article

Citrus × *paradisi* L. Fruit Waste: The Impact of Eco-Friendly Extraction Techniques on the Phytochemical and Antioxidant Potential

Jolita Stabrauskiene [1,2], Mindaugas Marksa [3], Liudas Ivanauskas [3], Pranas Viskelis [4], Jonas Viskelis [4] and Jurga Bernatoniene [1,2,*]

[1] Department of Drug Technology and Social Pharmacy, Lithuanian University of Health Sciences, LT-50161 Kaunas, Lithuania
[2] Institute of Pharmaceutical Technologies, Lithuanian University of Health Sciences, LT-50161 Kaunas, Lithuania
[3] Department of Analytical and Toxicological Chemistry, Lithuanian University of Health Sciences, LT-50161 Kaunas, Lithuania
[4] Lithuanian Research Centre for Agriculture and Forestry, Institute of Horticulture, LT-54333 Babtai, Lithuania
* Correspondence: jurga.bernatoniene@lsmuni.lt; Tel.: +370-6006-3349

Abstract: Citrus fruits have been the subject of extensive research over the years due to their impressive antioxidant properties, the health benefits of flavanones, and their potential use in the prevention and treatment of chronic diseases. Grapefruit have been shown in studies to improve overall health, with numerous potential benefits, including improved heart health, reduced risk of certain cancers, improved digestive health, and improved immune system function. The development of cyclodextrin complexes is an exciting approach to increasing the content of flavanones such as naringin and naringenin in the extraction medium while improving the profile of beneficial phenolic compounds and the antioxidant profile. This research aims to optimize the extraction conditions of the flavanones naringin and naringenin with additional compounds to increase their yield from different parts of grapefruit (*Citrus* × *paradisi* L.) fruits, such as albedo and segmental membranes. In addition, the total content of phenolic compounds, flavonoids, and the antioxidant activity of ethanolic extracts produced conventionally and with -cyclodextrin was examined and compared. In addition, antioxidant activity was measured using the radical scavenging activity assay (ABTS), radical scavenging activity assay (DPPH), and ferric reducing antioxidant power (FRAP) methods. The yield of naringin increased from 10.53 ± 0.52 mg/g to 45.56 ± 5.06 mg/g to 51.11 ± 7.63 mg/g of the segmental membrane when cyclodextrins (α, β-CD) were used; naringenin increased from 65.85 ± 10.96 µg/g to 91.19 ± 15.19 µg/g of the segmental membrane when cyclodextrins (α, β-CD) were used. Furthermore, the results showed that cyclodextrin-assisted extraction had a significant impact in significantly increasing the yield of flavanones from grapefruit. In addition, the process was more efficient and less expensive, resulting in higher yields of flavanones with a lower concentration of ethanol and effort. This shows that cyclodextrin-assisted extraction is an excellent method for extracting valuable compounds from grapefruit.

Keywords: *Citrus* × *paradisi* L.; grapefruit; flavanones; aglycones; excipients; cyclodextrins; extractions; antioxidant

check for updates

Citation: Stabrauskiene, J.; Marksa, M.; Ivanauskas, L.; Viskelis, P.; Viskelis, J.; Bernatoniene, J. *Citrus* × *paradisi* L. Fruit Waste: The Impact of Eco-Friendly Extraction Techniques on the Phytochemical and Antioxidant Potential. *Nutrients* **2023**, *15*, 1276. https://doi.org/10.3390/nu15051276

Academic Editor: Huihui Xiao

Received: 9 February 2023
Revised: 1 March 2023
Accepted: 1 March 2023
Published: 3 March 2023

1. Introduction

Natural bioactive compounds are in demand as humans become more health conscious, especially regarding a balanced diet. Epidemiological studies have shown that consumers of polyphenolic compounds are less susceptible to chronic diseases [1,2]. From this perspective, the fruits of *Citrus* × *paradisi* L. are rich in physiologically active components such as phenolic compounds, vitamins, carotenoid pigments, and fiber [3]. Grapefruit

(*Citrus* × *paradisi* L.) is one of the world's most popular fruits. In Eastern medicine, it is used as an appetite stimulant, antidiarrheal, emetic, and expectorant to treat flatulence, scurvy, acne, and eczema [4]. In addition, recent studies have shown that extracts of citrus peels and juices, as well as the biologically active components isolated from them, have a wide range of beneficial effects on living organisms, including antioxidant, antimicrobial, cardiovascular, anticancer, and antidiabetic activity (Figure 1) [5–9]. Due to the great pharmacological potential of citrus fruits, flavonoids and phenolic chemicals are the most studied biologically active molecules in the pharmaceutical field.

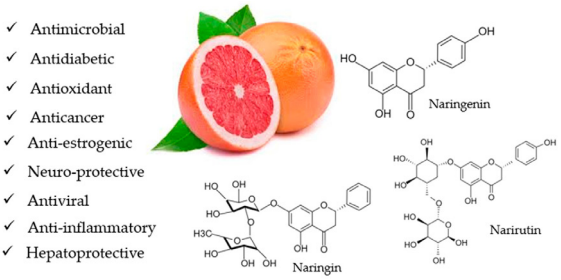

Figure 1. The effects of grapefruit (*Citrus* × *paradisi* L.) and the main flavonoids found in its extracts.

Two of the most important flavanones in grapefruit fruits are naringin and narirutin [10]. Naringenin (5,7,4′-trihydroxy flavanone), a polyphenolic flavonoid, is an aglycone derivative of hydrogenated flavone [11]. The bacteria of the gut microbiome convert naringin into active naringenin [12]. This flavonoid molecule is an essential part of the human diet and responsible for our foods' color and bitter–sour taste.

The anticancer, antiproliferative, and antitumor effects of naringenin are based on its DNA repair ability [13,14]. It has inhibited breast, liver, prostate, melanoma, and spinal cord glioblastoma cells. Naringenin also influences the intrinsic (mitochondrial) and extrinsic (receptor) apoptotic pathways. The effect of naringenin on apoptosis inhibits proliferation and angiogenesis [15].

Naringenin reduces leukocyte accumulation by inhibiting macrophages' chemotaxis molecules, which draw leukocytes to inflammation [14,16]. In addition, it activates NF-E2–related factor 2 (Nrf2), an anti-inflammatory factor, in macrophages which is another way it influences. It can also reduce pro-inflammatory cytokines such as IL-33, TNF-, IL-1, and IL-6, suppressing nuclear factor-κB (NF-kB) activation [17], boosting antioxidant ability, and reducing superoxide anions and other reactive oxygen species (ROS) [18].

Antidiabetic activity: Studies conducted in vitro and in vivo show that naringenin is essential in preventing and treating insulin resistance and type 2 diabetes [6]. This bioflavonoid can reduce the amount of glucose absorbed by the intestinal brush and the amount of sugar stored in the kidneys [19]. In addition, naringenin improves glucose uptake and utilization and contributes to glucose reabsorption by muscle and adipose tissue. According to the research, naringenin stimulates the growth of pancreatic cells, which has a beneficial effect. These cells have enhanced glucose-sensing abilities because of their training. It has been hypothesized that naringenin causes pancreatic cells to be more sensitive to the effects of glucose and has a pro-apoptotic effect on these cells [12].

Naringenin reduces inflammation caused by phenyl-β-benzoquinone, acetic acid, formalin, capsaicin, carrageenan, and superoxide anions [20]. This bioflavonoid also possesses antinociceptive and analgesic properties in vivo. Naringenin also regulates transient receptor potential (TRP) channels in nociceptors. Hence, it helps in analgesia [21].

Antibiotic resistance is a global problem. Bacteria are resistant to all groups of antibiotics [22]. The use of antibiotics in the food, veterinary, and medical industries has

raised this concern. Overprescribing antibiotics to asymptomatic patients, the COVID-19 pandemic, and broad-spectrum antibiotics have worsened this situation. *Acinetobacter Baumann*, vancomycin-resistant *Enterococcus faecalis*, methicillin-resistant *Staphylococcus aureus*, and beta-lactam-resistant *Klebsiella pneumonia* result from overuse. Naringenin kills Gram-positive bacteria, including *S. aureus* and *MRSA* [23,24]. However, only a few clinical studies are using this bioflavonoid as an antibiotic. Unfortunately, neither the US nor the EU databases have registered any clinical trials, so these results are unavailable. Pharmacological safety is shown at 900 mg [25].

Flavanones are also liver protective. Naringenin reduces hyperglycemia, hyperlipidemia, and gluconeogenesis [26], reduces triglyceride formation, and significantly reduces low-density lipoproteins (LDL) and triglycerides in diabetic mice. Furthermore, based on articles, naringenin increased high-density lipoproteins (HDL) levels in Wistar albino rats [19,27].

Antioxidant activity in the traditional sense is identified by the hydroxy substituents (OH) on their molecules showing a high reactivity towards reactive oxygen species (ROS) and reactive nitrogen species (RNS) [5,22,28]. Because of this, the ability of a given molecule to function as an antioxidant increases when that molecule contains OH radicals; in the case of naringenin, there are three of these residues. After this, OH donates its hydrogen to free radicals (R), eventually stabilizing naringenin by resonance. Ring B is an essential part of the typical structure of flavonoids. This is because when hydroxyl groups are present in the ring, flavonoids can stabilize hydroxyl (OH), peroxyl (ROO), and peroxynitrite (ONOO) radicals, thereby forming relatively stable flavonoid radicals (Figure 2) [29,30].

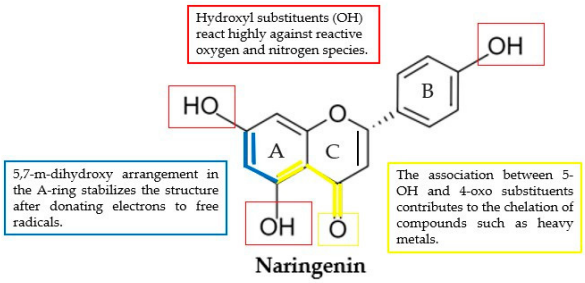

Figure 2. Naringenin: the relationship between antioxidant activity and structure. In red: Hydroxyl substituents (OH) react highly against reactive oxygen and nitrogen species. In blue: 5,7-m-dihydroxy arrangement in the A-ring stabilizes the structure after donating electrons to free radicals. In yellow: The association between 5-OH and 4-oxo substituents contributes to the chelation of compounds such as heavy metals.

UV spectrophotometry is the most common method for measuring phenolic compounds, flavonoids, and phenolic acids [31]. They measure the absorption of the reaction mixture in the visible spectrum. These methods are fast, simple, and reliable but lack chromatographic selectivity. Colorimetric techniques are used to quantify phenolic compounds based on their abundance and the complexity of the plant matrix [32]. One of these methods is that of Folin–Ciocalteu, which uses a specific reagent composed of several chemicals (sodium molybdate, sodium tungstate, etc.) [33]. The method is based on electron transfer reactions. However, the method requires a reference substance (in this case, gallic acid) to measure the total phenolic content of the extract.

Next, the method with aluminum chloride ($AlCl_3$) is used to test the total amount of flavonoids. These forms chelate complexes of aluminum and flavonoids [34]. DPPH (2,2-diphenyl1-picrylhydrazyl), ABTS (2,2′-azino-bis(3-ethylbenzothiazoline-6-sulfonic acid),

and FRAP (Ferric Reducing Antioxidant Power) are spectrophotometric techniques for the preliminary testing of the antioxidant activity of plant extracts [35,36].

ABTS uses ABTS•+, a stable blue-green radical with a maximum absorbance of 734 nm. Before use, allow the ABTS solution and potassium persulfate ($K_2S_2O_8$) to react in the dark at room temperature for 12–16 h to generate the ABTS radical cation. Next, this ion reacts with phenolic chemicals to change the blue color to greenish or colorless. Data are Trolox equivalents [34].

The FRAP method is comparable to the ABTS and DPPH methods; however, the reaction is carried out in an acidic medium. The effectiveness of the antioxidant in reducing Fe (III) in an acidic solution is the focus of this approach [35].

Pharmacologically active chemicals usually contain excipients. Excipients help in the formulation of drugs, and they increase drug stability, dosage uniformity, and bioavailability [36]. Cyclodextrins are composed of a ring of glucose molecules linked in a specific arrangement. The structure creates a cavity within the molecule, which can be used to bind to other molecules. This property makes cyclodextrins useful for drug delivery, as they can bind to drugs and deliver them to the desired location in the body. Additionally, cyclodextrins have a high degree of solubility in water, which makes them useful for water purification applications.

Another property of cyclodextrins is their ability to form complexes with other molecules. This property makes them useful for food processing applications, as they can be used to bind to food additives and other compounds to improve their stability and shelf life. Additionally, cyclodextrins can be used to bind to flavors and aromas, which can be used to enhance the flavor and aroma of food products.

Cyclodextrins (CDs) form inclusion complexes in aqueous solutions, making them suitable for assisted extraction. Lipophilic guest molecules or fragments reside within these inclusion complexes [37], so complexation can increase flavanone solubility and antioxidant properties [38]. In addition, CDs decrease the taste of naringin generations and decrease their interaction with intestinal CYP3A4 metabolized drugs [39]. The most common types of cyclodextrins are α-CD, β-CD, and γ-CD, which contain six, seven, and eight glucopyranose units, respectively (Figure 3).

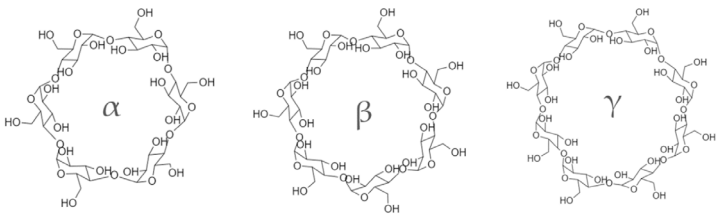

Figure 3. Chemical formulas of α-, β-, and γ-CD.

The exterior of these molecules is hydrophilic, which helps CDs interact favorably with water. Furthermore, the hydrophobic cavity of these molecules can accommodate a variety of guest molecules, including polar compounds (alcohols, acids, amines, and small inorganic anions) and nonpolar compounds (aliphatic and aromatic hydrocarbons) [40,41]. Figure 4 shows a graphical representation of the structure of CDs.

Recently, CDs have been used to separate polyphenols, including phenolic acid and flavonoids, from various natural sources. For example, Li Cui et al. (2012) found that β-CD inclusion complexation increased the solubility of naringin in water, which accelerated enzyme hydrolysis to form naringenin [42,43]. In addition, the inclusion complex foundation protects CDs from oxidation and decay [44].

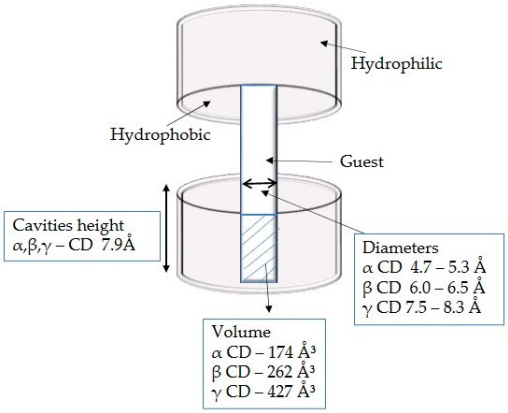

Figure 4. The heights, internal diameters, and cavity volumes of α, β, and γ CDs.

Based on these assessments, it becomes clear why there is so much interest in conducting additional in-depth studies on treated grapefruit peel as a natural, economical, and accessible antioxidant source.

The purpose of this research is twofold: (I) to describe and optimize the extraction conditions of the flavanones naringin and naringenin with additional compounds to increase their yield from different parts of the grapefruit fruit, such as albedo and segmental membranes; and (II) to describe and quantify the flavonoid profiles and antioxidant activity of processed grapefruit peel and juice. Both objectives are addressed in this study.

2. Materials and Methods

2.1. Material

The grapefruit's segmental membranes and skins were gathered for secondary raw materials when the juice was extracted from grapefruit (*Citrus* × *paradisi* L., variety Star Ruby, Italy, unknown place). After being diced up in a food processor, these components were frozen at −18 ± 0.9 °C until extraction. Figure 5 depicts the fruit slices that were utilized in this investigation.

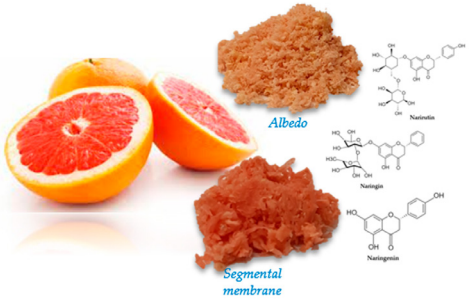

Figure 5. Fresh Albedo, and segmental membrane of *Citrus* × *paradisi* L.

Standards of naringin, naringenin, and narirutin were obtained from Sigma Aldrich in Steinheim, Germany. Hydrochloric acid, sodium hydroxide, acetic acid, methanol, acetonitrile, Trolox, α-, β-, and γ-CDs were obtained from Sigma Aldrich in HH, DE. Ethanol (96%) was obtained from Vilniaus Degtine in Vilniaus, LT. GFL2004 was used to manufacture filtered water (Burgwedelis, DE). The following reagents were also utilized: aluminum chloride, hexamethylenetetramine, acetic acid, 2,20-azino-bis(3-ethylbenzothiazoline-6-sulfonic acid) (ABTS), 2,4,6-Tris(2-pyridyl)-s-triazine (TPTZ), potassium persulfate, ferrous sulfate heptahydrate, saline phosphate buffer, and hydrogen peroxide from Sigma Aldrich (Schnelldorf, Germany); disodium hydrogen phosphate obtained from Merck (Darmstadt, Germany); 2,2-diphenyl1-picrylhydrazyl radical (DPPH).

2.2. Methods

2.2.1. Extracts' Preparation

Control sample: a control batch was performed based on previous studies using a combined extraction method with 50 and 70% ethanol (*v*/*v*). The extraction process used in this study is shown in Figure 6 [45].

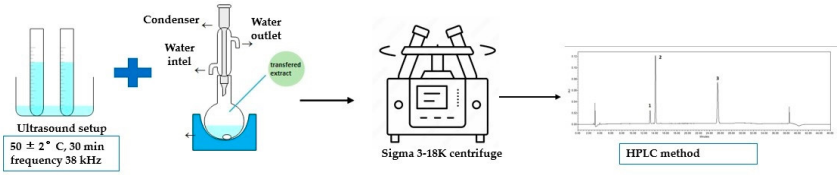

Figure 6. Combined extraction method schema.

Test sample: The extracts were made under the same conditions. The 50% or 70% ethanol (*v*/*v*) was employed as the solvent (10 mL), and the additional substances (0.1 ± 0.105 g of α-, β-, γ-CDs) were added with plant material (1 ± 0.05 g). After centrifuging the materials for 10 min at 1789× *g*, the supernatant was discarded by decantation. The extracts were then filtered using PVDF syringe filters with a pore size of 0.22 m, and an HPLC analysis was used to determine the total quantity of flavanones. A list of samples prepared in the UAE with thermal hydrolysis and excipients is given in Table 1.

Table 1. Extract ID and preparation condition.

Extract ID *	Extraction Method	Solvent (Ethanol *v*/*v*)	Excipient (Cyclodextrins CD)
AT1 (control sample)		50%	
AT2 (control sample)		70%	
ST1 (control sample)		50%	
ST2 (control sample)		70%	
AA1		50%	α
AA2		70%	α
SA1		50%	α
SA2	UAE combined with	70%	α
AB1	thermal hydrolysis	50%	β
AB2		70%	β
SB1		50%	β
SB2		70%	β
AG1		50%	γ
AG2		70%	γ
SG1		50%	γ
SG2		70%	γ

* First letter demonstrated fruit parts (A-albedo; S-segmental membrane); second letter (T-control sample, A-α-CD, B-β-CD, G-γ-CD); numbers (1–50% solvent *v*/*v*, 2–70% solvent *v*/*v*).

2.2.2. HPLC–PDA Conditions

Waters 2695 liquid chromatography with a photodiode array detector was used (Waters 996, 200–400 nm wavelength range). We used an ACE C18 chromatography column (250 mm × 4.6 mm) with a sorbent particle size of 5 µm to separate physiologically active substances. The process details of the HPLC method were as follows. Gradient elution was used to separate the tested substances. Each extract was injected in a volume of 10 L and measured at 280 nm. Eluent A: acetonitrile at a rate of 1 mL/min; Eluent B: water. 0.0 min, 10% A; 5 min, 20% A; 25 min, 40% A; 30 min, 100% A; 35 min, 100% A; 36 min, 10% A. The temperature of the column was set at 25 °C. Peaks were found by comparing the UV-Vis spectra of each peak to valid reference standards and measuring their retention times. The samples were subjected to two different analyses. The chromatograms of the standards for naringenin, naringin, and narirutin are shown in Figure 7.

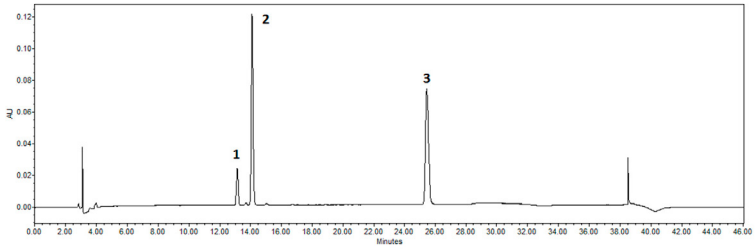

Figure 7. Chromatograms of standards detected by HPLC. 1–narirutin, 2–naringin, and 3–naringenin were identified as peak.

The Methodological Review of Natural Products by Wolfender (2009) [29,46] was used for quantification and validation. Standard stock solutions with primary concentrations of 100 µg/mL of naringin, narirutin, and naringenin were prepared in 70% methanol, and calibration curves were constructed using six standard solution concentrations. Three injections per concentration were performed to determine linearity. To construct calibration equations, naringin, naringenin, and narirutin were plotted against known concentrations of the respective standard solutions. The least squares approach was used to calculate a linear regression equation. The regression coefficients of all calibration curves were $R^2 > 0.999$, confirming the linearity of the concentration ranges.

The sensitivity of the approach was determined by determining the limit of detection (LOD) and the quantification (LOQ). The concentrations that produced a signal-to-noise ratio of 3 and 10, respectively, were used to determine LOD and LOQ.

A standard mixture of naringin, naringenin, and narirutin was used during the intraday and inter-day precision testing. Five repeated non-consecutive injections of the regular combination on the same day on four different days proved the method's accuracy. Relative standard deviation (RSD) is used to describe the results. The retention times and spectra of standards (naringin, naringenin, and narirutin) were compared to those prepared in extracts in this work. Linearity was determined by calculating the correlation coefficient R^2 of the calibration curve (naringin R^2 = 0.99992, naringenin R^2 = 0.99992, narirutin R^2 = 0.99999) and the peak areas were used for quantification. The linearity range of naringin was 1.166 to 33.34 µg/mL, 0.472 to 15.12 µg/mL for naringenin, and 1.2757 to 80.5 µg/mL for narirutin. The concentrations of naringenin, naringin, and narirutin were expressed as µg/g, mg/g, and mg/g dry weight (DW), respectively (Table 2).

Table 2. The linearities of calibration curves of flavanones.

Component	Calibration Equation	Coefficient of Determination R^2	Correlation Coefficient	LOD µg/mL	LOQ µg/mL
Naringin	Y = 25.50x + 6720	0.99992	0.99996	0.146	0.583
Naringenin	±Y = 33.30x + 3570	0.99992	0.99996	0.118	0.430
Narirutin	Y = 18.60x + 8100	0.99999	0.99999	0.281	0.5032

LOD—limit of detection; LOQ—limit of quantification.

2.3. Statistical Data Analysis

SSPS version 20.0 (IBM Corporation, Armonk, NY, USA) was used to analyze the data. Data are presented as mean and standard deviation (SD). All quantitative data were performed in triplicate. The Friedman and Wilcoxon tests were used to make the comparisons that should be made between the three different metrics. In addition, Spearman's test was used to determine correlation and regression coefficients. At the end, a comparison was made between the two groups using the Mann–Whitney U test. Results were considered statistically significant ($p < 0.05$).

2.4. Preparation of Extracts for Total Phenolic, Flavonoid, and Antioxidant Activity

We used a modification of this ultrasound-assisted extraction method to adapt it for our application to determine the total phenolic, flavonoid amount, and antioxidant activity. An ultrasound-assisted extraction method (UP-250; frequency range: 19–25 kHz, 250 W, probe amplitude: 35 µm) was used to prepare the extraction from grapefruit waste product and fresh juice. Control sample: the total content of phenols, flavonoids, DPPH, ABTS, and FRAP was determined using the flavedo, albedo, segmental membrane. A total of 10 g of plant material was poured with a solvent (50% ethanol v/v) and treated with an ultrasonic bath at 50 ± 5 °C for 30 min. The tested sample was produced under the same conditions but with additional excipients (0.1 g ± 0.01 g β-CDs) (Figure 8). A fresh juice tested sample was created; 10 mL of fresh juice and 0.1 g ± 0.01 g of β-cyclodextrins were added and treated for 30 min at 50 ± 5 °C using an ultrasound bath.

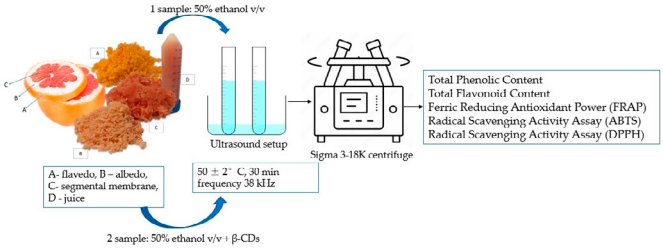

Figure 8. Extraction procedure to determine total phenolic, flavonoid, and antioxidant activity.

2.4.1. Analysis of Total Phenolic Content

A spectrophotometric analysis method determined the total amount of phenolic compounds in *Citrus* × *paradisi* L. The extract was mixed with the Folin-Ciocalteu phenol reagent, 2 mL of 7% sodium carbonate (Na_2CO_3) was added, and the mixture was kept in a dark place for 60 min. A gallic acid calibration curve y = 12.069x; R^2 = 0.9978 was used to create the calibration curve. The data were given in milligrams of gallic acid equivalent per gram of dry weight (mg GAE/g DW) [47].

2.4.2. Total Flavonoid Content Evaluation

The colorimetric aluminum chloride technique was modified to determine the total flavonoid concentration of the extracts [48]. First, 0.2 mL of the extract was combined with 2 mL of 96% (*v*/*v*) ethanol, 0.1 mL of 30% acetic acid, 0.3 mL of 10% aluminum chloride ($AlCl_3$), and 0.4 mL of 5% hexamethylenetetramine solutions. After 30 min of incubation, the absorbance of the reaction mixture was measured at 475 nm using a spectrophotometer (Shimadzu UV-1800; Kyoto, Japan). Then, the total flavonoid content was determined using a calibration curve (y = 5.0867x; R^2 = 0.9985). The result was computed using the following procedure and expressed as mg of rutin equivalent per gram of dry weight (RE/g DW):

$$TFC = C \times Ve \times F/m,$$

where

TFC–total flavonoid content; mg RE/g DW;
C–concentration of standards used mg/L;
Ve–the volume of solvent used;
F–dilution coefficient of the sample; m–a mass of the sample, g.

2.5. Antioxidant Activity

2.5.1. Radical-Scavenging Assay (ABTS)

ABTS (2,2′-Azino-bis-(3-ethylbenzthiazoline-6-sulonic acid) was oxidized using potassium persulfate to generate the $ABTS^{\bullet+}$ radical. It showed absorption maxima at wavelengths 645, 734, and 815 nm. A 7 mM (ABTS) aqueous solution was created and stored in the dark for 12 to 16 h to generate a dark solution containing the radical cation. Before usage, the ABTS radical cation was diluted with water, and its initial absorbance at 734 nm was measured using a spectrophotometer to be about 0.70 ± 0.01. To assess radical scavenging activity, 2.0 mL of the ABTS working standard was combined with 200 µL in a test cuvette. Using Trolox, the calibration curve was created (y = 0.0001728x; R^2 = 0.9832). Results were reported regarding the Trolox equivalent per gram of dry weight (TE per g DW) [49].

2.5.2. Radical Scavenging Assay (DPPH)

The free radical scavenging activity of the extract was carried out with slight modifications. For the first step, 10 µL of each ethanolic solution was mixed with 3 mL of 2,2-diphenyl-1-picrylhydrazyl (DPPH) solution. Then, the reaction mixture was incubated in the dark at room temperature for 1 h, and the absorbance at 517 nm was measured using a spectrophotometer (Shimadzu UV-1800; Kyoto, Japan). The calibration curve was obtained with Trolox (y = 0.00623x; R^2 = 0.9923). The results were expressed as Trolox equivalent per gram dry weight (TE/g DW) [50].

2.5.3. Ferric Reducing Antioxidant Power (FRAP)

The FRAP test was performed by combining 0.3 M of acetate buffer with a pH of 3.6, 10 mM of a solution containing 2,4,6-tripiridil-s-triazino, 40 mM of hydrochloric acid, and 20 mM of a solution containing ferric (III) chloride (10:1:1). After that, 10 µL of the sample was combined with 3 mL of the FRAP reagent, and the resulting mixture was well combined. After 30 min incubation, using a spectrophotometer, the level of absorption was determined to be 593 nm (Shimadzu UV-1800; Kyoto, Japan). Ferrous sulfate was used to obtain the calibration curve, which had the following equation: y = 0.00010x + 0.0646; R^2 = 0.9915 [51].

3. Results and Discussion

The flavanones most prevalent in grapefruit fruit are glycosides, specifically naringin and narirutin. On the other hand, naringenin (in the form of aglycone) is not very soluble in water; as a result, the majority of the extracts that were tested either had very low amounts of aglycone or only traces of it [42]. Consequently, one of the essential tasks is to increase

the amount of naringenin in the extracts and to do so in the simplest, most viable way. We selected the most optimal extraction conditions based on the previous research methods and used the conjugated extraction method. Using only ultrasound extraction method (UAE) without thermal hydrolysis showed poor results compared with thermal hydrolysis. Thermal hydrolysis is necessary to obtain a higher yield of naringenin (Table 3).

Table 3. Yields of flavanones from control samples using ultrasound extraction method modified with thermal hydrolysis. Results are means ± SD (n = 3).

Extract ID	Naringin mg/g	Narirutin mg/g	Naringenin μg/g
AT1 *	13.97 ± 0.698	2.24 ± 0.12	23.58 ± 1.17
AT2 *	14.07 ± 0.70	2.36 ± 0.18	25.06 ± 1.25
ST1 *	10.53 ± 0.526	2.34 ± 0.17	65.84 ± 3.29
ST2 *	7.8 ± 0.39	1.95 ± 0.09	67.59 ± 3.37

* Extract ID are provided in Table 1. The highest amount of naringin and narirutin was determined from the albedo part 13.97 ± 0.698 mg/g, 14.07 ± 0.71 mg/g (50 and 70% ethanol v/v), and 2.24 ± 0.12 mg/g, 2.36 ± 0.12 mg/g (50 and 70% ethanol v/v), respectively. Meanwhile, naringenin's highest quantity was detected from the segmental membrane—67.59 ± 2.81 μg/g using 70% of ethanol v/v.

First, the control extraction with the α, β, and γ-CDs was performed using the conjugated extraction method described in Section 2.2.1 and compared to the test extraction (prepared under the same conditions). Table 3 illustrates the findings that were obtained from the control extraction.

3.1. The Quantity of Flavanones Using the Additional Substances α-, β-, γ-Cyclodextrins

The structure of cyclodextrins (CD) can explain the increased yield of flavanones in the extracts from plant material. Additionally, the CD encapsulation can change the physicochemical features, such as water solubility and the substance's stability [36].

CDs can protect chemically unstable drug molecules from environmental factors, reducing or preventing drug hydrolysis, oxidation, and enzymatic degradation. One common application is reducing bitterness in citrus fruit juice by forming a naringin-β-CD complex [38]. The research of Pereira et al. in 2021 revealed that by using inclusion complexes, an impressive conversion rate from naringin to naringenin could be achieved, reaching up to 98.7% and 56.2%. On top of this remarkable success, β-CD has been noted as having a positive effect on water solubility; therefore, enzymatic hydrolysis of naringin will likely improve significantly [44].

Based on previous studies, we picked the albedo and segmental membrane parts for our investigation. The most significant quantities of naringenin were detected using combination extraction methods (ultrasonic extraction method with thermal hydrolysis).

Due to its polarity for flavonoids, research shows that methanol, among other organic solvents, is exceptionally capable of extraction. Because of this, efforts are being undertaken to find non-toxic and entirely biodegradable alternatives, such as ethanol, that can produce the same or similar outcomes without harming the environment [52,53].

The primary goal was to improve the flavanone yield in the extract; an organic solvent was chosen as a co-solvent with CDs because aglycones are more hydrophobic than hydrophilic chemicals and have limited solubility in water. As a result, once the combination with CD degrades, flavanone deposits might develop in water. This procedure may be avoided by using an organic solvent.

In control, the maximum level of naringenin was detected in the part of the segmental membrane using 70% ethanol (67.59 ± 3.37 μg/g). By using cyclodextrins, this amount could be increased by more than 34%. Comparing α, β, and γ-cyclodextrins, a statistically significant increase was observed in the AA1 sample (α-CDS, 50% ethanol v/v) 43.44 ± 2.17 μg/g compared to AT1 (23.58 ± 1.17 μg/g), AB1 (16.21 ± 0.81 μg/g), AG1 (0.84 ± 0.042 μg/g), and SA1 (91.19 ± 4.55 μg/g) compared to ST1 (65.84 ± 3.29 μg/g) and SB1 (0.45 ± 0.02 μg/g).

The results of our samples concluded that the combination of naringenin and α-CD with the smallest cavity size provided a higher yield of the aglycone compared to other cyclodextrins. Statistical analysis indicated that this significant increase was remarkable ($p < 0.05$).

According to the results of our research, 50% ethanol generated a higher concentration of naringenin than 70% (v/v) ethanol using α-CD: (AA1) 43.44 ± 2.17 μg/g–(AA2) 28.77 ± 1.44 μg/g from albedo, and (SA1) 91.19 ± 4.55 μg/g–(SA2) 86.69 ± 4.33 μg/g from segmental membrane parts, (50% and 70%, respectively). In addition, control samples AT1, AT2, and ST1 and ST2 were compared to test samples using α, β, and γ-CDs yielding statistically significant findings for naringenin using α-CD. The quantitative yield of naringenin using excipients (1%) is shown in Figure 9.

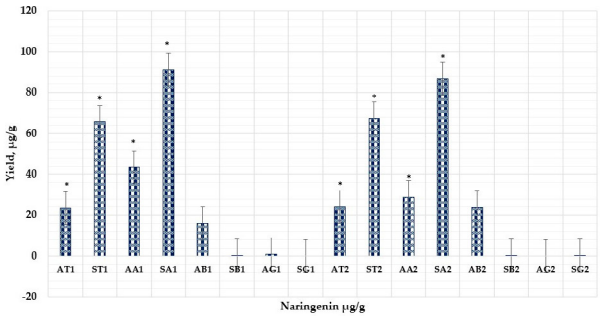

Figure 9. The quantitative yield of naringenin using excipients (1%). First letter demonstrated fruit parts (A—lbedo; S—segmental membrane); second letter (T—control sample; A—α-CD; B—β-CD; G—γ-CD); numbers (1–50% solvent v/v; 2–70% solvent v/v). AA1 $p < 0.05$ vs. AT1; AA2 $p < 0.05$ vs. AT2; SA1 $p < 0.05$ vs. ST1; SA2 $p < 0.05$ vs. ST2; AA1 $p < 0.05$ vs. AA2; AB2 $p < 0.05$ vs. AB1. * Results are means ± SD ($n = 3$).

Both naringin and narirutin are examples of hydrophobic polyphenols with a low water solubility of 38 and 500 μg/mL, respectively, at room temperature [54]. In addition, these polyphenols are inherently polar due to at least one sugar moiety in their molecular structures [55]. They are unable to form a stable complex with α-CD because they have the lowest affinity for it. In contrast to the findings obtained with control samples, extracts obtained with α-CD in this investigation showed statistically significant improvement (Figure 10) ($p < 0.05$). The results of flavanones showed in Table 4.

Based on the literature and previous research, our study chose 50 or 70% ethanol v/v. The extraction with water did not show any meaningful results, even after adding additional substances. Meanwhile, using 50% ethanol and α-CD significantly increased the amount of aglycones from the albedo and segmental membrane parts by an average of 1.6 and 1.05. Naringin from the albedo part (18.87 ± 0.94 mg/g–11.58 ± 0.58 mg/g, 50–70%, respectively) and narirutin in the sample from the albedo part 3.33 ± 0.16 mg/g–2.25 ± 0.11 mg/g, 50–70%, respectively.

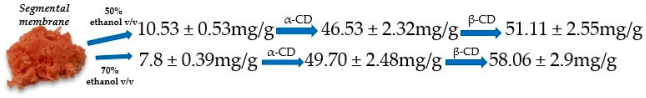

Figure 10. Naringin yield (control sample < α-CD < β-CD, respectively). Results are means ± SD ($n = 3$).

Table 4. Flavanone concentrations retrieved from samples using CDs.

Extract ID *	Naringin mg/g	Narirutin mg/g	Naringenin μg/g
AT1	13.99	2.24	23.58
ST1	10.53	2.34	65.84
AA1	18.87	3.33	43.44
SA1	46.53	0.70	91.19
AB1	6.87	1.74	16.21
SB1	51.11	0.81	0.45
AG1	5.99	1.79	0.84
SG1	7.52	2.29	0
AT2	14.07	2.36	24.06
ST2	7.80	1.95	67.59
AA2	11.58	2.25	28.77
SA2	49.72	0.80	86.69
AB2	8.75	1.74	23.80
SB2	58.08	0.98	0.20
AG2	10.59	2.13	0
SG2	6.76	2.15	0.45

The quantitative yield of naringin, naringenin, and narirutin using (1%) additional components α-, β-, γ-CDs. Results are means ± SD (n = 3). Naringin–AA1 $p < 0.05$ AT1; SB1 $p < 0.05$ SA1, ST1; SB2 $p < 0.05$ SA2; AA1 $p < 0.05$ AA2; SB2 $p < 0.05$ SB1; narirutin–AA1 $p < 0.05$ AT1; naringenin–AA1 $p < 0.05$ AT1; SA1 $p < 0.05$ ST1; AA2 $p < 0.05$ AT2; SA1 $p < 0.05$ SA2. * Extract ID are provided in Table 1.

The results of this study demonstrate that the quantity of flavanone in the extracts examined was significantly elevated when α and β cyclodextrins were used as compared to extracts used as controls. This study also showed that CDs increased flavanone yield while requiring a lower solvent concentration. Figure 11 displays the quantitative yield of naringin and naringenin when using excipients at a concentration of 1%.

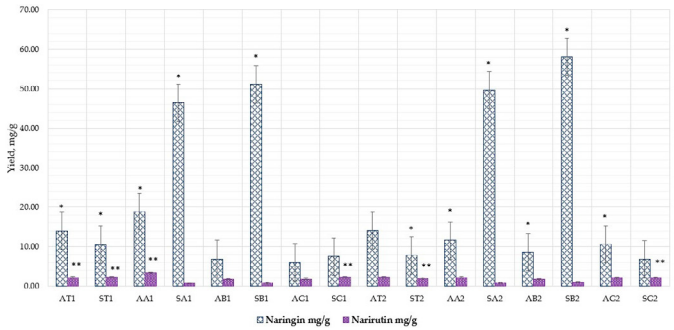

Figure 11. The quantitative yield of naringin and naringenin using excipients (1%). Sample codes are provided in Table 1. Results are means ± SD (n = 3). Naringin *: AA1 $p < 0.05$ vs. AT1 *; SA1 * $p < 0.05$ vs. ST1 *; SB1 * $p < 0.05$ vs. ST1 *; SB1 * $p < 0.05$ vs. SA1 *; AA2 $p < 0.05$ vs. AB2; SB2 * $p < 0.05$ vs. ST2 *; SB2 * $p < 0.05$ vs. SA2 *; SB2 * $p < 0.05$ vs. SB1 *; SA2 * $p < 0.05$ vs. SA1 *. Narirutin **: AA1 ** $p < 0.05$ vs. AT1 **; SG1 ** $p < 0.05$ vs. ST1 **; SG2 ** $p < 0.05$ vs. ST2 **.

The amount of naringin increased statistically significantly in the test sample with β-CDs, AA1, SA1, SA2, and SB2 compared to the control group AT1, ST1 AT2, and ST2. In addition, when comparing the test samples, higher amounts of naringin were found in the segmental membrane with β-CD using solvent 70% ethanol v/v (SB2) 58.08 ± 2.90 mg/g versus SB1 (50% ethanol v/v) 51.11 ± 2.55 mg/g.

The amount of narirutin was increased by α-CD in the albedo part, compared to the control sample (3.33 ± 0.16 mg/g vs. 2.24 ± 0.12 mg/g) and slightly increased by γ-CD in the segmental membrane 2.15 ± 0.11 mg/g). For naringin, the best results were obtained with β-CD from segmental membrane, using solvent 70% ethanol v/v.

3.2. Total Phenolic and Flavonoid Content Determination

It was evaluated how many total phenolic and flavonoids were determined using the ultrasound assistant extraction method (control sample) versus conjunction with 1% β-cyclodextrins (CDs) (tested sample), as described in Section 2.4.

Many medicinal plant species exhibit interspecific chemical diversity, which is important to study and evaluate. Chemical diversity studies provide information on the active ingredient's composition across species, varieties, and plant parts. Because of this, using UV–visible light spectrophotometry, pilot tests were carried out to measure the total content of phenolic compounds and flavonoids from various parts of *Citrus* × *paradisi* L. fruits. According to the findings of the tests, the total phenolic content varied from 2.48 ± 0.124 mg GAE/g DW (flavedo), 3.58 ± 0.17 mg GAE/g DW (albedo), 2.56 ± 0.12 mg GAE/g DW (segmental membrane), and 2.89 ± 0.14 mg GAE/g DW (juice). Most samples prepared with excipients contained more total phenolic compounds than control samples ($p < 0.05$).

This finding is significant because it shows that excipients can enhance the number of phenolic compounds found in a sample and shows promise for future pharmacology developments. Furthermore, the fact that these results have been statistically significant at $p \leq 0.05$ reinforces their credibility. Using β-CDs, the highest amount was found in the albedo part and increased from 3.58 ± 0.17 to 18.42 ± 0.92 mg GAE/g DW; the segmental membrane increased from 2.56 ± 0.128 to 17.8 ± 0.89 mg GAE/g DW. The total phenolic TPC content in grapefruit ethanol extract is shown in Figure 12.

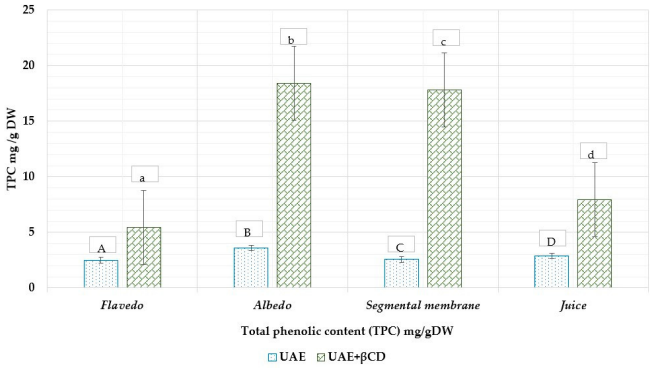

Figure 12. The total phenolic content TPC in grapefruit ethanolic extract with and without β-CDs. A, B, C, D—ultrasound extraction method (UAE), a, b, c, d—ultrasound extraction method (UAE) + β-CDs. The result is the mean value ($n = 3$) a, b, c, d $p < 0.05$ vs. A, B, C, D.

According to Gorinsten et al., total phenolic content (TPC) content was significantly higher in fresh grapefruit peel (155 ± 10.3 mg/100 g) than in peeled grapefruits (135 ± 10.1 mg/100 g) [56]. The difference in total flavonoid content across studies might be attributed to differences in variety, location, or analytical methodologies [34]. Xi et al. observed that the total phenolic content varied by variety and fruit portion, varying from 3.17 to 4.63 mg/g GAE FW in the peel, 2.43 to 3.46 mg/g FW in the pulp, 0.29 to 0.52 mg/g FW

in the juice, and 2.12 to 3.36 mg/g FW in the seeds [57]. According to the findings of the studies, the concentration of phenolic compounds present in albedo is higher than that found in any of the other portions of the fruit. This disparity may be attributable to the distinct parts of the fruit having a unique phenolic compound profile and a unique quantity of phenolic compounds. In addition, the solvent used to extract the substance, the method used to remove it, and the quality of the raw material might all contribute to the variations.

The concentration of flavonoids varies depending on the plant's development stage since they are the most abundant group of chemicals found in plants and substantially influence the plant when growing. The majority of flavonoids, also known as flavanone glycosides, are only found in citrus trees. Other types of plants have very few of these compounds. Grapefruit contains several flavonoid glycosides, the most important of which are naringin, hesperidin, and narirutin [34,52].

Flavonoids are abundant in various parts of the fruit, resulting in significant differences between fruit types. Another study found that fruit parts and cultures had different total flavonoid levels. For example, the peel has values between 5.12 mg and 8.30 mg per gram fresh weight; the pulp can range from 3.86 to 5.38 mg/g, from 0.26 to 0.44 mg/g in juice, from 3.16 to 9.27 mg/g in whole fruits and from 18, 61 to 25.33 mg/g in seeds. As a result, seeds contained more flavonoids than juices (5496 times as much as the juice) [57].

Nurcholis et al. investigated the effects of extraction procedures and durations on total flavonoid and phenolic contents (TFCs and TPCs) in a solvent such as methanol. According to the researchers, different extraction procedures and durations significantly influenced the TFCs, TPCs, and antioxidant activities of Java cardamom fruit methanol extracts [58].

Using the aluminum chloride technique, the flavonoid content of grapefruit fruit was analyzed, and the findings are presented in Figure 13. The TFC ranged from 1.26 ± 0.08 to 4.91 ± 0.24 mg RE/g DW. Flavedo extracts had the highest flavonoid levels (2.52 ± 0.13 mg RE/g DW). The total flavonoid content ranged from 1.78 ± 0.09 to 4.66 ± 0.23 mg RE/g DW using β-CDs using 50% ethanol (*v*/*v*) as a solvent. When comparing grapefruit extracts made under the same conditions but with an additional excipient, the total flavonoid content increases by 2.516 ± 0.1278 mg RE/g DW to 4.66 ± 1.26 mg RE/g DW in the flavedo parts. Meanwhile, using $AlCl_3$ to determine the total flavonoids reduces the number of flavonoids from 4.91 ± 0.24 mg RE/g DW to 1.887 ± 0.094 mg RE/g DW in fresh juice.

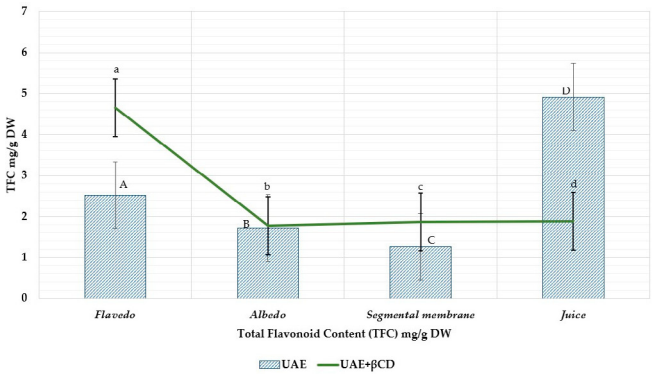

Figure 13. The total flavonoid content (TFC) in grapefruit ethanolic extract with and without β-CDs. A, B, C, D—ultrasound extraction method (UAE), a, b, c, d—ultrasound extraction method (UAE) + β-CDs. The result is the mean value (n = 3) a, b, c, d $p < 0.05$ vs. A, B, C, D.

3.3. Antioxidant Activity

After researching the total phenolic and flavonoid content of *Citrus* × *paradisi* L., the next step is to investigate and evaluate the antioxidant activity of the various parts of the fruit. The findings will be useful in evaluating and standardizing the quality of raw materials and their products. Furthermore, they will make it possible to anticipate the antioxidant activity of grapefruit extracts derived from various parts of the fruit when tested in vivo [59]. The antioxidant capacity of plant extracts can be affected by a wide variety of factors, including the extraction process, the solvent used, the kind of fruit, and the stage of ripeness at which the fruit was harvested [60]. Consequently, we decided to assess the number of antioxidants present in grapefruit using different methods (radical scavenging, antioxidant activity, and reducing power) [61].

Cyclodextrins, for example, can assist overcome the disadvantages of antioxidants in functional foods. In addition, cyclodextrins are also used as anti-browning agents to prevent the enzymatic browning of food. Finally, research shows that cyclodextrins act as secondary antioxidants and help typical antioxidants resist enzymatic browning.

Based on the literature review, the antioxidant capacity in the flavedo, albedo, segmental membrane, and fresh juice was determined. Extracts were extracted using ultrasound (as described in Section 2.4) (control test) and compared to extracts with the addition of β-cyclodextrins (test sample). To this end, the variation in antioxidant capacity was determined by assessing the effect of cyclodextrin on antioxidant capacity.

Figure 14 depicts the results of calculations made with DPPH to determine the radical-scavenging activity of grapefruit fruit in its various areas. After determining the antioxidant activity by the DPPH method, it was observed that the fresh juice and *flavedo* parts of the studied fruit neutralized the DPPH radical the most. The order of action was juice > flavedo > segmental membrane > albedo (1429.25 ± 71.01 µmol/g > 517.14 ± 25.86 µmol/g > 500.27 ± 22.54 µmol/g > 368.50 ± 15.42 µmol/g). β-CD was only slightly increased by DPPH radical inhibition in flavedo extracts from 517.14 ± 25.86 µmol TE/g DW to 630.76 ± 31.54 µmol TE/g DW. However, the CDs reduced the antioxidant activity in segmental membranes and juice.

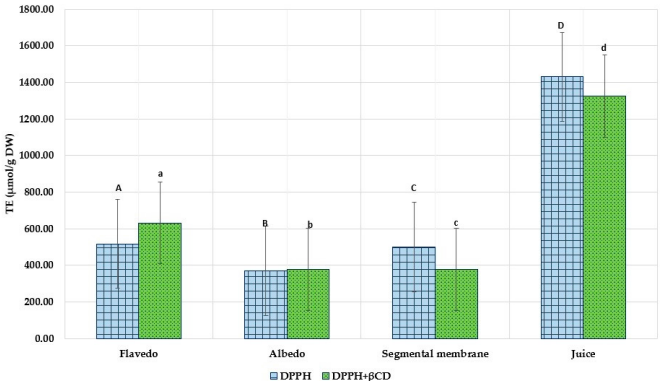

Figure 14. DPPH radical scavenging activity (DPPH) of ethanolic extracts with excipients and control sample (DPPH). Results are mean values (n = 3). A, B, C, D—ultrasound extraction method (UAE), a, b, c, d—ultrasound extraction method (UAE) + β-CDs. a, b $p < 0.05$ vs. A, B; a $p < 0.05$ b, c; D $p < 0.05$ A, B, C; d $p < 0.05$ a, b, c.

The ABTS radical cation decolorization test is a method used to measure the antioxidant activity level of a substance. A solution of ABTS (2,2′-azino-bis (3-ethylbenzthiazoline-6-sulfonic acid)) and potassium persulfate is used. When these two compounds are mixed, they form a stable radical cation that can be used to measure the antioxidant activity of a substance. The radical cation ABTS is blue and can be decolorized by antioxidants. The extent of discoloration is proportional to the antioxidant activity of the substance to be tested [62].

The free radical scavenging activity of *Citrus* × *paradisi* L. extract varied considerably: from 4.36 ± 0.218 µg TE/g to 18.61 ± 0.93 µg TE/g. The highest ABTS radical-cation binding activity was observed in fresh grapefruit juice at 18.61 ± 0.93 µg TE/g.

In this study, all test samples developed using CDs had significantly increased antioxidant activity than the control samples. In the sample with flavedo (from 8.97 ± 0.448 µg TE/g to 18.61 ± 0.93 µg TE/g) and fresh juice (from 18.61 ± 0.93 µg TE/g to 20.56 ± 1.028 µg TE/g), the highest binding of the ABTS radical showed (Figure 15). Conversely, the segmental membrane had the lowest antioxidant activity (4.36 ± 0.218 µg TE/g).

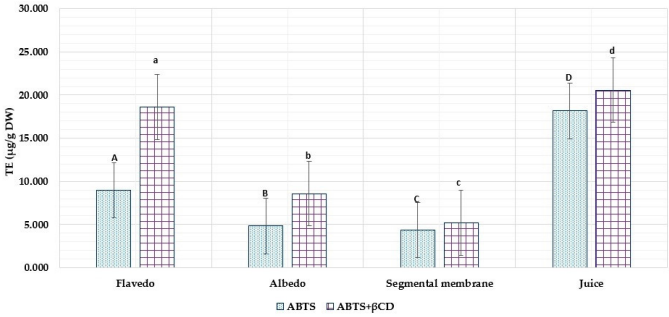

Figure 15. ABTS radical scavenging activity of ethanolic grapefruit extracts with excipients and without. The results are mean values (n = 3). All the test samples (a, b, c, d) were statistically ($p < 0.05$) significant to controls (A, B, C, D); D $p < 0.05$ A, B, C; d $p < 0.05$ a, b, c; A $p < 0.05$ B, C; a $p < 0.05$ b, c.

A compound's ability to reduce other substances might be a valuable signal of its prospective antioxidant action. Combinations with reducing power imply that they are electron donors and can decrease the oxidized intermediates produced during the process of lipid peroxidation, functioning as both primary and secondary antioxidants [63].

It was discovered by Gupta et al., who investigated two distinct harvests of pomelo fruit, that the flavedo of the fruit had the highest antioxidant capacity and FRAP activity. On the other hand, the albedo of the fruit was found to have the highest accumulation of naringin. These findings were based on the findings that the flavedo of the fruit had the highest antioxidant capacity and FRAP activity. On the other hand, pomelo juice showed the most increased DPPH free-radical scavenging activity and the highest tannin concentration [59].

The results of a FRAP experiment that was conducted on various grapefruit components may be found in Figure 16. Compared to their capacity to scavenge free radicals, the ability of some samples to reduce iron ions (Fe^{3+}) to iron ions (Fe^{2+}) was significantly more impressive. Applying β-CD resulted in a one- to two-fold increase in the ethanol samples' reduction power. In this investigation, the outcomes of the test samples (which had β-CDs) were noticeably superior to those of the control samples (devoid of β-CD).

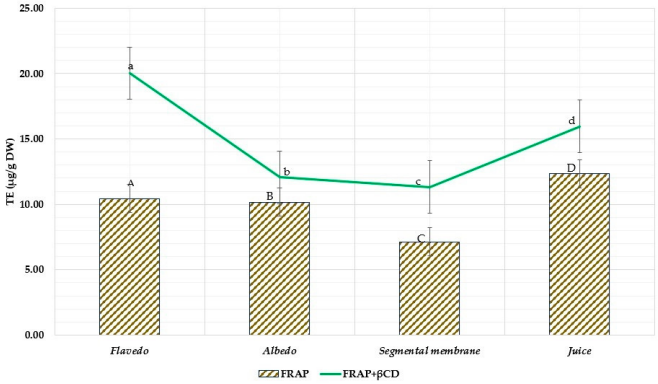

Figure 16. FRAP assay of ethanolic grapefruit extracts with excipients and without. The results are mean values (n = 3). All the test samples (a, b, c, d) were statistically ($p < 0.05$) significant to controls (A, B, C, D); D $p < 0.05$ A, B, C; a $p < 0.05$ b, c, d; d $p < 0.05$ c, d; A $p < 0.05$ B, C.

The spectrophotometric FRAP method determined that fresh grapefruit juice and extracts from the flavedo showed the highest reducing activity among the tested extracts, and the lowest reducing activity was found in the segmental membrane. The use of β-cyclodextrins showed statistically significant results in all tested extracts. In some samples, the reductive activity doubled; for example, the sample from flavedo parts increased reduction from 10.44 ± 0.522 µg TE/g to 20.44 ± 1.02 µg TE/g. Figure 16 depicts the FRAP assay of ethanolic grapefruit extracts with and without excipients.

According to the findings of our research, the segmental membrane extract was the sample that possessed the least amount of antioxidant potential, as indicated by its TE values of 500.27 ± 25.89 µmol/g, 4359.57 ± 24.89 µmol/g, and 7136.00 ± 304.87 µmol/g for DPPH, ABTS, and FRAP, respectively. These numbers are expressed as standard errors. On the other hand, the fresh juice exhibited the highest level of antioxidant activity; the results for DPPH, ABTS, and FRAP were as follows: 1429.25 ± 90.86 µmol/g, 18152.01 ± 698.72 µmol/g, and 12336 ± 616.8 µmol/g, respectively. In addition, the extract from the flavedo part of the grapefruit showed significant results for both DPPH and ABTS (TE 517.14 ± 25.15 and 8969.91 ± 448.50 µmol/g, respectively), and the extracts from the albedo part showed strong FRAP reducing activity (TE 10169.33 ± 508.46 µmol/g).

4. Conclusions

In summary, waste derived from grapefruit can be recycled in the manufacture of future pharmaceutical and medical consumables. Therefore, the extraction of natural products and the research of natural goods and their possible uses are attracting increasing attention. However, to achieve the main goal, such as achieving higher yields of bioactive chemicals from natural sources in less time, new and safe, economically feasible, environmentally friendly extraction processes must first be created.

Cyclodextrins are a type of carbohydrate molecule that exhibit various unique properties that make them useful for various applications. These properties include their ability to form complexes with other molecules, their high solubility in water, and their ability to bind to drugs and other compounds. As a result, cyclodextrins have a variety of uses in the medical, food processing, and water purification industries and are essential tools in improving the safety and effectiveness of these industries.

The results of this study demonstrate that the quantity of flavanone in the extracts examined was significantly elevated when α and β cyclodextrins were used as compared to extracts used as controls. This study also showed that CDs increased flavanone yield while requiring a lower solvent concentration. The highest yield of naringenin was found in SA1, 91.19 ± 2.93 µg/g, prepared with α-CD and 50% ethanol v/v, and for naringin 58.68 ± 2.93 mg/g, prepared with β-CD and 70% ethanol v/v. The highest narirutin amount was observed in AA1 3.33 ± 0.166 mg/g using α-CD in 50% ethanol v/v. In contrast, γ-CD did not provide a statistically significant outcome in this investigation. In the culinary, nutraceutical, and medicinal industries, increasing the naturally occurring flavanone aglycones in fruit materials may generate new potential for utilizing these beneficial chemicals in various applications.

Grapefruit contains many nutrients and biologically active compounds. The results show that grapefruit's albedo parts and segmental membranes have the highest total content of phenols, naringin, and naringenin. Grapefruit (*Citrus* × *paradisi* L.) extracts from the fresh juice and flavedo parts have greater levels of antiradical activity. These findings will be beneficial for processing grapefruit and creating products because there is a lack of literature on the phytochemical and taste qualities. According to the findings of this study, discarded fruit parts possess varied qualities and can also be employed to produce high-quality nutritional supplements and medicines.

Author Contributions: Conceptualization, J.B. and J.S.; investigation, J.S., M.M. and J.V.; resources, J.B., P.V. and L.I.; writing—production of the initial draft, J.S.; writing—review and editing, J.B. and J.S.; visualization, J.S.; supervision, J.B. All authors have read and agreed to the published version of the manuscript.

Funding: This research received no external funding.

Institutional Review Board Statement: Not applicable.

Informed Consent Statement: Not applicable.

Data Availability Statement: Not applicable.

Acknowledgments: The authors would like to express gratitude to the Open Access Centre for the Advanced Pharmaceutical and Health Technologies at the Lithuanian University of Health Sciences and Lithuanian Research Centre for Agriculture and Forestry, Institute of Horticulture for the opportunity to use their research infrastructure and carry out this study.

Conflicts of Interest: The authors state that there is no potential bias in their work.

References

1. Barreca, D.; Mandalari, G.; Calderaro, A.; Smeriglio, A.; Trombetta, D.; Felice, M.R.; Gattuso, G. Citrus Flavones: An Update on Sources, Biological Functions, and Health Promoting Properties. *Plants* **2020**, *9*, 288. [CrossRef] [PubMed]
2. Liu, W.; Zheng, W.; Cheng, L.; Li, M.; Huang, J.; Bao, S.; Xu, Q.; Ma, Z. Citrus fruits are rich in flavonoids for immunoregulation and potential targeting ACE2. *Nat. Prod. Bioprospect.* **2022**, *12*, 14. [CrossRef] [PubMed]
3. Deng, M.; Lin, Y.; Dong, L.; Jia, X.; Shen, Y.; Liu, L.; Chi, J.; Huang, F.; Zhang, M.; Zhang, R. Physicochemical and functional properties of dietary fiber from pummelo (Citrus grandis L. Osbeck) and grapefruit (Citrus paradisi Mcfad) cultivars. *Food Biosci.* **2021**, *40*, 100890. [CrossRef]
4. Mohd Zaid, N.A.; Sekar, M.; Bonam, S.R.; Gan, S.H.; Lum, P.T.; Begum, M.Y.; Mat Rani, N.N.; Vaijanathappa, J.; Wu, Y.S.; Subramaniyan, V.; et al. Promising Natural Products in New Drug Design, Development, and Therapy for Skin Disorders: An Overview of Scientific Evidence and Understanding Their Mechanism of Action. *Drug Des. Dev. Ther.* **2022**, *ume 16*, 23–66. [CrossRef] [PubMed]
5. Chen, Q.; Wang, D.; Tan, C.; Hu, Y.; Sundararajan, B.; Zhou, Z. Profiling of Flavonoid and Antioxidant Activity of Fruit Tissues from 27 Chinese Local Citrus Cultivars. *Plants* **2020**, *9*, 196. [CrossRef]
6. Qurtam, A.A.; Mechchate, H.; Es-Safi, I.; Al-Zharani, M.; Nasr, F.A.; Noman, O.M.; Aleissa, M.; Imtara, H.; Aleissa, A.M.; Bouhrim, M.; et al. Citrus Flavanone Narirutin, In Vitro and In Silico Mechanistic Antidiabetic Potential. *Pharmaceutics* **2021**, *13*, 1818. [CrossRef] [PubMed]
7. Mahmoud, A.M.; Bautista, R.J.H.; Sandhu, M.A.; Hussein, O.E. Beneficial Effects of Citrus Flavonoids on Cardiovascular and Metabolic Health. *Oxidative Med. Cell. Longev.* **2019**, *2019*, 5484138. [CrossRef] [PubMed]
8. Kopustinskiene, D.M.; Jakstas, V.; Savickas, A.; Bernatoniene, J. Flavonoids as anticancer agents. *Nutrients* **2020**, *12*, 457. [CrossRef]

9. Memariani, Z.; Abbas, S.Q.; ul Hassan, S.S.; Ahmadi, A.; Chabra, A. Naringin and naringenin as anticancer agents and adjuvants in cancer combination therapy: Efficacy and molecular mechanisms of action, a comprehensive narrative review. *Pharmacol. Res.* **2021**, *171*, 105264. [CrossRef]
10. Peterson, J.J.; Beecher, G.R.; Bhagwat, S.A.; Dwyer, J.T.; Gebhardt, S.E.; Haytowitz, D.B.; Holden, J.M. Flavanones in grapefruit, lemons, and limes: A compilation and review of the data from the analytical literature. *J. Food Compos. Anal.* **2006**, *19*, S74–S80. [CrossRef]
11. Di Majo, D.; Giammanco, M.; La Guardia, M.; Tripoli, E.; Giammanco, S.; Finotti, E. Flavanones in Citrus fruit: Structure–antioxidant activity relationships. *Food Res. Int.* **2005**, *38*, 1161–1166. [CrossRef]
12. Duda-Madej, A.; Stecko, J.; Sobieraj, J.; Szymańska, N.; Kozłowska, J. Naringenin and Its Derivatives—Health-Promoting Phytobiotic against Resistant Bacteria and Fungi in Humans. *Antibiotics* **2022**, *11*, 1628. [CrossRef]
13. Arafah, A.; Rehman, M.U.; Mir, T.M.; Wali, A.F.; Ali, R.; Qamar, W.; Khan, R.; Ahmad, A.; Aga, S.S.; Alqahtani, S.; et al. Multi-Therapeutic Potential of Naringenin (4′,5,7-Trihydroxyflavonone): Experimental Evidence and Mechanisms. *Plants* **2020**, *9*, 1784. [CrossRef] [PubMed]
14. Salehi, B.; Fokou, P.V.T.; Sharifi-Rad, M.; Zucca, P.; Pezzani, R.; Martins, N.; Sharifi-Rad, J. The Therapeutic Potential of Naringenin: A Review of Clinical Trials. *Pharmaceuticals* **2019**, *12*, 11. [CrossRef] [PubMed]
15. Stabrauskiene, J.; Kopustinskiene, D.M.; Lazauskas, R.; Bernatoniene, J. Naringin and Naringenin: Their Mechanisms of Action and the Potential Anticancer Activities. *Biomedicines* **2022**, *10*, 1686. [CrossRef]
16. Zhao, Z.; Jin, G.; Ge, Y.; Guo, Z. Naringenin inhibits migration of breast cancer cells via inflammatory and apoptosis cell signaling pathways. *Inflammopharmacology* **2019**, *27*, 1021–1036. [CrossRef]
17. TuTunchi, H.; Naeini, F.; Ostadrahimi, A.; Hosseinzadeh-Attar, M.J. Naringenin, a flavanone with antiviral and anti-inflammatory effects: A promising treatment strategy against COVID -19. *Phytother. Res.* **2020**, *34*, 3137–3147. [CrossRef]
18. Ginwala, R.; Bhavsar, R.; Chigbu, D.G.I.; Jain, P.; Khan, Z.K. Potential Role of Flavonoids in Treating Chronic Inflammatory Diseases with a Special Focus on the Anti-Inflammatory Activity of Apigenin. *Antioxidants* **2019**, *8*, 35. [CrossRef]
19. Hartogh, D.J.D.; Tsiani, E. Antidiabetic Properties of Naringenin: A Citrus Fruit Polyphenol. *Biomolecules* **2019**, *9*, 99. [CrossRef]
20. Manchope, M.F.; Calixto-Campos, C.; Coelho-Silva, L.; Zarpelon, A.C.; Pinho-Ribeiro, F.A.; Georgetti, S.R.; Baracat, M.M.; Casagrande, R.; Verri, W.A., Jr. Naringenin Inhibits Superoxide Anion-Induced Inflammatory Pain: Role of Oxidative Stress, Cytokines, Nrf-2 and the NO−cGMP−PKG−KATPChannel Signaling Pathway. *PLoS ONE* **2016**, *11*, e0153015. [CrossRef]
21. Eom, S.; Lee, B.-B.; Lee, S.; Park, Y.; Yeom, H.D.; Kim, T.-H.; Nam, S.-H.; Lee, J.H. Antioxidative and Analgesic Effects of Naringin through Selective Inhibition of Transient Receptor Potential Vanilloid Member 1. *Antioxidants* **2021**, *11*, 64. [CrossRef]
22. Baba, S.A.; Malik, S.A. Determination of total phenolic and flavonoid content, antimicrobial and antioxidant activity of a root extract of *Arisaema jacquemontii* Blume. *J. Taibah Univ. Sci.* **2015**, *9*, 449–454. [CrossRef]
23. Min, K.Y.; Kim, H.J.; Lee, K.A.; Kim, K.-T.; Paik, H.-D. Antimicrobial activity of acid-hydrolyzed Citrus unshiu peel extract in milk. *J. Dairy Sci.* **2014**, *97*, 1955–1960. [CrossRef] [PubMed]
24. Tomar, A.; Broor, S.; Kaushik, S.; Bharara, T.; Arya, D.S. Synergistic effect of naringenin with conventional antibiotics against methicillin resistant staphylococcus aureus. *Clin. Med.* **2021**, *8*, 15.
25. Rebello, C.J.; Beyl, R.A.; Lertora, J.J.L.; Greenway, F.L.; Ravussin, E.; Ribnicky, D.M.; Poulev, A.; Kennedy, B.J.; Castro, H.F.; Campagna, S.R.; et al. Safety and pharmacokinetics of naringenin: A randomized, controlled, single-ascending-dose clinical trial. *Diabetes Obes. Metab.* **2020**, *22*, 91–98. [CrossRef]
26. Rotimi, S.O.; Adelani, I.B.; Bankole, G.E.; Rotimi, O.A. Naringin enhances reverse cholesterol transport in high fat/low streptozocin induced diabetic rats. *Biomed. Pharmacother.* **2018**, *101*, 430–437. [CrossRef]
27. Mulvihill, E.E.; Allister, E.M.; Sutherland, B.G.; Telford, D.E.; Sawyez, C.G.; Edwards, J.Y.; Markle, J.M.; Hegele, R.A.; Huff, M.W. Naringenin Prevents Dyslipidemia, Apolipoprotein B Overproduction, and Hyperinsulinemia in LDL Receptor–Null Mice With Diet-Induced Insulin Resistance. *Diabetes* **2009**, *58*, 2198–2210. [CrossRef]
28. Fu, L.; Xu, B.T.; Xu, X.R.; Gan, R.Y.; Zhang, Y.; Xia, E.Q.; Li, H.B. Antioxidant capacities and total phenolic contents of 62 fruits. *Food Chem.* **2011**, *129*, 345–350. [CrossRef]
29. Losada-Barreiro, S.; Sezgin-Bayindir, Z.; Paiva-Martins, F.; Bravo-Díaz, C. Biochemistry of Antioxidants: Mechanisms and Pharmaceutical Applications. *Biomedicines* **2022**, *10*, 3051. [CrossRef]
30. Latos-Brozio, M.; Masek, A.; Piotrowska, M. Polymeric Forms of Plant Flavonoids Obtained by Enzymatic Reactions. *Molecules* **2022**, *27*, 3702. [CrossRef]
31. Platzer, M.; Kiese, S.; Herfellner, T.; Schweiggert-Weisz, U.; Eisner, P. How Does the Phenol Structure Influence the Results of the Folin-Ciocalteu Assay? *Antioxidants* **2021**, *10*, 811. [CrossRef] [PubMed]
32. Liew, S.S.; Ho, W.Y.; Yeap, S.K.; Bin Sharifudin, S.A. Phytochemical composition and in vitro antioxidant activities of *Citrus sinensis* peel extracts. *PeerJ* **2018**, *6*, e5331. [CrossRef] [PubMed]
33. Chen, L.-Y.; Cheng, C.-W.; Liang, J.-Y. Effect of esterification condensation on the Folin–Ciocalteu method for the quantitative measurement of total phenols. *Food Chem.* **2015**, *170*, 10–15. [CrossRef] [PubMed]
34. Fang, H.; Zhang, H.; Wei, X.; Ye, X.; Tian, J. Phytochemicals and Antioxidant Capacities of Young Citrus Fruits Cultivated in China. *Molecules* **2022**, *27*, 5185. [CrossRef]
35. Su, D.; Liu, H.; Zeng, Q.; Qi, X.; Yao, X.; Zhang, J. Changes in the phenolic contents and antioxidant activities of citrus peels from different cultivars after in vitro digestion. *Int. J. Food Sci. Technol.* **2017**, *52*, 2471–2478. [CrossRef]

36. Sharma, N.; Baldi, A. Exploring versatile applications of cyclodextrins: An overview. *Drug Deliv.* **2014**, *23*, 729–747. [CrossRef]
37. Cai, R.; Yuan, Y.; Cui, L.; Wang, Z.; Yue, T. Cyclodextrin-assisted extraction of phenolic compounds: Current research and future prospects. *Trends Food Sci. Technol.* **2018**, *79*, 19–27. [CrossRef]
38. Guan, M.; Shi, R.; Zheng, Y.; Zeng, X.; Fan, W.; Wang, Y.; Su, W. Characterization, in Vitro and in Vivo Evaluation of Naringenin-Hydroxypropyl-β-Cyclodextrin Inclusion for Pulmonary Delivery. *Molecules* **2020**, *25*, 554. [CrossRef]
39. Lu, W.J.; Ferlito, V.; Xu, C.; Flockhart, D.A.; Caccamese, S. Enantiomers of naringenin as pleiotropic, stereoselective inhibitors of cytochrome P450 isoforms. *Chirality* **2011**, *23*, 891–896. [CrossRef]
40. Wüpper, S.; Lüersen, K.; Rimbach, G. Cyclodextrins, Natural Compounds, and Plant Bioactives—A Nutritional Perspective. *Biomolecules* **2021**, *11*, 401. [CrossRef]
41. Kazlauskaite, J.A.; Ivanauskas, L.; Marksa, M.; Bernatoniene, J. The Effect of Traditional and Cyclodextrin-Assisted Extraction Methods on *Trifolium pratense* L. (Red Clover) Extracts Antioxidant Potential. *Antioxidants* **2022**, *11*, 435. [CrossRef]
42. Shulman, M.; Cohen, M.; Soto-Gutierrez, A.; Yagi, H.; Wang, H.; Goldwasser, J.; Lee-Parsons, C.W.; Benny-Ratsaby, O.; Yarmush, M.L.; Nahmias, Y. Enhancement of Naringenin Bioavailability by Complexation with Hydroxypropoyl-β-Cyclodextrin. *PLoS ONE* **2011**, *6*, e18033. [CrossRef] [PubMed]
43. Ndayishimiye, J.; Kumeria, T.; Popat, A.; Blaskovich, M.A.; Falconer, J.R. Understanding the relationship between solubility and permeability of γ-cyclodextrin-based systems embedded with poorly aqueous soluble benznidazole. *Int. J. Pharm.* **2022**, *616*, 121487. [CrossRef] [PubMed]
44. Pereira, A.G.; Carpena, M.; Oliveira, P.G.; Mejuto, J.; Prieto, M.; Gandara, J.S. Main Applications of Cyclodextrins in the Food Industry as the Compounds of Choice to Form Host–Guest Complexes. *Int. J. Mol. Sci.* **2021**, *22*, 1339. [CrossRef] [PubMed]
45. Stabrauskiene, J.; Marksa, M.; Ivanauskas, L.; Bernatoniene, J. Optimization of Naringin and Naringenin Extraction from *Citrus* × *paradisi* L. Using Hydrolysis and Excipients as Adsorbent. *Pharmaceutics* **2022**, *14*, 890. [CrossRef] [PubMed]
46. Wolfender, J.L. HPLC in natural product analysis: The detection issue. *Planta Med.* **2009**, *75*, 719–734. [CrossRef]
47. Chandra, S.; Khan, S.; Avula, B.; Lata, H.; Yang, M.H.; ElSohly, M.A.; Khan, I.A. Assessment of Total Phenolic and Flavonoid Content, Antioxidant Properties, and Yield of Aeroponically and Conventionally Grown Leafy Vegetables and Fruit Crops: A Comparative Study. *Evid.-Based Complement. Altern. Med.* **2014**, *2014*, 253875. [CrossRef]
48. Ghafar, M.F.; Prasad, K.N.; Weng, K.K.; Ismail, A. Flavonoid, hesperidine, total phenolic contents and antioxidant activities from Citrus species. *Afr. J. Biotechnol.* **2010**, *9*, 6.
49. Pudziuvelyte, L.; Liaudanskas, M.; Jekabsone, A.; Sadauskiene, I.; Bernatoniene, J. Elsholtzia ciliata (Thunb.) Hyl. Extracts from Different Plant Parts: Phenolic Composition, Antioxidant, and Anti-Inflammatory Activities. *Molecules* **2020**, *25*, 1153. [CrossRef]
50. Yim, S.-H.; Nam, S.-H. Physiochemical, nutritional and functional characterization of 10 different pear cultivars (Pyrus spp.). *J. Appl. Bot. Food Qual.* **2016**, *89*, 7381. [CrossRef]
51. Vijayalakshmi, M.; Ruckmani, K. Ferric reducing anti-oxidant power assay in plant extract. *Bangladesh J. Pharmacol.* **2016**, *11*, 570–572. [CrossRef]
52. Khan, M.K.; Huma, Z.E.; Dangles, O. A comprehensive review on flavanones, the major citrus polyphenols. *J. Food Compos. Anal.* **2014**, *33*, 85–104. [CrossRef]
53. Chaves, J.O.; de Souza, M.C.; Da Silva, L.C.; Lachos-Perez, D.; Torres-Mayanga, P.C.; Machado, A.P.D.F.; Forster-Carneiro, T.; Vázquez-Espinosa, M.; González-De-Peredo, A.V.; Barbero, G.F.; et al. Extraction of Flavonoids From Natural Sources Using Modern Techniques. *Front. Chem.* **2020**, *8*, 507887. [CrossRef]
54. Chen, M.; Li, R.; Gao, Y.; Zheng, Y.; Liao, L.; Cao, Y.; Li, J.; Zhou, W. Encapsulation of Hydrophobic and Low-Soluble Polyphenols into Nanoliposomes by pH-Driven Method: Naringenin and Naringin as Model Compounds. *Foods* **2021**, *10*, 963. [CrossRef]
55. Slámová, K.; Kapešová, J.; Valentová, K. "Sweet Flavonoids": Glycosidase-Catalyzed Modifications. *Int. J. Mol. Sci.* **2018**, *19*, 2126. [CrossRef] [PubMed]
56. Gorinstein, S.; Martin-Belloso, O.; Park, Y.-S.; Haruenkit, R.; Lojek, A.; Číž, M.; Caspi, A.; Libman, I.; Trakhtenberg, S. Comparison of some biochemical characteristics of different citrus fruits. *Food Chem.* **2001**, *74*, 309–315. [CrossRef]
57. Xi, W.; Lu, J.; Qun, J.; Jiao, B. Characterization of phenolic profile and antioxidant capacity of different fruit part from lemon (Citrus limon Burm.) cultivars. *J. Food Sci. Technol.* **2017**, *54*, 1108–1118. [CrossRef]
58. Nurcholis, W.; Alfadzrin, R.; Izzati, N.; Arianti, R.; Vinnai, B.; Sabri, F.; Kristóf, E.; Artika, I.M. Effects of Methods and Durations of Extraction on Total Flavonoid and Phenolic Contents and Antioxidant Activity of Java Cardamom (*Amomum compactum* Soland Ex Maton) Fruit. *Plants* **2022**, *11*, 2221. [CrossRef]
59. Gupta, A.K.; Dhua, S.; Sahu, P.P.; Abate, G.; Mishra, P.; Mastinu, A. Variation in Phytochemical, Antioxidant and Volatile Composition of Pomelo Fruit (*Citrus grandis* (L.) Osbeck) during Seasonal Growth and Development. *Plants* **2021**, *10*, 1941. [CrossRef]
60. Rajurkar, N.; Hande, S. Estimation of phytochemical content and antioxidant activity of some selected traditional Indian medicinal plants. *Indian J. Pharm. Sci.* **2011**, *73*, 146–151. [CrossRef]
61. Castro-Vazquez, L.; Alañón, M.E.; Rodríguez-Robledo, V.; Pérez-Coello, M.S.; Hermosín-Gutierrez, I.; Díaz-Maroto, M.C.; Jordán, J.; Galindo, M.F.; Arroyo-Jiménez, M.D.M. Bioactive Flavonoids, Antioxidant Behaviour, and Cytoprotective Effects of Dried Grapefruit Peels (*Citrus paradisi* Macf.). *Oxidative Med. Cell. Longev.* **2016**, *2016*, 8915729. [CrossRef] [PubMed]

62. Rakholiya, K.; Kaneria, M.; Nagani, K.; Patel, A.; Chanda, S. Comparative analysis and simultaneous quantification of antioxidant capacity of four terminalia species using various photometric assays. *World J. Pharm. Res.* **2015**, *4*, 1280–1296.
63. Benslama, A.; Harrar, A. Free radicals scavenging activity and reducing power of two Algerian Sahara medicinal plants extracts. *Int. J. Herb. Med.* **2016**, *4*, 158–161. [CrossRef]

Paper 3

Title: Naringin vs. *Citrus* × *paradisi* L. Peel Extract: An In Vivo Journey into Oxidative Stress Modulation
Authors: Jolita Stabrauskiene, Ilona Sadauskiene, Arunas Liekis, Zoja Mikniene and Jurga Bernatoniene.
Antioxidants 2025, 14, 157.

antioxidants

MDPI

Article

Naringin vs. *Citrus x paradisi* L. Peel Extract: An *In Vivo* Journey into Oxidative Stress Modulation

Jolita Stabrauskiene [1], Ilona Sadauskiene [2], Arunas Liekis [2], Zoja Mikniene [3] and Jurga Bernatoniene [1,4,*]

[1] Department of Drug Technology and Social Pharmacy, Lithuanian University of Health Sciences, Eiveniu St. 4, LT-50161 Kaunas, Lithuania; jolita.stabrauskiene@lsmu.lt
[2] Neuroscience Institute, Lithuanian University of Health Sciences, Eiveniu St. 4, LT-50161 Kaunas, Lithuania; ilona.sadauskiene@lsmu.lt (I.S.); arunas.liekis@lsmu.lt (A.L.)
[3] Large Animal Clinic, Lithuania University of Health Science, Veterinary Academy, LT-44307 Kaunas, Lithuania; zoja.mikniene@lsmu.lt
[4] Institute of Pharmaceutical Technologies, Lithuanian University of Health Sciences, Eiveniu St. 4, LT-50161 Kaunas, Lithuania
* Correspondence: jurga.bernatoniene@lsmuni.lt; Tel.: +370-6006-3349

Abstract: Citrus fruits, mainly grapefruit (*Citrus x paradisi* L.), are rich in bioactive compounds with potential antioxidant properties. This study investigated the antioxidant effects of naringin (NR) and ethanolic *Citrus x paradisi* L. peel (E) in reducing aluminum chloride ($AlCl_3$)-induced oxidative stress in mice. Quantitative analysis using HPLC identified optimal extraction conditions, combination ultrasound and reflux extraction (UH50), resulting in high concentrations of naringin (49.13 mg/g) and naringenin (63.99 µg/g). Mice were treated with NR and E to evaluate their effects on key markers of oxidative stress: reduced glutathione (GSH), malondialdehyde (MDA), and catalase (CAT). The E effectively reduced MDA levels in blood, brain, and liver tissues, with a more substantial effect on controlling lipid peroxidation. In contrast, NR was more effective in restoring GSH levels and CAT activity, suggesting a broader enhancement of antioxidant defense. These findings provide information about specific mechanisms of NR and E and their therapeutic potential in managing oxidative stress and developing products with synergistic efficacy.

Keywords: oxidative stress; naringin; naringenin; grapefruit extract; antioxidant biomarkers; GSH; MDA; CAT; aluminum chloride; *Citrus x paradisi* L.

Academic Editor: Antonio Barberis

Received: 3 January 2025
Revised: 21 January 2025
Accepted: 24 January 2025
Published: 28 January 2025

Citation: Stabrauskiene, J.; Sadauskiene, I.; Liekis, A.; Mikniene, Z.; Bernatoniene, J. Naringin vs. *Citrus x paradisi* L. Peel Extract: An *In Vivo* Journey into Oxidative Stress Modulation. *Antioxidants* **2025**, *14*, 157. https://doi.org/10.3390/antiox14020157

1. Introduction

Oxidative stress is an influential factor contributing to the development of chronic diseases, such as cardiovascular diseases, diabetes, neurodegenerative disorders, and cancer. This condition occurs when the balance between reactive oxygen species (ROS) production and antioxidant defenses is disrupted, damaging essential biomolecules such as lipids, proteins, and nucleic acids [1,2]. Research for effective strategies to reduce oxidative stress has become an essential area of study, focusing on natural antioxidants. For example, curcumin, a bioactive compound derived from turmeric, has shown significant promise in reducing malondialdehyde (MDA) levels and restoring glutathione (GSH) concentrations in oxidative stress models [3]. Similarly, stevia leaf extracts demonstrated the ability to reduce oxidative damage by enhancing enzymatic defenses [4]. These findings provide a comparative basis for evaluating the antioxidant properties of naringin and grapefruit extract, highlighting the need for targeted approaches to modulate oxidative stress.

1.1. Naringin and Its Pharmacological Effects

Citrus fruits, mainly grapefruit (*Citrus x paradisi* L.), are well known for their high content of bioactive compounds, such as flavonoids, vitamins, and minerals [5]. Grapefruit extract, derived from the fruit's pulp and peel, contains a variety of flavonoids, with naringin being one of the most well known.

Regarding the growing interest in both naringin and grapefruit extract, no direct studies have been identified that compare their effects in vivo, particularly regarding their ability to modulate oxidative stress. While several studies have explored their individual antioxidant properties, a side-by-side comparison in controlled in vivo models remains unexplored, highlighting a gap in current research.

Naringin (4′,5,7-trihydroxyflavanone-7-rhamnoglucoside), as illustrated in Figure 1, belongs to the flavanone class of flavonoids and is mainly found in citrus fruits like lemons, oranges, mandarins, and grapefruits. This essential compound is known for its potent antioxidant, anti-inflammatory, cardioprotective, and anticancer properties [6–9]. Naringin's ability to neutralize free radicals and its low toxicity make it a promising candidate for reducing cellular damage caused by oxidative stress [10].

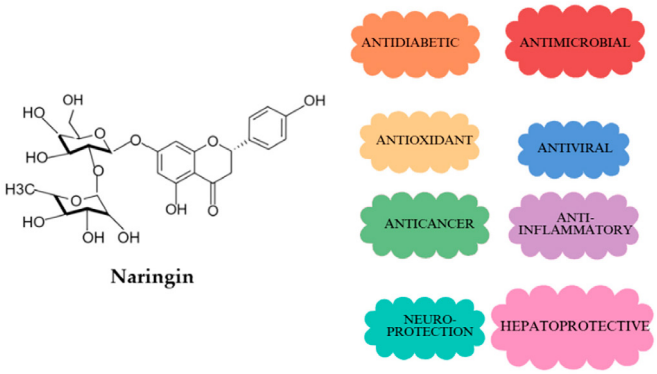

Figure 1. The structure and effects of naringin.

1.2. Free Radicals

Free radicals are molecules that contain one or more unpaired electrons in their outer shell, causing them to be highly reactive and unstable. Free radicals are generally short-lived and often originate from oxygen and nitrogen [11]. These elements form highly reactive molecules known as reactive oxygen species (ROS) and reactive nitrogen species (RNS). ROS include superoxide anion radicals (O_2^-•), reactive hydroxyl radicals (OH•), hydroperoxyl radicals (HO_2•), as well as other compounds like hydrogen peroxide (H_2O_2), hypochlorous acid (HOCl), and singlet oxygen (Figure 2) [12]. These molecules capture electrons from nearby molecules to stabilize themselves, which turns the nearby molecules into free radicals and initiates a chain reaction that can cause significant damage to cells and tissue. Free radicals can be generated in the body through enzymatic and non-enzymatic reactions (endogenous sources) or introduced from external sources (exogenous) such as pollution, smoking, and radiation [13]. Reactive oxygen species (ROS), including superoxide anions (O_2^-), hydroxyl radicals (OH^-), and nitrogen-based

radicals like nitric oxide (NO), are particularly harmful when their production exceeds the body's antioxidant defenses [14]. Figure 2 demonstrates the structure of free radicals.

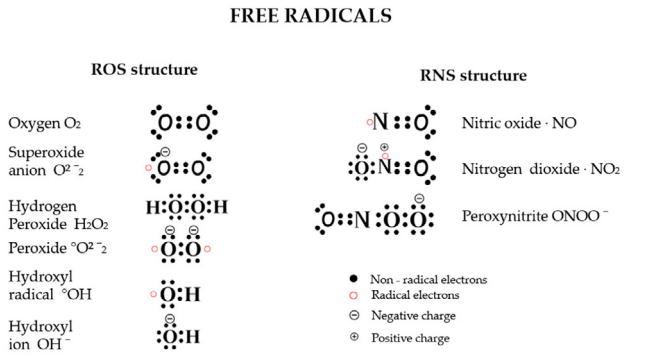

Figure 2. The structure of free radicals: Free radicals are highly reactive molecules with an unpaired electron count, capable of damaging cells. Reactive oxygen species (ROS), such as •OH, O_2•$^-$, •HO_2, and H_2O_2, represent types of free radicals containing oxygen. Reactive nitrogen species (RNS) are highly active molecules derived from nitric oxide compounds, including •NO, $ONOO^-$, and •NO_2.

1.3. Oxidative Stress

Oxidative stress is a form of biochemical imbalance where the formation of free radicals overwhelms the body's antioxidant defense systems [15]. This imbalance damages cells and tissues by modifying essential biomolecules, including lipids, proteins, and nucleic acids. This oxidative stress is associated not only with xenobiotic toxicity but also with various conditions such as ischemia–reperfusion injury, vascular endothelium, deep injury, organ dysfunction, shock, inflammation, sepsis, diabetic retinopathy, cancer, cognitive impairment, cataract, pathophysiology and heart disease [16]. In addition, oxidative stress accelerates ageing by promoting tissue and organ dysfunction, highlighting its wide-ranging effects on health—Figure 3.

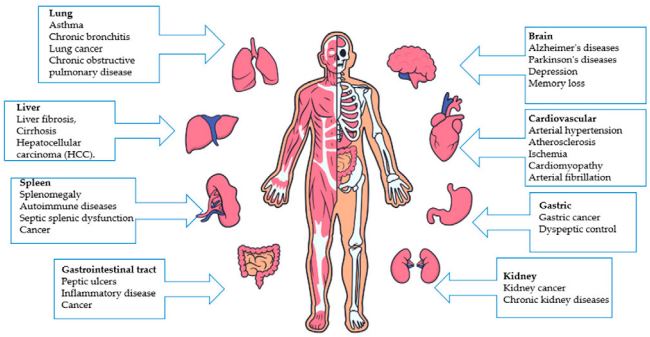

Figure 3. Schema illustrating human diseases caused by oxidative stress [17–23].

1.4. Oxidative Stress Markers

Reactive oxygen species (ROS) are compounds that are difficult to measure when assessing oxidative stress, primarily due to their short half-life, making them impractical as biomarkers [20]. However, ROS interacting with specific biological molecules leaves a unique chemical "fingerprint". Biomarkers derived in this way can be used to evaluate oxidative damage or the effects of antioxidants, including therapeutic substances. ROS interacts with their surroundings in vivo as highly reactive substances, triggering and stimulating various endogenous mechanisms. They also react with many molecules, leaving fingerprints as reference points for specific assessments [24].

Therefore, oxidative stress biomarkers are molecules that change in response to oxidative damage, allowing us to understand the level of stress and the effectiveness of antioxidant protection [25]. One example of an oxidative stress marker is malondialdehyde (MDA), a marker of lipid peroxidation. Lipids are sensitive to oxidation due to the double bonds in their molecular structure, which are reactive and less stable [26]. MDA can react with cellular components such as proteins, DNA, and lipids, causing cellular damage and dysfunction. The presence of MDA in cells and tissues is often used as an indicator of oxidative stress because it reflects the degree of lipid peroxidation and ROS-induced damage. Measurement of MDA levels can be used as a biomarker of oxidative stress and lipid peroxidation in clinical and experimental settings [27]. In addition, MDA can also be used as a therapeutic target to reduce the harmful effects of ROS, as antioxidants and other agents that reduce ROS production or scavenge free radicals can reduce MDA levels and reduce oxidative stress [28]. Figure 4 illustrates the involvement of reactive oxygen species (ROS) and lipoxygenase activity in lipid peroxidation, leading to the formation of malondialdehyde (MDA) as a biomarker of oxidative stress.

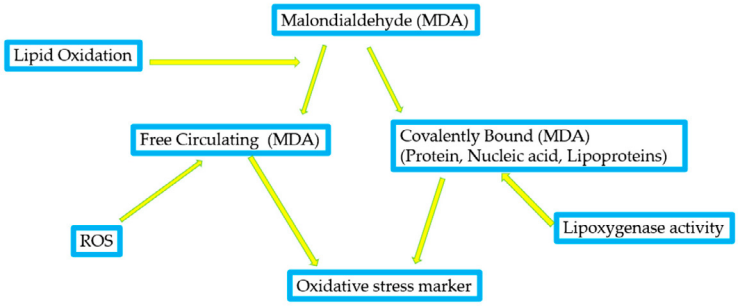

Figure 4. The involvement of reactive oxygen species (ROS) and lipoxygenase activity in lipid peroxidation and the formation of MDA involving free circulating MDA or covalently bound to proteins, nucleic acids, or lipoproteins during oxidative damage MDA is shown as a biomarker of oxidative stress linked with lipid oxidation [29,30].

Lipid peroxidation is a key process contributing to cellular damage during oxidative stress, significantly influencing the development of various diseases, including neurodegenerative and cardiovascular conditions [31]. Figure 5 illustrates the three stages of lipid peroxidation—initiation, propagation, and termination—and how ROS initiate chain reactions leading to lipid radicals, propagating oxidative damage until neutralized by antioxidants.

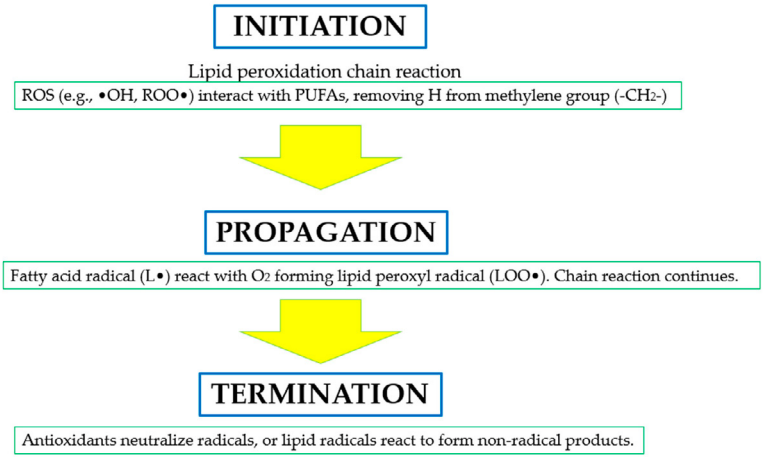

Figure 5. The three stages of lipid peroxidation, a critical oxidative process affecting polyunsaturated fatty acids (PUFAs) in biological membranes. During the initiation phase, reactive oxygen species (ROS), such as hydroxyl radicals (•OH) or peroxyl radicals (ROO•), abstract a hydrogen atom from the methylene group (-CH_2-) in PUFAs, generating lipid radicals (L•). In the propagation phase, these lipid radicals react with molecular oxygen (O2), forming lipid peroxyl radicals (LOO•), propagating further chain reactions and amplifying oxidative damage. The termination phase involves neutralizing these radicals with antioxidants or forming non-radical products, halting the chain reaction [32–34].

Other markers include glutathione S-transferase (GST), superoxide dismutase (SOD), catalase (CAT), glutathione peroxidase (GPx), and glutathione reductase (GR), as well as oxidized glutathione (GSSG) and reduced glutathione (GSH) [30,35,36]. During oxidative stress, (GST) levels may increase due to an activated antioxidant defense mechanism, as GST and reduced glutathione neutralize ROS [37]. An increase in (SOD) levels is also observed, which may be a compensatory mechanism by the body to protect itself from oxidative stress, as this enzyme is involved in breaking down superoxide anions. During oxidative stress, the activity of (CAT), as well as the levels of (GSH) and (GPx), diminish due to the insufficient availability of these enzymes to neutralize reactive oxygen species (ROS) effectively. Consequently, oxidized glutathione (GSSG) and glutathione reductase (GR) levels also decrease due to the intensified synthesis of ROS caused by oxidative stress [16,38].

The (GSH) is a thiol compound, an endogenous intracellular antioxidant that ensues naturally in the body. It is a tripeptide comprising the well-known amino acids glycine, cysteine, and glutamic acid (Figure 6). One of its fundamental properties is its sensitivity to hydrogen peroxide due to the SH group in its structure, making it more reactive than catalase [39].

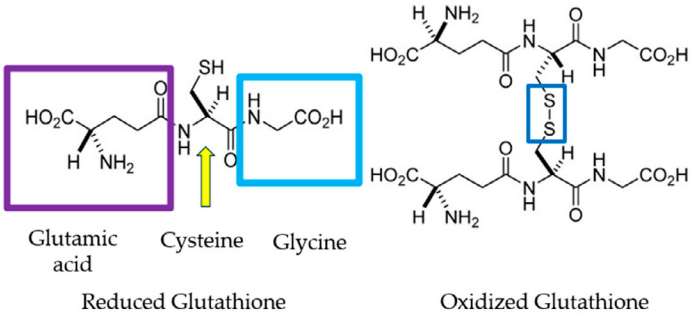

Figure 6. The figure illustrates the structural difference between reduced glutathione (GSH) and oxidized glutathione (GSSG). The reduced form (GSH) on the left consists of three amino acids: glutamic acid (highlighted by the purple square), cysteine, and glycine (highlighted by the blue square). The key feature is the thiol (–SH) group on the cysteine, which is marked by the yellow arrow and plays a crucial role in redox reactions. On the right, in the oxidized form (GSSG), two glutathione molecules are linked by a disulfide bond (S–S) between the sulfur atoms of the cysteine residues, indicated by the blue square. This bond replaces the free thiol groups in the reduced form, representing oxidative stress conditions.Glutathione exists in reduced glutathione (GSH) and oxidized glutathione (GSSG). The enzyme glutathione peroxidase catalyzes the conversion from GSH to GSSG, while the reverse process—from GSSG to GSH—is facilitated by glutathione reductase, using NADPH [38]. During oxidative stress, intracellular GSSG accumulates, leading to a decrease in the GSH/GSSG ratio. This ratio can indicate oxidative stress levels in tissues [40].

1.5. Antioxidants and Their Effects

Antioxidants have been and still constitute an exciting subject of investigation in the scientific world as their importance towards general human health and well-being has become apparent. Naturally occurring compounds, such as antioxidants, are crucial in eliminating free radicals, which would otherwise damage the cells and result in many other diseases, including cancer [41].

Antioxidants can be classified into enzymatic and non-enzymatic types. Enzymatic antioxidants function through biochemical reactions that neutralize (ROS), while non-enzymatic antioxidants directly scavenge free radicals or prevent their formation [42]. Also, their classification is based on their solubility factor in hydrophilic and lipophilic antioxidants. Hydrophilic antioxidants primarily act in the cell cytoplasm and blood plasma, while lipophilic antioxidants protect cell membranes by preventing lipid peroxidation [43,44]—Figure 7.

This study aims to evaluate the effects of grapefruit ethanolic extract (E) and naringin (NR) on biomarkers of antioxidant activity in the organs and blood of mice. It was hypothesized that the mechanisms by which E and NR reduce oxidative stress may differ. Grapefruit extract is expected to be more effective than naringin in reducing oxidative stress markers.

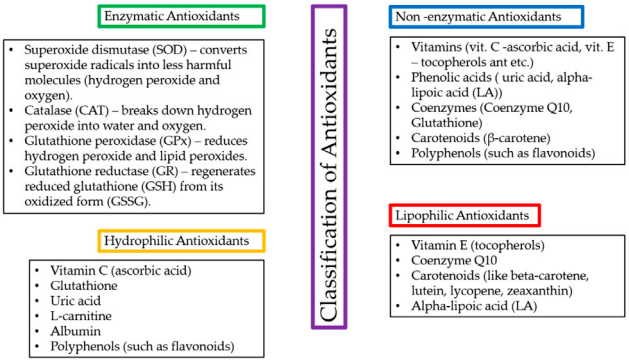

Figure 7. Classification of antioxidants with representative examples.

2. Results and Discussion

2.1. Quantitative Analysis of Phenolic Compounds and Selection of Extraction Sample

Before starting the in vivo study, the phenolic compounds naringin and naringenin were quantitatively analyzed on dried plant material using the HPLC method. The extraction process was carried out as described in the Materials and Methods Section 3.2, and the results are presented in Table 1.

Table 1. Quantification of naringin and naringenin in *Citrus x paradisi* L. peel extracts using different extraction methods and ethanol concentrations. The sample ID represents the extraction method and ethanol concentration used. U—ultrasonic extraction, UH—combines ultrasonic and reflux extraction—the numbers correspond to ethanol concentrations: 50 for 50% ethanol and 70 for 70% ethanol.

Sample ID	Naringin (mg/g)	Naringenin (μg/g)
U50	42.04 ± 2.1	56.81 ± 2.84
U70	40.36 ± 2.02	49.76 ± 2.49
UH50	49.13 ± 2.46	63.99 ± 3.17
UH70	51.94 ± 2.6	64.22 ± 3.21

The results demonstrated that ethanol concentration has a minor impact on the extraction efficiency. Instead, combining ultrasonic and reflux extraction plays a more significant role in achieving higher flavonoid yields. Similar findings were obtained from previous studies examining different parts of the citrus peel [45].

The UH70 sample had the highest naringin concentration (51.94 ± 2.6 mg/g), followed by UH50 (49.13 ± 2.46 mg/g). Both U50 and U70 samples yielded lower concentrations (42.04 ± 2.1 mg/g and 40.36 ± 2.02 mg/g, respectively), demonstrating the added benefit of combining ultrasonic and reflux extraction.

Similarly, the UH70 sample achieved the highest naringenin yield (64.22 ± 3.21 μg/g), with UH50 following closely (63.39 ± 3.17 μg/g).

Lower naringenin levels were found in U50 (56.81 ± 2.84 μg/g) and U70 (49.76 ± 2.49 μg/g), further showing the advantages of the combined extraction method. Meanwhile, UH70 provided slightly higher yields. However, its ethanol concentration

(70%) required more extensive dilution to achieve 10% for in vivo studies, which may introduce variability.

The UH50 sample was selected for in vivo experiments due to its higher flavonoid content and ease of dilution, which allowed it to reach a 10% ethanol concentration for the in vivo studies. In the prepared 10% solution of the UH50 sample, the naringin concentration was calculated to be approximately 4.91 mg/mL and naringenin 6.339 µg/mL.

2.2. Result of GSH and MDA in Mouse Blood

The changes in (GSH) levels observed in our study show the impact of ($AlCl_3$) on oxidative stress and the protective effects of naringin and ethanol grapefruit extract treatments. The concentrations of GSH in the blood of control and experimental mice are given in Figure 8.

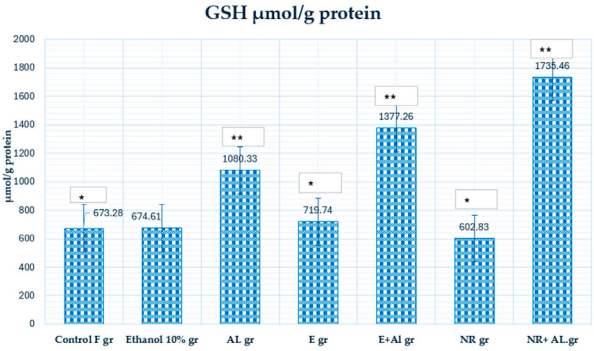

Figure 8. The concentration of GSH in mouse blood. * Indicates a statistically significant difference between the control group and the treated group with E and NR ($p \leq 0.05$); ** indicates a statistically significant difference between the Al group and the treated group with the E + Al and NR + Al groups ($p \leq 0.05$).

The reduced GSH levels in the NR-treated group (602.83 µmol/g) suggest that naringin was actively neutralize (ROS), resulting in depleted GSH reserves.

Conversely, the significant ($p \geq 005$) increase in GSH levels in the NR + $AlCl_3$ (1735.46 µmol/g protein) and E + $AlCl_3$ (1377.26 µmol/g protein) groups highlights the protective effects of treatments. It can lead to their ability to stimulate GSH synthesis or moderate ROS levels, accordingly, preventing GSH depletion. Meanwhile, the higher GSH levels in the NR + $AlCl_3$ group compared to the E + $AlCl_3$ group suggest that naringin might substantially enhance the body's natural antioxidant systems by activating GSH synthesis pathways.

NR and E demonstrated their efficacy in modulating GSH levels under oxidative stress conditions. However, GSH levels generally decrease during oxidative stress, so a compensatory mechanism is likely activated. Such observations are consistent with the results analyzed in the literature, highlighting the antioxidant properties of naringin and citrus peel extracts under oxidative stress conditions [46].

The (MDA) is a biomarker that assesses lipid peroxidation and indicates oxidative stress. Increased MDA levels, as shown in the $AlCl_3$ group, indicate increased oxidative stress, which can damage cell membranes, proteins, and DNA. This study observed changes

in MDA concentration caused by exposure to $AlCl_3$ and ethanol and the protective effect of treatment with naringin and extract (Figure 9).

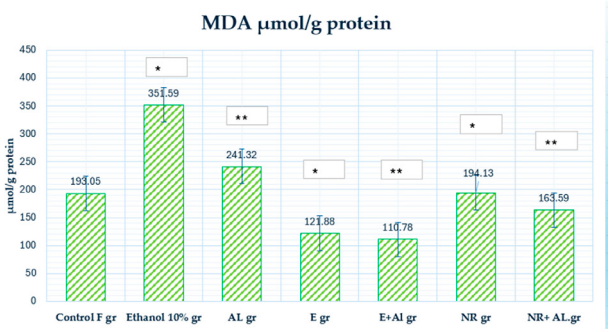

Figure 9. Demonstrates the concentration of MDA in mouse blood. * Indicates a statistically significant difference ($p \leq 0.05$) between the ethanolic and treated groups; ** indicates a statistically significant difference ($p \leq 0.05$) between the $AlCl_3$ and treated groups.

MDA levels in the control group (193.05 µmol/g protein) indicate the initial oxidative state under physiological conditions.

Ethanol (351.59 µmol/g protein) significantly increased MDA levels compared to the control group, indicating ethanol's pro-oxidative effect that enhances lipid peroxidation. This highlights the importance of controlling ethanol concentration in experimental designs to avoid misleading results.

The level of MDA in the $AlCl_3$ group (241.32 µmol/g protein) was increased compared to the control group, indicating $AlCl_3$-induced oxidative damage.

Treatment with the E alone (121.88 µmol/g protein) reduced MDA levels compared to the control group, indicating its antioxidant effect and ability to alleviate oxidative stress.

The observed decrease in MDA level (110.78 µmol/g protein) in the E + $AlCl_3$ group indicates the ethanol extract's protective effect against $AlCl_3$-induced oxidative damage.

The level of MDA in the NR group (194.13 µmol/g of protein) was similar to that in the control group, but compared to the ethanol group, it showed a statistically significant decrease.

The average MDA level (163.59 µmol/g protein) decreased in the NR + $AlCl_3$ group, but compared to the E + $AlCl_3$ group, the extract's effect on lipid peroxidation was higher. The results indicate that E substantially reduces lipid peroxidation more than NR, as evidenced by the lower MDA levels in the E + $AlCl_3$ group.

2.3. Result of GSH, MDA and CAT in Mouse Brain

In the control group (0.005 µmol/g protein), GSH levels showed baseline antioxidant capacity in healthy brain tissues. Ethanol-treated mice (0.004 µmol/g protein) exhibited reduced GSH levels compared to the control, indicating ethanol-induced oxidative stress and depletion of cellular antioxidant reserves. The $AlCl_3$ (0.0023 µmol/g protein) caused a higher decrease in GSH levels, confirming the severe oxidative stress caused by $AlCl_3$, which disrupts redox homeostasis. The results are presented in Figure 10.

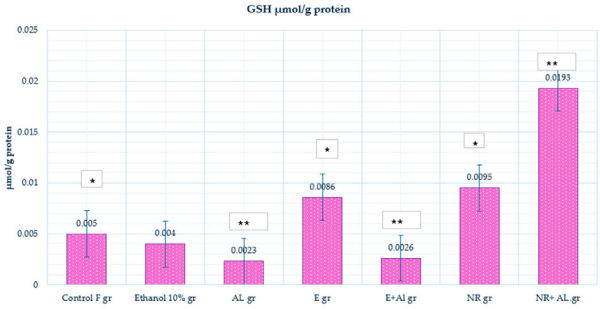

Figure 10. Glutathione reductase activity in the mouse brain. * Indicates a statistically significant difference ($p \leq 0.05$) between the control and treated groups; ** indicates a statistically significant difference ($p \leq 0.05$) between the $AlCl_3$ and treated groups.

Treatment with the E alone (0.0086 µmol/g protein) significantly increased GSH levels compared to the control, indicating that the E enhances antioxidant capacity and promotes GSH synthesis under normal conditions. However, in the E + $AlCl_3$ group (0.0026 µmol/g protein), GSH levels showed only a slight increase compared to $AlCl_3$ alone, suggesting that the E provided limited protection against oxidative stress caused by $AlCl_3$. In contrast, the NR-treated group (0.0095 µmol/g protein) significantly increased GSH levels, indicating its ability to enhance antioxidant capacity under normal conditions. Meanwhile, in the NR + $AlCl_3$ group (0.0193 µmol/g protein), GSH levels were significantly restored, reaching the control levels, suggesting that NR neutralized oxidative stress and strongly promoted GSH synthesis.

MDA, a marker of lipid peroxidation, reflects the extent of oxidative damage. In the control group (77.01 µmol/g protein), MDA levels represent baseline oxidative conditions with minimal lipid peroxidation. The ethanol-treated group (104.07 µmol/g protein) increased MDA levels, highlighting ethanol's role in generating ROS and promoting lipid peroxidation. Similarly, the $AlCl_3$ group increase (87.66 µmol/g protein) MDA level in mice brains indicated oxidative stress. The results are presented in Figure 11.

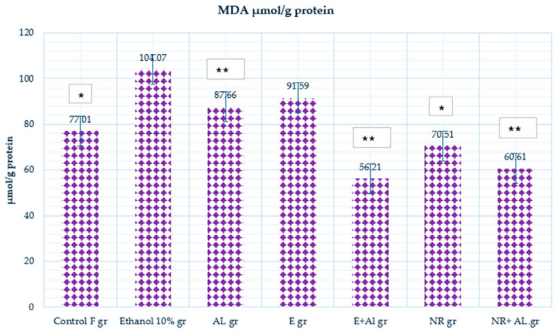

Figure 11. MDA activity in the mouse brain. * Indicates a statistically significant difference ($p \leq 0.05$) between the control and treated groups; ** indicates a statistically significant difference ($p \leq 0.05$) between the $AlCl_3$ and treated groups.

The combination of the E and $AlCl_3$ (56.21 µmol/g protein) significantly lowered MDA levels, showing that the E effectively neutralized oxidative stress caused by $AlCl_3$. The NR-treated group (70.51 µmol/g protein) showed reduced MDA levels compared to the control, reflecting naringin's preventive role against oxidative damage. In the NR + $AlCl_3$ group (60.61 µmol/g protein), naringin reduced MDA levels, demonstrating its strong ability to mitigate lipid peroxidation and oxidative damage under $AlCl_3$ exposure. In this case, E has a significantly more potent effect on the MDA level than NR.

CAT is an essential antioxidant enzyme detoxing hydrogen peroxide, protecting cells from oxidative damage. The control group (73.11 U/mg protein) indicates regular CAT activity, reflecting strong enzymatic antioxidant defenses. CAT activity decreased significantly in the ethanol-treated group (24.24 U/mg protein), indicating that ethanol impairs enzymatic antioxidant defenses. Similarly, $AlCl_3$ (22.69 U/mg protein) reduced CAT activity, confirming that $AlCl_3$ suppresses antioxidant enzymes to increase oxidative stress. The results are presented in Figure 12.

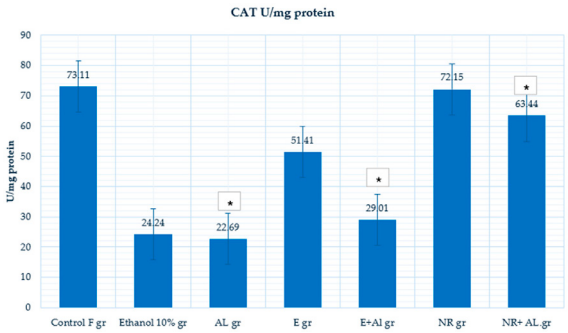

Figure 12. CAT activity in the mouse brain. * Indicates a statistically significant difference ($p \leq 0.05$) between the $AlCl_3$ and treated groups.

However, in the E + $AlCl_3$ group (29.01 U/mg protein), CAT activity showed only a slight increase, indicating limited protection against $AlCl_3$-induced oxidative stress, but did not reach a control group. The NR-treated group (72.15 U/mg protein) maintained CAT activity at near control levels, highlighting its ability to sustain enzymatic antioxidant defenses under normal conditions. In the NR + $AlCl_3$ group (63.44 U/mg protein), CAT activity was significantly restored, compared with the Al group, but did not reach the control group (73.11 U/mg protein).

The E showed a stronger ability to reduce MDA levels, demonstrating its effectiveness in preventing lipid peroxidation under the oxidative stress caused by $AlCl_3$. Meanwhile, NR significantly increases GSH levels and restores CAT activity.

2.4. Result of GSH, MDA and CAT in Mouse Liver

The effects of treatments on reduced (GSH), (MDA), and (CAT) activity in the liver are shown in Figures 13–15. During cervical dissection, notable physical changes were observed in the livers of $AlCl_3$-treated mice. These livers appeared enlarged, had irregular edges, and, in some cases, adhered to surrounding organs, indicating pathological changes likely caused by $AlCl_3$-induced oxidative stress and toxicity.

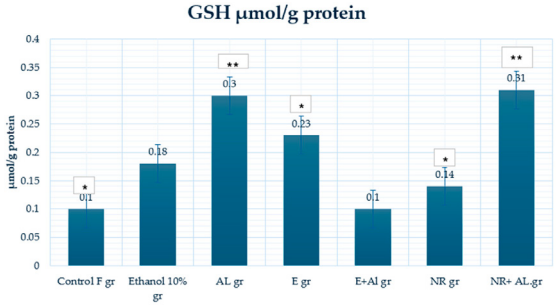

Figure 13. GSH activity in the mouse liver. * Indicates a statistically significant difference ($p \leq 0.05$) between the control and treated groups; ** indicates a statistically significant difference ($p \leq 0.05$) between the $AlCl_3$ and treated groups.

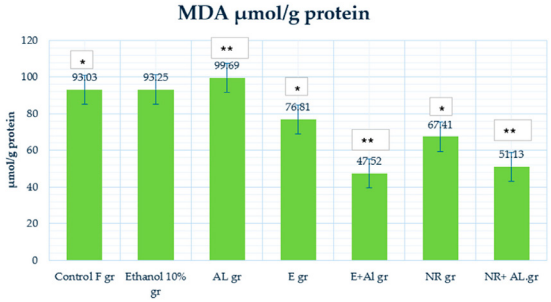

Figure 14. MDA activity in the mouse liver. * Indicates a statistically significant difference ($p \leq 0.05$) between the control and treated groups; ** indicates a statistically significant difference ($p \leq 0.05$) between the $AlCl_3$ and treated groups.

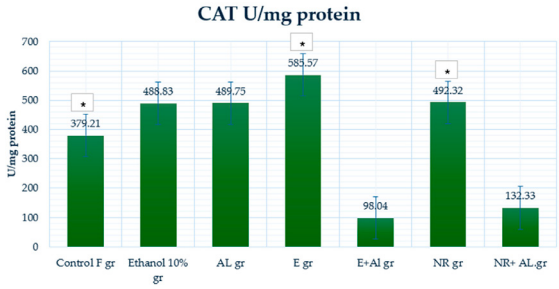

Figure 15. CAT activity in the mouse liver. * Indicates a statistically significant difference ($p \leq 0.05$) between the ethanolic and treated groups.

In the control group (0.1 µmol/g protein), baseline GSH levels show standard antioxidant capacity. The ethanol-treated group (0.18 µmol/g protein) showed a slight increase

in GSH, likely due to a compensatory response to oxidative stress caused by ethanol metabolism. The $AlCl_3$ group have the highest GSH levels (0.3 µmol/g protein), possibly reflecting an acute cellular response to counteract $AlCl_3$-induced oxidative stress.

The E group (0.23 µmol/g protein) increases on average GSH levels, suggesting its role in enhancing antioxidant defenses under normal conditions. However, in the extract (E) + $AlCl_3$ group (0.1 µmol/g protein), GSH levels dropped to control levels, indicating that the E provided limited protection against $AlCl_3$-induced oxidative stress in the liver. In contrast, the NR group (0.14 µmol/g protein) slightly increased GSH levels compared to the control. In comparison, the NR + $AlCl_3$ group (0.31 µmol/g protein) significantly restored GSH levels, indicating NR capacity to stimulate GSH synthesis and neutralize $AlCl_3$ toxicity.

The MDA control group (93.03 µmol/g protein) demonstrated baseline lipid peroxidation levels. The ethanol-treated group (93.25 µmol/g protein) showed similar MDA levels, indicating that ethanol did not significantly increase lipid peroxidation in the liver. However, the $AlCl_3$ group (99.69 µmol/g protein) increase MDA levels, confirming $AlCl_3$-induced oxidative stress and membrane lipid damage.

Treatment with the E alone (76.81 µmol/g protein) significantly reduced MDA levels, demonstrating its protective effect in lipid peroxidation under normal conditions. The E + $AlCl_3$ group (47.52 µmol/g protein) decreases MDA levels compared to the $AlCl_3$ group, highlighting the E strong antioxidative properties against $AlCl_3$-induced lipid damage. Similarly, the NR group (67.41 µmol/g protein) reduced MDA levels compared to the control, indicating its preventive effect on oxidative damage. The NR + $AlCl_3$ group (51.13 µmol/g protein) decreased MDA levels, demonstrating that NR effectively counteracts $AlCl_3$-induced lipid peroxidation.

The control group (379.21 U/mg protein) displayed baseline CAT activity and enzymatic defense mechanisms. The ethanol-treated group (488.83 µmol/g protein) and $AlCl_3$ group (489.75 U/mg protein) showed higher CAT activity, likely reflecting an adaptive response to increased ROS production.

The E group (585.57 U/mg protein) demonstrates the highest CAT activity, suggesting that the E strongly enhances enzymatic antioxidant defenses under normal conditions. However, in the E + $AlCl_3$ group (98.04 U/mg protein), CAT activity dropped significantly compared to the $AlCl_3$ group, indicating that the E had limited efficacy in restoring CAT activity under oxidative stress. The NR group (492.32 U/mg protein) maintained CAT activity, demonstrating NR's ability to support enzymatic defenses under normal conditions. In the NR + $AlCl_3$ group (132.33 U/mg protein), CAT activity improved significantly compared to the E + $AlCl_3$ group, indicating that NR provided better protection and restoration of enzymatic activity under oxidative stress.

Our findings on the effects of NR and E on oxidative stress markers GSH, MDA, and CAT are in close agreement with other studies using plant-derived antioxidants. These comparisons demonstrate natural extracts' unique properties and mechanisms in reducing oxidative stress.

M. Papaefthimiou et al. demonstrated that Stevia leaf extracts significantly reduced MDA levels while restoring GSH concentrations and antioxidant enzyme activity in experimental rat models [4]. It is similar to our findings that E effectively reduced MDA levels in liver and brain tissues, demonstrating its potential to limit lipid peroxidation under oxidative stress

G. M. Iova et al. found that curcumin and rutin restored GSH and reduced MDA levels in rats with experimentally induced oxidative stress [3]. Similarly, in our study, NR restored GSH levels, particularly in the brain and liver, highlighting its strong ability to counteract oxidative damage.

The findings from the *Origanum onites* L. study align closely with our research, as both demonstrate the effectiveness of plant-based antioxidants in reducing oxidative stress. In the *O. onites* study, the essential oil effectively reduced MDA levels, similar to the firm lipid peroxidation control observed with E in our study. Meanwhile, *O. onites* extract remarkably restored GSH levels and enhanced enzymatic protection, which parallels the effects of NR in our findings. Both studies highlight these antioxidants' complementary and tissue-specific roles in protecting against oxidative damage [47].

Sadauskienė et al. highlighted the ability of natural extracts to enhance GSH levels and restore CAT activity in liver and brain tissues under oxidative stress conditions [48]. It is consistent with our results, where NR effectively restored GSH and CAT activity, especially in the brain and liver, indicating its broad-spectrum antioxidant capacity.

The results of our study are strongly aligned with findings from another plant-based antioxidant research. While ethanolic grapefruit extract reduced lipid peroxidation (MDA) in the liver and brain, naringin showed broader antioxidant effects by restoring GSH levels and CAT activity. Future studies could explore their synergistic application to optimize therapeutic strategies related to oxidative stress.

3. Materials and Methods

3.1. Material

Naringin (NR) (≥95% purity)—Sigma Aldrich (Steinheim, Germany); ethanol (96%)—Vilniaus Degtinė (Vilnius, Lithuania); $AlCl_3$ (aluminum chloride)—Sigma Aldrich (Steinheim, Germany); GSH (reduced glutathione)—Sigma Aldrich (Steinheim, Germany); MDA (malondialdehyde)—Sigma Aldrich (Steinheim, Germany); TBA (thiobarbituric acid), tris-HCl (tris-hydrochloride), DTNB (5,5-dithiobis-(2-nitrobenzoic acid) were supplied by Serva, Heidelberg, Germany; TCA (trichloroacetic acid)—Merck (Darmstadt, Germany).

Analytical balance—Kern ABT 120-4M (Kern & Sohn GmbH, Balingen, Germany) max 120 g, min 10 mg, e = 1 mg, d = 0.1 mg; ultrasonic bath—Grant Instruments™ XUB12 Digital Bath (Grant Instruments Ltd., Shepreth, UK); Memmert UN 55 Laboratory Oven (Memmert GmbH + Co. KG, Büchenbach, Germany); centrifuge Sigma 3-18K, (Sigma Laborzentrifugen GmbH, Osterode am Harz, Germany); HPLC System—Waters 2695 Liquid Chromatography (Waters Corporation, Milford, MA, USA) with photodiode array detector (Waters 996, wavelength range 200–400 nm); chromatographic column—ACE C18 (250 mm × 4.6 mm, 5 µm particle size) (Advanced Chromatography Technologies Ltd., Aberdeen, UK); spectrophotometer—PerkinElmer Lambda 25 UV/Vis Spectrometer (PerkinElmer, Shelton, CT, USA).

3.2. Preparation of Naringin Solution for In Vivo Studies

Based on the scientific literature, a 500 mg/kg naringin concentration was selected to evaluate its antioxidant effects in an $AlCl_3$-induced oxidative stress mouse model. This dosage was chosen based on previous in vivo studies demonstrating its efficacy in mitigating oxidative stress and restoring antioxidant defense biomarkers [49,50]. To prepare 100 mL of solution, 5 g of naringin powder was dissolved in a 10% ethanol solution. The low ethanol concentration (10%) was chosen to minimize potential effects on the mice. The final naringin solution concentration was 50 mg/mL, and it was stored at ±4 °C until use [51,52].

3.3. Preparation and Extraction of Flavonoids from Citrus x paradisi L. Peels

Citrus x paradisi L. peels, a commonly discarded plant material, were dried at 60 °C for 8 h in the Department of Drug Technology and Social Pharmacy, Lithuanian University of Health Sciences, using a Memmert UN 55 Laboratory Oven (Memmert GmbH + Co. KG,

Büchenbach, Germany). The dried peels were then ground to a fine powder. Flavonoid extraction was conducted following methodologies shown in previous studies, with a detailed schematic of the process presented in Figure 16 [45,53].

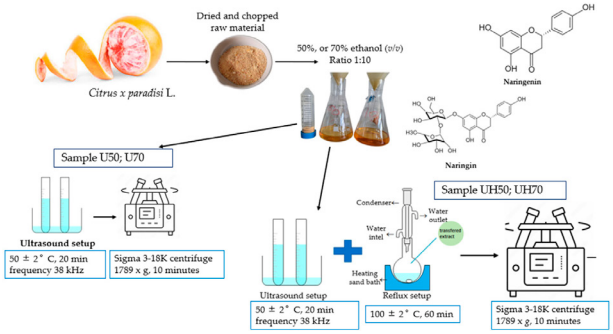

Figure 16. The sample ID represents the extraction method and ethanol concentration used. U indicates ultrasonic extraction, while UH combines ultrasonic and reflux extraction—the numbers correspond to ethanol concentrations: 50 for 50% ethanol and 70 for 70% ethanol.

For the extraction, ethanol solutions at concentrations of 50% and 70% (v/v) were used with a ratio of 1:10. Two extraction processes were evaluated. In the first process, ultrasonic extraction was performed using a Grant Instruments™ XUB12 Digital bath (Grant Instruments Ltd., Shepreth, UK), operating at 38 kHz for 20 min under controlled conditions of 50 ± 2 °C. The second step involved transferring the ultrasonically treated mixture to a reflux system for an additional 60 min extraction at 100 ± 2 °C temperature.

The extract was allowed to cool to room temperature and centrifuged with Sigma 3-18K centrifuge at room temperature (25 ± 5 °C) (Sigma Laborzentrifugen GmbH, Osterode am Harz, Germany) at 1789× g for 10 min to separate the solid residue from the liquid extract. The supernatant was filtered through a 0.22 µm PVDF membrane to remove residual particles. The samples were further analyzed, and their quantities were evaluated using HPLC.

3.4. Chromatographic Analysis of Citrus x paradisi L. Peels Ethanolic Extract: HLPC Analysis for Phenolic Compounds

A Waters 2695 liquid chromatography with a photodiode array detector (Waters 996, 200–400 nm wavelength range) was used in this study. In addition, a chromatographic column ACE C18 (250 mm × 4.6 mm) (Advanced Chromatography Technologies Ltd., Aberdeen, UK) with a sorbent particle size of 5 µm was used to separate the biologically active compounds. The following are the details of the procedure for the HPLC method. The HPLC analysis was performed to separate and quantify biologically active compounds in the ethanolic extract of *Citrus x paradisi* L. peels, including naringin and naringenin. The gradient elution method was applied to these extracts to achieve optimal separation of the target flavonoids. Then, 10 µL of each extract was injected and analyzed at 280 nm. Eluent A: acetonitrile; eluent B: water at a 1 mL/min rate. Gradient elution:10% of A from 0 to 5 min, from 5 to 25 min 20%, from 25 to 30 min 40%, from 30 to 35 min 100%, 35 min 100%, 36 min 10%. The temperature of the column was 25 °C. The peaks were identified by comparing their UV–vis spectra and retention times to those of authentic reference standards. Each extract was analyzed in duplicate as a technical repetition to confirm the

reproducibility of the HPLC method. Naringin and naringenin were used as reference standards for calibration, retention time identification, and quantification validation.

The quantification and validation followed the methodical revision of natural products presented by Wolfender (2009) [54]. Standard stock solutions of 100 µg/mL primary concentrations for naringin and naringenin were prepared in 70% methanol, and calibration curves were constructed using 6 different standard solution concentrations (Naringin: 1.166, 3.499, 8.332, 16.666, 25.000, and 33.343 µg/mL; Naringenin: 0.472, 1.889, 3.774, 7.547, 11.386, and 15.125 µg/mL). Three injections per concentration were performed to determine linearity. Naringin and naringenin were plotted against the known concentrations of their associated standard solutions to establish calibration equations. A linear regression equation was calculated using the least-squares method. The regression coefficients of all calibration curves were $R^2 > 0.999$, confirming the linearity of the concentration ranges. The method sensitivity was evaluated by determining the limit of detection (LOD)and quantitation (LOQ) Table 2. LOD and LOQ were calculated as the concentrations that gave signal-to-noise ratios of 3 to 10, respectively. A standard mixture of naringin and naringenin was used for intra-day and inter-day precision testing. The method precision was demonstrated by performing five replication-consecutive injections of the usual mix on the same day on four different days. The results are reported in terms of RSD. This study analyzed standards (naringin and naringenin), and their retention time and spectra were compared with the prepared extracts. The linearity was determined by estimating the correlation coefficient '$R^{2\prime}$ of the calibration curve (Figure 17) (naringin '$R^{2\prime}$ = 0.999923, naringenin '$R^{2\prime}$ = 0.999924), and the peak areas were used for quantification, Table 2. The linearity range of naringin was 1.166 to 33.343 µg/mL, and naringenin was 0.472 to 15.125 µg/mL. The results were expressed as µg/g and mg/g dry weight (DW) of naringenin and naringin, respectively.

Table 2. The linearities of calibration curves of flavanones.

Component	Calibration Equation	Coefficient of Determination '$R^{2\prime}$	Coefficient of Correlation R	LOD * µg/mL	LOQ ** µg/mL
Naringin	Y = 25.500x + 6720	0.999923	0.99996	0.146	0.583
Naringenin	±Y = 33.300x + 3570	0.999924	0.99996	0.118	0.430

LOD *—limit of detection; LOQ **—limit of quantification.

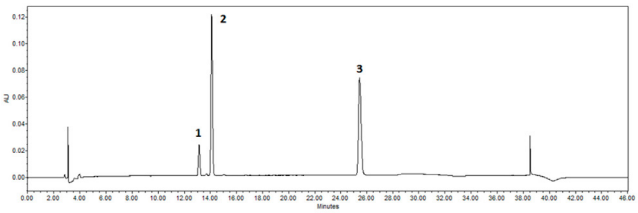

Figure 17. Chromatograms of standards detected by HPLC. Peaks identified: 1—narirutin, 2—naringin, 3—naringenin.

3.5. Animal Model

Experiments were performed with 4- to 6-week-old Balb C white laboratory mice weighing 20–25 g. All experiments were performed according to the Republic of Lithuania Law on the Care, Keeping, and Use of Animals (License of State Veterinary Service for Working with Laboratory Animals Nr. G2-275). Although this study observed ethical guidelines for animal research, further studies are needed to confirm the findings of clinical trials in humans, given species-specific differences in oxidative stress responses.

The mice were housed under standard laboratory conditions, maintained at a temperature of 22 ± 2 °C, with 55 ± 5% relative humidity, and a 12-h light-dark cycle. They had constant access to feed and water throughout the experiment. The diet consisted of Ab "Kauno Grūdai" Visaverčiai pašarai triušiams KG NATURE, a GMO-free complete feed formulated to provide balanced nutrition. The animals were supplied with filtered tap water, free from chemical additives.

This study involved 7 groups housed in separate cages containing 5 mice per group. The ethanolic *Citrus x paradisi* L. peel extract, and naringin solution (50 mg/mL body weight) was administered intragastrically for 21 days. The experimental design is illustrated in Figure 18.

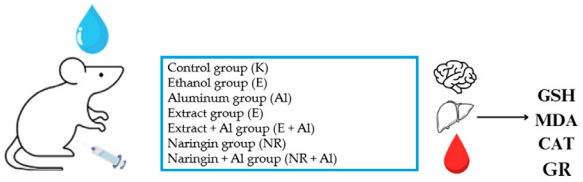

Figure 18. Experimental design and biomarkers assessed: reduced glutathione (GSH), malondialdehyde (MDA), and catalase (CAT), glutathione reductase (GR).

The control 1 group received NaCl 0.9% (the saline solution) for 21 days.

The control 2 group received 10% ethanol solution for 21 days.

The control 3 group $AlCl_3$ group (dissolved in saline) was injected intraperitoneally at 7.5 mg of Al^{3+}/kg body weight (0.15 LD50) in the $AlCl_3$ for 21 days.

The 4th group received ethanolic *Citrus x paradisi* L. peel extract intragastrical for 21 days.

The 5th group received ethanolic naringin 50 mg/mL solution intragastrical for 21 days.

The 6th group in which $AlCl_3$ (7.5 mg Al^{3+}/kg body weight) was administered intraperitoneally, followed by an intragastric administration of naringin solution (50 mg/mL) after a 20 min interval for 21 days.

The 7th group was treated with $AlCl_3$ intraperitoneally at the exact dosage, followed by intragastric administration of ethanolic *Citrus x paradisi* L. extract after a 20 min interval for 21 days.

This study involves collecting data on the body weight of mice in each group and monitoring changes in body mass continuously over 21 days. $AlCl_3$ solution was selected to induce oxidative stress due to its ability to indirectly promote ROS (reactive oxygen species) production via the Fenton reaction [55]. This reaction generates highly reactive hydroxyl radicals. The $AlCl_3$ solution was prepared by dissolving $AlCl_3$ in 0.9% sodium chloride. The concentration of the Al solution for the mice was determined based on scientific literature and calibrated according to the median lethal dose (LD50) of Al, which is 7.5 mg (0.15 LD50) per kilogram of body weight [56].

The $AlCl_3$ solution was administered to the mice intraperitoneally using a 1 mL insulin syringe. The ethanolic *Citrus x paradisi* L. peel extracts and naringin solution were delivered orally to the stomach using a specialized 1 mL syringe equipped with a probe designed for laboratory mice. The dosage of the test solutions was adjusted according to the body weight of the mice and any changes in their weight observed throughout this study.

After the 21-day study period, laboratory mice were weighed and euthanized via cervical dislocation followed by decapitation. This procedure complied with the European

Convention for the Protection of Vertebrate Animals used for Experimental and Other Scientific Purposes [57]. Blood samples were collected into heparin-treated tubes to prevent coagulation. Blood analyses were performed immediately on the same day to ensure reliable results.

The organs of the laboratory mice, including the liver and brain, were carefully prepared for further analysis. They were rinsed with physiological saline to remove residual blood and placed in Petri dishes. The organs were frozen at −40 °C to preserve their integrity until subsequent experiments. Weighed organs were homogenized in 9 volumes of cold 1.15% KCl solution relative to the organ weight, resulting in a 10% homogenate. The homogenate was then centrifuged at 15,000× *g* for 15 min.

3.6. Determination of GSH Concentration in Laboratory Mice Blood

The reduced glutathione (GSH) concentration in laboratory mice blood was determined using the method described by Sedlak and Lindsay [58]. This method relies on a reduction reaction in which GSH reacts with Ellman's reagent DTNG (5,5′-dithiobis-(2-nitrobenzoic acid). GSH and DTNB form a yellow-colored complex in an alkaline medium during this reaction.

To determine GSH concentration, 200 µL of blood was mixed with 1.8 mL deionized water and 2 mL of 0.6 M $HClO_4$. The prepared mixture was centrifuged at 3000 rpm for 10 min. After centrifugation, 1 mL of the supernatant was mixed with 3 mL of 0.4 M Tris–HCl buffer solution (pH 9.2) and 50 µL of Ellman's reagent solution. The same procedure was followed to prepare the control solution, except that 1 mL of deionized water was used instead of the supernatant. The color intensity of the reaction mixture was measured spectrophotometrically at a wavelength of 412 nm. The GSH concentration in the blood was expressed in µmol/L and calculated using the appropriate formula [59].

$$C\mu\frac{\text{mol}}{\text{L}} = A \times 1488.9705 \times V_0 \quad (1)$$

C—GSH concentration in µmol/L; A—absorbance of the supernatant at 412 nm wavelength; 1488.9705—coefficient; V_0—volume of the supernatant in ml.

3.7. Determination of MDA Concentration in Laboratory Mice Blood

The concentration of MDA in laboratory mice blood was determined using the method described by Seliutina and Selutin, which is based on the reaction between MDA and TBR (thiobarbituric acid) [60]. During the reaction, MDA reacts with TBR to form MDA-TBR_2 complexes, which exhibit a pink color and quantify MDA concentration in erythrocytes [47].

For the determination of MDA concentration, both test and control mixtures were prepared. The test mixtures comprised 2 mL of deionized water, 100 µL of mouse blood, 1 mL of 10% trichloroacetic acid, and 2 mL of 0.5% thiobarbituric acid solution. 2 mL of deionized water was used instead of the 0.5% TBR solution for the control mixtures. The mixtures were stirred with a glass rod and incubated in a water bath for 30 min. After incubation, the samples were cooled in an ice bath.

Once cooled, the samples were centrifuged at 3000 rpm for 15 min. The upper, transparent layer of the centrifuged mixture was analyzed using a spectrophotometer to measure absorbance at a wavelength of 540 nm. The MDA concentration in mice blood was calculated using the following formula, with results expressed in µmol/L:

$$c = E \times 1250 \quad (2)$$

where c MDA concentration in the blood (µmol/L); E—absorbance of the test sample at 540 nm; 1250—coefficient.

3.8. Determination of GSH Concentration in Laboratory Mouse Organs

The concentration of GSH was measured following the method outlined by Sadauskiene et al. [48,61]. Mouse liver or brain tissues were homogenized in 5% trichloroacetic acid at a ratio of six volumes of the solution to one of tissue weight. The homogenate was then centrifuged at 10,000× *g* for 7 min.

The supernatant was reacted with DTNB (Ellman's reagent, 5,5-dithiobis (2-nitrobenzoic acid)). Each reaction mixture (3 mL) was prepared by combining 2 mL of 0.6 mM DTNB in 0.2 M sodium phosphate buffer (pH 8.0), 0.2 mL of the supernatant, and 0.8 mL of 0.2 M phosphate buffer. The resulting compound exhibited maximum light absorption at 412 nm. GSH content was calculated and expressed as μmol/g of fresh tissue weight.

$$\text{C}\mu\text{mol/g} = \frac{\text{A} \times 3 \times \text{V}_{\text{gal}}}{2.72 \times \text{w}} \quad (3)$$

C—GSH concentration in tissues (μmol/g); A—absorbance value of the test sample; 3—coefficient; V_{gal}—volume of the supernatant; 2.72—coefficient; w—tissue weight.

3.9. GR Activity Assay

The method for determining glutathione reductase (GR) activity is based on measuring the decrease in absorbance at 340 nm due to $NADP^+$ oxidation during the reduction in oxidized glutathione (GSSG) catalyzed by GR.

The reaction mixture (2 mL, excluding sample volume) contains 0.05 M phosphate buffer (pH 7.8), 1 mM EDTA, 0.16 mM $NADP^+$, and 0.8 mM oxidized glutathione. The reaction is initiated by adding 20 μL of the sample, and the absorbance is measured at 340 nm at 0 min (E_0) and 3.5 min (E_a) [62].

GR activity is calculated using the formula:

$$\text{A} = \frac{(\text{E}_0 - \text{E}_\text{a})}{(\text{T} \times \text{V}_{\text{total}} \times \text{P})} \times \frac{1}{6.22 \times \text{C}} \quad (4)$$

T—reaction time (min), V_{total} is cuvette volume (2 mL), P—dilution factor, 6.22—extinction coefficient for glutathione (cm^{-1} mM^{-1}), and C—protein concentration (mg/mL).

3.10. Determination of MDA Concentration in Laboratory Mouse Organs

The final product of lipid peroxidation, (MDA), reacts with TBA (thiobarbituric acid) to form a colored complex, which can be quantified spectrophotometrically. The results are expressed as μmol/g of wet tissue weight [61]. Brain or liver tissues were excised and homogenized in a 9-fold volume (relative to tissue weight) of cold 1.15% potassium chloride (KCl) solution to produce a 10% homogenate.

To 0.5 mL of the homogenate, 3 mL of 1% phosphoric acid (H_3PO_4) and 1 mL of 0.6% TBA solution were added. The mixture was heated in a boiling water bath for 45 min to facilitate the reaction. After cooling, 4 mL of n-butanol was added to the sample, and the mixture was thoroughly mixed. The butanol phase was separated by centrifugation, and the absorbance of the supernatant was measured spectrophotometrically at 535 nm and 520 nm. This method enables accurate quantification of MDA as formula.

$$\text{C}\mu\text{mol/g} = \frac{\Delta\text{O.V.} \times 100,000}{133} \quad (5)$$

C—MDA concentration in tissues (μmol/g); ΔO.V.—difference in absorbance at 520 nm and 535 nm wavelengths; 100,000 and 133—coefficients.

3.11. (CAT) Activity Assay

Catalase activity in brain and liver homogenates was measured using the method described by Sadauskiene et al. [62]. This assay relies on the catalase decomposition of hydrogen peroxide (H_2O_2). The reaction mixture consisted of 50 mM Tris-HCl buffer (pH 7.4) containing 18 mM H_2O_2 (buffer-substrate mixture) and 100 µL of tissue homogenate. The mixture was incubated at 37 °C for 180 s to allow the enzymatic reaction to occur.

The reaction was terminated by adding 2.0 mL of 4.5% ammonium molybdate, which forms a yellow complex with residual hydrogen peroxide. The absorbance of this complex was measured at 410 nm using a spectrophotometer (PerkinElmer Lambda 25 UV/Vis Spectrometer (PerkinElmer, Shelton, CT, USA). A blank control was prepared by incubating the buffer-substrate mixture for 180 s, adding ammonium molybdate and 100 µL of the tissue homogenate.

The catalase activity was expressed as units per mg of protein (U/mg protein). One unit of CAT (U) corresponds to the decomposition of 1 µmol of H_2O_2 per minute under the assay conditions. This method provides a reliable measure of CAT activity in tissue samples.

$$A = \frac{(E_K - E_B) \times 12 \times 10^3 \times 4.1 \times 10^6}{22.2 \times 10^6 \times t} \quad (6)$$

A—CAT activity (U/mL); E_K—mean absorbance of the control sample at 410 nm wavelength; E_B—mean absorbance of the test sample at 410 nm wavelength; 12×10^3—dilution factor; 4.1×10^6—conversion coefficient to µmol; 22.2×10^6—molar extinction coefficient of H_2O_2; t—incubation time (3 min).

3.12. Statistical Analysis

The statistical analysis evaluated the effects of naringin, and grapefruit extract on oxidative stress markers (GSH, MDA, and CAT) in mice's blood, liver, and brain, comparing the treatment groups to control groups. Data were expressed as the mean ± SD (standard error of the mean). Statistical significance was determined using one-way analysis of difference (ANOVA) and the unpaired Student t-test. The value of $p < 0.05$ was considered statistically significant (SPSS version 20.0, IBM, Armonk, NY, USA).

4. Conclusions

This study demonstrates the effectiveness of combining ultrasound and reflux extraction (UH) methods (as example by the UH50 sample) to achieve higher yields of naringin and naringenin from *Citrus x paradisi* L. Our in vivo findings show different mechanisms through which grapefruit extract and naringin mitigate oxidative stress E significantly reduced lipid peroxidation, as evidenced by a marked decrease in (MDA) levels in the blood (Al group 241.32 µmol/g protein, E + AL group 110.78 µmol/g protein), respectively; in the liver (Al group 76.81 µmol/g protein, E + AL group 47.52 µmol/g protein), respectively; in the brain (Al group 87.66 µmol/g protein, E + AL group 56.21 µmol/g protein), respectively. Meanwhile, NR significantly impacted the antioxidant defense system by restoring (GSH) levels: in the blood (Al group 1080.33 µmol/g protein, E + AL group 1735.46 µmol/g protein), respectively; in the brain (Al group 0.0023 µmol/g protein, E + AL group 0.0193 µmol/g protein) respectively; in the liver (Al group 0.3 µmol/g protein, E + AL group 0.31 µmol/g protein) respectively, and (CAT) activity: in the brain (Al group 23.69 U/mg protein, E + AL group 63.44 U/mg protein) respectively; in the liver (Al group 489.75 U/mg protein, E + AL group 132.33 U/mg protein) respectively.

The hypothesis that E surpasses NR in reducing oxidative stress markers was only partially confirmed. However, E demonstrated excellent control over lipid oxidative damage, and NR proved more effective in restoring key antioxidant biomarkers, particularly

under aluminum chloride ($AlCl_3$)-induced oxidative stress. These findings suggest that combining E and NR may offer synergistic benefits, improving protection against oxidative damage through complementary pathways.

This research highlights the potential of grapefruit-derived bioactive compounds and lays the foundation for exploring combined therapeutic strategies to manage oxidative stress in future studies.

Author Contributions: Conceptualization, J.B., J.S., I.S., A.L. and Z.M.; investigation, J.S., I.S., A.L. and Z.M.; resources, J.B.; writing—production of the initial draft, J.S.; writing—review and editing, J.B. and J.S.; visualization, J.S.; supervision, J.B. All authors have read and agreed to the published version of the manuscript.

Funding: This project was funded by the Research Council of Lithuania (LMTLT), Agreement No. S-A-UE-23-7.

Institutional Review Board Statement: The Lithuanian State Food and Veterinary Service approved the animal study protocol, License no. G2-275.

Informed Consent Statement: Not applicable.

Data Availability Statement: The data presented in this study are available on request from the corresponding author.

Acknowledgments: The authors sincerely appreciate the Open Access Centre for Advanced Pharmaceutical and Health Technologies at the Lithuanian University of Health Sciences and the Lithuanian Research Centre for providing access to their state-of-the-art research infrastructure, which was essential for this study. We also acknowledge the Neuroscience Institute, Lithuanian University of Health Sciences, and the Large Animal Clinic, Veterinary Academy, Lithuanian University of Health Sciences for their support.

Conflicts of Interest: The authors declare no conflicts of interest.

References

1. Arias, A.; Feijoo, G.; Moreira, M.T. Exploring the potential of antioxidants from fruits and vegetables and strategies for their recovery. *Innov. Food Sci. Emerg. Technol.* **2022**, *77*, 102974. [CrossRef]
2. Kurutas, E.B. The importance of antioxidants which play the role in cellular response against oxidative/nitrosative stress: Current state. *Nutr. J.* **2015**, *15*, 71. [CrossRef] [PubMed]
3. Iova, G.M.; Calniceanu, H.; Popa, A.; Szuhanek, C.A.; Marcu, O.; Ciavoi, G.; Scrobota, I. The Antioxidant Effect of Curcumin and Rutin on Oxidative Stress Biomarkers in Experimentally Induced Periodontitis in Hyperglycemic Wistar Rats. *Molecules* **2021**, *26*, 1332. [CrossRef]
4. Papaefthimiou, M.; Kontou, P.I.; Bagos, P.G.; Braliou, G.G. Antioxidant Activity of Leaf Extracts from *Stevia rebaudiana* Bertoni Exerts Attenuating Effect on Diseased Experimental Rats: A Systematic Review and Meta-Analysis. *Nutrients* **2023**, *15*, 3325. [CrossRef]
5. Stabrauskiene, J.; Kopustinskiene, D.M.; Lazauskas, R.; Bernatoniene, J. Naringin and Naringenin: Their Mechanisms of Action and the Potential Anticancer Activities. *Biomedicines* **2022**, *10*, 1686. [CrossRef]
6. Alam, M.A.; Subhan, N.; Rahman, M.M.; Uddin, S.J.; Reza, H.M.; Sarker, S.D. Effect of Citrus Flavonoids, Naringin and Naringenin, on Metabolic Syndrome and Their Mechanisms of Action. *Adv. Nutr.* **2014**, *5*, 404–417. [CrossRef]
7. Bai, Y.; Peng, W.; Yang, C.; Zou, W.; Liu, M.; Wu, H.; Fan, L.; Li, P.; Zeng, X.; Su, W. Pharmacokinetics and Metabolism of Naringin and Active Metabolite Naringenin in Rats, Dogs, Humans, and the Differences Between Species. *Front. Pharmacol.* **2020**, *11*, 364. [CrossRef]
8. Eom, S.; Lee, B.-B.; Lee, S.; Park, Y.; Yeom, H.D.; Kim, T.-H.; Nam, S.-H.; Lee, J.H. Antioxidative and Analgesic Effects of Naringin Through Selective Inhibition of Transient Receptor Potential Vanilloid Member 1. *Antioxidants* **2021**, *11*, 64. [CrossRef]
9. Erdogan, S.; Doganlar, O.; Doganlar, Z.B.; Turkekul, K. Naringin sensitizes human prostate cancer cells to paclitaxel therapy. *Prostate Int.* **2018**, *6*, 126–135. [CrossRef]
10. Arafah, A.; Rehman, M.U.; Mir, T.M.; Wali, A.F.; Ali, R.; Qamar, W.; Khan, R.; Ahmad, A.; Aga, S.S.; Alqahtani, S.; et al. Multi-Therapeutic Potential of Naringenin (4′,5,7-Trihydroxyflavonone): Experimental Evidence and Mechanisms. *Plants* **2020**, *9*, 1784. [CrossRef]

11. Lobo, V.; Patil, A.; Phatak, A.; Chandra, N. Free radicals, antioxidants and functional foods: Impact on human health. *Pharmacogn. Rev.* **2010**, *4*, 118. [CrossRef] [PubMed]
12. Li, J.-K.; Liu, X.-D.; Shen, L.; Zeng, W.-M.; Qiu, G.-Z. Natural plant polyphenols for alleviating oxidative damage in man: Current status and future perspectives. *Trop. J. Pharm. Res.* **2016**, *15*, 1089. [CrossRef]
13. Chaudhary, P.; Janmeda, P.; Docea, A.O.; Yeskaliyeva, B.; Abdull Razis, A.F.; Modu, B.; Calina, D.; Sharifi-Rad, J. Oxidative stress, free radicals and antioxidants: Potential crosstalk in the pathophysiology of human diseases. *Front. Chem.* **2023**, *11*, 1158198. [CrossRef] [PubMed]
14. Martemucci, G.; Costagliola, C.; Mariano, M.; D'andrea, L.; Napolitano, P.; D'Alessandro, A.G. Free Radical Properties, Source and Targets, Antioxidant Consumption and Health. *Oxygen* **2022**, *2*, 48–78. [CrossRef]
15. Sies, H. Oxidative Stress: Concept and Some Practical Aspects. *Antioxidants* **2020**, *9*, 852. [CrossRef]
16. Abdelazim, A.M.; Abomughaid, M.M. Oxidative stress: An overview of past research and future insights. *Life* **2024**, *17*, 2316092. [CrossRef]
17. Rogers, L.K.; Cismowski, M.J. Oxidative stress in the lung—The essential paradox. *Curr. Opin. Toxicol.* **2018**, *7*, 37–43. [CrossRef]
18. Senoner, T.; Dichtl, W. Oxidative Stress in Cardiovascular Diseases: Still a Therapeutic Target? *Nutrients* **2019**, *11*, 2090. [CrossRef]
19. Braga-Neto, M.B.; Costa, D.V.S.; Queiroz, D.M.M.; Maciel, F.S.; De Oliveira, M.S.; Viana-Junior, A.B.; Santos, F.A.; Leitao, R.F.C.; Brito, G.A.C.; Vasconcelos, P.R.L.; et al. Increased Oxidative Stress in Gastric Cancer Patients and Their First-Degree Relatives: A Prospective Study from Northeastern Brazil. *Oxidative Med. Cell. Longev.* **2021**, *2021*, 6657434. [CrossRef]
20. Gyurászová, M.; Gurecká, R.; Bábíčková, J.; Tóthová, Ľ. Oxidative Stress in the Pathophysiology of Kidney Disease: Implications for Noninvasive Monitoring and Identification of Biomarkers. *Oxidative Med. Cell. Longev.* **2020**, *2020*, 5478708. [CrossRef]
21. Allameh, A.; Niayesh-Mehr, R.; Aliarab, A.; Sebastiani, G.; Pantopoulos, K. Oxidative Stress in Liver Pathophysiology and Disease. *Antioxidants* **2023**, *12*, 1653. [CrossRef] [PubMed]
22. Afshari-Kaveh, M.; Abbasalipourkabir, R.; Nourian, A.; Ziamajidi, N. The Protective Effects of Vitamins A and E on Titanium Dioxide Nanoparticles (nTiO2)-Induced Oxidative Stress in the Spleen Tissues of Male Wistar Rats. *Biol. Trace Elem. Res.* **2021**, *199*, 3677–3687. [CrossRef] [PubMed]
23. Ganapathy, E.; Rajasekaran, D.; Sivalingam, M.; Farooq, M.; Abdul, E.; Dhanapal, S. Naringenin Inhibits Oxidative Stress Induced Macromolecular Damage in N-methyl N-nitro N-nitrosoguanidine Induced Gastric Carcinogenesis in Wistar Rats. In *Gastric Carcinoma—New Insights into Current Management*; Lazar, D., Ed.; InTech: Houston, TX, USA, 2013; ISBN 978-953-51-0914-3.
24. Ghezzi, P. Environmental risk factors and their footprints in vivo—A proposal for the classification of oxidative stress biomarkers. *Redox Biol.* **2020**, *34*, 101442. [CrossRef]
25. Cammisotto, V.; Nocella, C.; Bartimoccia, S.; Sanguigni, V.; Francomano, D.; Sciarretta, S.; Pastori, D.; Peruzzi, M.; Cavarretta, E.; D'Amico, A.; et al. The Role of Antioxidants Supplementation in Clinical Practice: Focus on Cardiovascular Risk Factors. *Antioxidants* **2021**, *10*, 146. [CrossRef]
26. Haro Girón, S.; Monserrat Sanz, J.; Ortega, M.A.; Garcia-Montero, C.; Fraile-Martínez, O.; Gómez-Lahoz, A.M.; Boaru, D.L.; De Leon-Oliva, D.; Guijarro, L.G.; Atienza-Perez, M.; et al. Prognostic Value of Malondialdehyde (MDA) in the Temporal Progression of Chronic Spinal Cord Injury. *J. Pers. Med.* **2023**, *13*, 626. [CrossRef]
27. Bergin, P.; Leggett, A.; Cardwell, C.R.; Woodside, J.V.; Thakkinstian, A.; Maxwell, A.P.; McKay, G.J. The effects of vitamin E supplementation on malondialdehyde as a biomarker of oxidative stress in haemodialysis patients: A systematic review and meta-analysis. *BMC Nephrol.* **2021**, *22*, 126. [CrossRef]
28. Kong, A.S.-Y.; Lai, K.S.; Hee, C.-W.; Loh, J.Y.; Lim, S.H.E.; Sathiya, M. Oxidative Stress Parameters as Biomarkers of Cardiovascular Disease Towards the Development and Progression. *Antioxidants* **2022**, *11*, 1175. [CrossRef]
29. Cordiano, R.; Di Gioacchino, M.; Mangifesta, R.; Panzera, C.; Gangemi, S.; Minciullo, P.L. Malondialdehyde as a Potential Oxidative Stress Marker for Allergy-Oriented Diseases: An Update. *Molecules* **2023**, *28*, 5979. [CrossRef]
30. Noori, S.; Rezaei Tavirani, M.; Deravi, N.; Mahboobi Rabbani, M.I.; Zarghi, A. Naringenin Enhances the Anti-Cancer Effect of Cyclophosphamide Against MDA-MB-231 Breast Cancer Cells via Targeting the STAT3 Signaling Pathway. *Iran. J. Pharm. Res.* **2020**, *19*, 122–133. [CrossRef]
31. Zuleta, E.C.; Baena, L.; Rios, L.A.; Calderón, J.A. The oxidative stability of biodiesel and its impact on the deterioration of metallic and polymeric materials: A review. *J. Braz. Chem. Soc.* **2012**, *23*, 2159–2175. [CrossRef]
32. Ayala, A.; Muñoz, M.F.; Argüelles, S. Lipid Peroxidation: Production, Metabolism, and Signaling Mechanisms of Malondialdehyde and 4-Hydroxy-2-Nonenal. *Oxid. Med. Cell. Longev.* **2014**, *2014*, 360438. [CrossRef] [PubMed]
33. Iuchi, K.; Takai, T.; Hisatomi, H. Cell Death via Lipid Peroxidation and Protein Aggregation Diseases. *Biology* **2021**, *10*, 399. [CrossRef] [PubMed]
34. Valgimigli, L. Lipid Peroxidation and Antioxidant Protection. *Biomolecules* **2023**, *13*, 1291. [CrossRef] [PubMed]
35. Ighodaro, O.M.; Akinloye, O.A. First line defence antioxidants-superoxide dismutase (SOD), catalase (CAT) and glutathione peroxidase (GPX): Their fundamental role in the entire antioxidant defence grid. *Alex. J. Med.* **2018**, *54*, 287–293. [CrossRef]

36. Lee, C.-W.; Huang, C.C.-Y.; Chi, M.-C.; Lee, K.-H.; Peng, K.-T.; Fang, M.-L.; Chiang, Y.-C.; Liu, J.-F. Naringenin Induces ROS-Mediated ER Stress, Autophagy, and Apoptosis in Human Osteosarcoma Cell Lines. *Molecules* **2022**, *27*, 373. [CrossRef] [PubMed]
37. Dasari, S.; Ganjayi, M.S.; Meriga, B. Glutathione S-transferase is a good biomarker in acrylamide induced neurotoxicity and genotoxicity. *Interdiscip. Toxicol.* **2018**, *11*, 115–121. [CrossRef]
38. Carmo De Carvalho E Martins, M.D.; Martins; Da Silva Santos Oliveira, A.S.; Da Silva, L.A.A.; Primo, M.G.S.; De Carvalho Lira, V.B. Biological Indicators of Oxidative Stress [Malondialdehyde, Catalase, Glutathione Peroxidase, and Superoxide Dismutase] and Their Application in Nutrition. In *Biomarkers in Nutrition*; Patel, V.B., Preedy, V.R., Eds.; Biomarkers in Disease: Methods, Discoveries and Applications; Springer International Publishing: Cham, Switzerland, 2022; pp. 1–25, ISBN 978-3-030-81304-8.
39. Da Silva, J.K.; Cazarin, C.B.B.; Colomeu, T.C.; Batista, Â.G.; Meletti, L.M.M.; Paschoal, J.A.R.; Bogusz Júnior, S.; Furlan, M.F.; Reyes, F.G.R.; Augusto, F.; et al. Antioxidant activity of aqueous extract of passion fruit (*Passiflora edulis*) leaves: In vitro and in vivo study. *Food Res. Int.* **2013**, *53*, 882–890. [CrossRef]
40. Gajewska, J.; Chełchowska, M.; Rychłowska-Pruszyńska, M.; Klepacka, T.; Ambroszkiewicz, J. Oxidative and Antioxidative Status Expressed as OSI Index and GSH/GSSG Ratio in Children with Bone Tumors After Anticancer Therapy Completion. *J. Clin. Med.* **2022**, *11*, 1663. [CrossRef]
41. Kotha, R.R.; Tareq, F.S.; Yildiz, E.; Luthria, D.L. Oxidative Stress and Antioxidants—A Critical Review on In Vitro Antioxidant Assays. *Antioxidants* **2022**, *11*, 2388. [CrossRef]
42. Munteanu, I.G.; Apetrei, C. Analytical Methods Used in Determining Antioxidant Activity: A Review. *Int. J. Mol. Sci.* **2021**, *22*, 3380. [CrossRef]
43. Pardo-Botello, R.; Chamizo-Calero, F.; Monago-Maraña, O.; Rodríguez-Corchado, R.; De La Torre-Carreras, R.; Galeano-Díaz, T. Evaluation of Hydrophilic and Lipophilic Antioxidant Capacity in Spanish Tomato Paste: Usefulness of Front-Face Total Fluorescence Signal Combined with Parafac. *Food Anal. Methods* **2022**, *15*, 981–992. [CrossRef]
44. Flieger, J.; Flieger, W.; Baj, J.; Maciejewski, R. Antioxidants: Classification, Natural Sources, Activity/Capacity Measurements, and Usefulness for the Synthesis of Nanoparticles. *Materials* **2021**, *14*, 4135. [CrossRef] [PubMed]
45. Stabrauskiene, J.; Marksa, M.; Ivanauskas, L.; Viskelis, P.; Viskelis, J.; Bernatoniene, J. *Citrus* × *paradisi* L. Fruit Waste: The Impact of Eco-Friendly Extraction Techniques on the Phytochemical and Antioxidant Potential. *Nutrients* **2023**, *15*, 1276. [CrossRef] [PubMed]
46. Nobile, V.; Pisati, M.; Cestone, E.; Insolia, V.; Zaccaria, V.; Malfa, G.A. Antioxidant Efficacy of a Standardized Red Orange (*Citrus sinensis* (L.) Osbeck) Extract in Elderly Subjects: A Randomized, Double Blind, Controlled Study. *Nutrients* **2022**, *14*, 4235. [CrossRef]
47. Kubiliene, A.; Munius, E.; Songailaite, G.; Kokyte, I.; Baranauskaite, J.; Liekis, A.; Sadauskiene, I. A Comparative Evaluation of Antioxidant Activity of Extract and Essential Oil of *Origanum onites* L. In Vivo. *Molecules* **2023**, *28*, 5302. [CrossRef]
48. Sadauskiene, I.; Liekis, A.; Bernotiene, R.; Sulinskiene, J.; Kasauskas, A.; Zekonis, G. The Effects of Buckwheat Leaf and Flower Extracts on Antioxidant Status in Mouse Organs. *Oxidative Med. Cell. Longev.* **2018**, *2018*, 6712407. [CrossRef]
49. Salehi, B.; Fokou, P.; Sharifi-Rad, M.; Zucca, P.; Pezzani, R.; Martins, N.; Sharifi-Rad, J. The Therapeutic Potential of Naringenin: A Review of Clinical Trials. *Pharmaceuticals* **2019**, *12*, 11. [CrossRef]
50. Ghanbari-Movahed, M.; Jackson, G.; Farzaei, M.H.; Bishayee, A. A Systematic Review of the Preventive and Therapeutic Effects of Naringin Against Human Malignancies. *Front. Pharmacol.* **2021**, *12*, 639840. [CrossRef]
51. Yang, S.-Y.; Li, N.; Zhang, J.; Wooley, P.; Xu, Z. Therapeutic potentials of naringin on polymethylmethacrylate induced osteoclastogenesis and osteolysis, in vitro and in vivo assessments. *Drug Des. Devel. Ther.* **2013**, *8*, 1–11. [CrossRef]
52. Bharti, S.; Rani, N.; Krishnamurthy, B.; Arya, D. Preclinical Evidence for the Pharmacological Actions of Naringin: A Review. *Planta Med.* **2014**, *80*, 437–451. [CrossRef]
53. Stabrauskiene, J.; Marksa, M.; Ivanauskas, L.; Bernatoniene, J. Optimization of Naringin and Naringenin Extraction from *Citrus* × *paradisi* L. Using Hydrolysis and Excipients as Adsorbent. *Pharmaceutics* **2022**, *14*, 890. [CrossRef] [PubMed]
54. Wolfender, J.-L. HPLC in Natural Product Analysis: The Detection Issue. *Planta Medica* **2009**, *75*, 719–734. [CrossRef]
55. Bakare, O.; Adedugbe, O.; Owoloye, A. Aluminum Chloride-Induced Oxidative Damage to Serum and Combined Intervention of Ascorbic Acids and Massularia Acuminata On Selected Markers Of In Vivo Antioxidant Enzymes in Wistar Rats. *J. Chem. Nutr. Biochem.* **2021**, *2*, 13–28. [CrossRef]
56. Staneviciene, I.; Ivanov, L.; Kursvietiene, L.; Viezeliene, D. Short-term effects of aluminum and selenium on redox status in mice brain and blood. *Trace Elem. Electrolytes* **2017**, *34*, 74–80. [CrossRef]
57. Official Journal of the European Union Directive 2010/63/EU of the European Parliament and of the Council of 22 September 2010 on the Protection of Animals Used for Scientific Purposes. 2010. Available online: https://eur-lex.europa.eu/LexUriServ/LexUriServ.do?uri=OJ:L:2010:276:0033:0079:en:PDF (accessed on 23 January 2025).
58. Sedlak, J.; Lindsay, R.H. Estimation of Total, Protein-Bound, and Non Protein Sulfhydryl Groups in Tissue by Ellman's Reagent. *Anal. Biochem.* **1968**, *25*, 192–208. [CrossRef]

59. Rajurkar, N.; Hande, S. Estimation of phytochemical content and antioxidant activity of some selected traditional Indian medicinal plants. *Indian. J. Pharm. Sci.* **2011**, *73*, 146. [CrossRef]
60. Seliutina, C.N.; AIu, S.; Pal, A.I. Modifikatsiia opredeleniia kontsentratsii TBK-aktivnykh produktov syvorotki krovi [Modification of estimation the concentrations of serum TBA-active product]. *Klin. Lab. Diagn.* **2000**, *2*, 8–10.
61. Bernotiene, R.; Ivanoviene, L.; Sadauskiene, I.; Liekis, A.; Ivanov, L. Effects of cadmium and zinc ions on mice brain lipid peroxidation and amounts of thiol-rich compounds. *Trace Elem. Electrolytes* **2016**, *33*, 83–88. [CrossRef]
62. Sadauskiene, I.; Liekis, A.; Staneviciene, I.; Naginiene, R.; Ivanov, L. Effects of Long-Term Supplementation with Aluminum or Selenium on the Activities of Antioxidant Enzymes in Mouse Brain and Liver. *Catalysts* **2020**, *10*, 585. [CrossRef]

Paper 4

Title: Optimizing Encapsulation: Comparative Analysis of Spray-Drying and Freeze-Drying for Sustainable Recovery of Bioactive Compounds from *Citrus* × *paradisi* L. Peels.
Authors: Jolita Stabrauskiene, Lauryna Pudziuvelyte and Jurga Bernatoniene.
Pharmaceuticals 2024, 17, 596.

pharmaceuticals

MDPI

Article

Optimizing Encapsulation: Comparative Analysis of Spray-Drying and Freeze-Drying for Sustainable Recovery of Bioactive Compounds from *Citrus x paradisi* L. Peels

Jolita Stabrauskiene [1,2], Lauryna Pudziuvelyte [1,2] and Jurga Bernatoniene [1,2,*]

[1] Department of Drug Technology and Social Pharmacy, Lithuanian University of Health Sciences, LT-50161 Kaunas, Lithuania; jolita.stabrauskiene@lsmu.lt (J.S.); lauryna.pudziuvelyte@lsmu.lt (L.P.)
[2] Institute of Pharmaceutical Technologies, Lithuanian University of Health Sciences, LT-50161 Kaunas, Lithuania
* Correspondence: jurga.bernatoniene@lsmu.lt; Tel.: +370-6006-3349

Abstract: Spray-drying and freeze-drying are indispensable techniques for microencapsulating biologically active compounds, crucial for enhancing their bioavailability and stability while protecting them from environmental degradation. This study evaluates the effectiveness of these methods in encapsulating *Citrus x paradisi* L. (grapefruit) peel extract, focusing on sustainable recovery from waste peels. Key objectives included identifying optimal wall materials and assessing each encapsulation technique's impact on microencapsulation. The investigation highlighted that the choice of wall material composition significantly affects the microencapsulation's efficiency and morphological characteristics. A wall material mixture of 17 g maltodextrin, 0.5 g carboxymethylcellulose, and 2.5 g β-cyclodextrin was optimal for spray drying. This combination resulted in a sample with a wettability time of 1170 (s), a high encapsulation efficiency of 91.41%, a solubility of 60.21%, and a low moisture content of 5.1 ± 0.255%. These properties indicate that spray-drying, particularly with this specific wall material composition, offers a durable structure and can be conducive to prolonged release. Conversely, varying the precise compositions used in the freeze-drying process yielded different results: quick wettability at 132.6 (s), a solubility profile of 61.58%, a moisture content of 5.07%, and a high encapsulation efficiency of 78.38%. The use of the lyophilization technique with this latter wall material formula resulted in a more porous structure, which may facilitate a more immediate release of encapsulated compounds and lower encapsulation efficiency.

Keywords: encapsulation; spray-drying; freeze-drying; *Citrus x paradisi* L. peels

Citation: Stabrauskiene, J.; Pudziuvelyte, L.; Bernatoniene, J. Optimizing Encapsulation: Comparative Analysis of Spray-Drying and Freeze-Drying for Sustainable Recovery of Bioactive Compounds from *Citrus x paradisi* L. Peels. *Pharmaceuticals* **2024**, *17*, 596. https://doi.org/10.3390/ph17050596

Academic Editor: Serge Mordon

Received: 8 April 2024
Revised: 24 April 2024
Accepted: 2 May 2024
Published: 7 May 2024

1. Introduction

Phenolic compounds such as flavanones naringin and naringenin are abundant bioactive components in *Citrus x paradisi* L (grapefruit) [1]. These compounds have attracted the scientific community's attention due to their unique health-promoting properties and diverse biological activities [2,3]. However, limited solubility, bioavailability, and stability often hinder their practical application in the pharmaceutical and food industries [4,5].

Microencapsulation technology is used in various industries, including food, cosmetics, and pharmaceuticals, to protect, isolate, and control the release of bioactive substances [6]. Microcapsules are particles of an outer shell enclosing an inner core containing the active ingredient (Table 1). The particle size of microcapsules can vary from 0.2 to 5000 µm, depending on the materials and processing methods used [7,8]. Methods such as spray drying, cooling, extrusion coating, liquid layer coating, liposome entrapment, lyophilization, coacervation, centrifugal suspension separation, crystallization, and inclusion complexation can produce microcapsules [9].

Table 1. Encapsulation coating materials and their applications [10–14].

Microencapsulation Materials	Material Examples	Common Use
Polysaccharides	Dextrines (maltodextrin, cyclodextrins), Ethylcellulose, Methylcellulose, Hydroxypropyl methylcellulose, Carboxymethylcellulose, Carrageenan	Food, Pharmaceuticals, Nutraceuticals
Proteins	Gelatin, Casein, Whey protein, Skim milk, Egg white	Food, Pharmaceuticals, Nutraceuticals
Lipids	Waxes (beeswax, carnauba wax), Animal sources, Fats, and Plant sources	Food, Pharmaceuticals, Nutraceuticals
Synthetics	Poly-lactic-co-glycolic acid (PLGA)	Target drug delivery, Bioengineering

Spray-drying is widely used for converting liquid extracts into powder form [15]. It is practical and universal and can preserve phenolic compounds' stability, solubility, and controlled-release characteristics [16]. Spray-drying also allows for the creation of microcapsules with different particle sizes, which can be customized to meet specific usage and formulation requirements, storage conditions, and desired shelf life [17–19].

Before spray-drying, it is essential to emulsify the liquid extracts. Emulsification significantly influences the encapsulation efficiency, powder attributes, and stored materials' stability [20,21] (Figure 1).

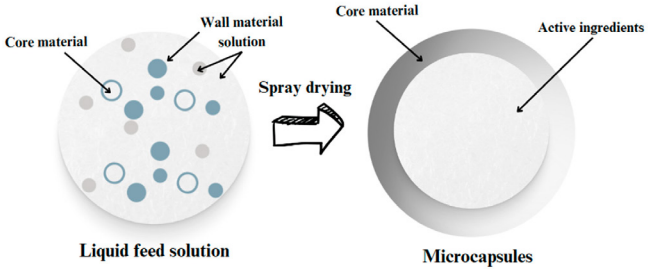

Figure 1. This schematic illustrates the encapsulation process, where a shell is formed around particles during the spray-drying procedure.

The stability of the emulsions, critical for effective microencapsulation, largely depends on the pH level. The acidic conditions (pH 3.0–6.0) are optimal for stabilizing grapefruit extracts rich in flavonoids and ascorbic acid; the latter is particularly vulnerable to degradation at higher pH levels [22]. Excipients such as β-cyclodextrin and carboxymethylcellulose enhance the solubility and stability of these bioactive compounds under acidic conditions, playing pivotal roles in maintaining the integrity of the emulsion [10,23].

Freeze-drying–lyophilization is a method of dehydration that delicately removes the solvent from a sample through sublimation during the primary drying phase and desorption during the secondary drying phase [24]. The process comprises three stages. The first is sample freezing; in this phase, the sample is frozen quickly to solidify the solvent and maintain the material's structural integrity. This step is crucial in stabilizing the sample in a fixed geometry, which helps retain the sample's physical structure during drying. During the primary drying (sublimation) phase, the solid solvent (such as water) transitions directly from the solid phase (ice) to the vapor phase under a high vacuum without passing through the liquid phase [25]. This phase is responsible for most of the solvent removal, and controlled heat is applied cautiously to provide the energy required for sublimation while preserving the integrity of the temperature-sensitive materials. In the secondary drying (desorption) phase, residual solvent, usually bound to the product,

is removed by desorption (Figure 2). The temperature is raised above the primary drying levels to break the intermolecular forces holding the solvent molecules, helping to release them from the sample matrix. This phase ensures the complete removal of water, resulting in a dry product with an extended shelf life [26,27].

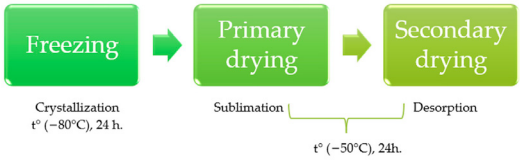

Figure 2. An overview of the three stages involved in the freeze-drying process.

Freeze-drying is widely recognized as the best method for encapsulating sensitive bioactive compounds due to its gentle dehydration process, one which does not expose substances to high temperatures, unlike spray-drying [24]. This technique, known for its simplicity and quick reconstitution capabilities, is particularly effective for encapsulating products like vaccines and antibodies that require rapid administration [25].

Recent advancements in material science, such as the development of novel scaffold fabrication methods like those proposed by Ilaria Silvestro et al., incorporate techniques like thermally induced phase separation enhanced by freeze-gelation and photo cross-linking. These innovative methods avoid chemical cross-linkers and allow precise control over porosity, which is crucial for applications in tissue engineering. Claire M. Brougham et al. further demonstrate the potential of freeze-drying in creating complex scaffold geometries for biomedical applications, showcasing a novel method to produce a collagen-based, heart valve-shaped scaffold with controlled porosity. These cutting-edge techniques are at the forefront of our research, promising exciting new possibilities in microencapsulation [28,29].

This study aims to deepen the understanding of wall material selection for encapsulating bioactive compounds in grapefruit extract using both spray-drying and freeze-drying methods. By evaluating the roles of skim milk, maltodextrin, carboxymethylcellulose, and β-cyclodextrin as encapsulating agents, this investigation seeks to guide effective strategies for microencapsulation, focusing on the enhancement of powder quality and encapsulation efficiency Figure 3.

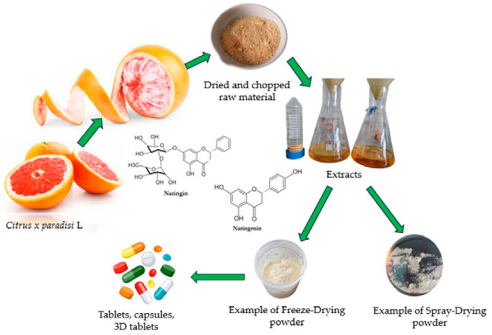

Figure 3. Converting grapefruit peels (*Citrus x paradisi.* L) into different pharmaceutical forms. The process starts with preparing the raw material by drying and chopping it, and then extracting the active compounds naringin and naringenin. Next, the emulsion is processed into powders using freeze-drying and spray-drying techniques.

2. Materials and Methods

2.1. Citrus x paradisi.L Extracts Preparation

For these studies, we utilized the residual peels of *Citrus x paradisi* L., which are typically discarded post-juice-extraction. These peels were dried and ground into powder using a coffee grinder. The powdered peels underwent ultrasonic extraction in a Grant Instruments™ XUB12 Digital bath at 38 kHz with a 50% ethanol solution in a 1:10 ratio for 30 min at 50 ± 2 °C. After cooling to room temperature, the mixture was centrifuged at 1789× *g* for 10 min. The supernatant was filtered through a 0.22 µm PVDF filter for further microencapsulation.

2.2. Formulation of Emulsion for Spray-Drying and Freeze-Drying Processes

The wall material for spray- and freeze-drying comprised varying concentrations of maltodextrin, skim milk, beta-cyclodextrin, chitosan, and carboxymethylcellulose (CMC). The wall material, forming a 20% (*w*/*v*) concentration, was initially dissolved in purified water. Subsequently, all solutions were stirred using a magnetic stirrer (MSH-20A, Witeg, Wertheim, Germany) for 30 min at 25 °C. The solutions containing dissolved encapsulants were combined with a 50 mL ethanolic extract from *Citrus x paradisi* L. The resulting emulsion was stirred for another 30 min at 25 °C. Directly following this process, the resultant emulsion was used for microencapsulation purposes.

2.3. Parameters for Spray-Drying Process

Spray-drying was carried out using a Buchi B-291 Mini Spray-Dryer (BÜCHI Labortechnik AG, Flawil, Switzerland) under varying experimental conditions. These included inlet temperatures of 90, 120, and 160 °C, outlet temperatures ranging from 25 to 80 °C, a spray flow feed rate of 30 mL/min, and air pressure in the 8-bar range. The resulting spray-dried powders were collected and stored in a refrigerator at +4–7 °C to prevent avoidable changes in material properties.

2.4. Freeze-Drying Procedure

The prepared mixtures were initially subjected to freezing using a FORMA™ 88,000 Series laboratory freezer (Therma Scientific, Waltham, MA, USA) at a temperature of −80 °C for 24 h. Later, the frozen samples underwent lyophilization in a LyoQuest Telstar laboratory freeze-dryer (Wertheim, Germany) operating at −50 °C and 0.05 bar for 24 h. The resultant powders were collected, securely sealed in foil bags, and stored in a desiccator to ensure preservation and stability until further analysis.

2.5. Characterizations of the Microcapsules

The powders produced by spray-drying and freeze-drying were analyzed in detail, including moisture content, wettability, solubility, bulk and tapped volumes, product yield, encapsulation efficiency, and morphology.

2.5.1. Determination of Moisture Content

The moisture content of the powder is determined by oven-drying the sample at 105 °C until it reaches a constant weight. The heating rate is approximately 0.11 °C per minute. The weight loss observed during this process, quantified as a percentage, accurately reflects the product's moisture content [30]. These tests were performed in triplicate, and results were reported as the mean ± (n = 3).

2.5.2. Wettability Analysis of Spray-Dried and Freeze-Dried Powders

Wettability for both spray-dried powder and freeze-dried powder was evaluated using methods adapted from Zhang et al. [31] and Wang et al. [32], respectively. In each test, 1 g of the sampler was added to 100 mL of water at room temperature, and the time until complete dissolution or disappearance from the water's surface was recorded. These tests were performed in triplicate, and results were reported as the mean ± (n = 3).

2.5.3. SEM Analysis of Microcapsules: Morphological Evaluation

The morphological properties of the microcapsules, as formulated using various wall materials and processed at 160 °C, were examined using scanning electron microscopy (SEM). Tiny quantities of the spray-dried powders were adhered to the surface of double-sided tape attached to stubs. The Hitachi TM 3000 scanning electron microscope, sourced from Tokyo, Japan, was employed to capture photomicrographs at magnifications ranging from 100× to 5000× under an accelerating voltage of 5 kV.

2.5.4. Assessment of Process Yield (Y%)

For this study, the yield of each production process was calculated based on the amount of solid material initially introduced into the equipment compared to the quantity of powder collected after the process. The yield percentage was determined using the following adapted equation, Equation (1):

$$Yield\ (\%) = \frac{Weight\ of\ Powder\ Collected}{Weight\ of\ Solids\ Fed\ into\ Equipment} \times 100 \quad (1)$$

2.5.5. Measurement of Bulk and Tapped Volumes for Spray-Dried and Freeze-Dried Powders

The evaluations of bulk (V_0) and tapped volumes (Vtapped) of both spray-dried and freeze-dried powders were conducted using the SVM 102 Erweka (Germany) density tester, following the protocols outlined in the Pharmacopeia (Ph. Eur., USP). These collected volume measurements were then applied to calculate each powder variant's Carr index (2) and Hausner ratio (3). The tapped volume was determined after performing 750 tappings. These tests were performed in triplicate, and results were reported as the mean ± (n = 3).

$$CarrIndex = \frac{100 \times (V_0 - Vtapped)}{V_0} \quad (2)$$

$$HausnerRatio = \frac{V_0}{Vtapped} \quad (3)$$

2.5.6. Solubility Assessments

The solubility of the samples was assessed using a modification of the method described in [33]. A 0.5 g sample was mixed with 12.5 mL of distilled water and stirred with a magnetic stirrer at 350 rpm at 25 °C for 30 min. The solution was centrifuged at 3500× g for 10 min at the same temperature. A 10 mL portion of the supernatant was dried overnight at 105 ± 5 °C. The weight difference determined the solubility percentage (%). These tests were performed in triplicate, and results were reported as the mean ± (n = 3).

$$Solubility\ (\%) = \frac{Residue\ after\ drying}{Theoretical\ residue\ after\ drying} \times 100 \quad (4)$$

$$Theoreticalresidue = \frac{W\ (supernatant\ to\ be\ dried) + W\ (microcapsules)}{W\ (microcapsules) - W\ (purified\ water)} \times 100 \quad (5)$$

2.5.7. Quantification of Total and Surface Phenolic Content in Powdered Samples

To find the total phenolic content (TPC) and surface phenolic content (SPC) of the powdered samples, an assay was made following a modified version of the method described in Pudziuvelyte et al. [6,25]. For the TPC determination, a 100 mg sample of the test powder was dissolved in a 1 mL solution of ethanol, acetic acid, and water, as mixed in a volume ratio of 20:8:42, respectively. This mixture was stirred for 2 min with a magnetic stirrer and then subjected to an ultrasonic bath for 20 min at 30 °C. After sonication, the mixture was filtered through a microfilter with a 0.45 µm pore size. A quantity of 100 µL of the filtered sample was mixed with 2.5 mL of Folin–Ciocalteu reagent and left in a dark

place for 5 min. Following this incubation, 2 mL of a 7.5% Na_2CO_3 solution was added to the mixture, which was then thoroughly mixed and left in the dark for an additional hour at 25 °C. The TPC was quantified by measuring the absorbance at 760 nm using a UV/VIS 1800 Shimadzu spectrophotometer, with results expressed in mg of gallic-acid-equivalent per gram of powder.

To assess the SPC, another 100 mg sample of the test powder was mixed with 10 mL of ethanol–methanol solution in a 1:1 volume ratio and filtered similarly.

The encapsulation efficiency TPC EE% (7) and SPC% (6) were calculated using the following specific formulas:

$$SPC\ \% = \frac{surface\ phenolic\ compounds}{total\ phenolic\ compounds} \times 100 \quad (6)$$

$$TPC\ EE\ (\%) = 100 - SPC\ (\%) \quad (7)$$

3. Results and Discussion

3.1. Influences of Different Conditions of Microencapsulation on the Physicochemical Properties

A study was conducted, beginning with the creation of an extract from *Citrus x paradisi.* L fruit peels using 50% v/v ethanol. The extract was used to make encapsulated powders. The process involved drying and grinding the peels, followed by extraction, centrifugation, and filtration. (Section 2). The resulting flavanone extracts were used for encapsulation.

First, the properties of spray-dried powders were determined using a consistent composition of 10% skim milk and 10% maltodextrin to establish optimal conditions for microencapsulation. Four samples (M1, M2, M3, and M7) were prepared under this formulation, and the effects of temperature on the yield and moisture content of the powders were evaluated. The results are summarized in Table 2, illustrating the variations in yield percentages and moisture levels under different conditions.

Table 2. Spray-drying conditions and microencapsulation results for *Citrus x paradisi.* L phenolics using maltodextrin (MD) 10% and skim milk (SK) 10% as wall materials (M1, M2, M3, and M7).

Inlet T (°C)	Outlet T (°C)	Flow Rate (mL/min)	Air Pressure	Yield (%)	Moisture Content (%)	Sample ID
90	25	30	8 bars	48.10 ± 2.40	7.60 ± 0.38	M1
120	65	30	8 bars	51.65 ± 2.58	6.57 ± 0.32	M2
160	80	30	8 bars	52.95 ± 2.64	5.97 ± 0.298	M3
170	116	30	8 bars	48.00 ± 2.40	5.31 ± 0.265	M7

The study found that the yield range extended from 48% to approximately 53%, while the moisture content ranged from about 5.31% to 7.60%. The differences in yield and moisture content were attributed to the various conditions employed during the spray-drying process.

Based on these studies, the optimal conditions for obtaining the highest yield with the lowest moisture content were an inlet temperature of 160 °C and an outlet temperature of 80 °C. The yield achieved under these conditions was approximately 52.95 ± 2.64%. The moisture content was also the lowest, at about 5.97 ± 0.298%.

Meanwhile, when the inlet temperature was increased to 170 °C and the outlet temperature to 116 °C, the yield decreased to 48.0 ± 2.4%, while evincing a slightly lower moisture content of 5.31 ± 0.265%. This could be because of the increased temperature in the drying process. Higher temperatures may lead to the degradation of phenolic compounds or the formation of impermeable skin around the microcapsules, which can trap moisture and reduce the yield.

3.2. Impact of Wall Material Composition on the Physicochemical Characteristics of Microcapsules

During the initial phase of the study, different wall materials were selected for evaluation, including maltodextrin (MD), skim milk (SK), β-cyclodextrin (β-CD), and carboxymethylcellulose (CMC). These materials were used to understand the physical and chemical properties of the resulting powders, in addition to the release characteristics of the powders. The concentration of the encapsulating agents was set at 20%. The microencapsulation conditions were optimized based on the study's parameters as reported in Section 2.1.

Using different wall materials significantly impacts the parameters of the spray-drying process. For example, experiments using samples MBC2 and MBC3, which had varying amounts of MD, β-CD, and CMC under identical conditions, resulted in reduced quantities. However, improvements in yield were observed by modifying the temperature and flow rate. The temperature was decreased from 160 °C to 145 °C and the flow rate increased from 30 mL/min to 60 mL/min. These findings highlight the importance of both wall materials and operational parameters in determining the efficiency and result of the spray-drying process. The graph in Figure 4 illustrates how temperature and flow affect bulk quantities.

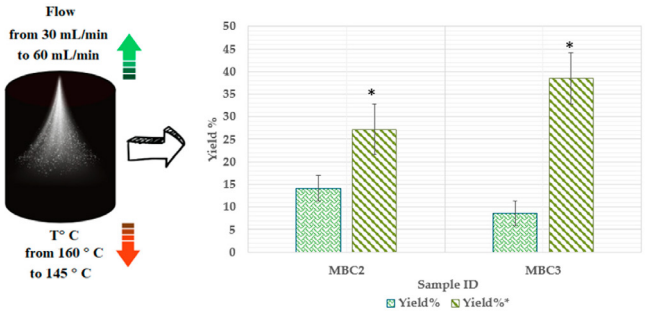

Figure 4. Illustration of how temperature and flow affect bulk quantities (Yield%). MBC2 * (MD 15%, β-CD 4.1%, and CMC 0.9%) $p < 0.05$ MBC2 (MD 15%, β-CD 4.1%, and CMC 0.9%); MBC3 * (MC 17%, β-CD 2.5%, and CMC 0.5%) $p < 0.05$ MBC3 (MC 17%, β-CD 2.5%, and CMC 0.5%).

It was observed that yield improvements occurred for two bulk compositions, MBC2 and MBC3, when the temperature was reduced and the flow rate increased. The yield of MBC2 increased from 14.15% to 27.2%, while MBC3's yield increased significantly, from 8.55% to 38.5%. This improvement is attributed to the lower temperature, which enhances solubility and stability. At the same time, the higher flow rate promotes better mixing and mass transfer. The specific composition of MBC3 was found to be more responsive to the process changes, resulting in the most significant yield increase.

3.2.1. Examining Moisture Content and Wettability in Microcapsule Formulations

In a previous study, we determined suitable spray-drying parameters for microcapsules' qualitative aspects. This study aims to examine how different wall materials, processed with the same parameters, affect moisture content and wettability.

Figure 5 illustrates the variations in moisture content and wettability among different microcapsule formulations that employ distinct combinations of encapsulating agents. For instance, M3, which utilizes a balance of maltodextrin and skim milk, exhibited a moderate moisture content of 5.97 ± 0.29%. MD is recognized for its ability to confer low moisture content, which is advantageous for the stability of microcapsules over time, as supported by references [34,35]. Our findings indicate that increased maltodextrin correlates with

decreased moisture levels, as demonstrated by MBC2 and MBC3 (5.52 ± 0.276% and 5.1 ± 0.255%, respectively), under consistent spray-drying conditions.

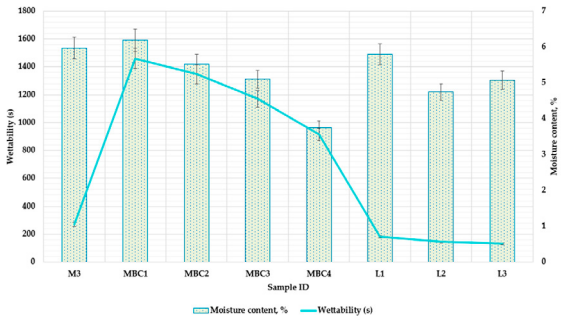

Figure 5. Comparative moisture content and wettability time analysis across different microcapsule formulations. M3 (MD 10%, SK 10%); MBC1 (MD 13%, β-CD 5.8%, CMC 1.2%); MBC2 (MD 15%, β-CD 4.1%, CMC 0.9%); MBC3 (MD 17%, β-CD 2.5%, CMC 0.5%); MBC4 (MD 10%, SK 9%, β-CD 1%). L1 (MD 13%, β-CD 5.8%, CMC 1.2%); L2 (MD 15%, β-CD 4.1%, CMC 0.9%); L3 MBC3 (MD 17%, β-CD 2.5%, CMC 0.5%); M indicates the spray-dry method, and the L–lyophilization method is used.

The integration of β-CD in formulations of MBC1, MBC2, and MBC3 seems to impact the surface characteristics of the microcapsules, leading to increased wettability times as the concentration of β-CD rises (Figure 5). This alteration may be due to the formation of more-structured and less-permeable surfaces, which is attributed to the β-CD [36]. β-CD is a cyclic oligosaccharide that can create complexes with various hydrophobic compounds within its structure while its exterior remains hydrophilic. This means that the surface of β-CD is predominantly hydrophilic, enhancing the wettability of microcapsules. However, the hydrophilic/hydrophobic properties of β-CD can be altered when other components are present in the composition of the microcapsules [37].

Carboxymethylcellulose (CMC), due to its hydrophilic properties, significantly influences the moisture content and wettability times of microcapsules, which are crucial for controlled release mechanisms [38]. In the MBC series, we observe that the wettability time decreases with decreasing CMC content: MBC1 (1.2% CMC) has a wettability time of 1461 s, MBC2 (0.9% CMC) 1347 s, and MBC3 (0.5% CMC) 1170 s.

Meanwhile, the sample MBC4 exhibited a lower moisture content and wettability time (3.75 ± 0.018% and 915 s, respectively), suggesting a synergistic interaction between SK and β-CD. This combination, involving the protein matrix and the encapsulating function of β-CD, results in a less hygroscopic product, and one which is more rapidly wettable [37].

Samples L1, L2, and L3 showcase the benefits of lyophilization in producing microcapsules with lower moisture content (5.8 ± 0.29%, 4.74 ± 0.19%, and 5.07 ± 0.25%). Freeze-drying typically produces a more porous structure that retains less moisture than those produced with spray-drying [15]. The rapid wettability of L2 (despite having a composition like L1) indicates that optimizing the ratio of MD to β-CD and CMC is crucial for improving water uptake. It suggests that the specific proportions of these components are critical to the microcapsules' properties, beyond just the overall concentration of wall materials. L3 displayed a moisture content comparable to MBC3 but lower wettability due to the different drying methods.

3.2.2. Impacts of Composition and Drying Methods on the Flowability of Microencapsulated Powders

The compressibility index and Hausner ratio are essential for assessing the powder characteristics of spray-dried and freeze-dried formulations. The compressibility index reflects the ability of a powder to settle and the degree to which it can be compacted [39]. The powder flowability, characterized by the Carr index and Hausner ratio, ranged from 30.43% to 38.89% and 1.438 to 1.636, respectively (Figure 6). Based on the European Pharmacopoeia article Ph. Eur. 01/2010:20936, the flowability of the powders is classified from 'poor' to 'very, very poor' based on these measurements.

Figure 6. Assessment of compressibility (Carr index) and flowability (Hausner ratio) in spray-dried and freeze-dried powders formulated with varied wall materials. M3 (MD 10%, SK 10%); MBC1 (MD 13%, β-CD 5.8%, CMC 1.2%); MBC2 (MD 15%, β-CD 4.1%, CMC 0.9%); MBC3 (MD 17%, β-CD 2.5%, CMC 0.5%); MBC4 (MD 10%, SK 9%, β-CD 1%). L1 (MD 13%, β-CD 5.8%, CMC 1.2%); L2 (MD 15%, β-CD 4.1%, CMC 0.9%); L3 MBC3 (MD 17%, β-CD 2.5%, CMC 0.5%). M indicates the spray-dry method, and the L–lyophilization method is used.

Mainly, the MBC1 sample exhibits a Hausner ratio of 1.636, one of the highest, indicating lower flowability. This is possibly due to its higher β-CD and CMC content, substances that tend to enhance cross-linking, which could diminish flow.

Conversely, incorporating more maltodextrins tends to lower the cohesiveness, thereby improving flow. This is demonstrated by the MBC3 sample, which has an increased MD content and reflects this principle.

SK is part of the microencapsulation process, as evidenced by samples like M3 and MBC4 (1.5–1.545 and 31.47% and 30.11%). The proteins in SK can enhance the integrity of the powder through protein–protein interactions, which may reflect increased compressibility indices and Hausner ratios, suggesting a reduction in flow. Nevertheless, statistical analyses have not found significant differences between groups of samples, suggesting that skim milk's inclusion does not significantly impact flowability or compressibility when compared to the influence of other components.

The preparation method also plays a significant role in these properties. Although spray-drying typically results in more uniform and spherical particles, which should theoretically improve flow compared to the irregular particles from lyophilization, the composition's influence is more pronounced than that of the drying technique. However, interestingly, lyophilized samples have shown better compressibility indices and Hausner ratios in cases where the compositions are similar, such as with MBC1 and L1.

3.2.3. Optimization of Solubility and Release Profiles in Microencapsulated Phenolic Compounds

During our research, we observed significant variations in the solubility of different samples, indicating that the choices of composition and preparation method significantly impact their solubility. The samples were prepared using lyophilization (L1, L2, and L3) and spray-drying (M3, MBC1, MBC2, MBC3, and MBC4). Figure 7 displays the solubility percentages of microencapsulated formulations using spray-drying and lyophilization methods with different wall materials.

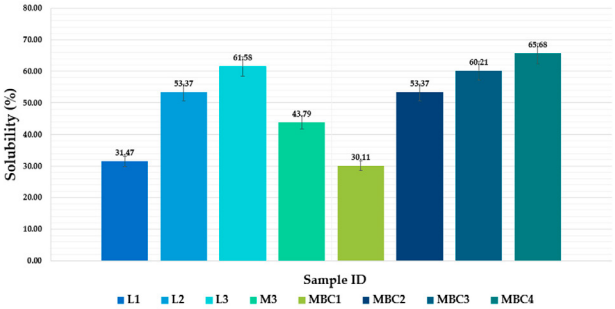

Figure 7. Solubility (%) of microencapsulated formulations using spray-drying and lyophilization methods with a different wall material. M3 (MD 10%, SK 10%); MBC1 (MD 13%, β-CD 5.8%, CMC 1.2%); MBC2 (MD 15%, β-CD 4.1%, CMC 0.9%); MBC3 (MD 17%, β-CD 2.5%, CMC 0.5%); MBC4 (MD 10%, SK 9%, β-CD 1%). L1 (MD 13%, β-CD 5.8%, CMC 1.2%); L2 (MD 15%, β-CD 4.1%, CMC 0.9%); L3 MBC3 (MD 17%, β-CD 2.5%, CMC 0.5%). M indicates the spray-dry method, and the L–lyophilization method is used.

Samples prepared using the lyophilization method showed an increasing tendency towards increased solubility with a decrease in β-CD and CMC content and an increase in MD content. The solubility ranged from 31.47 ± 1.57% for L1 to 61.58 ± 3.079% for L3. We suggest that MD, a polysaccharide, can increase the solubility of samples, while β-CD and CMC may decrease it [40].

A similar tendency can be observed for samples prepared using the spray-dry method. Solubility increased with the decrease in β-CD and CMC content and an increase in MD content. The solubility ranged from 30.11 ± 1.50% for MBC1 to 65.68 ± 3.35% for MBC4.

Lyophilization produces formulations with a more porous structure, which could lead to faster release rates [15]. Nonetheless, our data indicate that with a careful selection of wall materials, even lyophilized samples can achieve a degree of solubility suitable for controlled release.

Spray-drying is known for producing denser particles, which should, in theory, contribute to a slower release due to reduced solubility [35]. Based on our research data for the spray-dried samples (marked as M), the MBC3 sample is the most suitable for producing modified-release microcapsules to encapsulate grapefruit phenolic compounds. This sample has a wettability time of 1170 s, indicating a potentially slower release rate, which is desirable for sustained release. Additionally, its moisture content is 5.1% and it has a high solubility of 67.05%. These factors make it beneficial for controlled release and bioavailability.

In the lyophilized (freeze-dried) sample series (marked as L), the L2 sample appears to be the most suitable choice. This sample has a relatively low moisture content of 4.74%, suggesting improved stability. It also exhibits excellent flowability, with a Hausner ratio of 1.438, which is crucial for manufacturing processes. Furthermore, its solubility is relatively

high at 60.21%, and with a wettability time of 144 s, it might provide a rapid initial release while maintaining a controlled release profile.

3.2.4. The Impact of Wall Material Composition on the Encapsulation Efficiency of Active Ingredients

In examining the M and L series' encapsulation efficiency (EE%), sample MBC3 from the M series achieves the highest encapsulation efficiency, at 91.41%. Figure 8 illustrates the encapsulation efficiency percentages (TPC EE%) for various microencapsulated formulations. M3 with equal parts MD and SK (both at 10%) shows a high EE% at 89.04, suggesting that combining these two components at these specific ratios is conducive to effective encapsulation. In comparison, MBC1 has the lowest value within this group, at 76.72%. These results indicate that the optimal ratio of maltodextrin, as observed in MBC3, is crucial for enhancing encapsulation efficiency. EE% increases recorded with increasing MD in the formulation M sample were 76.72% < 87.27% < 91.41%. MBC4, with a high proportion of SK comparable to MD and a minimal amount of β-CD, shows an EE% of 83.97, which is lower than M3 but higher than MBC1. The presence of SK at a high level seems beneficial but the impact is not as pronounced as that of a high MD content. L1 is the highest for the L series, at 88.57%, with L2 at the lower end at 76.77%. However, the L series overall exhibits lower encapsulation efficiencies than their MBC counterparts.

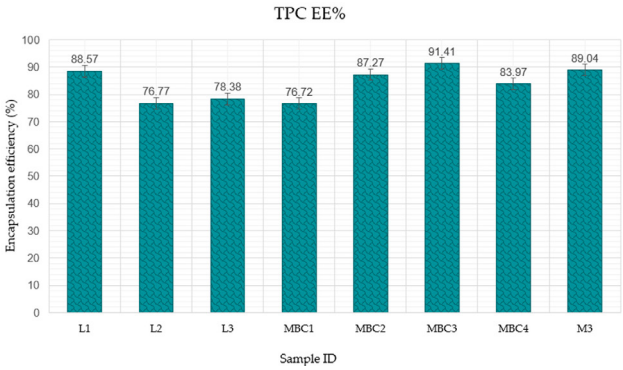

Figure 8. Encapsulation efficiency of *Citrus x paradisi.* L phenolic compounds in various microencapsulation formulations. M3 (MD 10%, SK 10%); MBC1 (MD 13%, β-CD 5.8%, CMC 1.2%); MBC2 (MD 15%, β-CD 4.1%, CMC 0.9%); MBC3 (MD 17%, β-CD 2.5%, CMC 0.5%); MBC4 (MD 10%, SK 9%, β-CD 1%). L1 (MD 13%, β-CD 5.8%, CMC 1.2%); L2 (MD 15%, β-CD 4.1%, CMC 0.9%); L3 MBC3 (MD 17%, β-CD 2.5%, CMC 0.5%).

3.2.5. Scanning Electron Microscopy of Spray-Dried and Freeze-Dried Powders

Figure 9 presents scanning electron microscope (SEM) images of various microencapsulated formulations identified as M3, MBC1, MBC2, MBC3, MBC4, L1, and L2. The images show the surface morphology and particle size distribution of each sample at high magnifications, providing insight into the physical characteristics of the microcapsules produced by different methods and with various wall materials. Each panel highlights unique structural differences, from spherical and smooth to irregular and crumpled textures, which are critical in understanding the encapsulation efficiencies and potential release behaviors of the encapsulated compounds.

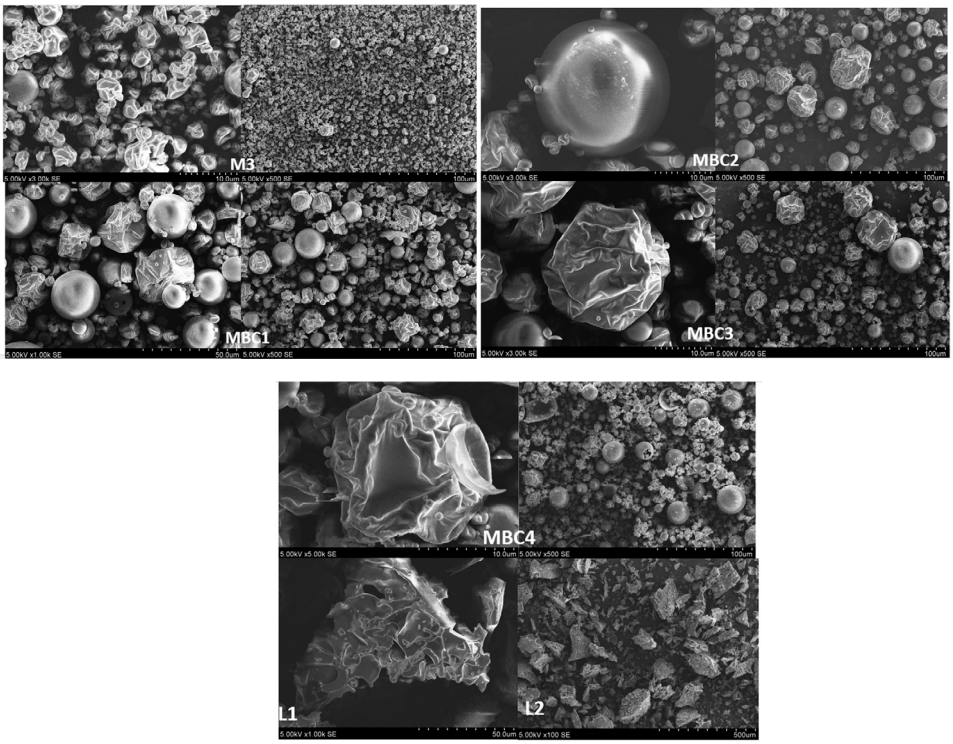

Figure 9. Microcapsules were observed using scanning electron microscopy (SEM) to capture their morphology at 100×, 500×, 1000×, 3000×, and 5000× magnifications. M3 (MD 10%, SK 10%); MBC1 (MD 13%, β-CD 5.8%, CMC 1.2%); MBC2 (MD 15%, β-CD 4.1%, CMC 0.9%); MBC3 (MD 17%, β-CD 2.5%, CMC 0.5%); MBC4 (MD 10%, SK 9%, β-CD 1%). L1 (MD 13%, β-CD 5.8%, CMC 1.2%); L2 (MD 15%, β-CD 4.1%, CMC 0.9%).

SEM images of M3 show semi-spherical microcapsules with a wrinkled surface, likely due to the combination of maltodextrin and skim milk. This texture could influence the microcapsules' release profile and surface area, potentially enhancing their interaction with the environment. MBC1 (MD 13%, β-CD 5.8%, CMC 1.2%) combines smooth and wrinkled particles with a softer surface due to the higher β-CD content. MBC2 (MD 15%, β-CD 4.1%, CMC 0.9%) shows fewer wrinkles and a more uniform surface with increased MD and decreased β-CD and CMC content compared to MBC1. The MBC3 (MD 17%, β-CD 2.5%, CMC 0.5%) sample has the most uniform and smoothest surface morphology due to the high MD content. MBC4 (MD 10%, SK 9%, β-CD 1%), with a high proportion of skim milk, produces a unique texture, possibly showing a balance between smooth and wrinkled surfaces.

L1 (MD 13%, β-CD 5.8%, CMC 1.2%) and L2 (MD 15%, β-CD 4.1%, CMC 0.9%) samples were lyophilized, and they exhibited a more porous and irregular structure than those associated with spray-drying. SEM images provide crucial information on how the different wall material ratios influence the physical structure of the microcapsules, which in

turn affects their functional properties. The micrographs reveal any agglomerations, cracks, or inconsistencies within the microcapsules that could impact their effectiveness.

4. Conclusions

In this investigation, the ethanolic extract of *Citrus x paradisi* L. was subjected to microencapsulation through spray drying and freeze-drying techniques, employing combinations of skim milk, maltodextrin, carboxymethylcellulose, and beta-cyclodextrin as wall materials. The chosen matrix components were necessary for forming microparticles and encapsulating the ethanolic extract, with each constituent playing a distinct role in the microcapsules' structural and release properties.

Maltodextrin (MD), as a polysaccharide, was essential in the microcapsule's structural formation, providing a protective matrix for the active compounds. Beta-cyclodextrin (β-CD), a cyclic oligosaccharide, was used to enhance the solubility and stability of hydrophobic molecules by forming inclusion complexes. This characteristic of β-CD was beneficial in improving the bioavailability of the active compounds. Carboxymethylcellulose (CMC), with its hydrophilic properties, acted as a release modulator within the microcapsules. The formation of hydrogels by CMC was essential in controlling the release rate of the encapsulated actives in the intestinal tract.

The comparative analysis of spray-dried and freeze-dried samples showed notable differences in morphologies and encapsulation efficiencies. In the spray-dried methodology, sample ID MBC3 (MD 17%, β-CD 2.5%, CMC 0.5%) showed the best results. It was characterized by its wettability time (1170 s), a higher encapsulation efficacy EE% (91.41%), a better solubility (60.21%), and lower moisture content (5.1 $\pm$ 0.255%), which can be attributed to the higher maltodextrin content, indicating a solid structure conducive to prolonged release. Meanwhile, the freeze-dried sample ID L1 (MD 13%, β-CD 5.8%, CMC 1.2%) displayed a quick weldability (132.6 s), rapid solubility profile (61.58%), low moisture content (5.07%) and high EE% (78.38%), which may result from the lyophilization process and the wall material composition, which facilitated a more porous structure.

This research contributes to the field of pharmaceutical sciences by illustrating the criticality analysis of wall material selection and process optimization in microencapsulation. It highlights the necessity for a multidisciplinary approach which considers material science and pharmacokinetics in order to develop advanced delivery systems for active bioactive compounds.

Author Contributions: Conceptualization, J.B., J.S., and L.P; investigation, J.S. and L.P.; resources, J.B.; writing—production of the initial draft, J.S.; writing—review and editing, J.B. and J.S.; visualization, J.S.; supervision, J.B. All authors have read and agreed to the published version of the manuscript.

Funding: This research received no external funding.

Institutional Review Board Statement: Not applicable.

Informed Consent Statement: Not applicable.

Data Availability Statement: Data is contained within the article.

Acknowledgments: The authors express their sincere appreciation to the Open Access Centre for Advanced Pharmaceutical and Health Technologies at the Lithuanian University of Health Sciences and the Lithuanian Research Centre. These institutions provided us with access to their state-of-the-art research infrastructure, which was essential for conducting this study. Their support facilitated our experimental efforts and significantly contributed to advancing our research objectives. We are deeply grateful for the opportunity to utilize such exceptional resources and collaborate within these esteemed scientific communities.

Conflicts of Interest: The authors declare no conflicts of interest.

References

1. Stabrauskiene, J.; Marksa, M.; Ivanauskas, L.; Bernatoniene, J. Optimization of Naringin and Naringenin Extraction from Citrus × paradisi L. Using Hydrolysis and Excipients as Adsorbent. *Pharmaceutics* **2022**, *14*, 890. [CrossRef] [PubMed]
2. Stabrauskiene, J.; Kopustinskiene, D.M.; Lazauskas, R.; Bernatoniene, J. Naringin and Naringenin: Their Mechanisms of Action and the Potential Anticancer Activities. *Biomedicines* **2022**, *10*, 1686. [CrossRef] [PubMed]
3. Stabrauskiene, J.; Marksa, M.; Ivanauskas, L.; Viskelis, P.; Viskelis, J.; Bernatoniene, J. Citrus × paradisi L. Fruit Waste: The Impact of Eco-Friendly Extraction Techniques on the Phytochemical and Antioxidant Potential. *Nutrients* **2023**, *15*, 1276. [CrossRef] [PubMed]
4. Jiang, H.; Zhang, M.; Lin, X.; Zheng, X.; Qi, H.; Chen, J.; Zeng, X.; Bai, W.; Xiao, G. Biological Activities and Solubilization Methodologies of Naringin. *Foods* **2023**, *12*, 2327. [CrossRef] [PubMed]
5. Ravetti, S.; Garro, A.G.; Gaitán, A.; Murature, M.; Galiano, M.; Brignone, S.G.; Palma, S.D. Naringin: Nanotechnological Strategies for Potential Pharmaceutical Applications. *Pharmaceutics* **2023**, *15*, 863. [CrossRef] [PubMed]
6. Pudziuvelyte, L.; Marksa, M.; Jakstas, V.; Ivanauskas, L.; Kopustinskiene, D.M.; Bernatoniene, J. Microencapsulation of Elsholtzia ciliata Herb Ethanolic Extract by Spray-Drying: Impact of Resistant-Maltodextrin Complemented with Sodium Caseinate, Skim Milk, and Beta-Cyclodextrin on the Quality of Spray-Dried Powders. *Molecules* **2019**, *24*, 1461. [CrossRef] [PubMed]
7. Binesh, N.; Babaloo, H.; Farhadian, N. Chapter 14—Microencapsulation: Spray drying. In *Principles of Biomaterials Encapsulation: Volume One*; Sefat, F., Farzi, G., Mozafari, M., Eds.; Woodhead Publishing: Sawston, UK, 2023; Volume 1, pp. 271–296. ISBN 978-0-323-85947-9.
8. Mehta, N.; Kumar, P.; Verma, A.K.; Umaraw, P.; Kumar, Y.; Malav, O.P.; Sazili, A.Q.; Domínguez, R.; Lorenzo, J.M. Microencapsulation as a Noble Technique for the Application of Bioactive Compounds in the Food Industry: A Comprehensive Review. *Appl. Sci.* **2022**, *12*, 1424. [CrossRef]
9. Poshadri, A.; Kuna, A. Microencapsulation technology: A review. *J. Res. ANGRAU* **2010**, *38*, 86–102.
10. Lukova, P.; Katsarov, P.; Pilicheva, B. Application of Starch, Cellulose, and Their Derivatives in the Development of Microparticle Drug-Delivery Systems. *Polymers* **2023**, *15*, 3615. [CrossRef]
11. Safeer Abbas, M.; Afzaal, M.; Saeed, F.; Asghar, A.; Jianfeng, L.; Ahmad, A.; Ullah, Q.; Elahi, S.; Ateeq, H.; Shah, Y.A.; et al. Probiotic viability as affected by encapsulation materials: Recent updates and perspectives. *Int. J. Food Prop.* **2023**, *26*, 1324–1350. [CrossRef]
12. Garg, A.; Chhipa, K.; Kumar, L. MICROENCAPSULATION. Available online: https://www.jetir.org/papers/JETIR2404766.pdf (accessed on 1 May 2024).
13. Sánchez-Osorno, D.M.; López-Jaramillo, M.C.; Caicedo Paz, A.V.; Villa, A.L.; Peresin, M.S.; Martínez-Galán, J.P. Recent Advances in the Microencapsulation of Essential Oils, Lipids, and Compound Lipids through Spray Drying: A Review. *Pharmaceutics* **2023**, *15*, 1490. [CrossRef] [PubMed]
14. Lu, Y.; Cheng, D.; Niu, B.; Wang, X.; Wu, X.; Wang, A. Properties of Poly (Lactic-co-Glycolic Acid) and Progress of Poly (Lactic-co-Glycolic Acid)-Based Biodegradable Materials in Biomedical Research. *Pharmaceuticals* **2023**, *16*, 454. [CrossRef] [PubMed]
15. Da Silva Júnior, M.E.; Araújo, M.V.R.L.; Martins, A.C.S.; Dos Santos Lima, M.; Da Silva, F.L.H.; Converti, A.; Maciel, M.I.S. Microencapsulation by spray-drying and freeze-drying of extract of phenolic compounds obtained from ciriguela peel. *Sci. Rep.* **2023**, *13*, 15222. [CrossRef] [PubMed]
16. Shirsath, P.R.; Khandre, R.A. A Review: Microencapsulation. *Int. J. Creat. Res. Thoughts (IJCRT)* **2022**, *10*, 2320–2882.
17. Mohammed, N.K.; Tan, C.P.; Manap, Y.A.; Muhialdin, B.J.; Hussin, A.S.M. Spray Drying for the Encapsulation of Oils—A Review. *Molecules* **2020**, *25*, 3873. [CrossRef]
18. Gullifa, G.; Risoluti, R.; Mazzoni, C.; Barone, L.; Papa, E.; Battistini, A.; Martin Fraguas, R.; Materazzi, S. Microencapsulation by a Spray Drying Approach to Produce Innovative Probiotics-Based Products Extending the Shelf-Life in Non-Refrigerated Conditions. *Molecules* **2023**, *28*, 860. [CrossRef]
19. Kandansamy, K.; Somasundaram, P.D. Microencapsulation of Colors by Spray Drying—A Review. *Int. J. Food Eng.* **2012**, *18*. [CrossRef]
20. Sarabandi, K.; Tamjidi, F.; Akbarbaglu, Z.; Samborska, K.; Gharehbeglou, P.; Kharazmi, M.S.; Jafari, S.M. Modification of Whey Proteins by Sonication and Hydrolysis for the Emulsification and Spray Drying Encapsulation of Grape Seed Oil. *Pharmaceutics* **2022**, *14*, 2434. [CrossRef]
21. Lengyel, M.; Kállai-Szabó, N.; Antal, V.; Laki, A.J.; Antal, I. Microparticles, Microspheres, and Microcapsules for Advanced Drug Delivery. *Sci. Pharm.* **2019**, *87*, 20. [CrossRef]
22. Saftić Martinović, L.; Birkic, N.; Miletić, V.; Antolović, R.; Štanfel, D.; Wittine, K. Antioxidant Activity, Stability in Aqueous Medium and Molecular Docking/Dynamics Study of 6-Amino- and N-Methyl-6-amino-L-ascorbic Acid. *Int. J. Mol. Sci.* **2023**, *24*, 1410. [CrossRef]
23. Aiassa, V.; Garnero, C.; Zoppi, A.; Longhi, M.R. Cyclodextrins and Their Derivatives as Drug Stability Modifiers. *Pharmaceuticals* **2023**, *16*, 1074. [CrossRef]
24. Igual, M.; Cebadera, L.; Cámara, R.M.; Agudelo, C.; Martínez-Navarrete, N.; Cámara, M. Novel Ingredients Based on Grapefruit Freeze-Dried Formulations: Nutritional and Bioactive Value. *Foods* **2019**, *8*, 506. [CrossRef] [PubMed]

25. Pudziuvelyte, L.; Marksa, M.; Sosnowska, K.; Winnicka, K.; Morkuniene, R.; Bernatoniene, J. Freeze-Drying Technique for Microencapsulation of Elsholtzia ciliata Ethanolic Extract Using Different Coating Materials. *Molecules* **2020**, *25*, 2237. [CrossRef] [PubMed]
26. Álvarez-Castillo, E.; Bengoechea, C.; Felix, M.; Guerrero, A. Freeze-Drying versus Heat-Drying: Effect on Protein-Based Superabsorbent Material. *Processes* **2021**, *9*, 1076. [CrossRef]
27. Kubbutat, P.; Tauchnitz, A.; Kulozik, U. Water Vapor Pathways during Freeze-Drying of Foamed Product Matrices Stabilized by Maltodextrin at Different Concentrations. *Processes* **2020**, *8*, 1463. [CrossRef]
28. Silvestro, I.; Sergi, R.; Scotto D'Abusco, A.; Mariano, A.; Martinelli, A.; Piozzi, A.; Francolini, I. Chitosan scaffolds with enhanced mechanical strength and elastic response by combination of freeze gelation, photo-crosslinking and freeze-drying. *Carbohydr. Polym.* **2021**, *267*, 118156. [CrossRef]
29. Brougham, C.M.; Levingstone, T.J.; Shen, N.; Cooney, G.M.; Jockenhoevel, S.; Flanagan, T.C.; O'Brien, F.J. Freeze-Drying as a Novel Biofabrication Method for Achieving a Controlled Microarchitecture within Large, Complex Natural Biomaterial Scaffolds. *Adv. Healthc. Mater.* **2017**, *6*, 1700598. [CrossRef] [PubMed]
30. Thuong Nhan, N.P.; Tan Thanh, V.; Huynh Cang, M.; Lam, T.D.; Cam Huong, N.; Hong Nhan, L.T.; Thanh Truc, T.; Tran, Q.T.; Bach, L.G. Microencapsulation of Lemongrass (*Cymbopogon citratus*) Essential Oil Via Spray Drying: Effects of Feed Emulsion Parameters. *Processes* **2020**, *8*, 40. [CrossRef]
31. Zhang, Q.; Chen, Y.; Geng, F.; Shen, X. Characterization of Spray-Dried Microcapsules of Paprika Oleoresin Induced by Ultrasound and High-Pressure Homogenization: Physicochemical Properties and Storage Stability. *Molecules* **2023**, *28*, 7075. [CrossRef]
32. Wang, Y.; Ghosh, S.; Nickerson, M.T. Microencapsulation of Flaxseed Oil by Lentil Protein Isolate-κ-Carrageenan and -ι-Carrageenan Based Wall Materials through Spray and Freeze Drying. *Molecules* **2022**, *27*, 3195. [CrossRef]
33. Tomsone, L.; Galoburda, R.; Kruma, Z.; Durrieu, V.; Cinkmanis, I. Microencapsulation of Horseradish (*Armoracia rusticana* L.) Juice Using Spray-Drying. *Foods* **2020**, *9*, 1332. [CrossRef] [PubMed]
34. Ricci, A.; Arboleda Mejia, J.A.; Versari, A.; Chiarello, E.; Bordoni, A.; Parpinello, G.P. Microencapsulation of polyphenolic compounds recovered from red wine lees: Process optimization and nutraceutical study. *Food Bioprod. Process.* **2022**, *132*, 1–12. [CrossRef]
35. Díaz-Montes, E. Wall Materials for Encapsulating Bioactive Compounds via Spray-Drying: A Review. *Polymers* **2023**, *15*, 2659. [CrossRef] [PubMed]
36. Emadzadeh, B.; Ghorani, B.; Naji-Tabasi, S.; Charpashlo, E.; Molaveisi, M. Fate of β-cyclodextrin-sugar beet pectin microcapsules containing garlic essential oil in an acidic food beverage. *Food Biosci.* **2021**, *42*, 101029. [CrossRef]
37. Mohammadalinejhad, S.; Kurek, M.A. Microencapsulation of Anthocyanins—Critical Review of Techniques and Wall Materials. *Appl. Sci.* **2021**, *11*, 3936. [CrossRef]
38. Li, Y.; Zhang, H.; Zhao, Y.; Lv, H.; Liu, K. Encapsulation and Characterization of Proanthocyanidin Microcapsules by Sodium Alginate and Carboxymethyl Cellulose. *Foods* **2024**, *13*, 740. [CrossRef] [PubMed]
39. Afshari, K.; Javanmard Dakheli, M.; Ramezan, Y.; Bassiri, A.; Ahmadi Chenarbon, H. Physicochemical and control releasing properties of date pit (*Phoenix dactylifera* L.) phenolic compounds microencapsulated through fluidized-bed method. *Food Sci. Nutr.* **2023**, *11*, 1367–1382. [CrossRef] [PubMed]
40. Xiao, Z.; Xia, J.; Zhao, Q.; Niu, Y.; Zhao, D. Maltodextrin as wall material for microcapsules: A review. *Carbohydr. Polym.* **2022**, *298*, 120113. [CrossRef]

Paper 5

Title: Comparative *In Vitro* Evaluation of Buccal Films, Microcapsules, and Liposomal Systems for Naringin and *Citrus* × *paradisi* L. Peel Extract: Effects of Encapsulation Strategy and Compound Origin on Release Profiles

Authors: Jolita Stabrauskiene, Mindaugas Marksa and Jurga Bernatoniene. Pharmaceutics 2025, 17, 1311.

pharmaceutics

MDPI

Article

Comparative In Vitro Evaluation of Buccal Films, Microcapsules, and Liposomal Systems for Naringin and *Citrus* × *paradisi* L. Peel Extract: Effects of Encapsulation Strategy and Compound Origin on Release Profiles

Jolita Stabrauskiene [1,2], Mindaugas Marksa [3] and Jurga Bernatoniene [1,2,*]

[1] Department of Drug Technology and Social Pharmacy, Lithuanian University of Health Sciences, LT-50161 Kaunas, Lithuania; jolita.stabrauskiene@lsmu.lt
[2] Institute of Pharmaceutical Technologies, Lithuanian University of Health Sciences, LT-50161 Kaunas, Lithuania
[3] Department of Analytical and Toxicological Chemistry, Lithuanian University of Health Sciences, LT-50161 Kaunas, Lithuania; mindaugas.marksa@lsmuni.lt
* Correspondence: jurga.bernatoniene@lsmuni.lt; Tel.: +370-6006-3349

Abstract

Background/Objectives: *Citrus* × *paradisi* Macfad., Rutaceae. peel is a rich source of naringin (NR), but its poor solubility and low bioavailability limit applications. This study aimed to improve NR delivery by comparing microencapsulation, liposomal microencapsulation, and buccal films containing either pure NR or grapefruit peel extract. **Methods**: Four spray-dried powder formulations—spray-dried NR (NS), liposomal NR (NLS), spray-dried extract (ES), and liposomal extract (ELS)—were produced using maltodextrin, β-cyclodextrin, and HPMC as wall materials. Buccal films (EP1, EP2, NP1, NP2) were prepared via solvent casting with HPMC, alginate (ALG), or polyvinyl alcohol (PVA). All samples were evaluated for solubility, moisture content, mucoadhesion, and in vitro release under simulated gastric, intestinal, and salivary conditions. **Results**: NR powders had the highest absolute solubility (306.42 ± 10.34 μg/mL), whereas ELS showed the lowest due to low loading. However, relative to theoretical NR content, ELS achieved the highest dissolution efficiency (55.3%), followed by NLS (42.7%), outperforming NS (5.6%) and ES (91.8%) in sustained release potential. Dual encapsulation (NLS, ELS) slowed gastric release and maintained intestinal delivery, while non-liposomal powders released rapidly. In buccal films, NP2 (NR + PVA) showed the highest release (69.97 ± 3.01 μg/mL; 40.9% efficiency) and strongest mucoadhesion (0.47 N·s). Extract-based films had lower absolute NR release but higher relative efficiency to content, likely due to co-extracted compounds enhancing wettability and matrix erosion. **Conclusions**: Liposomal microencapsulation improves relative dissolution efficiency and sustains intestinal release, while PVA-based buccal films enhance both release and mucoadhesion. Polymer choice and active ingredient composition are critical for optimising oral delivery of NR. These results demonstrate the potential of the proposed systems in the pharmaceutical or dietary supplement field, especially in improving the oral delivery of poorly soluble flavonoids. A graphical summary is included, visually summarising the main formulation strategies and results.

Keywords: naringin; grapefruit peel extract; liposomes; microencapsulation; buccal films; dissolution; mucoadhesion

Academic Editor: Stefania Petralito

Received: 3 September 2025
Revised: 1 October 2025
Accepted: 6 October 2025
Published: 9 October 2025

Citation: Stabrauskiene, J.; Marksa, M.; Bernatoniene, J. Comparative In Vitro Evaluation of Buccal Films, Microcapsules, and Liposomal Systems for Naringin and *Citrus* × *paradisi* L. Peel Extract: Effects of Encapsulation Strategy and Compound Origin on Release Profiles. *Pharmaceutics* **2025**, *17*, 1311. https://doi.org/10.3390/pharmaceutics17101311

1. Introduction

Grapefruit (*Citrus* × *paradisi* Macfad., Rutaceae) by-products have recently attracted growing interest because of their high content of health-promoting phytochemicals. Among these, naringin (NR) and its aglycone naringenin (NAR) are the most important compounds. They are known for their antioxidant, anti-inflammatory, and anticancer properties [1–4]. Beyond naringin, grapefruit peel extract also contains flavonoid glycosides, organic acids, and natural sugars, which exhibit additional antioxidant, antimicrobial, and permeability-enhancing effects, potentially offering synergistic therapeutic or functional benefits in oral delivery systems.

However, both molecules face a common challenge: they are poorly soluble in water and have very low bioavailability in the human body. For example, naringin dissolves only at approximately 38 μg/mL and exhibits less than 5% oral bioavailability, classifying it as a BCS class IV [5–8]. These limitations reduce its effectiveness when used in foods, nutraceuticals, or therapeutic applications.

Different encapsulation technologies are being explored to address these problems. Microencapsulation, typically carried out with carriers such as maltodextrin or β-cyclodextrin, allows better stabilisation of NR and provides controlled release. In our previous work on the encapsulation of *C. paradisi* peel extracts, we compared different carrier compositions. We demonstrated that the combination of maltodextrin, β-cyclodextrin, and carboxymethylcellulose provided the most favourable results, achieving high encapsulation efficiency (>90%), improved solubility, and stable powder characteristics. These findings indicated that polysaccharides and cyclic oligosaccharides act synergistically to stabilise flavonoids and enhance their release properties [9]. Liposomes, which are vesicles formed from phospholipid bilayers, can further increase solubility and protect hydrophobic molecules such as NR [10–13]. Since liposomal dispersions in water are often unstable, they are commonly converted into dry powders through lyophilisation or spray drying. A promising strategy is dual encapsulation, where liposomes are trapped inside carbohydrate-based microcapsules to reduce release in the acidic stomach environment while supporting prolonged release in the intestine. Although this method has not yet been suggested, notable improvements in solubility and stability have been observed when directly applied to naringin [14–16].

Another innovative delivery method is the use of buccal films. These thin, mucoadhesive formulations adhere to the buccal mucosa, allowing drugs to be absorbed directly into the bloodstream and bypassing first-pass metabolism in the liver. Their swelling properties and polymer composition have a significant impact on the rate of release of the active compound. Studies have shown that selecting the polymer matrix can significantly improve the release and absorption profiles [17,18].

Summarising these limitations, it becomes evident that a systematic comparison of different encapsulation strategies is required. Therefore, this study compares three delivery paths for *C. paradisi*. peel extract and pure NR: (i) microencapsulated powder, (ii) spray-dried liposomal powder, and (iii) buccal films. All were evaluated in vitro for solubility, stability, and release under simulated gastric (pH ~1.2), intestinal (pH ~6.8), and artificial saliva (pH ~6.8) conditions.

2. Materials and Methods

Fresh grapefruit peels were collected post-juicing, dried at 60 ± 5 °C, ground, and stored in a dry, dark place. Naringin (≥98% purity) was obtained from Sigma-Aldrich (Buchs, Switzerland). Lipoid S100 and methanol (99%) were sourced from Lipoid GmbH and Carl Roth GmbH, respectively (Germany). Ethanol (96%) was sourced from Vilniaus Degtinė (Vilnius, Lithuania). Purified water was prepared using a Millipore system (Merck, Rahway, NJ, USA). Hydroxypropyl methylcellulose (HPMC, Methocel E5 Premium LV)

was obtained from Dow Chemical Co. (Midland, MI, USA). Sodium alginate (Protanal® LF 10/60, ALG) was sourced from FMC BioPolymer (Philadelphia, PA, USA). Polyvinyl alcohol (PVA) and glycerol (≥99.5%) were obtained from Sigma-Aldrich (St. Louis, MO, USA). Additional reagents for artificial saliva, simulated gastric fluid (SGF), and simulated intestinal fluid (SIF) were sourced from Sigma-Aldrich, Merck, and Farmalabor.

2.1. Preparation of Extract

Dried peel powder was mixed with 50%, 70%, or 90% ethanol (v/v) at a 1:10 (w/v) ratio and subjected to ultrasonic-assisted extraction (38 kHz, 30 min, 50 ± 2 °C). Extracts were cooled, centrifuged (1789× g, 10 min), filtered (0.22 µm PVDF membrane), and stored for further use. The process is demonstrated in Figure 1. The ethanol concentrations used for extraction (50%, 70%, and 90%) were based on our prior optimisation studies, which evaluated the influence of solvent strength on flavonoid yield and formulation compatibility [19,20].

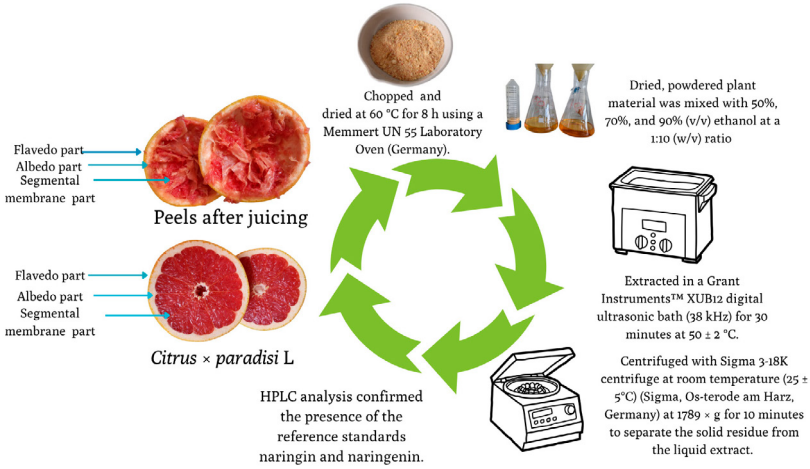

Figure 1. Extraction procedure of bioactive compounds from *C. paradisi* peels, including drying, ethanol extraction, ultrasonic treatment, centrifugation, and HPLC analysis.

Depending on the specific requirements of each formulation and the solubility properties of the active compounds, concentrations of 50%, 70%, and 90% ethanol were selected. For liposomal formulations, 90% ethanol was used to ensure efficient dissolution of the lipid components (Lipoid S100 and cholesterol) together with the active ingredients. For spray-dried formulations, 50% ethanol was chosen due to its favourable interaction with wall materials and its ability to form stable emulsions. For buccal film formulations, 70% ethanol ensured an optimal balance between extract solubility and compatibility with film-forming polymers, such as HPMC, ALG, and PVA, during the solvent casting process.

2.2. HPLC Methodology for the Quantification of Naringin and Naringenin

The study employed a Waters 2695 liquid chromatography system with a photodiode array detector (Waters 996, wavelength range 200–400 nm) to analyse biologically active compounds. The chromatographic separation was achieved using an ACE C18 column (250 mm × 4.6 mm, 5 µm particle size) with a gradient elution method. A total of 10 µL of

each extract was injected and analysed at a wavelength of 280 nm. A mixture of acetonitrile (A) and water (B) was employed as the mobile phase, pumped at a constant flow of 1 mL/min: at 0.0 min, 10% A; at 5 min, 20% A; at 25 min, 40% A; at 30 min, 100% A; at 35 min, 100% A; and returning to 10% A at 36 min. The column temperature was maintained at 25 °C. Peak identification was performed by comparing the UV-vis spectra and retention times of the compounds to those of authentic reference standards (Figure 2). Each sample was analysed in duplicate. A 100 µg/mL solution of naringin and naringenin was dissolved in 70% methanol to serve as the reference standard. From this, a series of six concentrations was prepared to generate calibration curves. Each concentration was injected three times to assess linearity. The calibration equations for naringin and naringenin were derived from plotting their peak areas against their respective concentrations, yielding regression coefficients (R^2) greater than 0.999, indicating excellent linearity. The method's sensitivity was assessed by determining the limit of detection (LOD) and limit of quantitation (LOQ), calculated based on signal-to-noise ratios of 3 and 10, respectively. Intra-day and inter-day precision were evaluated using a standard mixture of naringin and naringenin, with five consecutive injections performed on the same day over four different days. Results were expressed as relative standard deviation (RSD). The study confirmed the retention times and spectra of naringin and naringenin against the prepared extracts. The linearity of the calibration curves was established, with naringin exhibiting a linearity range of 1.166 to 33.343 µg/mL and naringenin from 0.472 to 15.125 µg/mL. Quantification results were reported in µg/g and mg/g dry weight (DW) for naringenin and naringin, respectively [21].

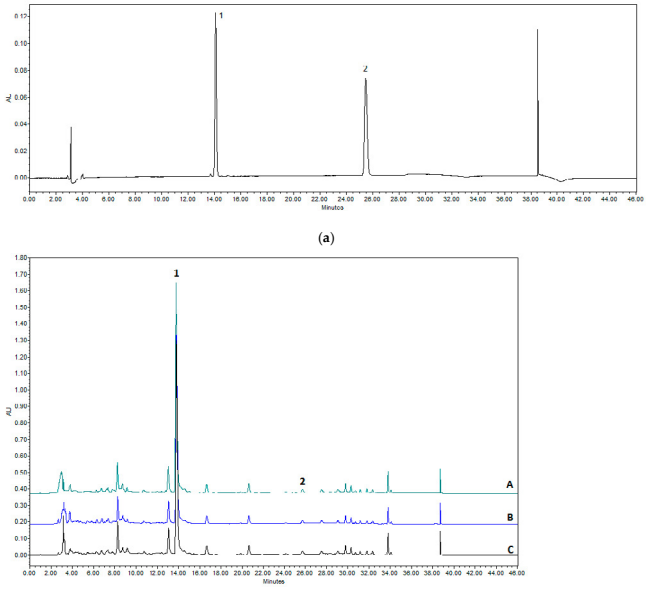

Figure 2. (**a**). Chromatograms of standards detected by HPLC. Peaks identified: 1—naringin; 2—naringenin. (**b**). HPLC chromatogram of the *C. paradisi* peel extract obtained using ethanol as extraction solvent at different concentrations: A—50%, B—70%, and C—90%. Peaks corresponding to naringin—1 and naringenin—2 are indicated. All experiments were conducted in triplicate (n = 3).

2.3. Preparation of C. paradisi Peel Extracts and Naringin-Loaded Liposomes

Liposomes were prepared by ethanol injections followed by probe sonication. Lipoid S100 and cholesterol were dissolved in 10 mL of 90% ethanolic solution containing either grapefruit peel extract or pure NR (10 mg/mL), then injected into the aqueous phase under constant stirring.

Sonication (5 cycles, 1 min on/1 min off, 16 ± 5% power) produced nanoscale vesicles, as represented in Figure 3. Formulations varied in lipid-to-core ratio (1:1 and 2:1) as described in Table 1. Liposomes were prepared according to a modified procedure based on the method reported by San Ang et al. [22].

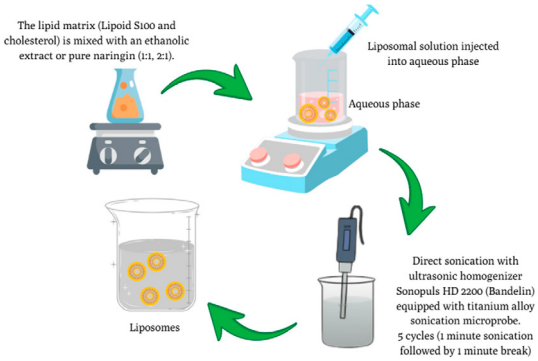

Figure 3. Schematic representation of the liposome preparation process using lipid matrix, aqueous phase injection, and ultrasonic homogenization.

Table 1. The composition of *C. paradisi* peel extract and NR-loaded liposome formulations.

Composition			
Formulation ID *	**Lipoid S100**	**Cholesterol**	**Total Lipid Phase: Extract or Naringin Ratio**
EL1	100 mg	10 mg	1:1
EL2	200 mg	20 mg	2:1
NL1	100 mg	10 mg	1:1
NL2	200 mg	20 mg	2:1

* EL: extract-loaded liposome; NL: NR-loaded liposome. All experiments were conducted in triplicate ($n = 3$).

2.4. Characterisation of Particle Size Distribution and Zeta Potential

The particle size and size distribution of the liposomal formulations were determined using dynamic light scattering (DLS) with a Nano ZS 3600 system (Malvern Instruments, Worcestershire, UK). Measurements provided both the mean hydrodynamic diameter and the polydispersity index (PDI).

Zeta potential was measured on the same instrument in zeta mode. For these measurements, the samples were placed in a dedicated cell equipped with electrodes, which ensured the generation of a stable electric field and improved the precision of the readings. The procedure followed the approach described by Németh et al. [23].

2.5. Spray-Drying Microencapsulation of C. paradisi Peel Extracts and NR Samples

Spray-drying conditions and wall material ratios were chosen based on previously optimised protocols developed in our earlier studies [9]. Based on our previous research, four different samples were prepared for microencapsulation using spray-drying: (1) *C. paradisi*. peel extract (ES), (2) pure NR solution (50 mg/mL) (NS), (3) liposomal *C. paradisi* peel extract (ELS), and (4) liposomal NR solution (10 mg/mL) (NLS).

The encapsulation matrix was prepared by dissolving maltodextrin (MD, 15% *w*/*v*), β-cyclodextrin (β-CD, 2.5% *w*/*v*), and carboxymethylcellulose sodium salt (HPMC, 0.5% *w*/*v*) in purified water. After the complete dissolution, each active ingredient was homogenised with the wall material solution to form stable emulsions.

Spray-drying was carried out using a BÜCHI B-291 Mini Spray-Dryer under the following optimised conditions: inlet temperature of 150 °C, outlet temperature of 98 °C, a flow rate set at 60%, aspiration at 100%, and a pump rate of 12%, as demonstrated in Figure 4. The resulting spray-dried powders were carefully collected and stored at +4–7 °C to preserve their stability and functional properties for further analysis [23,24].

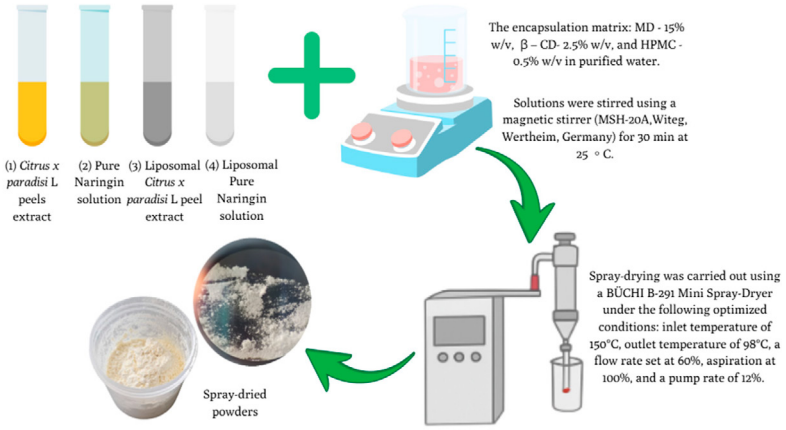

Figure 4. Schematic illustration of the microencapsulation process of different samples using spray-drying technology under optimised conditions. Sample ID: 1—ES, 2—NS, 3—ELS, 4—NLS.

2.6. SEM Analysis of Microcapsules: Morphological Evaluation

The surface morphology of spray-dried microcapsules was evaluated using a Hitachi TM 3000 SEM (Tokyo, Japan) at 100×–6000× magnification and 5 kV accelerating voltage. Samples were mounted on stubs using double-sided tape for imaging [25]. All experiments were conducted in triplicate ($n = 3$)

2.7. Encapsulation Efficiency (EE)

Encapsulation efficiency (EE) of the liposomes was evaluated by centrifuging the formulations at 10,000× *g* for 30 min. The supernatant containing the unencapsulated active compounds was carefully extracted [26]. All experiments were conducted in triplicate ($n = 3$).

The supernatant was analysed using HPLC to quantify the concentration of unencapsulated active compounds. The EE of NR were calculated using the formulation:

$$EE\ (\%) = \frac{QT - Q_{FREE}}{QT} \times 100 \quad (1)$$

QT represents the total active compound added (mg/g), *QFREE* denotes the non-encapsulated fraction in the supernatant (mg/g), and *EE* (%) indicates the encapsulation efficiency in the final powder.

2.8. Characterisation of Spray-Dried Powders

2.8.1. Yield Calculation

The powder yield obtained from the spray-drying process was calculated as the ratio between the total mass of dry powder collected and the total amount of solid raw materials initially present in the feed solution [27].

$$Yield\ (\%) = \frac{Total\ weight\ of\ dry\ powdrer\ collected}{Total\ weight\ of\ row\ materials\ in\ feed\ solution} \times 100 \quad (2)$$

2.8.2. Evaluation of Moisture Content in Spray-Dried Powders

Moisture content was determined using a Kern DBS60-3 moisture analyser (Kern & Sohn GmbH, Balingen, Germany). Approximately 1.0 ± 0.05 g of each sample was uniformly distributed on the weighing plate and analysed in triplicate. The mean value was calculated and expressed as a percentage of moisture content [28]. All experiments were conducted in triplicate (n = 3).

2.8.3. Aqueous Solubility Determination of the Spray-Dried Powders

The theoretical naringin content (mg) was calculated from the known concentration in the formulation and the mass of the powder used (500 mg). The dissolved amount was quantified using HPLC as described above.

The aqueous solubility of the spray-dried powders was determined following a modified equilibrium solubility method [22]. A total of 0.5 g of each powder was dispersed in 30 mL of distilled water in sealed vials. Samples were shaken at 25 °C for 24 h at 120 rpm to reach equilibrium. After incubation, suspensions were centrifuged at 10,000 rpm for 10 min. The supernatants were collected and filtered through a 0.22 µm syringe filter. The concentration of dissolved compounds was determined using HPLC and expressed in µg/mL. All experiments were conducted in triplicate (n = 3).

2.8.4. In Vitro Release Study of NR from Microcapsules and Liposomal Powders

The in vitro release study of the active compound, NR, from microcapsules and liposomal powder formulations was conducted using a Sotax AT7 Smart Dissolution System (SOTAX AG, Aesch, Switzerland). The experimental protocol was based on the previously reported methodology by Kazlauskaitė et al. [29], with minor modifications adapted for the tested formulations. Simulated gastric fluid (SGF, pH 1.2) was prepared in accordance with the European Pharmacopoeia by dissolving 2.0 g of NaCl, 3.2 g of pepsin, and 80 mL of 1 M HCl in distilled water, adjusting the final volume to 1000 mL. Simulated intestinal fluid (SIF) was prepared using 6.8 g of KH_2PO_4, 10 g of pancreatin, and 77.0 mL of 0.2 M NaOH, followed by dilution with distilled water to a final volume of 1000 mL.

Samples were first incubated in SGF for 0–90 min, followed by transfer to SIF for an additional 90–180 min, simulating gastrointestinal transit. Aliquots were collected every 30 min over a total release period of 0–180 min.

All collected samples were filtered through a 0.45 µm membrane filter and subsequently analysed using high-performance liquid chromatography (HPLC) for the quantitative detection of the flavanone naringin. All experiments were conducted in triplicate ($n = 3$).

2.9. Preparation of Buccal Films

Buccal films were obtained via solvent casting. Formulations EP1 and EP2 contained 70% ethanolic grapefruit peel extract, while NP1 and NP2 contained pure NR (50 mg/mL in 70% ethanol).

A 12% (w/v) HPMC solution was prepared using a 70:30 mixture of NR or extract solution (in 70% ethanol) and purified water, ensuring complete polymer dispersion before blending with secondary components. Separately, sodium alginate (2% w/v) for EP1 and NP1, or PVA (2% w/v) for EP2 and NP2, was dissolved in glycerol (4% w/v). Solutions were combined, homogenised, and cast using a ZUA 2000 film applicator (2 mm wet thickness) onto glass plates. Films were dried at 40 °C for 2 h, cut into 3 cm × 2.5 cm strips, sealed in foil pouches, and stored at 22 ± 2 °C [30,31]. The compositions of the prepared buccal film formulations are summarised in Table 2. All processes are demonstrated in Figure 5.

Table 2. Composition of buccal film formulations.

Component	EP1	EP2	NP1	NP2
(HPMC)	12%	12%	12%	12%
(ALG)	2%	–	2%	–
(PVA)	–	2%	–	2%
Glycerol	4%	4%	4%	4%
70% Ethanolic Peel Extract/NR Solution	70%	70%	70%	70%
Purified Water	30%	30%	30%	30%

"–" indicates that the component was not included in the formulation. Sample IDs: E1, E2, N1, N2. All experiments were conducted in triplicate ($n = 3$).

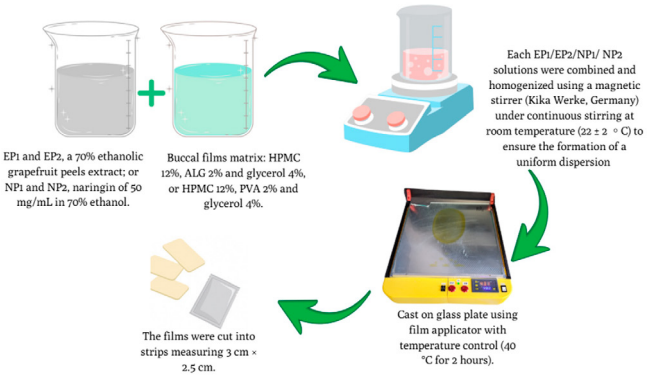

Figure 5. Schematic representation of buccal film preparation using the solvent casting method with naringin (NP1, NP2) or grapefruit peel extract (EP1, EP2), film-forming, drying, and cutting processes. All experiments were conducted in triplicate ($n = 3$).

2.9.1. Texture Analysis of Buccal Films

Film mechanical properties were measured using a TA.XT Plus texture analyser (Stable Micro Systems Ltd., Godalming, UK), based on modified procedures from prior literature [32].

For mucoadhesion, 3 cm × 2.5 cm dry film samples were adhered to a fixed plastic support to determine adhesive strength. A transparent plastic ring with a 1 cm central opening (A/MUC mucoadhesive probe) was aligned over the sample, leaving an exposed circular area. This area was hydrated with 100 µL of artificial saliva (pH 6.8) and allowed to equilibrate for 15 s. A cylindrical P/0.5R probe (slightly smaller diameter than the opening) was then lowered onto the moistened surface under a constant load of 5 N for 60 s. The force required to detach the probe from the film (adhesive strength, in N) was measured. Each test was performed three times under room temperature conditions. All experiments were conducted in triplicate (n = 3).

2.9.2. Buccal Film Moisture Content Determination

Film moisture content (%) was determined by drying to constant weight at 105 °C in an analyser (DBS 60-3, KERN & SOHN GmbH, Balingen, Germany), in triplicate [33,34]. All experiments were conducted in triplicate (n = 3).

2.9.3. In Vitro Release Profile of NR from Buccal Films

The dissolution of mucoadhesive polymeric films (n = 3) was tested in 25 mL of artificial saliva (pH 6.8) at 37 ± 1 °C. Each 3 cm × 2.5 cm film was placed in a Berzelius beaker under static conditions. The time to complete dissolution, with no visible residue, was recorded using a method adapted from Y. Maslii et al. [34].

For NR release studies, 3 cm × 2.5 cm buccal films were placed in 25 mL of artificial saliva at 37 °C under constant stirring. The average film weights were as follows: EP1—108.17 mg, EP2—163.27 mg, NP1—97.64 mg, and NP2—97.72 mg. Aliquots (1 mL) were withdrawn at 5, 10, 15, and 30 min, stored, and analysed by HPLC. Artificial saliva was prepared by dissolving $MgCl_2$ (100 mg/L), $CaCl_2 \cdot 2H_2O$ (220 mg/L), $Na_2HPO_4 \cdot 7H_2O$ (1350 mg/L), KH_2PO_4 (680 mg/L), KCl (750 mg/L), urea (600 mg/L), and NaCl (600 mg/L) in distilled water and adjusting pH to 6.8 [34,35]. All experiments were conducted in triplicate (n = 3).

2.10. Statistical Analysis

All data are presented as mean ± standard deviation (SD) from three independent experiments. Statistical significance ($p < 0.05$) was assessed using one-way ANOVA, with post hoc non-parametric tests (Friedman, Wilcoxon, Mann–Whitney U) where appropriate. Correlation and regression were analysed using Spearman's method. Analyses were performed using SPSS v20, GraphPad Prism 8, and Excel 2021.

3. Results and Discussion

3.1. Evaluation of Flavonoid Content in Hydroalcoholic Peel Extracts of C. paradisi

Quantitative HPLC analysis confirmed that NR was the predominant flavonoid in all hydroalcoholic extracts of *C. paradisi* peel, whereas NAR was only a minor component. The highest NR concentration was obtained in the 50% EtOH extract (15.62 mg/g), followed by the 90% extract (15.40 mg/g) and the 70% extract (14.58 mg/g). In contrast, NAR levels were low and relatively stable (1.41–1.82 µg/g), confirming its limited abundance in grapefruit peel.

These results indicate that solvent concentration in the tested range (50–90% ethanol) did not markedly affect NR yield, as the differences between extracts were within a narrow margin (<1.1 mg/g). Nevertheless, the slight superiority of the 50% EtOH extract suggests

that moderate ethanol content may facilitate better solubilisation of glycosylated flavonoids such as NR.

Importantly, variability between studies is evident: while our extracts contained ~14–16 mg/g naringin, our previous work reported up to 42.04 mg/g [19,20]. This discrepancy is most likely due to natural differences in raw material (ripeness, harvest season, or cultivation conditions) rather than methodological inconsistencies [36].

3.2. Characterisation of Liposomal Formulations: Particle Size, PDI, and Zeta Potential

The physicochemical properties of the liposomal formulations, including particle size, polydispersity index (PDI), and zeta potential, are summarised in Table 3.

Table 3. Data are presented as mean ± standard deviation ($n = 3$). Letters (a, b, c) indicate statistically significant differences within each column ($p < 0.05$). The formulation ID is listed in Table 1.

Formulation	Size (nm)	PDI	Zeta Potential (mV)
EL1	101.5 ± 5.08 a	0.362 ± 0.018 c	−17.5 ± 0.88 b
EL2	93.93 ± 4.70 b	0.144 ± 0.007 a	−20.3 ± 1.02 bc
NL1	98.57 ± 4.93 ab	0.225 ± 0.011 b	−10.4 ± 0.52 a
NL2	96.96 ± 4.85 ab	0.151 ± 0.017 c	−25.8 ± 1.29 c

The particle size of the liposomes ranged from 93.93 ± 4.70 nm to 101.5 ± 5.08 nm, placing all formulations within the nanoscale range, which is favourable for biomedical applications such as drug delivery [37]. EL2 had the smallest particle size (93.93 ± 4.70 nm), which was significantly smaller than that of EL1 (101.5 ± 5.08 nm, $p < 0.05$). NL1 and NL2 showed intermediate sizes with no statistically significant difference from the extract-based systems EL1 or EL2. These findings suggest that the 2:1 lipid-to-core ratio promoted smaller vesicle formation, consistent with previous reports that higher lipid concentrations enhance bilayer stability and reduce vesicle size [38]. NL2 (96.96 ± 4.85 nm), which had the same lipid composition as EL2 but contained naringin instead of extract, showed slightly smaller particles than NL1 (98.57 ± 4.93 nm), further suggesting that lipid content—not the encapsulated compound—was the main factor causing size reduction [39,40].

PDI values ranged from 0.144 to 0.362. EL2 had the lowest PDI (0.144 ± 0.007), indicating a highly uniform particle size distribution. EL1 and NL1 had significantly higher PDI values, suggesting greater heterogeneity. Higher lipid content in lipid nanoparticles likely improves homogeneity by stabilising vesicle formation. This stabilisation is due to the ability of lipids to interact with each other and with other components of lipid nanoparticles, such as cholesterol, which promotes a more uniform structure and prevents aggregation or phase separation [41].

Zeta potential ranged from −10.4 mV (NL1) to −25.8 mV (NL2). NL2 showed the most negative value (−25.8 ± 1.29 mV), indicating superior electrostatic stability and reduced risk of aggregation. NL1 had the least negative zeta potential (−10.4 ± 0.52 mV), while EL1 and EL2 were intermediate. Similar correlations between increased lipid content and more negative zeta potential have been found by Németh et al. [23], suggesting that higher lipid levels enhance the surface charge density of the vesicles. Based on physicochemical evaluation, EL2 and NL2 were selected for further studies. These size values (<120 nm) and zeta potentials below −20 mV suggest good colloidal stability and favourable biological behaviour, potentially enhancing mucosal permeation and systemic absorption after oral administration [42,43].

3.3. *Characterisation of Spray-Dried Microcapsules and Spray-Dried Liposomes*

3.3.1. Powder Yield, Moisture Content, and Encapsulation Efficiency

The spray-drying process produced powders with yields ranging from 36.7% to 43.0% (Table 4).

Table 4. Powder yield, moisture content, encapsulation efficiency (EE%) and aqueous solubility determination of different spray-dried formulations.

Sample ID	Powder Yield (%)	Moisture Content (%)	Encapsulation Efficiency (EE) (%)	Solubility NR (µg/mL)
ES	43.00 ± 2.15	4.12 ± 0.206	90.91 ± 4.54	138.80 ± 4.25 *
ELS	41.05 ± 1.60	3.81 ± 0.19	99.36 ± 4.96 *	17.36 ± 1.01
NS	36.70 ± 1.83	4.21 ± 0.21	81.08 ± 4.05	306.42 ± 10.34 *
NLS	38.15 ± 1.91	5.58 ± 0.279 *	94.60 ± 4.73 *	93.32 ± 6.01

Data are presented as mean ± standard deviation ($n = 3$). * Columns indicate statistically significant differences between groups ($p < 0.05$). Sample ID explanations: ES—Extract without liposomes (spray-dried); ELS—Extract-loaded liposomal powder; NS—Naringin without liposomes (spray-dried); NLS—Naringin-loaded liposomal powder.

Extract-based powders (ES, ELS) yielded higher amounts (41–43%) than NR-based powders (NS, NLS; 36–38%, $p < 0.05$). This difference likely reflects the higher solid content and greater compatibility of the natural extract with the carrier, which promotes droplet stability and efficient solvent removal during the drying process. Similar effects have been observed in studies comparing plant extracts with pure compounds in capsule manufacturing processes [44]. Moreover, liposomal formulations (ELS and NLS) yielded slightly lower results compared to non-liposomal formulations. This reduction is likely due to the additional lipid phases, which can affect atomization and increase wall deposition during the spray drying process. Similar observations have been reported in previous studies, where lipid-rich formulations reduced powder recovery due to nozzle clogging and increased wall deposition [45,46]. These findings align with reports that high fat content can adversely affect the retention of bioactive compounds and the overall efficiency of encapsulation processes [47].

Moisture content was below the 6% stability threshold for all samples [27]. NLS had the highest residual moisture (5.58 ± 0.279%, $p < 0.05$). This result can be explained by the interaction between crystalline NR and the lipid bilayer, which may prevent the complete removal of bound water during the drying process. Cegledi et al. [48] published a similar study on flavonoids and lipids, noting that a possible interaction between polyphenols and lipids may increase the residual moisture content.

3.3.2. Encapsulation Efficiency

Encapsulation efficiency (EE) showed apparent differences between the tested systems, ranging from 81.08% for the spray-dried NR sample (NS) to 99.36% for the extract-based liposomal powder (ELS). In general, liposomal systems (ELS, NLS) performed better than non-liposomal ones, supporting the well-known function of phospholipid bilayers in retaining both hydrophilic and lipophilic compounds within the carrier. The exceptionally high EE observed for ELS (99.36 ± 4.96%) suggests that the presence of multiple extract components may stabilise the liposomal structure and enhance the retention of NR during spray-drying. This result aligns with previous reports that complex plant matrices often interact more strongly with carrier materials than single, pure compounds, leading to improved entrapment and stability. The lower encapsulation efficiency observed for crystalline NR could also be attributed to partial precipitation or phase separation during

spray drying, as previously observed in similar flavonoid systems where crystalline nature interfered with uniform entrapment [47,49,50].

3.3.3. Solubility and Dissolution Efficiency

The aqueous solubility of NR was evaluated by measuring the concentration of the dissolved compound in 30 mL of distilled water from 500 mg of each spray-dried powder formulation. The results are summarised in Table 4.

The literature reports a wide range of solubility data for NR, ranging from 30–40 µg/mL under standard experimental conditions to a theoretical solubility of 0.5 g/L (500 µg/mL) at 20 °C and up to 1 mg/mL at 40 °C, confirming the significant influence of temperature [7]. The highest solubility was observed for the spray-dried pure NR formulation (NS), reaching 306.42 ± 10.34 µg/mL, nearly tenfold higher than the reported reference value. The extract-based microencapsulated powder (ES) also showed a significantly higher solubility at 138.80 ± 4.25 µg/mL. The solubility of the liposomal naringin formulation (NLS) reached 93.32 ± 6.01 µg/mL, more than twice the solubility of pure crystalline naringin. Meanwhile, liposomal grapefruit peel extract powder (ELS) had the lowest solubility among all tested samples—17.36 ± 1.01 µg/mL.

The increasing solubility observed in NS, ES, and NLS formulations can be attributed to the spray-drying process, combined with the use of appropriate carrier materials, which enhance wettability, reduce particle crystallinity, and increase surface area. Meanwhile, the low solubility of the ELS formulation, despite its high encapsulation efficiency (99.36 ± 4.96%), can be attributed to several factors. First, the initial amount of extract used in the formulation was relatively low, resulting in a limited absolute NR content in the final dried product (0.94 mg of theoretical NR in 500 mg of powder), as shown in Table 5. Second, liposomal encapsulation may limit the release of NR due to entrapment in lipid bilayers, especially when drug loading is low. Lastly, matrix entrapment and reduced wettability of lipid-rich particles may delay the diffusion of NR [48,50].

Table 5. Theoretical and dissolved amounts of naringin (NR) and dissolution efficiency (%) of different spray-dried formulations.

Sample ID	Theoretical Amount of NR (mg)	Dissolved Amount of NR (mg)	Dissolution Efficiency DE (%)
NS	163.82 ± 2.10	9.19 ± 0.31 *	5.6 ± 0.28
NLS	6.55 ± 0.22	2.80 ± 0.18 *	42.7 ± 2.13
ES	4.53 ± 0.15	4.16 ± 0.12	91.8 ± 4.59
ELS	0.94 ± 0.05	0.52 ± 0.03	55.3 ± 2.76

* The difference between the samples' parameters is statistically significant at $p * < 0.05$.

Meanwhile, these findings suggest that while liposomal systems, such as NLS, are valuable for enhancing NR stability and controlling its release, their apparent solubility may be lower than that of non-liposomal powders. This finding is compatible with previous studies, which have shown that liposomal carriers tend to slow down the initial dissolution phase while providing benefits for sustained release and improved absorption in vivo [6,51–53].

3.3.4. Theoretical and Dissolved Amounts of NR

To ensure clarity, dissolution data were expressed both as absolute NR concentrations and as dissolution efficiencies relative to the theoretical drug content. This approach enables a more direct comparison of different formulations, highlighting the higher relative efficiency of dual encapsulation (NLS, ELS) compared to single microencapsulation (NS, ES).

The spray-dried NR powder (NS) contained the highest theoretical amount of NR (163.82 ± 2.10 mg), but released only 9.19 ± 0.31 mg, corresponding to a very low DE of 5.6%.

This low percentage demonstrates the limitations of the solubility and slow dissolution kinetics of crystalline NR, even after encapsulation with maltodextrin, β-cyclodextrin, and HPMC. Similar limitations have been reported for flavonoids encapsulated in carbohydrate-based matrices [51], where strong intermolecular hydrogen bonding, high crystallinity, and limited wettability of the carrier system hinder complete dissolution.

In contrast, the NLS formulation with a much lower drug loading (6.55 ± 0.22 mg) achieved a DE of 42.7 ± 2.13%, indicating more efficient release relative to the available content. This suggests that liposomal encapsulation can increase the relative release efficiency even if the total amount of solute remains lower.

For the extract-based systems, ES achieved the highest DE among all tested samples (91.8 ± 4.59%), releasing nearly all its naringin content (4.16 ± 0.12 mg of 4.53 ± 0.15 mg theoretical). The presence of other phytochemicals and soluble matrix components in the extract may have enhanced solubilisation, acting as natural surfactants and dissolution promoters [49].

Interestingly, ELS, despite having the lowest absolute naringin loading (0.94 ± 0.05 mg), achieved a DE of 55.3 ± 2.76%. While lower than ES, this still demonstrates that more than half of the encapsulated naringin was released into the medium. This suggests that lipid encapsulation, even in low-loading systems, can sustain and control the release rate, reducing burst dissolution and potentially enhancing bioavailability in vivo [5,54].

Overall, the data indicate that while single-layer carbohydrate encapsulation (NS) offers some protection to NR, it does not overcome its intrinsic solubility limitations. Incorporating a lipid phase, as in NLS and ELS, markedly improves relative dissolution efficiency, although achieving high solubility still requires optimising both drug loading and release characteristics.

3.3.5. Scanning Electron Microscopy of Spray-Dried Powder

The surface morphology of the spray-dried formulations was examined by scanning electron microscopy (SEM) at magnifications of ×1000 and ×6000 (Figure 6). All samples were prepared using an encapsulation matrix consisting of maltodextrin (15% w/v), β-cyclodextrin (2.5% w/v), and hydroxypropyl methylcellulose (0.5% w/v). It ensures comparable structural characteristics across the different formulations. The only varying factor was the encapsulated core material: grapefruit peel extract (ES), pure naringin (NS), and their respective liposomal forms (ELS and NLS).

Across all samples, particles displayed predominantly spherical to quasi-spherical morphology, with sizes ranging approximately from 5 to 10 µm. The surfaces were generally smooth but showed typical spray-drying artefacts such as shrinkage, surface indentations, and wrinkles. This morphology is consistent with previously described spray-dried systems that use carbohydrate-based encapsulation materials [54,55].

Liposomal formulations (ELS and NLS) showed more uniform, rounded, and intact particle structures with fewer surface irregularities. This may be attributed to the presence of liposomal carriers in the matrix, which may improve the structural cohesion and film-forming properties of the droplets during drying. Similar improvements in particle integrity for lipid-containing spray-dried systems have been reported in previous microencapsulation studies [55,56].

Overall, the SEM analysis confirmed that despite minor visual differences related to the core material, all spray-dried samples maintained desirable morphological characteristics suitable for stable dry powder delivery systems.

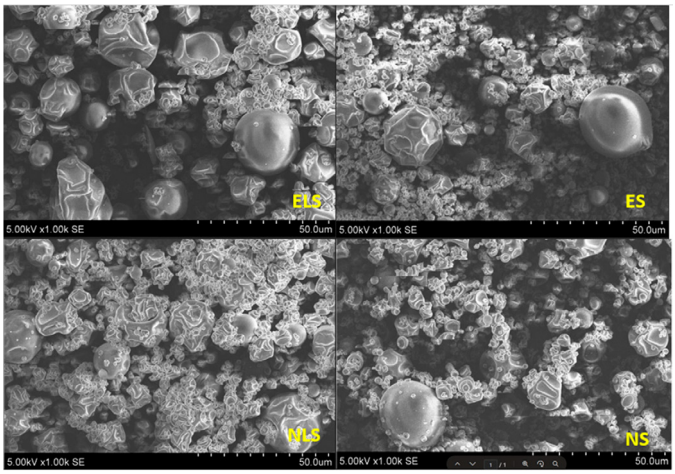

(**a**)

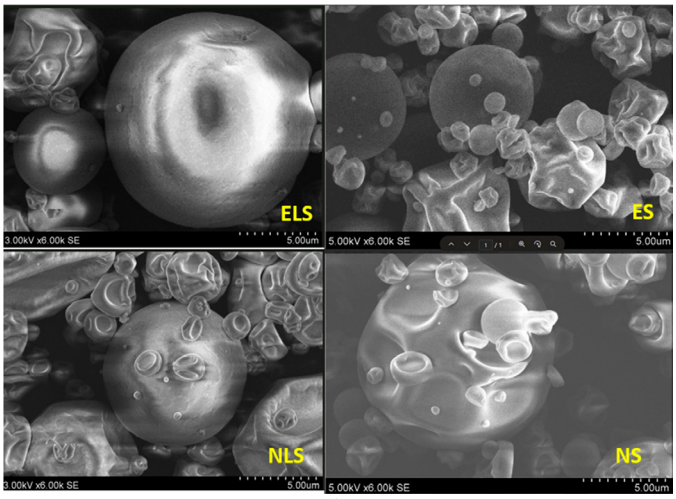

(**b**)

Figure 6. (**a**) SEM images of spray-dried powders (ELS, ES, NLS, NS) at ×1000 magnification. (**b**) SEM images of spray-dried powders (ELS, ES, NLS, NS) at ×6000 magnification. Quantitative image analysis of SEM micrographs (×6000 magnification) revealed a predominant particle size range below 1 µm, with a mean equivalent diameter of 1.45 µm, supporting the uniformity and nanoscale nature of the spray-dried formulations.

3.4. In Vitro Release Profile in Simulated Gastrointestinal Fluids

It was hypothesised that the application of a dual-encapsulation system consisting of liposomal entrapment and microencapsulation using carbohydrate-based wall materials would provide a modified and sustained release of naringin through simulated gastric (SGF,

pH 1.2) and intestinal (SIF, pH ~6.8) fluids compared to single microencapsulation. In total, 500 mg of powder was used in each test, allowing for standardised comparisons between different groups of formulations. Based on the formulation composition, the theoretical NR content in a 500 mg sample was NS—163.82 mg, NLS—6.55 mg, ES—4.53 mg, and ELS—0.94 mg. The result is demonstrated in Figure 7.

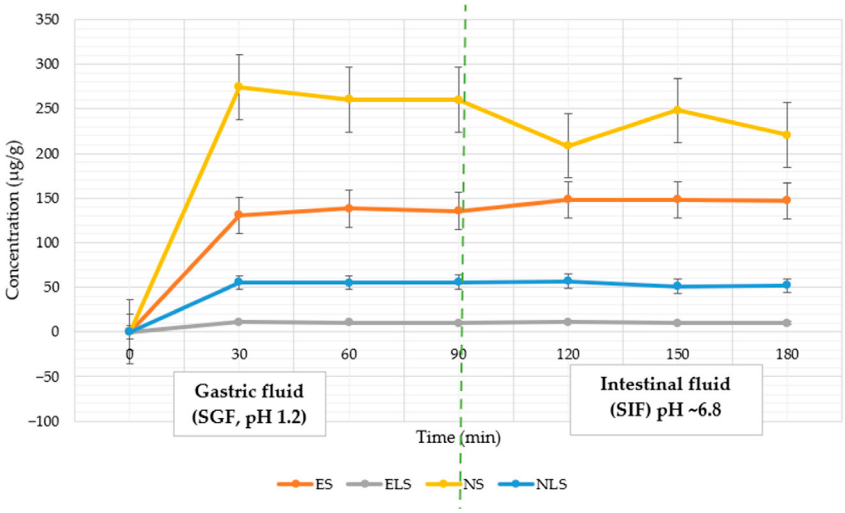

Figure 7. In vitro NR release from spray-dried formulations was evaluated in SGF (pH 1.2) and SIF (pH ~6.8). Results are expressed as mean ± SD (n = 3).

3.4.1. NR Release in Gastric Phase (30–90 min)

The release of NR during the gastric phase varied significantly, indicating the influence of the capsule on the kinetics of release. The non-liposomal formulation (NS) exhibited the highest release, reaching 274.26 ± 2.15 µg/mL after 30 min and 260.07 ± 1.73 µg/mL after 90. Despite this high initial release, the overall dissolution efficiency remained low (~5–6% of the theoretical drug content), likely due to rapid saturation of the medium followed by crystal recrystallisation or acid-induced degradation. This behaviour aligns with earlier findings that crystalline flavonoids display poor aqueous solubility and reduced stability in acidic environments due to strong intermolecular hydrogen bonding and high crystal lattice energy [41].

NLS (dual-encapsulated NR) released 55.36 ± 0.44 µg/mL at 30 min and 55.87 ± 0.33 µg/mL at 90 min, corresponding to ~59–60% of its measured aqueous solubility (93.3 µg/mL). This demonstrates that the lipid bilayer and carbohydrate shell act synergistically to limit drug diffusion under acidic conditions, in agreement with previous studies that have shown rigidified liposomal membranes reduce permeability in SGF [53].

For extract-based systems, ES showed rapid release (130.67 ± 3.21 µg/mL at 30 min; 135.71 ± 2.16 µg/mL at 90 min), corresponding to ~94–98% of theoretical content. The high efficiency (91.8%) is likely facilitated by co-extracted polar compounds, such as flavonoid glycosides and organic acids, acting as natural solubilising agents. In contrast, ELS (dual-encapsulated extract) exhibited the lowest absolute release (9.87–10.85 µg/mL), yet this represented ~32–36% of its theoretical loading, indicating that liposomal encapsulation

successfully retained NR in the gastric phase, allowing for delayed release into the intestinal stage.

3.4.2. NR Release in Intestinal Phase (120–180 min)

When the medium was changed to simulated intestinal fluid (SIF, pH 6.8), the release of NLS slightly increased to 56.89 ± 0.68 μg/mL after 120 min and remained stable at 52.07 ± 0.55 μg/mL after 180 min. It shows a pH-dependent release pattern where liposome destabilisation and capsule matrix hydration at neutral pH promote controlled diffusion.

NS, which excludes most of its content in SGF, showed lower concentrations in SIF (208.53 ± 1.95 μg/mL at 120 min and 220.82 ± 1.65 μg/mL at 180 min). ELS showed a delayed but sustained release, reaching 11.24 ± 0.41 μg/mL at 120 min and 9.94 ± 0.36 μg/mL at 180 min, confirming gut-mediated disintegration of the carbohydrate matrix. Despite the low absolute concentration, this behaviour supports the concept of site-specific delivery. ES peaked at 148.35 ± 2.37 μg/mL at 120 min, with a minor decline to 146.88 ± 2.01 μg/mL at 180 min, indicating passive diffusion without pH-triggered modulation.

These results confirm that dual-encapsulation systems (NLS, ELS) reduce early gastric release and promote sustained intestinal delivery more effectively than single-encapsulation systems (NS, ES). Similar dual-barrier effects—where a hydrophobic lipid bilayer protects against gastric acid and a carbohydrate shell modulates hydration and erosion—have been reported for other polyphenol delivery systems [56]. The synergistic effect of the double capsule is likely due to the lipid bilayer acting as a hydrophobic barrier, limiting diffusion in acidic environments. At the same time, the carbohydrate matrix inhibits hydration and erosion, while promoting pH-dependent release and penetration into the intestine [57].

4. Physical Characterisation of Buccal Films

4.1. Visual Appearance of Buccal Films

Buccal films were successfully prepared using the solvent casting method, and four formulations—EP1, EP2, NP1 and NP2—were developed based on different polymer combinations and active ingredients. Formulations EP1 and EP2 contained grapefruit peel extract prepared with 70% ethanol, while NP1 and NP2 were based on a pure naringin solution (50 mg/mL in 70% ethanol). The polymers used in all formulations were hydroxypropyl methylcellulose (HPMC), EP1 and NP1, which contained sodium alginate (ALG), and EP2 and NP2, which contained polyvinyl alcohol (PVA). All films contained glycerol as a plasticiser.

Visual inspection (Figure 8) revealed that all prepared films were homogeneous, smooth, and free from visible defects, such as air bubbles or cracks, indicating the proper dispersion of the film-forming components. However, apparent differences in transparency and colour were observed between the extract-based (EP1, EP2) and NR-based (NP1, NP2) films. EP1 and EP2 appeared to be light yellow to light brown, which is due to the natural pigmentation of the grapefruit extract, which contains flavonoids and other polyphenolic compounds. It is noteworthy that the surface of EP2 was slightly more transparent and uniform, most likely due to the clarifying properties of the PVA film.

In contrast, NP1 was almost colourless and the most transparent. At the same time, NP2 had a faint yellow tint, possibly due to the interaction of PVA and naringin or due to minor oxidative changes during drying.

These observations suggest that extract-based films typically exhibit higher pigmentation and opacity, which may impact consumer perception and acceptability, while also indicating the presence of multiple bioactive components compared to films containing a single active compound. The choice of secondary polymer (ALG or PVA) also affected the appearance and texture of the film. PVA-based films (EP2, NP2) showed higher visual

smoothness and flexibility, likely due to the better film-forming properties of PVA [58]. Meanwhile, ALG-based films (EP1, NP1) were slightly matte and stiffer, which may affect their mucoadhesive properties.

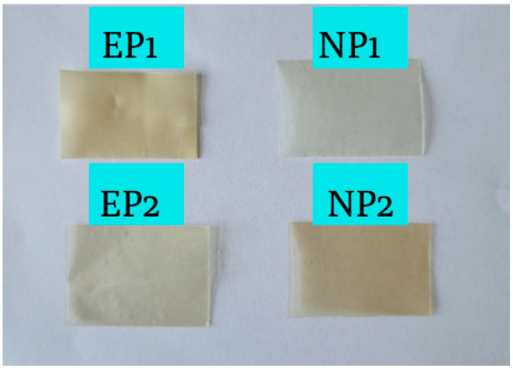

Figure 8. Visual appearance of buccal film samples. EP1 and EP2 (grapefruit peel extract), NP1 and NP2 (pure naringin). EP1/NP1: HPMC + ALG; EP2/NP2: HPMC + PVA.

4.2. Solubility, Moisture Content, and Mucoadhesive Properties of Buccal Films

The in vitro dissolution performance and mucoadhesive behaviour of the developed buccal films were evaluated using artificial saliva (pH 6.8) and texture analysis. Results are presented in Table 6.

Table 6. In vitro dissolution results, moisture content, and mucoadhesive properties of buccal film formulations (mean ± SD, n = 3). Dissolution efficiency is calculated relative to the theoretical maximum drug content in each film.

Sample ID *	In Vitro Dissolution Test (µg/mL)	Dissolution Efficiency (%)	Moisture Content (%)	Peak Force (Adhesiveness N)	Work of Adhesion (N·s)
EP1	27.08 ± 1.42	40.2	13.48 ± 0.45	0.02 ± 0.005	−0.53 ± 0.12
EP2	18.45 ± 1.05	26.6	15.25 ± 0.52	0.07 ± 0.01	−0.25 ± 0.008
NP1	63.99 ± 2.64	37.5	11.46 ± 0.40	0.08 ± 0.01	0.46 ± 0.10
NP2	69.97 ± 3.01	40.9	11.49 ± 0.42	0.09 ± 0.01	0.47 ± 0.11

* Sample ID codes and formulation compositions are listed in Table 2.

The highest release of naringin in artificial saliva was observed for NP2 (69.97 ± 3.01 µg/mL) and NP1 (63.99 ± 2.64 µg/mL), corresponding to dissolution efficiencies of 40.9% and 37.5%, respectively. These results reflect the efficient matrix hydration and polymer swelling, especially in PVA-based films, which promote faster wetting and better dispersion of molecules [59,60].

In contrast, extract-loaded films (EP1, EP2) released lower absolute amounts of NAR (27.08 ± 1.42 µg/mL and 18.45 ± 1.05 µg/mL, respectively), but achieved moderate dissolution efficiencies relative to their drug loading (40.2% and 26.6%, respectively). Notably, EP1 (ALG-based) exceeded EP2, consistent with the literature, which indicates that alginate matrices promote drug release at near-neutral pH through ion-exchange and gradual erosion mechanisms [61,62].

Figure 9 presents these findings along with the complete dissolution time of the films, defined as the time required for the entire buccal film to dissolve fully into artificial saliva.

EP1 exhibited the longest dissolution time (~35 min), suggesting a slower matrix erosion rate despite moderate drug release. EP2 shows the fastest dissolution (~5 min), likely due to PVA's rapid hydration and erosion properties. NP1 and NP2 dissolved more slowly, in 15 and 20 min, respectively, suggesting that variations in polymer structure and the way films absorb water influence the breakdown rate.

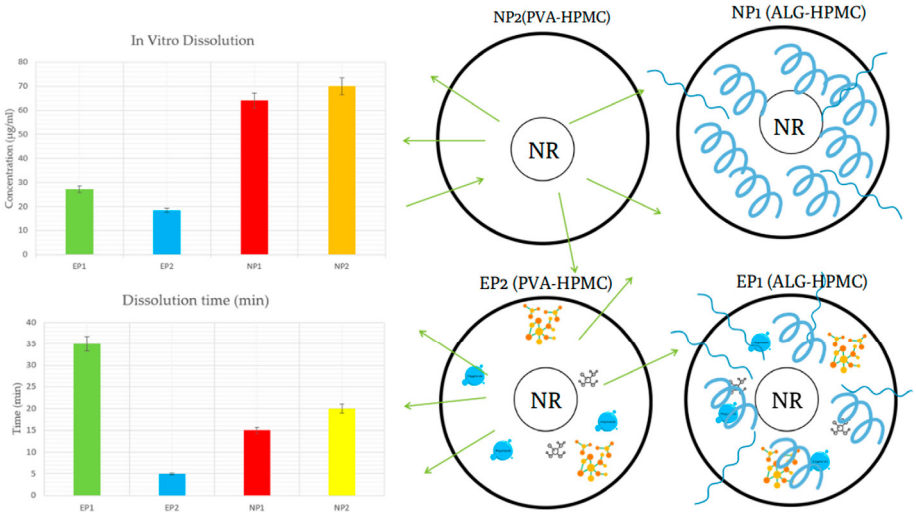

Figure 9. Dissolution time of buccal film formulations (EP1, EP2, NP1, NP2) in artificial saliva (pH 6.8), showing complete film disintegration time. Schematic diagrams illustrate the proposed release mechanisms based on polymer composition and the type of active ingredient. NP2 (PVA–HPMC, pure NR)—rapid hydration and diffusion; NP1 (ALG–HPMC, pure NR)—dense gel matrix restricting diffusion; EP1 (ALG–HPMC, grapefruit peel extract)—improved wettability due to polyphenols, organic acids, pectins, and essential oils; EP2 (PVA–HPMC, grapefruit peel extract)—faster erosion facilitated by co-extracted components but with lower absolute release due to reduced NR loading.

Mucoadhesion testing showed that NP2 exhibited the highest adhesion force (0.09 N) and work of adhesion (0.47 N·s), which can be attributed to PVA's hydrophilicity and ability to form hydrogen bonds with mucin. NP1 also exhibited good adhesion (0.46 N·s), likely due to the ionic interactions of alginate with mucosal surfaces. In contrast, EP1 and EP2 had lower or negative work of adhesion values, suggesting that specific extract components may interfere with optimal polymer–mucin interactions. This may be due to polyphenolic or flavonoid compounds in the extract forming non-specific interactions with mucin or the polymer chains, thus disrupting the formation of stable adhesive networks [60,63]. Additionally, extract constituents may increase interfacial tension or alter surface wettability, reducing effective contact with mucosal surfaces [64]. Interestingly, visual inspection during artificial saliva exposure revealed that all films softened rapidly upon contact with liquid and adhered well to the glass test surface. This suggests that localised swelling and hydration can still promote surface attachment, even when probe-measured mucoadhesion is low.

Moisture content varied among formulations, with extract-based films (EP1, EP2) having higher values (13.48–15.25%), likely due to the hygroscopic nature of sugars and

polyphenols in the extract [65]. In comparison, NP1 and NP2 had lower moisture levels (~11.5%), which showed better mechanical stability.

4.3. In Vitro Release Profile in Artificial Saliva

The release of NR from extract-based buccal films (EP1 and EP2) was assessed in artificial saliva and is presented alongside pure compound films in Table 6 and Figure 10. Dissolution assay evaluated by the actual maximum release of NR from fully dissolved films (Table 6).

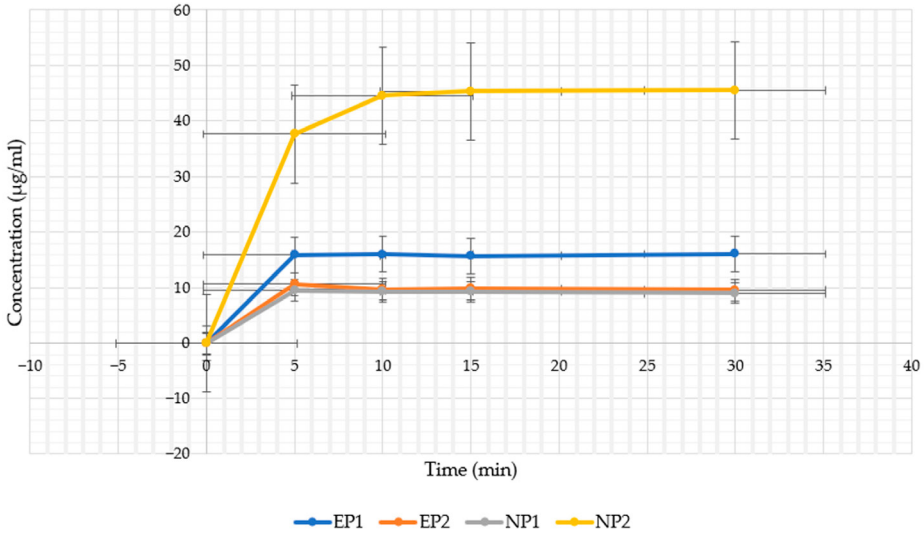

Figure 10. In vitro release profiles of naringin from buccal film formulations (EP1, EP2, NP1, NP2) over 30 min in artificial saliva (pH 6.8). Error bars represent standard deviations (n = 3).

The NP2 formulation exhibited the highest cumulative release, reaching 65.1% within 30 min. These results support the findings of El Sharawy et al. (2017) [65,66] and Elgharbawy et al. (2024) [67], who showed that polyvinyl alcohol (PVA) combined with hydroxypropyl methylcellulose (HPMC) promotes rapid hydration and facilitates diffusion of poorly soluble drugs (e.g., ibuprofen) by forming a highly conductive polymer matrix [31].

The EP1 and EP2 films released approximately 59.4% and 52.1% of their total naringin content, respectively, despite having substantially lower initial loading. This behaviour is consistent with previous reports suggesting that polyphenols and co-extracted phytochemicals can enhance wettability, disrupt polymer–polymer interactions, and accelerate film matrix erosion [68].

In contrast, NP1 showed the lowest release (14.1% in 30 min) despite containing the highest drug content. This reduced release may be related to sodium alginate forming a dense gel barrier in aqueous media, thereby limiting the diffusion of the drug. This reduced release may be attributed to sodium alginate forming a dense gel matrix upon hydration, which restricts drug diffusion, consistent with findings from recent studies using alginate-based buccal systems [62,69].

These findings confirm that both polymer selection (PVA vs. ALG) and the nature of the active ingredient (pure compound vs. plant extract) have a significant influence on buccal film productivity. Extract-based films, although showing lower mucoadhesive properties, appear to be more suited for rapid-release applications. In contrast, PVA–naringin films such as NP2 offer a favourable balance between release kinetics and adhesion.

5. Conclusions

In the present study, single microencapsulation of naringin with carbohydrate-based wall materials substantially increased its aqueous solubility compared to the crystalline form, reaching 306.42 μg/mL for the spray-dried powder. This value is markedly higher than the ~30–40 μg/mL reported under standard conditions by Zhang et al. (2015) [70]. Dual encapsulation combining liposomal entrapment with microencapsulation also enhanced solubility relative to pure naringin; however, the values (e.g., 93.32 μg/mL for NLS) were lower than those from single microencapsulation, as the liposomal barrier slowed immediate dissolution while providing greater stability. Buccal films, particularly the PVA–HPMC formulation (NP2), achieved dissolution efficiencies of 40.9% in artificial saliva, consistent with the rapid hydration and diffusion.

Release studies demonstrated that dual encapsulation slowed NR release under gastric conditions and sustained delivery in the intestinal phase, whereas single microencapsulation promoted faster but less controlled release. Among buccal films, NP2 provided the highest total release and mucoadhesive strength, highlighting the role of polymer selection in optimising both drug availability and mucosal retention. Interestingly, grapefruit peel extract-based formulations, despite lower absolute NR content, frequently showed higher relative release efficiencies, likely due to the presence of co-extracted phytochemicals—such as flavonoids, organic acids, and sugars—that improve wettability, matrix hydration, and molecular diffusion.

These results support the initial hypotheses of the study: (i) the double capsule effectively limits release in the acidic gastric environment, supporting intestinal delivery, (ii) PVA-based oral films outperform alginate-based films in terms of release and mucoadhesion, and (iii) grapefruit peel extract increases the relative release of NR compared to the pure compound, likely due to synergistic co-components.

Meanwhile, in vitro findings suggest that dual-encapsulation systems may enhance stability and site-specific release, supporting their potential for improved intestinal absorption and therapeutic efficacy in nutraceutical or pharmaceutical applications.

Although the in vitro results are promising, future in vivo investigations are needed to evaluate the impact of enzymatic degradation, mucosal penetration efficiency, and intestinal absorption mechanisms, which may influence the real-world applicability of these delivery systems.

Author Contributions: Conceptualisation, J.S., J.B. and M.M.; investigation, J.S., M.M. and J.B.; resources, J.B. and M.M.; writing—production of the initial draft, J.S.; writing—review and editing, J.S., M.M. and J.B.; visualisation, J.S.; supervision, J.B. All authors have read and agreed to the published version of the manuscript.

Funding: This project has received financial support from the Research Council of Lithuania (LMTLT) and the Ministry of Education, Science and Sport of the Republic of Lithuania, agreement No: S-A-UEI-23-7.

Institutional Review Board Statement: Not applicable.

Informed Consent Statement: Not applicable.

Data Availability Statement: The data presented in this study are available on request from the corresponding author.

Acknowledgments: The authors gratefully acknowledge the Open Access Centre for Advanced Pharmaceutical and Health Technologies at the Lithuanian University of Health Sciences and the Lithuanian Research Centre for providing access to research infrastructure that was essential to this study. Their support significantly contributed to the successful completion of the experimental work.

Conflicts of Interest: The authors declare no conflicts of interest.

References

1. Russo, C.; Maugeri, A.; Lombardo, G.E.; Musumeci, L.; Barreca, D.; Rapisarda, A.; Cirmi, S.; Navarra, M. The Second Life of Citrus Fruit Waste: A Valuable Source of Bioactive Compounds. *Molecules* **2021**, *26*, 5991. [CrossRef]
2. Eom, S.; Lee, B.-B.; Lee, S.; Park, Y.; Yeom, H.D.; Kim, T.-H.; Nam, S.-H.; Lee, J.H. Antioxidative and Analgesic Effects of Naringin through Selective Inhibition of Transient Receptor Potential Vanilloid Member 1. *Antioxidants* **2021**, *11*, 64. [CrossRef]
3. Ginwala, R.; Bhavsar, R.; Chigbu, D.G.I.; Jain, P.; Khan, Z.K. Potential Role of Flavonoids in Treating Chronic Inflammatory Diseases with a Special Focus on the Anti-Inflammatory Activity of Apigenin. *Antioxidants* **2019**, *8*, 35. [CrossRef] [PubMed]
4. Stabrauskiene, J.; Kopustinskiene, D.M.; Lazauskas, R.; Bernatoniene, J. Naringin and Naringenin: Their Mechanisms of Action and the Potential Anticancer Activities. *Biomedicines* **2022**, *10*, 1686. [CrossRef] [PubMed]
5. Chen, M.; Li, R.; Gao, Y.; Zheng, Y.; Liao, L.; Cao, Y.; Li, J.; Zhou, W. Encapsulation of Hydrophobic and Low-Soluble Polyphenols into Nanoliposomes by pH-Driven Method: Naringenin and Naringin as Model Compounds. *Foods* **2021**, *10*, 963. [CrossRef]
6. Bai, Y.; Peng, W.; Yang, C.; Zou, W.; Liu, M.; Wu, H.; Fan, L.; Li, P.; Zeng, X.; Su, W. Pharmacokinetics and Metabolism of Naringin and Active Metabolite Naringenin in Rats, Dogs, Humans, and the Differences Between Species. *Front. Pharmacol.* **2020**, *11*, 364. [CrossRef]
7. Ravetti, S.; Garro, A.G.; Gaitán, A.; Murature, M.; Galiano, M.; Brignone, S.G.; Palma, S.D. Naringin: Nanotechnological Strategies for Potential Pharmaceutical Applications. *Pharmaceutics* **2023**, *15*, 863. [CrossRef]
8. Budel, R.G.; da Silva, D.A.; Moreira, M.P.; Dalcin, A.J.F.; da Silva, A.F.; Nazario, L.R.; Majolo, J.H.; Lopes, L.Q.S.; Santos, R.C.V.; Antunes Soares, F.A.; et al. Toxicological Evaluation of Naringin-Loaded Nanocapsules In Vitro and In Vivo. *Colloids Surf. B Biointerfaces* **2020**, *188*, 110754. [CrossRef] [PubMed]
9. Stabrauskiene, J.; Pudziuvelyte, L.; Bernatoniene, J. Optimizing Encapsulation: Comparative Analysis of Spray-Drying and Freeze-Drying for Sustainable Recovery of Bioactive Compounds from *Citrus* × *Paradisi* L. Peels. *Pharmaceuticals* **2024**, *17*, 596. [CrossRef]
10. Elkhoury, K.; Sanchez-Gonzalez, L.; Lavrador, P.; Almeida, R.; Gaspar, V.; Kahn, C.; Cleymand, F.; Arab-Tehrany, E.; Mano, J.F. Gelatin Methacryloyl (GelMA) Nanocomposite Hydrogels Embedding Bioactive Naringin Liposomes. *Polymers* **2020**, *12*, 2944. [CrossRef]
11. Caddeo, C.; Pucci, L.; Gabriele, M.; Carbone, C.; Fernàndez-Busquets, X.; Valenti, D.; Pons, R.; Vassallo, A.; Fadda, A.M.; Manconi, M. Stability, Biocompatibility and Antioxidant Activity of PEG-Modified Liposomes Containing Resveratrol. *Int. J. Pharm.* **2018**, *538*, 40–47. [CrossRef] [PubMed]
12. Pearce, K.; Cairncross, S.I.; Benjeddou, M. Liposomal-Naringenin Radiosensitizes Triple-Negative Breast Cancer MDA-MB-231 Cells In Vitro. *IET Nanobiotechnol.* **2024**, *2024*, 3786627. [CrossRef]
13. Ruwizhi, N.; Aderibigbe, B.A. The Efficacy of Cholesterol-Based Carriers in Drug Delivery. *Molecules* **2020**, *25*, 4330. [CrossRef]
14. Krithika, R.; Ravilla, L.; Perumal, S.; Padmini, R. Formulation and Characterization of Naringin—Niosomes for Sustained Drug Delivery and Wound Healing Properties. *J. Adv. Zool.* **2023**, *44*, 1579–1598. [CrossRef]
15. Moammeri, A.; Chegeni, M.M.; Sahrayi, H.; Ghafelehbashi, R.; Memarzadeh, F.; Mansouri, A.; Akbarzadeh, I.; Abtahi, M.S.; Hejabi, F.; Ren, Q. Current Advances in Niosomes Applications for Drug Delivery and Cancer Treatment. *Mater. Today Bio.* **2023**, *23*, 100837. [CrossRef]
16. Imam, S.; Gilani, S.; Zafar, A.; Jumah, M.; Ali, R.; Ahmed, M.; Alshehri, S. Preparation and Optimization of Naringin Oral Nanocarrier: In Vitro Characterization and Antibacterial Activity. *Coatings* **2022**, *12*, 1230. [CrossRef]
17. Kaur, N.; Sharma, P.; Li, X.; Jasti, B. Sublingual Permeability of Model Drugs in New Zealand White Rabbits: In Vitro-In Vivo Correlation. *Int. J. Pharm.* **2025**, *668*, 124998. [CrossRef]
18. Mohamed, E.; Abu Hashim, I.; Yusif, R.; Shaaban, A.; El-Sheakh, A.; Hamed, M.; Badria, F. Polymeric Micelles for Potentiated Antiulcer and Anticancer Activities of Naringin. *Int. J. Nanomed.* **2018**, *13*, 1009–1027. [CrossRef]
19. Stabrauskiene, J.; Marksa, M.; Ivanauskas, L.; Bernatoniene, J. Optimization of Naringin and Naringenin Extraction from *Citrus* × *Paradisi* L. Using Hydrolysis and Excipients as Adsorbent. *Pharmaceutics* **2022**, *14*, 890. [CrossRef] [PubMed]

20. Stabrauskiene, J.; Marksa, M.; Ivanauskas, L.; Viskelis, P.; Viskelis, J.; Bernatoniene, J. Citrus × Paradisi L. Fruit Waste: The Impact of Eco-Friendly Extraction Techniques on the Phytochemical and Antioxidant Potential. *Nutrients* **2023**, *15*, 1276. [CrossRef] [PubMed]
21. Raudone, L.; Zymone, K.; Marksa, M.; Cesoniene, L. Phenolic Diversity in *Viburnum* L. Inflorescences: A Comparative Study of *V. Opulus*, *V. Trilobum*, and *V. Sargentii*. *Sci. Hortic.* **2025**, *350*, 114327. [CrossRef]
22. Ang, S.-S.; Thoo, Y.Y.; Siow, L.F. Encapsulation of Hydrophobic Apigenin into Small Unilamellar Liposomes Coated with Chitosan Through Ethanol Injection and Spray Drying. *Food Bioprocess Technol.* **2024**, *17*, 424–439. [CrossRef]
23. Németh, Z.; Csóka, I.; Semnani Jazani, R.; Sipos, B.; Haspel, H.; Kozma, G.; Kónya, Z.; Dobó, D.G. Quality by Design-Driven Zeta Potential Optimisation Study of Liposomes with Charge Imparting Membrane Additives. *Pharmaceutics* **2022**, *14*, 1798. [CrossRef] [PubMed]
24. Pudziuvelyte, L.; Siauruseviciute, A.; Morkuniene, R.; Lazauskas, R.; Bernatoniene, J. Influence of Technological Factors on the Quality of Chitosan Microcapsules with *Boswellia serata* L. Essential Oil. *Pharmaceutics* **2022**, *14*, 1259. [CrossRef]
25. Ghaferi, M.; Asadollahzadeh, M.J.; Akbarzadeh, A.; Ebrahimi Shahmabadi, H.; Alavi, S.E. Enhanced Efficacy of PEGylated Liposomal Cisplatin: In Vitro and In Vivo Evaluation. *Int. J. Mol. Sci.* **2020**, *21*, 559. [CrossRef]
26. Kubiliene, A.; Munius, E.; Songailaite, G.; Kokyte, I.; Baranauskaite, J.; Liekis, A.; Sadauskiene, I. A Comparative Evaluation of Antioxidant Activity of Extract and Essential Oil of *Origanum onites* L. In Vivo. *Molecules* **2023**, *28*, 5302. [CrossRef]
27. Ferreira, L.M.D.M.C.; Pereira, R.R.; Carvalho-Guimarães, F.B.D.; Remígio, M.S.D.N.; Barbosa, W.L.R.; Ribeiro-Costa, R.M.; Silva-Júnior, J.O.C. Microencapsulation by Spray Drying and Antioxidant Activity of Phenolic Compounds from Tucuma Coproduct (Astrocaryum Vulgare Mart.) Almonds. *Polymers* **2022**, *14*, 2905. [CrossRef] [PubMed]
28. Thuong Nhan, N.P.; Tan Thanh, V.; Huynh Cang, M.; Lam, T.D.; Cam Huong, N.; Hong Nhan, L.T.; Thanh Truc, T.; Tran, Q.T.; Bach, L.G. Microencapsulation of Lemongrass (*Cymbopogon Citratus*) Essential Oil Via Spray Drying: Effects of Feed Emulsion Parameters. *Processes* **2020**, *8*, 40. [CrossRef]
29. Kazlauskaite, J.A.; Matulyte, I.; Marksa, M.; Bernatoniene, J. Nutmeg Essential Oil, Red Clover, and Liquorice Extracts Microencapsulation Method Selection for the Release of Active Compounds from Gel Tablets of Different Bases. *Pharmaceutics* **2023**, *15*, 949. [CrossRef] [PubMed]
30. Pudžiuvelytė, L.; Drulytė, E.; Bernatonienė, J. Nitrocellulose Based Film-Forming Gels with Cinnamon Essential Oil for Covering Surface Wounds. *Polymers* **2023**, *15*, 1057. [CrossRef]
31. Bolko Seljak, K.; Grilc, B.; Gašperlin, M.; Gosenca Matjaž, M. Ibuprofen-Loaded, Nanocellulose-Based Buccal Films: The Development and Evaluation of Promising Drug Delivery Systems for Special Populations. *Gels* **2025**, *11*, 163. [CrossRef]
32. Khan, M.S.; Ahmad, R.N.K.; Badruddoja, A.; Akhtar, M.M.J.S.; Rafeeque, S.B.M.; Ahmed, A.A.M.Z.; Shafiullah, F.S.M.; Kha-war, M.M.A.A.; Ahmed, W.A.N.; Iftekhar, A.A. Development and Evaluation of Mucoadhesive Buccal Films for the Sustained Release of Diclofenac Sodium: An Innovative Approach for Pain Management. *World J. Adv. Eng. Technol. Sci.* **2024**, *13*, 814–830. [CrossRef]
33. Hassan, A.A.A.; Kristó, K.; Ibrahim, Y.H.-E.Y.; Regdon, G.; Sovány, T. Quality by Design-Guided Systematic Development and Optimization of Mucoadhesive Buccal Films. *Pharmaceutics* **2023**, *15*, 2375. [CrossRef] [PubMed]
34. Maslii, Y.; Herbina, N.; Dene, L.; Ivanauskas, L.; Matulis, G.; Bernatoniene, J. Mucoadhesive Polymeric Film with Plant-Based Compounds for Dental Applications: Formulation, Characterization and Evaluation. *Pharm. Dev. Technol.* **2025**, *30*, 505–520. [CrossRef]
35. Matulyte, I.; Marksa, M.; Bernatoniene, J. Development of Innovative Chewable Gel Tablets Containing Nutmeg Essential Oil Microcapsules and Their Physical Properties Evaluation. *Pharmaceutics* **2021**, *13*, 873. [CrossRef]
36. Chen, J.; Li, S.; Xu, J.; Ding, F.; Wang, Z.; Cheng, Y.; Deng, X. Concentration and Distribution of Main Bitter Compounds in Fruit Tissues of 'Oroblanco' (*Citrus grandis* L.× *Citrus paradisi* Macf.). *Sci. Hortic.* **2015**, *193*, 84–89. [CrossRef]
37. Lindsay, S.; Tumolva, O.; Khamiakova, T.; Coppenolle, H.; Kovarik, M.; Shah, S.; Holm, R.; Perrie, Y. Can We Simplify Liposome Manufacturing Using a Complex DoE Approach? *Pharmaceutics* **2024**, *16*, 1159. [CrossRef]
38. Opatha, S.A.T.; Titapiwatanakun, V.; Chutoprapat, R. Transfersomes: A Promising Nanoencapsulation Technique for Transdermal Drug Delivery. *Pharmaceutics* **2020**, *12*, 855. [CrossRef]
39. Soema, P.C.; Willems, G.-J.; Jiskoot, W.; Amorij, J.-P.; Kersten, G.F. Predicting the Influence of Liposomal Lipid Composition on Liposome Size, Zeta Potential and Liposome-Induced Dendritic Cell Maturation Using a Design of Experiments Approach. *Eur. J. Pharm. Biopharm.* **2015**, *94*, 427–435. [CrossRef]
40. Koehler, J.K.; Schnur, J.; Heerklotz, H.; Massing, U. Screening for Optimal Liposome Preparation Conditions by Using Dual Centrifugation and Time-Resolved Fluorescence Measurements. *Pharmaceutics* **2021**, *13*, 2046. [CrossRef]
41. Chen, C.; Chen, C.; Li, Y.; Gu, R.; Yan, X. Characterization of Lipid-Based Nanomedicines at the Single-Particle Level. *Fundam. Res.* **2023**, *3*, 488–504. [CrossRef] [PubMed]
42. Öztürk, K.; Kaplan, M.; Çalış, S. Effects of Nanoparticle Size, Shape, and Zeta Potential on Drug Delivery. *Int. J. Pharm.* **2024**, *666*, 124799. [CrossRef]

43. Calandra, P.; Abe, A.A.; Scavo, A.; Bruno, L.; Rossi, C.O.; Caputo, P. Novel Microscopic Approach to Particle Size Evaluation in Colloidal Systems. *Appl. Sci.* **2024**, *14*, 3567. [CrossRef]
44. Mardani, M.; Siahtiri, S.; Besati, M.; Baghani, M.; Baniassadi, M.; Nejad, A.M. Microencapsulation of Natural Products Using Spray Drying; an Overview. *J. Microencapsul.* **2024**, *41*, 649–678. [CrossRef]
45. Kyriakoudi, A.; Spanidi, E.; Mourtzinos, I.; Gardikis, K. Innovative Delivery Systems Loaded with Plant Bioactive Ingredients: Formulation Approaches and Applications. *Plants* **2021**, *10*, 1238. [CrossRef]
46. Safaeian Laein, S.; Samborska, K.; Can Karaca, A.; Mostashari, P.; Akbarbaglu, Z.; Sarabandi, K.; Jafari, S.M. Strategies for Further Stabilization of Lipid-Based Delivery Systems with a Focus on Solidification by Spray-Drying. *Trends Food Sci. Technol.* **2024**, *146*, 104412. [CrossRef]
47. Buljeta, I.; Pichler, A.; Šimunović, J.; Kopjar, M. Polysaccharides as Carriers of Polyphenols: Comparison of Freeze-Drying and Spray-Drying as Encapsulation Techniques. *Molecules* **2022**, *27*, 5069. [CrossRef]
48. Cegledi, E.; Garofulić, I.E.; Zorić, Z.; Roje, M.; Dragović-Uzelac, V. Effect of Spray Drying Encapsulation on Nettle Leaf Extract Powder Properties, Polyphenols and Their Bioavailability. *Foods* **2022**, *11*, 2852. [CrossRef]
49. Papoutsis, K.; Golding, J.B.; Vuong, Q.; Pristijono, P.; Stathopoulos, C.E.; Scarlett, C.J.; Bowyer, M. Encapsulation of Citrus By-Product Extracts by Spray-Drying and Freeze-Drying Using Combinations of Maltodextrin with Soybean Protein and ι-Carrageenan. *Foods* **2018**, *7*, 115. [CrossRef]
50. Jiang, H.; Zhang, M.; Lin, X.; Zheng, X.; Qi, H.; Chen, J.; Zeng, X.; Bai, W.; Xiao, G. Biological Activities and Solubilization Methodologies of Naringin. *Foods* **2023**, *12*, 2327. [CrossRef] [PubMed]
51. Katukam, L.P.; Padakanti, A.P.; Chella, N. Upscaling Co-Amorphous Formulation of Naringin-Quinacrine Dihydrochloride Translating from Laboratory to Pilot Scale Using Spray Drying for Improved Physicochemical and Mechanical Properties. *Powder Technol.* **2025**, *451*, 120458. [CrossRef]
52. Da Costa, R.S.; Teixeira, C.B.; Gabbay Alves, T.V.; Ribeiro-Costa, R.M.; Casazza, A.A.; Aliakbarian, B.; Converti, A.; Silva Júnior, J.O.C.; Perego, P. Optimization of Spray Drying Conditions to Microencapsulate Cupuassu (*Theobroma grandiflorum*) Seed by-Product Extract. *Nat. Prod. Res.* **2019**, *33*, 2600–2608. [CrossRef] [PubMed]
53. Mohammadalinejhad, S.; Kurek, M.A. Microencapsulation of Anthocyanins—Critical Review of Techniques and Wall Materials. *Appl. Sci.* **2021**, *11*, 3936. [CrossRef]
54. Gaćina, N.; Elez Garofulić, I.; Zorić, Z.; Pedisić, S.; Dragović-Uzelac, V. Influence of Encapsulation Parameters on the Retention of Polyphenols in Blackthorn Flower Extract. *Processes* **2022**, *10*, 2517. [CrossRef]
55. Dejeu, I.L.; Vicaș, L.G.; Marian, E.; Ganea, M.; Frent, O.D.; Maghiar, P.B.; Bodea, F.I.; Dejeu, G.E. Innovative Approaches to Enhancing the Biomedical Properties of Liposomes. *Pharmaceutics* **2024**, *16*, 1525. [CrossRef]
56. Ashfaq, R.; Rasul, A.; Asghar, S.; Kovács, A.; Berkó, S.; Budai-Szűcs, M. Lipid Nanoparticles: An Effective Tool to Improve the Bioavailability of Nutraceuticals. *Int. J. Mol. Sci.* **2023**, *24*, 15764. [CrossRef]
57. Tang, Y.; Liu, W.; Zhang, J.; Juan, B.; Zhu, Y.; Zhu, L.; Zhao, Y.; Daglia, M.; Xiao, X.; He, Y. Advances in Intestinal-Targeted Release of Phenolic Compounds. *Nutrients* **2025**, *17*, 2598. [CrossRef]
58. Desai, S.D.; Kundu, I.; Swamy, N.P.; Crull, G.B.; Pan, D.; Zhao, J.; Shah, R.P.; Venkatesh, C.; Vig, B.; Varia, S.A.; et al. Cross-Linking of Poly (Vinyl Alcohol) Films under Acidic and Thermal Stress. *Eur. J. Pharm. Sci.* **2020**, *152*, 105429. [CrossRef]
59. Bayer, I.S. Recent Advances in Mucoadhesive Interface Materials, Mucoadhesion Characterization, and Technologies. *Adv. Mater. Inter.* **2022**, *9*, 2200211. [CrossRef]
60. Al-Sahaf, Z.; Raimi-Abraham, B.; Licciardi, M.; De Mohac, L.M. Influence of Polyvinyl Alcohol (PVA) on PVA-Poly-N-Hydroxyethyl-Aspartamide (PVA-PHEA) Microcrystalline Solid Dispersion Films. *AAPS PharmSciTech* **2020**, *21*, 267. [CrossRef]
61. Hazt, B.; Read, D.J.; Harlen, O.G.; Poon, W.C.K.; O'Connell, A.; Sarkar, A. Mucoadhesion across Scales: Towards the Design of Protein-Based Adhesives. *Adv. Colloid Interface Sci.* **2024**, *334*, 103322. [CrossRef]
62. Lai, J.; Azad, A.K.; Sulaiman, W.M.A.W.; Kumarasamy, V.; Subramaniyan, V.; Alshehade, S.A. Alginate-Based Encapsulation Fabrication Technique for Drug Delivery: An Updated Review of Particle Type, Formulation Technique, Pharmaceutical Ingredient, and Targeted Delivery System. *Pharmaceutics* **2024**, *16*, 370. [CrossRef]
63. Shipp, L.; Liu, F.; Kerai-Varsani, L.; Okwuosa, T.C. Buccal Films: A Review of Therapeutic Opportunities, Formulations & Relevant Evaluation Approaches. *J. Control. Release* **2022**, *352*, 1071–1092. [CrossRef]
64. Pérez Zamora, C.M.; Michaluk, A.G.; Chiappetta, D.A.; Nuñez, M.B. Herbal Buccal Films with In Vitro Antibacterial and Anti-Inflammatory Effects. *J. Herb. Med.* **2022**, *31*, 100527. [CrossRef]
65. Jacob, S.; Nair, A.B.; Boddu, S.H.S.; Gorain, B.; Sreeharsha, N.; Shah, J. An Updated Overview of the Emerging Role of Patch and Film-Based Buccal Delivery Systems. *Pharmaceutics* **2021**, *13*, 1206. [CrossRef] [PubMed]
66. El Sharawy, A.M.; Shukr, M.H.; Elshafeey, A.H. Formulation and Optimization of Duloxetine Hydrochloride Buccal Films: In Vitro and In Vivo Evaluation. *Drug Deliv.* **2017**, *24*, 1762–1769. [CrossRef]

67. Elgharbawy, A.S.; El Demerdash, A.-G.M.; Sadik, W.A.; Kasaby, M.A.; Lotfy, A.H.; Osman, A.I. Enhancing the Biodegradability, Water Solubility, and Thermal Properties of Polyvinyl Alcohol through Natural Polymer Blending: An Approach toward Sustainable Polymer Applications. *Polymers* **2024**, *16*, 2141. [CrossRef]
68. Dołowacka-Jóźwiak, A.; Nawrot-Hadzik, I.; Matkowski, A.; Ciecieląg, T.; Gawin-Mikołajewicz, A.; Dudek-Wicher, R.; Prochoń, M.; Markowska, D.; Adamski, R.; Wiater, A.; et al. Mucoadhesive PVA Film for Sustained Resveratrol Delivery: Formulation, Characterization, and Release Profile. *Molecules* **2025**, *30*, 2642. [CrossRef] [PubMed]
69. Pamlényi, K.; Kristó, K.; Jójárt-Laczkovich, O.; Regdon, G. Formulation and Optimization of Sodium Alginate Polymer Film as a Buccal Mucoadhesive Drug Delivery System Containing Cetirizine Dihydrochloride. *Pharmaceutics* **2021**, *13*, 619. [CrossRef]
70. Zhang, J.; Zhang, P.; Liu, T.; Zhou, L.; Zhang, L.; Lin, R.; Yang, G.; Wang, W.; Li, Y. Solubility of Naringin in Ethanol and Water Mixtures from 283.15 to 318.15K. *J. Mol. Liq.* **2015**, *203*, 98–103. [CrossRef]